Critical function of superoxide dismutase 1 (SOD1) in relation to nitric oxide in mouse skeletal muscles

Alycia Noë

Department of Biology

McGill University

Montréal, Canada

December 2020

A thesis submitted to McGill University in partial fulfillment of the requirements of the degree of Doctor of Philosophy

© Alycia Noë 2020

Abstract

Superoxide dismutases (SODs) are the first line of defense against the potential damage from oxygen free radicals. The importance of SODs is highlighted by the expression of at least one SOD in most organisms today, even some anaerobic bacteria and that SODs emerged prior to the first Great Oxidation Event (GOE), over 2.7 billion years ago[1, 2]. SODs catalyze the dismutation, or removal, of superoxide ($O_2^{\bullet-}$), by converting it into hydrogen peroxide and oxygen ($2O_2^{\bullet-} + 2H^+ \rightarrow H_2O_2 + O_2$)[3]. This SOD-catalyzed dismutation is extremely efficient, as it occurs at a diffusion-limited rate of ~2 x 10^9 M^{-1} s^{-1}. This thesis focuses on a reaction that competes with superoxide dismutation – the formation of peroxynitrite by the reaction of superoxide with nitric oxide ($NO^{\bullet}$). The spontaneous reaction of superoxide with nitric oxide occurs three-times faster than the dismutation of superoxide by SODs[4]. Although superoxide has historically been considered a toxic molecule, the toxicity attributed to superoxide is puzzling as it is not a strong oxidizing agent. Previous work from other laboratories has shown that germline *Sod1*$^{-/-}$ knockout mice can live for up to two years, yet mouse embryonic fibroblasts isolated from the same mice cannot survive in culture[5]. SOD1 is the most abundant SOD isoform in mammals and is expressed in the cytoplasm and mitochondrial inner-membrane space. To better understand the toxicity of superoxide, we generated a conditional *Sod1* knockout mouse model, using the Cre/loxP system. This mouse model allows us to bypass any possible developmental adaptations of germline knockout mice and to see the consequence of losing SOD1 expression *in vitro* and in adult mice *in vivo*.

First, we studied inducible *Sod1* knockout mouse embryonic fibroblasts (MEFs) *in vitro*. Upon Cre recombinase expression, these cells do not express SOD1 and lose ~80% of their superoxide dismutase activity. Like their germline *Sod1*$^{-/-}$ counterparts, inducible *Sod1* knockout MEFs die upon the loss of SOD1 expression. We show that the viability of inducible *Sod1* knockout MEFs can be fully rescued by treatment with nitric oxide synthase (NOS) inhibitors (L-NAME and 7-NI) and a peroxynitrite decomposition catalyst (FeTPPS). Surprisingly, cells rescued with L-NAME show little to no SOD2 and SOD3 expression, meaning there is little removal of superoxide. These results suggest that peroxynitrite, rather than superoxide itself, is the damaging molecule and highlights the possibility that superoxide is not inherently strongly damaging in the absence

of nitric oxide. Furthermore, we show that cells can thrive with little to no SOD expression when nitric oxide formation is lowered by treatment with L-NAME (L-nitro-L-arginine methyl ester). Although this may be an *in vitro* phenomenon, this is the first evidence of mammalian cells that can survive without minimal SOD expression. Overall, these cells represent a new tool to study ROS/RNS metabolism. For example, cells lacking SOD1 expression and treated with NOS inhibitors are more sensitive when treated with N-acetylcysteine (NAC), an antioxidant that leads to an increase in hydrogen peroxide detoxification, pointing to a minimum need of hydrogen peroxide formation, for signaling, that is depleted by the lack of SOD1.

Next, we generated a whole-body adult-onset *Sod1* knockout mouse model. Interestingly, loss of *Sod1* as an adult leads to rapid skeletal muscle degeneration and death. These mice lose expression of SOD1 in most tissues, but there were pathological findings only in skeletal muscles. These marks of muscle damage also correlated with increased peroxynitrite damage (3-nitrotyrosine immunohistochemistry). This was surprising as the germline knockout *Sod1*$^{-/-}$ mice can live for two years, although they do show signs of accelerated sarcopenia, or muscle atrophy[6]. Guided by our *in vitro* studies, we wanted to see if L-NAME treatment could improve the phenotypes our adult-onset *Sod1* knockout mice. The knockout phenotype, viability and skeletal muscle degradation, were both rescued by intraperitoneal injections with L-NAME. These results are indicative that germline knockout *Sod1*$^{-/-}$ mice have developmental adaptations that likely impact nitric oxide handling or peroxynitrite formation to allow them to survive much longer than adult-onset *Sod1* knockout mice. I found that that the viable germline knockout *Sod1*$^{-/-}$ mice have altered blood composition and lower nNOS expression in skeletal muscle tissues. Both of these changes are likely to affect local nitric oxide levels and thus lead to slower peroxynitrite formation.

To conclude, the findings in my thesis present the first mammalian model of global adult-onset *Sod1* knockout and provide new insights into the strategies for the management of stresses from reactive oxygen and reactive nitrogen species. The results also underline that superoxide is not by itself key to oxidative stress, as believed by many, but rather that peroxynitrite should be where to focus.

Resumé

Les superoxydes dismutases (SOD) constituent la première ligne de défense contre les dommages potentiels des espèces réactives de l'oxygène (ERO). L'importance des SOD est soulignée par l'expression d'au moins une SOD dans la plupart des organismes aujourd'hui, même certaines bactéries anaérobies, et par le fait que les SOD sont apparues avant le premier grand événement d'oxydation (GOE), il y a ~2.7 milliards ans[1, 2]. Les SODs catalysent la dismutation, ou l'élimination, du superoxydes ($O_2^{\bullet-}$), en le transformant en peroxyde d'hydrogène et en oxygène ($2O_2^{\bullet-} + 2H^+ \rightarrow H_2O_2 + O_2$)[3]. Cette dismutation catalysée par les SODs est extrêmement efficace (~2×10^9 M^{-1} s^{-1}). Cette thèse se concentre sur une sur une réaction qui entre en concurrence avec la dismutation du superoxyde – la formation de peroxynitrite par la réaction du superoxyde et d'oxyde nitrique ($NO^{\bullet}$). Cette réaction est trois fois plus vite que la dismutation du superoxyde par les SODs[4]. Bien que le superoxyde ait été historiquement considéreé comme une molécule toxique, la toxicité attribuée au superoxyde est déroutante parce qu'il ne s'agit pas d'un agent oxydant puissant. Les souris germinales *Sod1*$^{-/-}$ knockout peuvent vivre jusqu'à deux ans, mais ses fibroblastes embryonnaires, isolés des mêmes souris, ne peuvent pas survivre en culture[5]. SOD1 est l'isoforme des SODs la plus abondante et s'exprime dans le cytoplasme et l'espace intra-membranaire mitochondrial. Pour mieux comprendre la toxicité du superoxyde, nous avons généré un modèle de souris *Sod1* knockout conditionnel, en utilisant le système Cre/loxP. Ce modèle de souris nous permet de contourner toutes les adaptations du développement possibles des souris germinales *Sod1*$^{-/-}$ knockout et de voir la conséquence de la perte de l'expression de SOD1 *in vitro* et *in vivo* (les souris adultes).

Nous avons d'abord étudié *in vitro* les fibroblastes embryonnaires (MEFs) de souris *Sod1* knockout conditionnel. Lors de l'expression de la recombinase Cre, ces cellules n'expriment pas SOD1 et perdent ~80% de leur activité superoxyde dismutase. Comme les MEFs de la lignée germinale *Sod1*$^{-/-}$ knockout, les MEFs de souris *Sod1* knockout conditionnel meurent lors de la perte de l'expression de SOD1. Nous montrons que la viabilité des MEFs de souris *Sod1* knockout conditionnel peut être entièrement rétablie par le traitement avec des inhibiteurs de l'oxyde nitrique synthase (NOS) (L-NAME et 7-NI) et un catalyseur de décomposition du peroxynitrite (FeTPPS). Étonnamment, les cellules sauvées avec L-NAME ont peu ou pas d'expression de SOD2

et SOD3. Cela signifie qu'il y a peu d'élimination du superoxyde. Ces résultats suggèrent que c'est le peroxynitrite, plutôt que le superoxyde lui-même, qui est la molécule nuisible, et souligne la possibilité que le superoxyde ne soit pas intrinsèquement fortement nuisible en l'absence d'oxyde nitrique. En outre, nous montrons que les cellules peuvent se développer avec une expression de la SOD faible ou nulle lorsque la formation d'oxyde nitrique est réduite par un traitement au L-NAME (ester méthylique de L-nitro-L-arginine). Bien qu'il puisse s'agir d'un phénomène *in vitro*, c'est la première preuve que des cellules de mammifères peuvent survivre sans une expression minimale de la SOD. Dans l'ensemble, ces cellules représentent un nouvel outil pour étudier le métabolisme de ERO/ERN (les espèces réactives de l'azote). Par exemple, les cellules manquant d'expression de la SOD1 et traitées avec L-NAME (l'inhibiteur de NOS) sont plus sensibles lorsqu'elles sont traitées avec de la N-acétylcystéine (NAC), un antioxydant qui augmente la détoxification du peroxyde d'hydrogène, ce qui indique un besoin minimal de formation de peroxyde d'hydrogène, pour la signalisation, qui est épuisé par l'absence de SOD1.

Ensuite, nous avons généré un modèle de souris knockout pour *Sod1* début à l'âge adulte. Il est intéressant de noter que la perte de *Sod1* à l'âge adulte entraîne une dégénérescence rapide des muscles squelettiques et la mort. Ces souris perdent l'expression de SOD1 dans la plupart des tissus, mais il n'y a eu des résultats pathologiques que dans les muscles squelettiques. Ces marques de dommages musculaires sont également corrélées à une augmentation des dommages causés par peroxynitrite (immunohistochimie de la 3-nitrotyrosine).Cela a été surprenant car les souris *Sod1*$^{-/-}$ knockout germinales peuvent vivre deux ans, bien qu'elles présentent des signes de sarcopénie accélérée, ou atrophie musculaire[6]. Guidés par nos études *in vitro*, nous avons voulu voir si le traitement L-NAME pouvait améliorer les phénotypes de nos souris Sod1 knockout adultes. Le phénotype de knockout, la viabilité et la dégradation des muscles squelettiques, ont été sauvés par des injections intrapéritonéales de L-NAME. Ces résultats indiquent que les souris *Sod1*$^{-/-}$ knockout germinales ont des adaptations de développement qui ont probablement un impact sur la manipulation de l'oxyde nitrique ou la formation de peroxynitrite, ce qui leur permet de survivre beaucoup plus longtemps que les souris *Sod1* knockout adultes. J'ai découvert que les souris *Sod1*$^{-/-}$ knockout germinales ont modifié la composition sanguine et réduit l'expression des nNOS dans les tissus musculaires

squelettiques. Ces deux changements sont susceptibles d'affecter les niveaux locaux d'oxyde nitrique et donc de ralentir la formation de peroxynitrite.

Pour conclure, les résultats de ma thèse présentent le premier modèle de mammifère d'élimination globale de *Sod1* à l'âge adulte et apportent de nouvelles idées sur les stratégies de gestion des stress aux espèces réactives de l'oxygène et de l'azote. Les résultats soulignent également que le superoxyde n'est pas la clé du stress oxydatif, comme beaucoup le croient, mais que le peroxynitrite devrait être le point central.

*To my parents for **always** being there.*

Acknowledgements

To begin, I would like to thank my thesis supervisor, Dr. Siegfried Hekimi, for believing in me all these years. His guidance, support, and encouragement were both good motivation and essential during the harder times when completing my degree. I will fondly remember conversations in his office where we parsed through data. I would walk in demoralized at times and he would see something interesting I had yet to note and it would set me off on a reinvigorated course.

Additionally, I would like to extend a thank you to the members of my supervisory committee – Dr. Alanna Watt and Dr. Hugh Clarke – for their valuable suggestions on my research. I would also like to recognize Dr. David Dankort. I always enjoyed our conversations, whether about research or the stock market, and your advice over these years is greatly appreciated.

A big thanks is also due to Dr. Ying Wang. When I began my Ph.D., it was just her and I that made up the "mouse side of the lab." We grew close over the years, bonding over our mutual love of food, but she is also boundless source of experimental knowledge that was priceless. In addition to Ying, I would like to that all members of the Hekimi Lab, past and present, and my compatriots of Bellini 2nd floor that I had the pleasure of working with.

I am also eternally grateful for the support and encouragement of my friends. I am quite fortunate to have friends, both from the lab and outside of the lab, that are a grounding force for me. Whether it be cooking nights, dinners at the restaurants where my friends work, café mornings, late night phone conversations, long walks, etc., all of them were key to keeping my head on straight.

I cannot forget to thank my animals. Although, they most certainly cannot read, my dog, Baylor, and my cats, Teak and Quartz, were imperative as continuous reminders of what is important and for showing me what unquestioning love is. They would stay up with me during late nights, processing data or writing. They would be patient with me on the nights when I needed to stay in the lab past midnight. They were always there.

Finally, but most importantly, I must expression my deepest appreciation for the love and support of my family. To my sister, thank you for being there, regardless of how much we annoy each other at times. To my Mum, thank you for being the calmest person I know and for always

believing I can do anything. To my Dad, thank you for being your sarcastic self, one of my best friends, and for the inspiration to pursue research. When it comes to family, I can say with confidence that no one is luckier than me.

Since I was a little kid, I wanted to end my thesis acknowledgements in the same way my father did in his thesis and now I finally have the chance to do so. “It seemed as it would never end but we finally made it.”

Contribution of Authors

All experiments and analysis were completed by A. Noë, unless stated below. Experimental design was a collaboration between A. Noë and S. Hekimi.

Chapter 2: qRT-PCR for *Sod1* and *Sod2* and superoxide dismutase activity assays were conducted in collaboration with Y. Wang.

Chapter 3: E. Bigras and E. Brasell aided with animal maintenance. E. Brasell also helped with cardiac blood draws for complete blood count analysis to ensure all mice could be sacrificed within three days of each other.

Contribution to Original Knowledge

All data chapters in this thesis represent contributions to original knowledge. Chapter 1 is a literature review and therefore not original knowledge. In Chapter 2, all findings except data represented by Figure 16 are unique contributions to the current knowledge in the field. In Chapter 3, all data presented are unique contributions to original knowledge.

Table of Contents

ABSTRACT ..... **II**

RESUME ..... **IV**

ACKNOWLEDGEMENTS ..... **VIII**

CONTRIBUTION OF AUTHORS ..... **X**

CONTRIBUTION TO ORIGINAL KNOWLEDGE ..... **XI**

LIST OF TABLES ..... **XV**

LIST OF FIGURES ..... **XVI**

LIST OF ABBREVIATIONS ..... **XIX**

CHAPTER 1: GENERAL INTRODUCTION **1**

1. Reactive Oxygen Species (ROS) 2
   a. What is a free radical? *2*
   b. Free Radical Theory of Aging *2*
   c. Sources of ROS *4*
      ROS generation in the mitochondria 4
      ROS production in the cytosol 7
   d. Superoxide *9*
      Historical perspective 9
      Structure 9
      Where is it formed and how does it move? 10
   e. Damage from ROS *10*
      DNA modifications 11
      Protein oxidation 12
      Lipid oxidation 12
   f. ROS signaling *13*
   g. Detoxification of ROS *15*
      Superoxide dismutase 15
      Catalase 16
      Glutathione 17
      N-acetyl cysteine 18
      Vitamin C 18
2. Reactive Nitrogen Species (RNS) 19
   a. Nitric oxide ($NO^{\bullet}$) *19*
   b. RNS sources *22*
   c. Damage resulting from RNS *23*
   d. RNS signaling *24*
      $NO^{\bullet}$/cGMP signaling pathway 24
      cGMP-independent $NO^{\bullet}$ signaling 26
3. Roles of ROS/RNS in disease pathology 27
   a. Cardiovascular diseases *27*
   b. Diabetes *27*
   c. Alzheimer's disease *28*
   d. Amyotrophic lateral sclerosis (ALS) *28*
   e. Cancer development *28*
4. Superoxide dismutases 29
   a. History *29*
   b. Function *31*
   c. Mechanism *31*

d. Isoforms *34*
5. NITRIC OXIDE SYNTHASES (NOS) 35
a. History *35*
b. Function *36*
c. Mechanism *37*
d. Isoforms *39*
6. THE REACTION OF SUPEROXIDE AND NITRIC OXIDE 41
a. Peroxynitrite *41*
b. Regulation of physiological processes by peroxynitrite *42*
c. Damage associated with peroxynitrite formation *43*
DNA damage 43
Lipid peroxidation 44
Reaction with transition metal centers 44
Oxidation of thiols 45
Tyrosine nitration 46
Tryptophan, methionine, and histidine oxidation 50
7. CELL WORK STUDYING SODS AND NOSS 51
a. Cells studying SOD *51*
b. Cells studying NOS *51*
8. MOUSE MODELS STUDYING SODS NOSS 52
a. Mouse models studying SOD *52*
Phenotypes associated with loss of Sod1 54
Lethality associated with loss of Sod2 58
Phenotypes associated with loss of Sod3 59
b. Mouse models studying NOS *60*
9. THESIS RATIONALE 63

CHAPTER 2: CONSEQUENCES OF THE LOSS OF THE CYTOPLASMIC SUPEROXIDE DISMUTASE SOD1 ON CELLULAR PHYSIOLOGY 64

1. ABSTRACT 65
2. INTRODUCTION 65
3. MATERIAL AND METHODS 69
a. Reagents and chemicals *69*
b. Mice *69*
c. Genotyping and detection of Sod1^{loxP} allele *70*
d. Genotyping and detection of KRas^{LSL} allele *71*
e. Preparation of mouse embryonic fibroblasts *71*
f. Construction of retroviral vector and retroviral infection *72*
g. Cells and tissue culture *73*
h. Cell viability assays *73*
i. Superoxide dismutase activity *74*
j. Microscopy *74*
k. Detection of apoptotic cells *74*
l. RNA preparation and qRT-PCR analysis *75*
m. Cell lysis and protein quantification *75*
n. Western blotting *75*
o. Statistical analysis *76*
4. RESULTS 76
a. Generation of mice with floxed Sod1 allele for conditional knockout *76*
b. Generation of inducible Sod1 knockout mouse embryonic fibroblasts (MEFs) *76*
c. Viability of inducible Sod1 knockout MEFs *77*
d. Rescue inducible Sod1 knockout MEFs by L-NAME *80*
e. Expression of SOD2 and SOD3 in inducible Sod1 knockout MEFs *86*
f. The regulation of SOD expression is not transcriptional *89*

g. Sensitivity of viable Sod1 knockout MEFs (rescued with L-NAME) to paraquat ($O_2^{\bullet-}$ generator) *91*
h. Sensitivity of viable Sod1 knockout MEFs (rescued with L-NAME) to N-acetyl cysteine (antioxidant) *93*
i. The sensitivity of $KRas^{G12D}$ cells to nitric oxide donors *95*
5. Discussion 96
a. Rescued inducible Sod1 KO MEFs are viable, despite lack of SOD expression *97*
b. Inducible Sod1 knockout MEFs are a new tool to understand ROS/RNS metabolism *99*

CHAPTER 3: ADULT-ONSET LOSS OF SOD1 IS LETHAL DUE TO PEROXYNITRITE DAMAGE TO SKELETAL MUSCLES 101

1. Abstract 102
2. Introduction 102
a. Superoxide dismutases *102*
b. Cre-loxP system *104*
c. Elimination of nitric oxide from the body *105*
3. Materials and Methods 106
a. Reagents and chemicals *106*
b. Mice *106*
c. Genotyping of mice *107*
d. Intraperitoneal injections *108*
e. Protein extraction and quantification from mouse tissue *109*
f. Western blotting *109*
g. Tissue processing and pathology *110*
h. Hematoxylin and Eosin *110*
i. Immunohistochemistry *111*
j. Microscopy *111*
k. Tail vein lactate measurements *111*
l. Urea assay *112*
m. Bloodwork *112*
n. Statistics *112*
4. Results 113
a. Construction of a mouse strain combining a floxed Sod1 allele and a broadly expressed tamoxifen (TM)-inducible Cre transgene *113*
b. Adult-onset global Sod1 knockout mice die within three weeks of Sod1 excision and are rescued by L-NAME treatment *114*
c. Dying adult-onset global Sod1 knockout mice show signs of muscle atrophy and degradation *118*
d. Peroxynitrite in adult-onset global Sod1 knockout mice *126*
e. Heart, brain, liver, and kidney are unaffected by loss of Sod1 ..... *127*
f. Developmental adaptations in germline Sod1 knockout mice *133*
5. Discussion 139
a. L-NAME rescues the lethality of Sod1 loss and skeletal muscle degradation in adult onset Sod1 knockout mice *139*
b. Lessons from $Sod1^{loxP/loxP}$ and $Sod1^{-/-}$ mice and mouse embryonic fibroblasts *141*

CHAPTER 4: GENERAL DISCUSSION 144

1. The SOD conundrum 145
2. Sod1 and skeletal muscles 147
3. Nitric oxide and skeletal muscles 148
4. A new perspective on superoxide and nitric oxide 149
5. Evolutionary perspective 150
6. Clinical applications 151

APPENDIX 154

LITERATURE CITED 158

List of Tables

Chapter 1:

Table 1: Nitrotyrosine formation in humans and mice 47
Table 2: Sod knockout mouse models and their phenotypes. 52

List of Figures

Chapter 1:

Figure 1: Superoxide dismutases are dispensable for normal lifespan in C. elegans. 3
Figure 2: Mice lacking *Sod1* expression are alive. 4
Figure 3: Cysteines as redox switches. 14
Figure 4: ROS are both beneficial and detrimental. 15
Figure 5: Identification of endothelial derived relaxing factor (EDRF) as nitric oxide (NO•). 21
Figure 6: Hemoglobin inhibits downstream effects of nitric oxide (NO•). 21
Figure 7: SOD1 crystal structure. 33
Figure 8: Mammalian isoforms of superoxide dismutase (SOD). 35
Figure 9: Formation of nitric oxide (NO•) by nitric oxide synthases (NOS). 38
Figure 10: Decreased SOD expression and its effect on superoxide, nitric oxide, and peroxynitrite levels. 50
56
Figure 11: Sarcopenia in *Sod1*$^{-/-}$ mice. 56
Figure 12: Decrease in skeletal muscle mass accounts for decrease in body mass of *Sod1*$^{-/-}$ mice. 57
Figure 13: Mice lacking all three NOS isoforms are alive. 61

Chapter 2:

Figure 14: Reactions of superoxide 66
Figure 15: SOD-dependent mammalian ROS signaling 67
Figure 16: *Sod1*$^{-/-}$ mouse embryonic fibroblasts undergo apoptotic cell death 69
Figure 17: Generation of *Sod1*$^{loxP/loxP}$ knockout mouse embryonic fibroblasts. 77
78
Figure 18: Induction of *Sod1* knockout in mouse embryonic fibroblasts leads to cell death. 78
Figure 19: Viability of *Sod1*$^{loxP/loxP}$ knockout mouse embryonic fibroblasts. 79
Figure 20: *Sod1*$^{-/-}$ mouse embryonic fibroblasts (MEFs) and *Sod1*$^{loxP/loxP}$ knockout MEFs both undergo apoptotic cell death. 80
Figure 21: Unsuccessful rescue attempts for *Sod1*$^{loxP/loxP}$ KO MEFs. 81
Figure 22: Downregulation of *Sod1* in rat adrenal medulla cells leads to cell death that can be rescued by a nitric oxide synthase inhibitor. 82
Figure 23: Nitric oxide synthase (NOS) inhibitors fully rescue viability of *Sod1*$^{loxP/loxP}$ knockout mouse embryonic fibroblasts. 83
Figure 24: Peroxynitrite decomposition catalyst, FeTPPS, rescues *Sod1*$^{loxP/loxP}$ knockout MEFs. 84
Figure 25: Resazurin cell viability assay on *Sod1*$^{loxP/loxP}$ cells. 85
Figure 26: SOD levels in control cells and *Sod1*$^{loxP/loxP}$ knockout cells (before and after rescue). 87
Figure 27: SOD activity in *Sod1* knockout MEFs. 87
Figure 28: Dose-dependent effects of L-NAME on the survival of *Sod1*$^{loxP/loxP}$ knockout MEFs and SOD2 expression. 88

Figure 29: The effect of L-NAME treatment on *Sod1* mRNA expression. 90
Figure 30: Relative *Sod2* mRNA expression level in L-NAME treated *Sod1* KO cells by qRT-PCR. 90
Figure 31: Paraquat (PQ) treatment on *Sod1*$^{loxP/loxP}$ mouse embryonic fibroblasts. 92
Figure 32: N-acetyl cysteine treatment on *Sod1*$^{loxP/loxP}$ mouse embryonic fibroblasts. 94
Figure 33: Sensitivity of *KRas*$^{lsl/+}$ cells to nitric oxide donors. 96

Chapter 3:
Figure 34: The dioxygenation reaction of hemoglobin and nitric oxide. 106
Figure 35: Schematic describing the steps involved in the generation of adult-onset *Sod1* global knockout mice. 114
..... 116
Figure 36: Tamoxifen successfully knockouts SOD1 in *Sod1*$^{loxP/loxP}$ mice. 116
Figure 37: Adult onset *Sod1* knockout mice degenerate and die quickly. 117
Figure 38: Adult onset *Sod1* knockout mice are rescued by L-NAME treatment. 118
..... 120
Figure 39: Loss of Sod1 in young adults leads to acute skeletal muscle degeneration. 120
..... 121
Figure 40: Further examples of muscle degeneration in adult onset *Sod1* knockout mice.... 121
..... 122
Figure 41: SOD1 is lost in degenerating skeletal muscle. 122
..... 123
Figure 42: L-NAME rescued adult onset *Sod1* knockout mice have healthy skeletal muscles. 123
Figure 43: Adult onset *Sod1* knockout mice have elevated lactate levels. 124
Figure 44: Body weight of adult onset *Sod1* knockout mice. 125
Figure 45: Peroxynitrite in skeletal muscles of adult onset Sod1 knockout mice. 127
Figure 46: Loss of *Sod1* does not alter the morphology of cardiac muscles. 129
Figure 47: Loss of *Sod1* causes no morphological changes in the brain. 130
Figure 48: Morphological changes in liver of mice lacking *Sod1* are a result of continuous intraperitoneal injections. 131
Figure 49: Changes in kidney morphology in inducible *Sod1* knockout mice result from continuous intraperitoneal injections. 132
Figure 50: NOS expression in *Sod1* germline knockout mice 134
..... 135
Figure 51: Red blood cells (RBC) of *Sod1* germline knockout mice 135
Figure 52: Hematocrit of *Sod1* germline knockout mice 136
..... 136
Figure 53: Hemoglobin of *Sod1* germline knockout mice 137
Figure 54: Mean corpuscular volume (MCV) of *Sod1* germline knockout mice 137
Figure 55: Mean corpuscular hemoglobin (MCH) of *Sod1* germline knockout mice 138

Appendix:
Figure A1: SOD expression in adult-onset Sod1 knockout mice 155

Figure A2: Replicates of L-NAME rescued adult-onset *Sod1* knockout skeletal muscles 156
Figure A3: Replicates of reduction in nNOS expression in *Sod1* germline knockout mice 157

List of abbreviations

Abbreviation	Full Name
3-NT	3-nitrotyrosine
5hmC	5-Hydroxymethylcytosine
8-oxo-dG	8-hydroxy-2’-deoxyguanosine
AA	arachidonic acid
ACE	angiotensin-converting enzyme
ACh	acetylcholine
AD	Alzheimer’s disease
ALS	amyotrophic lateral sclerosis
APOE4	apolipoprotein E4
ARB	angiotensin receptor blockers
Arg	arginine
Asp	aspartate
ATII	angiotensin II
ATP	adenosine triphosphate
A*β*	amyloid beta peptides
BER	base excision repair
bp	base pair
CaM	calmodulin
CAT	catalase
CBC	complete blood count
CCS	copper chaperone for superoxide dismutase
cGMP	cyclic guanosine monophosphate
CoQ	coenzyme Q/ubiquinone
COX	cyclooxygenases
Cu	copper
Cys	cysteine
DEAE	diethylaminoethyl
DETA-NO	diethylenetriamine-nitric oxide
DISC	death-inducing signaling complex
DMEM	Dulbecco’s Modified Eagle Medium
DNA	Deoxyribonucleic acid
DNPH	2,4-dinitrophenylhydrazine
dNTP	deoxyribonucleotide triphosphate
E	embryonic day
EDRF	endothelium-derived relaxing factor
EPO	erythropoietin
EPR	electron paramagnetic resonance
ER	endoplasmic reticulum
ERS	endoplasmic reticulum stress

ETC	electron transport chain
FBS	fetal bovine serum
Fe	iron
FeTPPS	Fe(III)5,10,15,20-tetrakis(4-sulfonatophenyl)porphyrinato chloride
FMN	flavin mononucleotide
FRTA	free radical theory of aging
GH	growth hormone
GRX	glutaredoxin
GSH	glutathione
GTP	guanosine triphosphate
H_2O_2	hydrogen peroxide
His	histidine
$HO^{\bullet}$	hydroxyl radical
H&E	hematoxylin and eosin
IL-8	interleukin-8
IP	intraperitoneal
JAK/STAT	Janus Kinase/Signal Transducer and Activator of Transcription
KO	knockout
L-NAME	Nω-Nitro-L-arginine methyl ester
LOOH	lipid hydroperoxide
LOX	lipoxygenases
MAO	monoamine oxidase
MAPK	mitogen-activated protein kinase
MCH	mean corpuscular hemoglobin
MCV	mean corpuscular volume
MEFs	mouse embryonic fibroblasts
MeSOX	methionine sulfoxide
MLEC	murine lung endothelial cell
MMO	membrane-bound microsomal monooxygenase system
MMP	matrix metalloproteinases
Mn	manganese
NAC	N-acetylcysteine
NADH	nicotinamide adenine dinucleotide
NADPH	nicotinamide adenine dinucleotide phosphate
NF-κB	nuclear factor κB
NI	nickel
NMJ	neuromuscular junction
$NO^{\bullet}$	nitric oxide

$-NO_2$	nitro group
NOS	nitric oxide synthase (e = endothelial, i = inducible, n= neuronal)
NOX	NADPH oxidase
O_2	molecular oxygen
$O_2^{\bullet-}$	superoxide
OGG1	8-oxoguanine DNA glycosylase
-OH	hydroxyl group
$ONOO^-$/PN	peroxynitrite
PARP	poly (ADP-ribose) polymerase
PBS	phosphate buffered saline
PCR	polymerase chain reaction
PDGF	platelet-derived growth factor
PDI	protein disulfide isomerase
PQ	paraquat
PRDX	peroxiredoxin
PTP	protein tyrosine phosphatases
PUFA	polyunsaturated fatty acids
RBC	red blood cell
RNA	ribonucleic acid
RNS	reactive nitrogen species
ROS	reactive oxygen species
$RS^{\bullet}$	thiyl radical
-RSSR	disulfide
-RSOH	sulfenic acid
RT-PCR	reverse transcription polymerase chain reaction
sGC	soluble guanylate cyclase
-SH	thiol
SMC	smooth muscle cell
SOD	superoxide dismutase
TdT	terminal transferase
TNF-α	tumour necrosis factor-α
TRX	thioredoxin
Tyr	tyrosine
UPR	unfolded protein response
VSMCs	vascular smooth muscle cells
WB	Western blot
Zn	zinc
Z-VAD-FMK	N-Benzyloxycarbonyl-Val-Ala-Asp(O-Me) fluoromethyl ketone

CHAPTER 1: GENERAL INTRODUCTION

1. Reactive Oxygen Species (ROS)

a. What is a free radical?

A free radical is any atom or molecule that has at least one unpaired electron in its outer electron shell, referred to as an unpaired valence electron[7]. Free radicals must also be stable enough to exist independently, meaning they are not simply reaction intermediates[8]. Many reactive oxygen and nitrogen species are radicals, but not all molecules that are considered as ROS are free radicals (e.g. H_2O_2).

Reactive species were first shown to be present in biological materials, ranging from plants to invertebrate and vertebrates in 1954 by Barry Commoner and colleagues[9]. They used electron paramagnetic resonance (EPR) to examine biological samples. The idea behind EPR is quite simple: unpaired electrons have a different response to the application of a magnetic field than paired electrons. When a magnetic field is applied, a paramagnetic electron (unpaired electron) orients itself in the magnetic field, either in a parallel or antiparallel way. Paramagnetic electrons can switch between these two orientations, allowing them to be detected as they switch between orientations[10].

b. Free Radical Theory of Aging

The free radical theory of aging (FRTA) was proposed by Denham Harman in 1956[11]. This theory asserts that organisms age due to accumulated damaged from reactive species[12]. According to a review by Denham Harman in 2003, his theory of FRTA suggests that antioxidants (e.g. vitamin E, ascorbic acid, N-acetylcysteine) can decrease the rate of aging and delay the onset of disease development[12]. Interestingly, many of the papers cited to support this idea are written by Harman himself[13, 14]. While it is not up for debate that oxidative damage resulting from the presence of reactive oxygen species (ROS) increases with aging, it is not clear if this oxidative stress is causal to aging[15]. Increasingly, there are studies of long-lived model organisms that challenge the idea that reactive species are solely toxic. For example, our lab showed that superoxide dismutases (SODs), the only enzymatic defense against superoxide, are dispensable

for normal lifespan in *C. elegans* (Figure 1)[16]. Furthermore, mice lacking the main, cytoplasmic, superoxide dismutase (SOD1) are alive, albeit with a reduced mean lifespan of 20.8 months, compared to 29.8 months in *Sod1*$^{+/+}$ mice (Figure 2)[17]. More on this later.

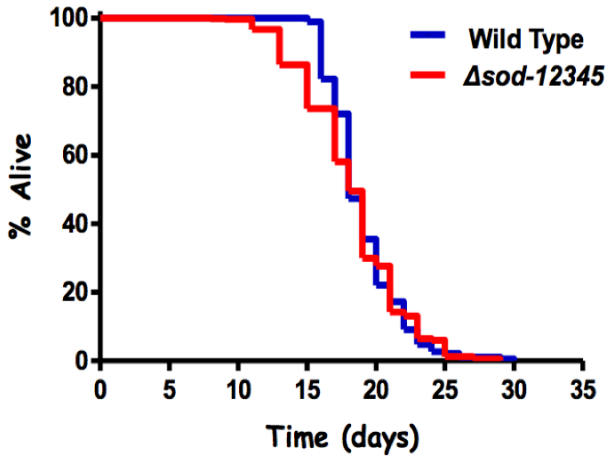

Figure 1: Superoxide dismutases are dispensable for normal lifespan in C. elegans.
C. elegans has five *sod* genes. *SOD-1*, *SOD-2*, and *SOD-4* are primarily cytoplasmic, mitochondrial, and extracellular, respectively. *SOD-3* and *SOD-5* are encoded by inducible *sod* genes, and are located in the mitochondria and cytoplasm, respectively. *sod* quintuple mutant worms lack all five *sod* genes (*sod-12345*), and thus all SOD activity. Examination of the lifespan of sod-12345 mutants revealed that there is no difference in overall survival between them and wild-type worms. The survival curve is an average of 17 independent trials with a total of 1,571 recorded deaths (Van Raamsdonk & Hekimi, 2012).

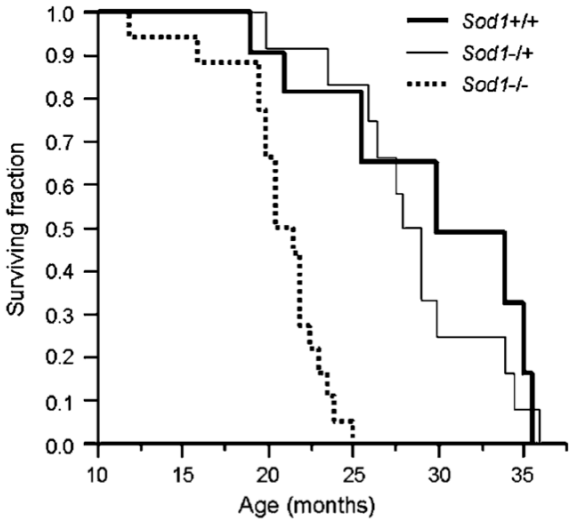

Figure 2: Mice lacking *Sod1* expression are alive.
Lifespan analysis comparing *Sod1*$^{+/+}$ to *Sod1*$^{+/-}$ to *Sod1*$^{-/-}$ mice shows that *Sod1*$^{-/-}$ mice have a reduced lifespan compared to mice with *Sod1* expression. The mean lifespan of *Sod1*$^{-/-}$ mice is 20.8 months, compared to the mean lifespan of *Sod1*$^{+/+}$ mice and *Sod1*$^{+/-}$ mice, 29.8 and 28.7 months, respectively (Elchuri et al., 2005). It is surprising that mice lacking *Sod1* expression live for as long as they do, since SOD1 is the 34th most abundant protein in mice, out of 17,698 identified proteins (Wang et al., 2015).

c. Sources of ROS

ROS generation in the mitochondria

Within mammalian cells, ROS are generated at numerous locations, by a variety of enzymatic systems. Notable sources of ROS are the mitochondria, NADPH oxidases (NOXs), often found in the plasma membrane, peroxisomes, cytochrome P450, and cytosolic enzymes like cyclooxygenases[18]. Although there are countless sources of ROS, an estimated 90% of ROS can be traced to the mitochondria[19]. An understanding of mitochondrial ROS is important to understand redox signaling, mitochondrial dysfunction, cell death, aging, and disease development[20]. In mitochondria, ROS are produced in the electron transport chain (ETC), mostly at complex I (NADH-ubiquinone oxidoreductase) and complex III (CoQ-cytochrome c reductase)[21]. In physiological conditions, approximately 0.2-2% electrons flowing through the ETC leak out of the transport chain to interact with oxygen and form hydrogen peroxide or superoxide[22]. The first findings of ROS generated by the ETC was in 1966. Later, in 1971, it was shown that mitochondria, isolated from pigeon hearts, produce hydrogen peroxide[23]. Subsequently, it was determined that the presence of this mitochondrial H_2O_2 results from superoxide dismutation in the mitochondria[24]. That same year, it was also uncovered that mitochondria have a superoxide dismutase of their own, SOD2[25]. Since these discoveries in the 1960s and 1970s, the roles mitochondrial ROS play in ROS signaling, disease, and aging have been hotly debated.

Superoxide ($O_2^{\bullet-}$) is produced in the mitochondria by transfer of one electron onto molecular oxygen (O_2). The ground state of O_2 is essential for aerobic life, but it also makes O_2 reactive. Molecular oxygen has two unpaired electrons in its outer shell[26]. This requires that reduction occurs in a univalent fashion, or one electron at a time[27]. In mitochondria, the

generation of superoxide by the one-electron reduction of molecular oxygen is a thermodynamically favoured reaction[20]. This favourability is due to the highly reducing environment of mitochondria, the abundance of many compounds that are capable of one-electron transfers (e.g. flavoproteins, iron-sulfur clusters, ubiquinone, etc.), and for the fact that one-electron transfers are the norm in the mitochondrial electron transport chain[28]. Interestingly, not all mitochondrial electron carriers that have the ability to reduce molecular oxygen to superoxide do. In fact, it is possible that most superoxide generation occurs at proteins and not in relation to small-molecule electron carriers (e.g. NADH, NADPH, $CoQH_2$, glutathione)[20].

Typically, in the mitochondrial electron transport chain, oxygen is the terminal electron acceptor. Oxygen is an ideal candidate to be the terminal electron acceptor in the ETC because when reduced to water a great amount of energy is released. It is the unpaired valence electrons that cause O_2 to have a high affinity for accepting electrons[21]. Aerobic cellular respiration harnesses this property and enables more energy production than with anaerobic respiration. O_2 is essential for energy production in the ETC, but because O_2 is a strong oxidant, electrons can prematurely interact with it leading to superoxide production[29]. Most mitochondrial superoxide formation occurs at complex I and complex III, but these are not the only mitochondrial locations where superoxide can be made. Currently, there are 7 generally-accepted mitochondrial sites where superoxide formation is known to occur – pyruvate dehydrogenase, 2-oxoglutarate dehydrogenase, the FMN-containing NADH binding site in complex I, the ubiquinone binding site in complex I, electron-transferring flavoprotein ubiquinone oxidoreductase, glycerol 3-phosphate dehydrogenase, and the outer-quinone binding site in complex III[30].

Complex I, NADH-ubiquinone oxidoreductase, is a mitochondrial inner membrane protein complex[31]. This means that it is shown to both the intermembrane space and the mitochondrial matrix. In the ETC, complex I oxidizes NADH and reduces coenzyme Q. This reaction is coupled with protons pumping across the mitochondrial membrane to generate a transmembrane potential[32]. This gradient of protons is later used in ATP generation[33]. In 1977, Cadenas et al. demonstrated for the first time that both complex I and complex III, isolated from beef heart mitochondria, have the capability to produce superoxide when NADH is present[34]. This very intriguing paper also showed that these mitochondria, that typically produce superoxide from

NADH, appear to produce hydrogen peroxide when SODs are present and little to no superoxide. Superoxide production was determined using an adrenochrome assay and hydrogen peroxide production was determined using a cytochrome c peroxidase assay. The adrenochrome assay can measure how much epinephrine A is oxidized by superoxide because this reaction leads to the generation of adrenochrome, a coloured product[35]. The cytochrome c peroxidase is another spectrophotometric assay, first proposed in 1972 by Boverise et al., that exploits the high specificity of yeast cytochrome c peroxidase for hydrogen peroxide[36]. This NADH-dependent superoxide production at complex I also appeared to require ubiquinone because rotenone inhibited superoxide formation[34]. Rotenone is a known inhibitor of electron transfer from the Fe-S centers of complex I to ubiquinone[37]. Studies delving deeper into the complex I ROS production have yet to conclude on a definitive mechanism of how superoxide is produced[38, 39]. The major debates include, but are not limited to, what site(s) are ROS produced at within complex I and what does ROS production require (e.g. NAD, FMN, ubiquinone, iron-sulfur centers, etc.)[38, 40, 41].

Another site of ROS production in mitochondria is complex III, CoQ-cytochrome c reductase. Unlike ROS originating from complex I, the mechanism leading to ROS at complex III is much better understood. In general terms, complex III is responsible for the transfer of electrons from ubiquinol/coenzyme Q to cytochrome c. This process is referred to as the Q-cycle[42]. Superoxide is thought to form as a result of semiquinone ($Q^{\bullet -}$) formation at the Q_0 site of complex III[43]. This was first demonstrated in experiments using mitochondria isolated from mung bean plants and confirmed to be the case in mammals with the use of inhibitors known to affect rates of superoxide production at complex III[44]. Complex III is generally capable of a large amount of superoxide formation and antimycin A, an inhibitor of Complex III, further stimulates this superoxide formation[24]. Antimycin A causes semiquinone build-up because it prevents transfer of a second electron onto Q[45]. Interestingly, two other complex III inhibitors, myxothiazol and stigmatellin, both inhibit superoxide formation at complex III. This is because these inhibitors inhibit the Q0 site. Myxothiazol displaces ubiquinol and stigmatellin block electron transfer from the quinol[46].

ROS production in the cytosol

In addition to mitochondrial sources of ROS, ROS can also be produced outside of the electron transport chain. There are many enzymes located in the cytosol whose enzymatic reactions produce ROS as a by-product. Xanthine oxidase (XOR), a highly conserved metalloflavoprotein, is one such enzyme. XOR catalyzes the oxidation of hypoxanthine to xanthine and the oxidation of xanthine to uric acid[47]. These reactions are key for purine catabolism in mammals[48]. XOR can transport electrons to molecular oxygen, providing the perfect opportunity to produce ROS, both superoxide, via one-electron reduction, and hydrogen peroxide, via two-electron production[49]. For this reason, XOR is tightly regulated at transcriptional and post-translational levels[50]. Curiously, in hypoxic-acidic conditions, XOR has a reduced affinity for xanthine and an increased affinity for nitrites. This leads to XOR reactions with nitric oxide that can produce reactive nitrogen species (RNS), most notably peroxynitrite ($ONOO^-$)[51, 52].

Similar to XOR, cytochrome P450 oxidases, a family of heme-thiolate enzymes that are part of the membrane-bound microsomal monooxygenase system (MMO), can also generate superoxide. The MMO is a collection of enzymes localized to the endoplasmic reticulum (ER) where they oxidize many compounds, such as drugs, carcinogens, and xenobiotics[53]. In the catalytic cycle of cytochrome P450, electrons are moved to activate oxygen and to attach oxygen to the substrate in question. Mediocre coupling of this catalytic cycle results in the production of ROS. Just like XOR, cytochrome P450 is also transcriptionally regulated to reduce the potential amounts of ROS produced[54, 55].

Monoamine oxidases (MAOs) are enzymes responsible for the catabolism of a variety of neurotransmitters, such as dopamine, epinephrine, and serotonin[56]. MAOs are often found bound to the outer membrane of mitochondria[57]. In order to breakdown these neurotransmitters, MAOs oxidatively deaminate amines and a possible by-product of these reactions, as they involve oxygen, are ROS (superoxide, hydrogen peroxide, and hydroxyl radicals)[58, 59].

Yet another source of ROS in the cytosol are NADPH oxidases (NOXs). These enzymes transfer electrons from NADPH to molecular oxygen to produce superoxide[60]. NOXs are found in phagocytes involved in innate immune responses, such as neutrophils, monocytes, macrophages,

and eosinophils[61]. Cells involved in innate immune responses circulate in blood and "eat" foreign bacteria, fungi, and debris from other apoptotic or necrotic cells[62]. It was first noted back in 1933 by Baldridge and Gerrard that neutrophils showed "extra respiration" or a large increase in oxygen consumption associated with their phagocytotic roles[63]. This respiratory burst was later shown to be due to NOX consumption of oxygen, not due to mitochondria as originally thought[64].

ROS from NOXs can go on to serve signaling functions. It is specifically the superoxide from NOX2 that is key for the respiratory burst seen in phagocytes during immune response[65]. But another role for the NOX-produced superoxide and hydrogen peroxide is the reversible modifications of proteins to regulate their activity, localization, and stability[66, 67]. These reversible modifications as a result of NOX activity allows NOX to modulate physiological processes such as cellular growth and differentiation, apoptosis, cytoskeletal remodeling, host defense, inner ear formation, iodination of thyroid hormone, and vascular tone control[68-70].

NOXs are a well-recognized source of cytoplasmic ROS, but another important source of ROS generation is the metabolism of arachidonic acid (AA) by lipoxygenases (LOX) and cyclooxygenases (COX)[71]. AA is produced due to the activity of cytosolic phospholipase A_2 in the nuclear envelope and plasma membrane. This AA is then oxidized by LOX and COX into various bioactive compounds (e.g. prostaglandins and leukotrienes)[72]. During this process of breaking down AA, ROS are produced as a by-product[73].

Additionally, hydrogen peroxide can also be produced by peroxisomal β-oxidation of fatty acids. Peroxisomes, named and identified in 1965 by Christian de Duve, are defined as a membrane-bound organelle with at least one method of H_2O_2 production and one catalase, an enzyme that degrades H_2O_2[74]. This idea was highlighted when it was shown that, in rat liver, peroxisomes are responsible for 20% of the oxygen consumed and up to 35% of the hydrogen peroxide produced[75]. Fatty acid oxidation that occurs in peroxisomes is the breakdown of fatty acids to acyl-CoA units via a multi-step process[76]. The enzymes that participate in this process of fatty acid oxidation produce ROS and RNS as by-products of their activities[77]. Some of these enzymes that produce hydrogen peroxide in peroxisomes include, but are not limited to, acyl-CoA oxidases, D-amino acid oxidase, and polyamine oxidase[78]. When considering the countless

sources of ROS, it is quite remarkable that organisms can live with lower, or completely lacking, superoxide dismutase (SOD) expression despite the fact that only SOD directly act on superoxide.

d. Superoxide

Historical perspective

Superoxide is an interesting molecule let alone because Linus Pauling, arguably one of the greatest scientists of the twentieth century, conceived that it might exist three years before others did the experiment to prove that it does[79, 80]. In 1979, Pauling glowingly reflected: "It is a source of satisfaction to me that the superoxide radical, whose existence was predicted through arguments based upon the theory of quantum mechanics, should have turned out to be important in biology and medicine"[81]. Superoxide was formally discovered in 1934, when Edward W. Neuman isolated potassium superoxide. These experiments were guided by Pauling, who suggested Neuman prepare a potassium oxide sample and measure its magnetic susceptibility. When this was done, the measurement supported the conclusion that this prepared oxide sample had an odd number of electrons per unit of molecular oxygen[82]. Although the Free Radical Theory of Aging was proposed in 1956, Fridovich was the first to directly outline a role for superoxide in "oxygen toxicity" in 1978[83]. Many publications in the years that followed supported this idea of superoxide being toxic to cells, organs, and animals. In 1986, it was even stated that "aerobic life forms are possible despite and not thanks to the presence of oxygen!"[84]. More recently, the perspective on the toxicity of superoxide has shifted and become much more nuanced and this thesis will contribute to this shift. For example, the Hekimi lab showed that *C. elegans* that lack all 5 isoforms of superoxide dismutase (SOD) live just as long as wild-type worms. This would not be possible if physiological levels of superoxide production were the cause of aging or acutely toxic[16].

Structure

Molecular oxygen (O_2) is known to exist in four oxidation states. These oxidation states are described by the notation $(O_2)^n$, where n changes based on the charge of the compound. When n is 0, this is molecular oxygen (O_2). When n is +1, this is the dioxygen cation (O_2^+). When n is -1,

this is superoxide ($O_2^{\bullet-}$). And finally, when n is -2, this is the peroxide dianion ($O_2^{\bullet 2-}$)[85]. Superoxide is both a radical and an anion that is formed as a result of the monovalent reduction (involves one electron) of O_2[3]. There is disagreement in the literature as to how reactive superoxide is. Many studies have stated that superoxide is highly reactive, but some have also proposed that it is not very reactive despite its free radical nature[86].

Where is it formed and how does it move?

As previously discussed, the major source of reactive oxygen species, and therefore superoxide, is believed by many to be the mitochondria, specifically complex I in the electron transport chain (NADH:ubiquinone oxidoreductase). The most likely course of events leading to superoxide formation at complex I is that one electron is transferred from a fully reduced flavin to molecular oxygen[87]. Mitochondrial superoxide was traditionally thought to be only relevant in the mitochondria, because superoxide, unlike hydrogen peroxide, cannot freely cross the mitochondrial membrane. However, it was shown recently that there are voltage-gated channels that allow superoxide to be released from the mitochondria into the cytosol[88, 89]. Note, paraquat (1,1'-dimethyl-4,4'-bipyridinium dichloride) is an exogenous "source" of superoxide[90]. Paraquat (PQ) has been shown to stimulate superoxide production, specifically at complex I in the mitochondrial ETC, leading to extensive oxidative damage[91]. PQ is a redox cycler. PQ^{2+} (the paraquat di-cation) can accept an electron, leading to formation of PQ^{+} (the paraquat mono-cation), which can then go to react with O_2 at a rate of $k \sim 7.7 \times 10^8\ M^{-1}\ s^{-1}$ to produce superoxide. Superoxide production also regenerates PQ^{2+} and the cycle begins again[92]. Superoxide formation at complex I is favoured because there is a greater proton-motive force and pool of reduced coenzyme Q (Q) than at other complexes in the ETC[93]. Superoxide is also produced at complex III in the ETC. Complex III superoxide is released into both the matrix and intermembrane space, unlike complex I superoxide which is released exclusively into the mitochondrial matrix. This is an important note given the likely presence of SOD in the mitochondrial intermembrane space[42].

e. Damage from ROS

For years, it has been shown that loss of SOD activity in organisms ranging from bacteria to mice is associated with increased oxidative damage. Oxidative damage can be measured by membrane

lipid peroxidation, protein carbonylation, and DNA breakage and base modification[17, 94-96]. The traditional interpretation of these results is that insufficient removal of superoxide is deleterious; however, in this thesis, it is shown that the majority of the toxicity of superoxide is due to the generation of peroxynitrite ($ONOO^-$)[4]. Peroxynitrite is itself a much stronger oxidant than superoxide and its decomposition also leads to the formation of reactive species such as $HO^\bullet$, $NO_2^\bullet$, and $CO3^{\bullet-}$[97]. More on peroxynitrite will be discussed later.

Even if the responsible species of ROS is not always agreed upon, it is accepted that oxidative damage can result when ROS levels reach a high concentration. Damage from ROS can occur to various types of macromolecules, ranging from DNA to proteins to lipids.

DNA modifications

The DNA sugar-phosphate backbone and bases alike can be oxidized by ROS[98]. ROS-mediated modifications of DNA can lead to strand breakage, deoxyribose oxidation, DNA-protein crosslinking, and mutations from modification of DNA bases. Deoxyribose oxidative damage is primarily a result of hydrogen abstraction from this sugar and oxidative modifications of DNA bases usually involve the addition of $OH^\bullet$. ROS have been shown to attack both nuclear and mitochondrial DNA. Nuclear DNA extracted from rat livers showed that every 1 in 130,000 nucleotides had evidence of ROS damage, whereas mitochondrial DNA from those same livers showed ROS damage every 1 in 8,000 nucleotides. The presence of damage was assessed by 8-hydroxy-2'-deoxyguanosine (8-oxo-dG)[99]. Base excision repair (BER) is the major approach for ROS-damaged DNA bases. There is evidence that this nucleotide excision repair can be defective through mutations in human pathologies, so the effects of ROS DNA damage are compounded by the effects of ineffective DNA repair. Accumulation of DNA damage and mutations has been associated with human disease and cancer development[100].

Let us explore some typical ROS-modifications of DNA. First, the presence of hydroxyl radicals can result in the formation of 5hmC, or the removal of a hydrogen atom from the methyl group of cytosine[101]. 5hmC has been shown to result in improper methylation patterning and demethylation of CpG sites[102]. ROS can also affect DNA via the formation of 8-hydroxy-2'-deoxyguanosine (8-oxo-dG), as briefly discussed above. Most of these residues can be removed

by 8-oxoguanine DNA glycosylase (OGG1) and then the resulting gap filled by BER[103]. 8-oxodG can lead to DNA mutations, mainly G to T transversions, and, on an epigenetic level, changes in methylation patterns that can affect transcription regulation[104]. High 8-oxodG have been associated with many diseases, for example, elevated levels have been found in atherosclerotic blood vessels[105].

Protein oxidation

High levels of ROS can impact a protein's ability to carry out its functions. Oxidative modifications can lead to altered protein conformations (e.g. active site), protein fragmentation, protein-protein crosslinking, changes in protein-partner interactions, and increased or decreased protein turnover[106, 107]. ROS/RNS can cause nitrosylation, carbonylation, disulfide bond formation, and glutathionylation[98]. Protein carbonylation is oxidation that forms ketones or aldehydes on amino acid side chains. These ketones and aldehydes can be measured because they readily react with 2,4-dinitrophenylhydrazine (DNPH) to form hydrazones. These carbonyl forming oxidations often occur on side chains of lysine, arginine, proline, and threonine amino acid residues[108]. High protein carbonyl levels have been correlated with many diseases ranging from Alzheimer's to diabetes to renal failure[109].

Cysteine and methionine residues are particularly susceptible to oxidations by ROS. Cysteine residues have a thiol group that can readily be converted to disulfides and methionine residues can easily be converted to methionine sulfoxide (MeSOX) residues. Oxidations of both cysteine and methionine residues, unlike other protein oxidations, can be repaired. It has been hypothesized that methionine residues, in particular, serve as a sort of ROS scavenger system to protect against other amino acid residues from being oxidatively modified[110]. Another possible oxidative modification to proteins is metal catalyzed oxidization, as seen in proteins with active site metal, and often leads to enzymatic inactivation[111].

Lipid oxidation

Lipid peroxidation, once induced by ROS damage, can be propagated to adjacent lipids. These alterations to lipids can inactivate membrane-bound receptors and enzymes and can change

membrane permeability, thus affecting cellular functions[112]. ROS-mediated oxidation of lipids, typically polyunsaturated fatty acids (PUFA), occurs with a primary initiation step where an oxidant abstracts a hydrogen atom from a PUFA, resulting in the formation of a lipid peroxyl radical ($LOO^{\bullet}$). This lipid peroxyl radical can then remove another hydrogen atom from a neighbouring lipid, leading to the formation of a lipid hydroperoxide (LOOH). This neighbouring lipid is then available to react with another oxidant, continuing the cycle[113].

f. ROS signaling

Although initially thought to be toxic, ROS have now been established as key players in cellular signalling. Even though ROS involvement in signalling has been well-documented in the literature, there still is skepticism in the field. This skepticism stems from the idea that to be an effective signaller, a high level of specificity is required and ROS are reactive by nature, which makes it difficult to imagine how ROS can discriminate between targets[114]. In stereotypical signalling, specificity is obtained by what could be compared to a lock and key model, where the ligand can only bind to its receptor due to complementary shapes. However, ROS signal by covalent protein modifications[115].

ROS vary in their signalling based on their chemical reactivity, lipid solubility, and half-life[116]. The hydroxyl radical ($HO^{\bullet}$) reacts with most biological material it comes in contact with, however, superoxide and hydrogen peroxide both seem to prefer certain targets over others. Superoxide is drawn to iron-sulfur (FeS) clusters as a result of electrostatic attraction[117]. Fe-S centers are commonly used in enzymes that are responsible for oxidation-reduction transformations of many small molecules. The simplest Fe-S center is a Fe atom surrounded by 4 cysteine residues, where the iron is bound to the sulfur in cysteine residues[118]. Cysteine is the most common protein residue found in these Fe-S centers as it has a high affinity for iron, however, other residues have been found in clusters such as histidine, aspartate, and arginine[119]. Cysteine act as redox switches in enzymes regulated by ROS (Figure 3)[120]. The thiol of cysteines can be converted between reduced, oxidized, and alkylated forms post-translationally, thereby changing catalytic properties of enzymes[121]. At physiological pH, the thiol of cysteine exists as a thiolate anion ($Cys\text{-}S^{-}$)[122]. This anionic form of sulfur is particularly vulnerable to oxidations[123]. Hydrogen peroxide specifically can oxidize this thiolate anion to a sulfenic form (Cys-SOH). This

can lead to both allosteric changes and changes in protein function. This sulfenic cysteine can then be reduced back to a thiolate anion cysteine by thioredoxin (Trx) and glutaredoxin (Grx)[120]. Hydrogen peroxide can, in some cases, further oxidize the thiol group to sulfinic (SO_2H) and sulfonic (SO_3H) forms. These oxidized forms are not reversible modifications to a protein, unlike the sulfenic form[124]. Interestingly, during oxidation of Fe-S clusters by superoxide, an iron atom is released which can reduce hydrogen peroxide and lead to further generation of $HO^{\bullet}$ radicals[125].

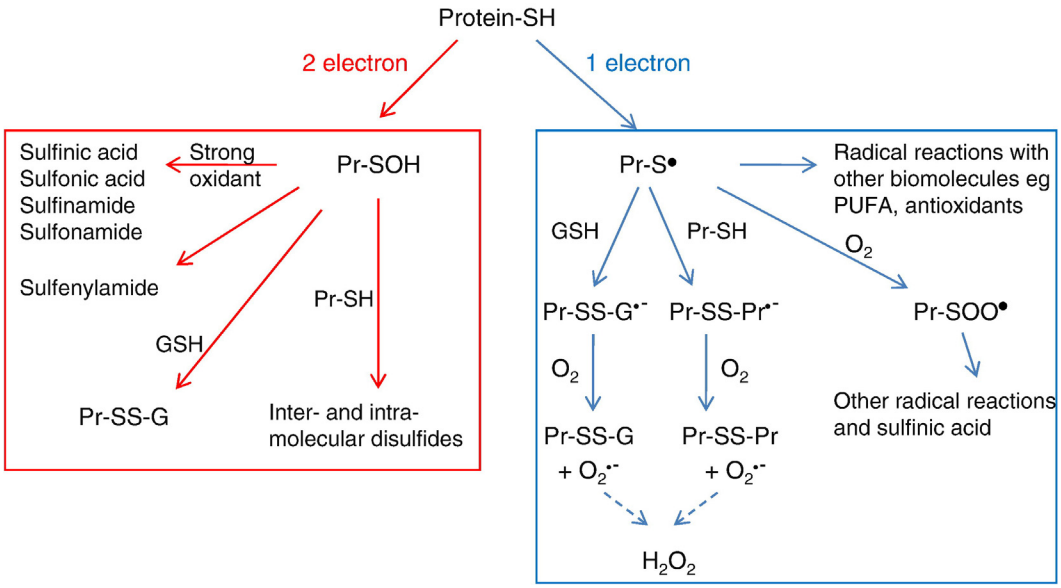

Figure 3: Cysteines as redox switches.
Post-translational modification of cysteine (Cys) residues is one of the most common mechanisms of redox signaling. Cysteine is well-equipped for signaling due to its thiol (-SH) side chain. This thiol can easily switch between reduced and oxidized states in response to various reactive oxygen and reactive nitrogen species. Therefore, cysteine thiols have been referred to as redox switches. Protein thiol can undergo both one-electron and two-electron oxidation. One-electron oxidation, shown on the right-hand side of the figure, initially gives rise the thiyl radical ($-S^{\bullet}$). In aerobic conditions, this radical can easily form disulfide bridges upon reaction with another thiol group. The thiyl radical formed by a one-electron oxidation of a thiol group can also propagate the formation of additional radicals. In the circumstance of a two-electron oxidation of a protein thiol, shown by the left-hand side of the figure, sulfenic acid (-SOH) is initially formed and quickly undergoes a secondary reaction. It can go on to form higher oxidation products (e.g. sulfinic acid, sulfonic acid, etc.), react with an adjacent amide to form sulfenylamide, or react with an addition thiol to form disulfide bonds. The figure illustrates the diversity of the oxidative modifications that a thiol group can undergo and highlights why thiol groups are modulators of signaling (Winterbourn and Hampton, 2008).

g. Detoxification of ROS

As there are several mechanisms of ROS production, there are also numerous mechanisms of ROS detoxification to preserve the integrity of the cell and organism. Remember, protection against ROS formation is essential as the impacts of ROS on organisms can be plotted into an inverted U-shaped curve, where up until a certain threshold ROS are beneficial and maybe even required (i.e. because of their signalling functions) but beyond that threshold ROS become detrimental and deleterious (i.e. their damaging qualities overwhelm) (Figure 4)[126, 127]. There are both endogenous and exogenous mechanisms of ROS detoxification, of which superoxide dismutases (SOD), catalases (CAT), glutathione, N-acetyl cysteine, and vitamin C/ascorbic acid will be reviewed in this section.

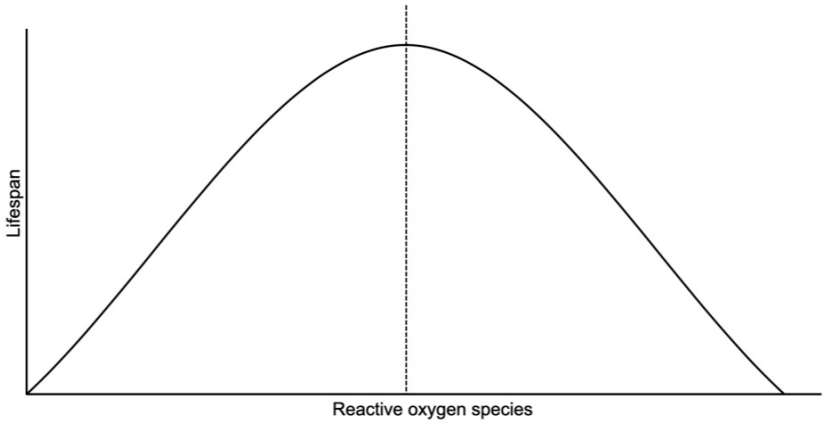

Figure 4: ROS are both beneficial and detrimental.
Traditionally, reactive oxygen species have been considered to be damaging compounds that cells and organisms must properly manage to survive. However, there is mounting evidence that ROS are required for cellular signalling but can produce beneficial effects in terms of aging. This is not to say that ROS cannot be damaging, but instead their effects can be represented by an inverted-U curve, whereby before a certain threshold, ROS are mainly beneficial, can be properly managed by cellular detoxification systems, and fulfill signalling functions. However, after this threshold, indicated by the dotted line in the figure, ROS become deleterious and begin to affect survival negatively. Cellular detoxification systems appear unable to manage the gradual increase in ROS that comes with age and are therefore unable to prevent age-related oxidative damage.

Superoxide dismutase

SOD catalyzes the dismutation of superoxide to hydrogen peroxide. In mammals, there are three SOD isoforms – SOD1 mostly cytoplasmic, SOD2 mitochondrial, and SOD3 extracellular[128].

Surprisingly, even though SODs are the only known endogenous protection against superoxide formation, mice lacking SOD1 and SOD3 remain alive, albeit mice lacking SOD2 die within three weeks of birth[129]. Furthermore, *C. elegans* lacking all 5 isoforms of SOD (in worms, there are 5 isoforms, rather than the 3 isoforms in mammals) live just as long as wild-type worms, albeit are more sensitive to exogenous sources of oxidative stress[16]. Later in this thesis, more about SOD will be discussed as SODs are the focus of much of the work in this thesis.

Catalase

Catalases (CAT) convert hydrogen peroxide (H_2O_2) to water (H_2O) and molecular oxygen (O_2). The reaction that CAT catalyzes is: $2H_2O_2 \rightarrow 2H_2O + O_2$[130]. The term catalase was coined in 1900 by Loew and colleagues when they noted: "there seems to exist no plant and no animal which is without that peculiar enzyme.[131]" Finally, in 1937, the first catalase was isolated from a mammal, specifically bovine liver, by Sumner and Dounce[132]. From there, catalases became one of the most studied family of enzymes[133]. There are three classes of enzymes in this family that are capable of catalyzing the conversion of hydrogen peroxide to water. Two of these classes, typical catalases and catalase-peroxidases, are heme-containing enzymes, whereas the third class, only found in bacteria, are manganese catalases. The heme or manganese is found in the active sites of these catalases and is required for the reaction[134].

The mammalian CAT is a homotetramer with a molecular weight of approximately 60kDa[135]. Each of the 4 subunits contain a heme and these hemes form the active site of the enzyme. The active site of CAT is relatively narrow and allows for selection of only small substrates[136]. Intriguingly, even though CAT have been described for their role in removal of hydrogen peroxide before the molecule can cause harm, catalases found in human and mouse keratinocytes have been shown to also generate ROS upon irradiation[137]. Note, mice lacking catalase do develop normally and only show a slight disparity in their response to oxidative stress[138]. These results and the ubiquitous expression of CAT across all aerobic organisms highlight both how elevated levels of hydrogen peroxide can be tolerated by organisms but also how improved modulation of these levels does seem to contribute an obvious survival advantage under laboratory conditions.

Glutathione

The glutathione system of detoxification is perhaps the most prominent system of ROS detoxification[139]. This system relies on several enzymes to support the unique ROS detoxification qualities of glutathione. In fact, reduced glutathione (GSH) is the most abundant non-protein thiol found in animal cells, reaching millimolar concentration levels in various tissues[140]. GSH is a tripeptide, composed of the amino acids glutamine, cysteine, and glycine that are water-soluble and thereby easily able to move throughout cells[141]. The thiol (-RS) present in GSH makes it an efficient reducing agent. The importance of GSH for life is underlined by its widespread abundance, not only in mammals but in plants, fungi, and prokaryotes alike[140]. Intracellularly, glutathione can exist in an oxidized state (GSSG) or a reduced state (GSH).

GSH is synthesized in the cell by γ-glutamylcysteine and GSH synthases. Cysteine is typically the rate limiting substrate during the synthesis of GSH[142]. Oxidants, such as hydrogen peroxide, have been shown to promote uptake of cysteine into cells and this cysteine uptake is accompanied by an increase in γ-glutamylcysteine expression[143, 144]. After GSH has been produced, in concert with GSH peroxidase (GPx), GSH helps to protect against uncontrolled ROS formation. GPx detoxifies hydrogen peroxide, with the requirement of GSH acting as an electron donor. This results in detoxification of peroxides and formation of GSSG, the oxidized form of glutathione. Conversion of GSSG back to GSH requires glutathione reductase (GR) and NADPH. GR is a flavoprotein disulfide oxidoreductase and is a dimer. Oxidative stress contributes to the transcriptional and posttranslational modification of GR expression[145]. Similarly, GPx expression can be induced by oxidative stress. Aberrant expression of GPx is linked to many diseases and viruses, including cancers, HIV, and hepatitis[146-148].

Also included within the glutathione system are peroxiredoxins (PRDX), thioredoxins (TRX), and glutaredoxins (GLRX). PRDX are a conserved family of peroxidases responsible for the reduction of peroxides and other ROS[149]. PRDX3, found exclusively in the mitochondria, has also been shown, in both human and murine models, to be important for the reduction of peroxynitrite and has interfered with peroxynitrite-mediated neurotoxicity and tyrosine nitration[150]. The catalytic mechanism of PRDXs relies on a conserved cysteine residue, termed

the peroxidatic cysteine[151]. TRX and GLRX are also both found in mammalian cells and are reliant on a thiol group for ROS detoxification. TRX require thioredoxin reductase (TXRX) and NADPH to return to a form that can detoxify and GLRX require only glutathione[152].

N-acetyl cysteine

N-acetylcysteine (NAC) is not an antioxidant, but rather a precursor to the antioxidant glutathione[153]. NAC is a modified version of the amino acid cysteine (acetyl group attached to the nitrogen of cysteine), which as stated earlier is rate-limiting in glutathione synthesis[154]. This modified amino acid was first reported in the early 1960s when it was used as a mucolytic agent in cystic fibrosis patients[155]. Currently, the most common use for NAC in a clinical setting is to treat acetaminophen overdose[156]. The addition of an acetyl group on NAC, when compared to cysteine, allows it to be less susceptible to oxidation and therefore more readily able to cross cellular membranes[157]. De-acetylation of NAC occurs once NAC enters the cell. After the acetyl group is removed, cysteine remains and can contribute to GSH synthesis[158]. Note, although NAC has been reported to have mild antioxidant effects, GSH is approximately 10 times more effective as an antioxidant[159]. In this thesis, NAC is used as to boost antioxidant levels in cell culture.

Vitamin C

Since the discovery of vitamin C in 1933 by Albert Szent-Györgyi, there has been seemingly a never-ending continually expanding list of biological functions attributed to this chemical[160]. Pertaining to the work in this thesis, the most important function is its antioxidant effects. Vitamin C, also known as ascorbic acid or simply ascorbate, can act as an electron donor to free radicals. Donation of one electron results in the formation of the ascorbate radical ($Asc^{\bullet -}$) and donation of the second available electron generates dehydroascorbic acid (DHA)[161]. Ascorbic acid can be regenerated, by both enzymatic and non-enzymatic mechanisms, from both the ascorbate radical and DHA[162]. Ascorbic acid was used in several cell culture experiments in this thesis.

2. Reactive Nitrogen Species (RNS)

a. Nitric oxide (NO•)

Nitric oxide (NO•) was discovered in 1772 when a British minister, Joseph Priestley, exposed iron shavings to common air. He was intensely interested in understanding the chemical makeup of the air[163]. The eighteenth century has rather astutely been referred to as "the century of gases" or "airs," as gases were termed at the time. Joseph Priestley was the first to hypothesize that air, the atmosphere, is not just one substance, but rather a mixture of gases. This revolutionary idea, at the time, led Priestley to discover not only nitric oxide, but also oxygen, ammonia, and carbon monoxide, to name a few[164].

Since its discovery, NO• was considered a key component of the atmosphere, but it took a couple hundred years before the physiological role of NO• was acknowledged. First, in 1979, it was shown that NO• had the ability to relax smooth muscle when Gruetter and colleagues were able to relax isolated strips of pre-contracted bovine artery by adding NO• to the bath that the strips of artery were soaking in[165]. This was the first evidence that NO• could have a physiological role; however, in the late 1970s, the presence of NO• in the mammalian body had yet to be confirmed. A year later (1980), Furchgott demonstrated that acetylcholine (ACh) requires endothelial cells for relaxation of arterial smooth muscle cells, as mechanical removal by rubbing the surface or enzymatic removal with collagenase treatment of the endothelial cells eliminated smooth muscle relaxation[166]. As a reminder, the main cell types composing smooth muscle are endothelial cells and smooth muscle cells. Endothelial cells form a lining between the flowing blood and the smooth muscle tissue[167]. Furchgott and colleagues were then able to go on to show that ACh induces endothelial cells to secrete a factor, unknown at the time, that eventually leads to smooth muscle relaxation. This was demonstrated by sandwiching two strips of aorta together. Sandwiching refers to placing a strip of aorta without endothelial cells directly in contact with another strip of aorta that has intact endothelial cells. When these two strips were placed together, both relaxed[168]. The factor secreted by endothelial cells that is responsible for this smooth muscle relaxation was termed as the endothelium-derived relaxing factor (EDRF)[169].

Only in 1987, EDRF was proven to be NO• and this is where the drama began. Separately, within six months of one another, the Ignarro lab and the Moncada lab showed that nitric oxide accounts for the biological activity of EDRF, meaning nitric oxide is the unknown compound that is responsible for smooth muscle relaxation[170, 171]. To prove that nitric oxide is EDRF, various substances were flowed over arteries or veins stripped on the endothelium. Perfusate from intact arteries, acetylcholine, and nitric oxide all led to relaxation of the artery or vein. Also important, pyrogallol, a substance that generates superoxide from molecular oxygen present in solutions, inhibited this relaxation and superoxide dismutases (SODs) accelerated the relaxation (Figure 5)[171]. This finding that superoxide seems to inhibit the function of NO• is noteworthy because this thesis focuses on demonstrating that peroxynitrite, formed by the reaction of superoxide with nitric oxide, is what is toxic to cells and organisms, rather than superoxide, which has been historically considered to be toxic. Another interesting finding is that hemoglobin has a similar effect of inhibiting relaxation induced by nitric oxide in an endothelium-stripped artery or vein (Figure 6)[172]. Finally, in 1988, Moncada and colleagues went on to show that L-arginine is the precursor to NO•[173].

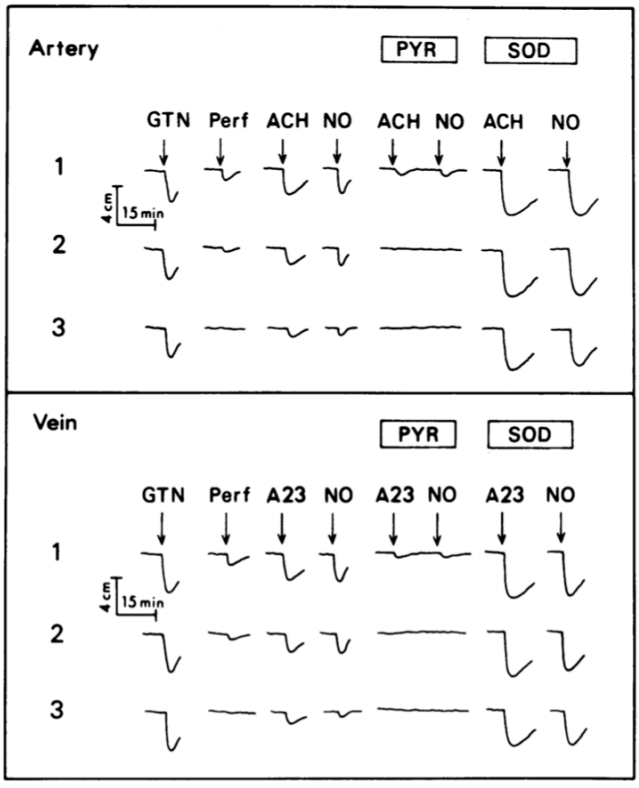

Figure 5: Identification of endothelial derived relaxing factor (EDRF) as nitric oxide ($NO^{\bullet}$).
The similarity between patterns of vasodilation in both arteries and veins by endothelial-derived relaxing factor (EDRF; perfusate in above figure), nitric oxide donors, and nitric oxide ($NO^{\bullet}$) itself led to the identification of EDRF as nitric oxide. Arteries and veins used in these experiments were stripped of their endothelium, the source of EDRF. They were also pre-contracted with 10uM phenylephrine. Before delving into the experiment, the abbreviations are the following – GTN is glyceryl trinitrate (0.1uM for 1 minute), Perf is perfusate from intact arteries or veins that contains the elusive EDRF, ACH and A23 are both acetylcholine (1uM ACH or 0.1uM A23 for 3 minutes), NO is nitric oxide (0.1uM for 3 minutes), PYR is pyrogallol, a substance that generates superoxide (20uM), and SOD is superoxide dismutase (100 units/mL). In arteries and veins alike, GTN, perfusate, ACH (signals via increases in nitric oxide), and NO all induce relaxation. This relaxation is inhibited by PYR, presumably due to increased superoxide reaction with nitric oxide, and is intensified by the addition of SOD, presumably due to decreased superoxide reaction with nitric oxide (Ignarro et al., 1987).

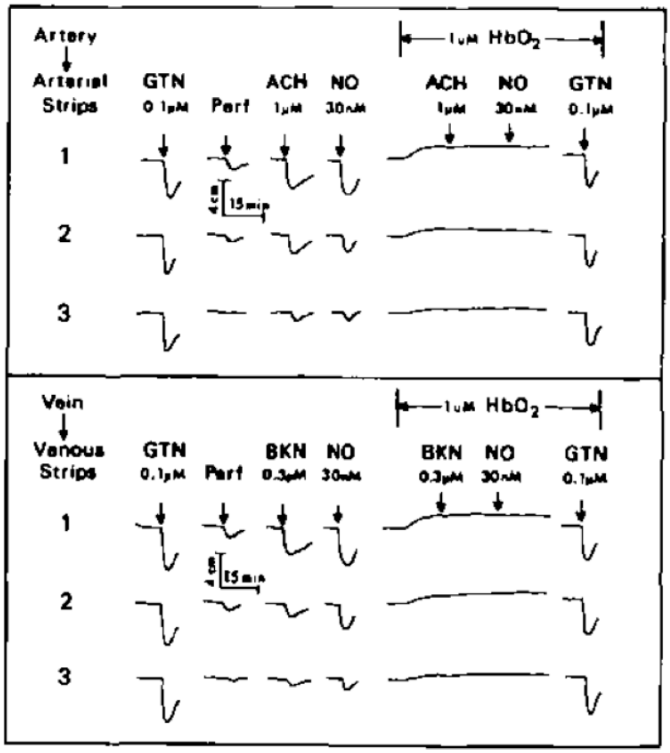

Figure 6: Hemoglobin inhibits downstream effects of nitric oxide ($NO^{\bullet}$).
HbO_2 (hemoglobin) inhibits the relaxation of endothelium-stripped arteries and veins. As in the above figure, these arteries and veins were pre-contracted with phenylephrine. Normally, GTN (glyceryl trinitrate), NO (nitric oxide), acetylcholine (ACH), and bradykinin (BKN) induce relaxation of arteries and veins. However, the presence of hemoglobin alone is sufficient to completely inhibit the relaxation cause by NO and ACH/BKN and the greatly reduce the relaxation caused by

GTN. This was the first evidence that hemoglobin can affect the bioavailability of nitric oxide and thereby affect physiological processes such as vasodilation (Ignarro et al., 1989).

Few discoveries have had such an impact on biological knowledge as the discovery of the physiological relevance of nitric oxide[174]. In the years since its identification in a physiological setting, $NO^{\bullet}$ has been linked to pretty much every disease and implicated in various processes throughout the mammalian body. Nitric oxide garnered so much attention that it was identified as molecule of the year in 1992 and winning the Nobel Prize in 1998[175, 176]. Because two separate labs had simultaneously identified nitric oxide as EDRF, this is where the drama arose. The three American scientists (Robert F. Furchgott, Louis J. Ignarro, and Ferid Murad) involved in the identification of EDRF as nitric oxide were awarded the Nobel Prize, whereas Salvador Moncada, a Honduras native whose research is based out of University College London, was notably left out. This was surprising as the Moncada paper identifying EDRF as nitric oxide was actually published six months prior to the Ignarro paper[177]. Murad was recognized by the Nobel committee for the medical significance of his contributions, showing that vasodilators such as nitroglycerin, and thereby nitric oxide, relaxes smooth muscle by activating soluble guanylate cyclase (sGC) and elevating levels of cyclic guanosine monophosphate (cGMP)[178].

A fun fact, Alfred Nobel, the man who establish the Nobel Prizes and the inventor of dynamite (explosion of nitroglycerine in a controlled manner), was told by doctors to take nitroglycerin to control a heart condition, but he refused[177]. It is now known that nitroglycerin can help a patient suffering from chest pain, or angina, feel significantly better in a matter of minutes because nitroglycerin aids in heart blood vessel dilation[179].

b. RNS sources

All reactive nitrogen species (RNS) formation requires nitric oxide synthases (NOS). NOS are the only endogenous sources of $NO^{\bullet}$ [180]. NOS convert L-arginine to L-citrulline and as a result produce $NO^{\bullet}$[181]. $NO^{\bullet}$ goes to react with oxygen-containing molecules to form further RNS. When $NO^{\bullet}$ is reduced, this gives rise to the nitroxyl (HNO) and its nitroxyl anion (NO^{-})[182]. $NO^{\bullet}$ can also be

modified to higher oxides of nitrogen (e.g. NO_2, N_2O_4, etc.)[183]. Other derivatives of NO• include – S-nitrothiols (RSNO) and dinitrosyl-iron complexes[184].

c. Damage resulting from RNS

NO• has been reported to have many toxic outcomes, but it is more likely that these toxic effects are mediated by oxidation products of NO•, such as peroxynitrite (PN), rather than NO• itself. For example, in 1991, it was shown that NO• is not able to directly attack DNA and that rather this can only be achieved by nitrogen oxides[185]. Furthermore, NO• was thought to inactivate Fe-S centers in mitochondria. However, this effect has now been shown to be mediated by PN[186, 187].

Akin to ROS, RNS can be extremely toxic[188]. Examples of RNS include, but are not limited to, nitric oxide, nitrogen dioxide, peroxynitrite, nitroxyl anion, and nitrosium cation[189]. Damage through RNS often occurs via nitration that can result in protein dysfunction and often, in the brain, neuron loss[190]. Excessive NO• production has been linked to various neurodegenerative diseases. When NO• is produced in high quantities, it acts like a neurotoxin rather than a neurotransmitter[191].

RNS also has an impact on the response to stress in the endoplasmic reticulum. This occurs mostly because NO• can S-nitrosylate endoplasmic reticulum chaperones, as seen with protein disulfide isomerase (PDI), causing their inactivation. This leads to accumulation of polyubiquitinated proteins and the activation of the unfolded protein response (UPR), resulting in endoplasmic reticulum stress (ERS) and corresponding neuronal cell death[192].

NO• and its derivatives are known to have both pro- and anti-apoptotic outcomes. Influences on whether or not RNS promote or prevent apoptosis are – the concentration of RNS, the source of RNS, and the conditions in which RNS are studied (the simplest example being *in vitro* versus *in vivo* studies)[193]. NO•-containing species can regulate apoptosis from many angles as NO• signalling is involved in countless physiological processes. For example, NO• can stimulate the Fas ligand to bind to its receptor (APO-1/CD95) which initiates apoptosis, marked by assembly of the death-inducing signaling complex (DISC) and activation of caspase-8. The binding of the ligand is facilitated by S-nitrosylation, a consequence of NO• production, of cysteine 199 and 304

on the Fas receptor[194]. There is also evidence that suggest that NO• promotes an increase in the Bax/Bcl-2 ratio, which leads to increased mitochondrial permeability and cytochrome c release[195]. Both NO• and peroxynitrite can inhibit the ETC[196, 197]. Furthermore, NO•-mediated caspase activation has been found in various cell types, ranging from smooth muscle cells to retinal ganglion cells[198, 199]. As stated earlier, NO• also has anti-apoptotic roles that have been highlighted. For example, the maintenance of an inactive population of caspase-3 requires NO•-mediated S-nitrosylation. This reversible post-translational modification allows for rapid modulation of apoptosis[200].

d. RNS signaling

NO• is a key modulator of numerous physiological processes ranging from neurotransmission to vasodilation to inflammatory and immune responses[201]. NO• is unique because it is small, has no charge, which obviates the need for a transport system as it is freely diffusible, is relatively unreactive for a free radical, and is oxidized to both NO_2^- and NO_3^-, which are readily destroyed under physiological conditions, meaning that there are no specific mechanisms of NO• removal[202]. The exception to the relative unreactive nature of NO• may be its reaction with superoxide to form peroxynitrite (as discussed below). However, if NO• does not have readily available access to proteins and metals, its removal in a physiological setting is slow[183]. One of the main reasons why NO• makes an excellent, while unorthodox, signaling molecule is because of its ability to bind hemes at low, non-toxic, concentrations, especially that of soluble guanylate cyclase[203]. Nitric oxide has been shown to signal through both cGMP-dependent (involving soluble guanylate cyclase) and cGMP-independent mechanisms[204].

NO•/cGMP signaling pathway

Soluble guanylate cyclase (sGC, also referred to as guanylyl cyclase) is a heterodimeric enzyme that converts guanosine triphosphate (GTP) to cyclic guanosine monophosphate (cGMP)[205]. sGC, much like NOS itself, is a heme-containing protein. It is through NO• interaction with this heme that sGC is activated[206]. sGC is the only proven receptor of NO•. Both sGC and cGMP were uncovered in the 1960s, but the NO•/cGMP signalling pathway only began to be unraveled in the 1990s. After the finding of cAMP in 1958, the search began for other physiological relevant cyclic

nucleotides[207]. From there, cGMP was first identified in rat urine in 1963 and guanylate cyclase was purified and confirmed to be the source of cGMP production in mammalian tissues in 1969[208-210]. In 1977, the link between guanylate cyclase and NO• was made when it was shown that NO• gas and NO• originating from vasodilators (e.g. nitroglycerin) activate guanylate cyclase[178, 211]. However, in 1977, NO• was still not considered significant, as it was not known to be endogenously produced *in vivo*. The only biological application of NO• in 1977 was exogenously-supplied drugs, such as nitroglycerin as a vasodilator[212]. When NO• was shown to be EDRF, all of a sudden, the activation of sGC by NO• became relevant[171]. Since the initial connection by NO• and cGMP was made, this signalling pathway has been shown to be important in smooth muscle relaxation, regulation of blood pressure, blood platelet aggregation, immune responses, and neurotransmission[213-217].

Binding of NO• to sGC heme catalyzes the production of cGMP[218]. In the context of smooth muscle relaxation, cGMP expression leads to a lowering of the concentration of intracellular Ca^{2+} and thereby muscle relaxation[201]. Studies of the structure of sGC show that sGC is an αβ-heterodimer with one heme. Two isoforms - α1β1, α2β1 – have thus far been proven to exist in a physiological context[219]. Most studies of sGC function are carried out using the α1β1 isoform. From these studies, it is known that NO• interacts with the heme moiety of sGC that is attached to histidine 105 (His105) of the β1 subunit. The current model for sGC activation by NO• is a two-step process – 1) NO• binds to the heme forming a six-coordinate complex and 2) the bond attaching the heme moiety to His105 is broken leading to the formation of a five-coordinate complex. This breaking of the bond between His105 and heme leads to a conformational change in sGC and enhances the catalytic abilities of the enzyme[220]. Until recently, this model has been generally well accepted. But in the past few years, several studies have challenged the accuracy of this model of sGC activation by NO•. Zhao et al. used stopped-flow spectroscopy to follow changes in heme absorption during the process of sGC activation. These experiments suggest that the mechanism for sGC activation is a three step process that could include a second NO•-binding step[221]. Fernhoff et al. have also challenged the assumption that only the sGC heme is involved in its activation, as sGC has many readily accessible cysteines that NO• could react with.

From this study, it is shown that sGC can be inhibited by methyl methanethiosulfonate by blocking a non-heme site[222].

cGMP-independent NO• signaling

NO• signalling through the secondary messenger cGMP is the most well-defined but several other cGMP-independent NO• signaling pathways have recently been proposed. For example, NO• is a regulator of mitochondria respiration via its inhibition of mitochondrial cytochrome oxidase at low concentrations[223]. NO• serves as an indicator of oxygen levels. Under hypoxic conditions, NO• is free to act in place of oxygen and will inhibit the mitochondrial electron transport chain by directly binding to cytochrome oxidase, as NO• and O_2 closely resemble one another structurally[224]. If oxygen is present at normal levels, this inhibition occurs to a lesser degree. This inhibition of the mitochondrial electron transport chain would allow for redistribution and increased bioavailability of molecular oxygen to surrounding cell types and/or tissues[225]. NO• has also been reported to activate calcium-sensitive potassium channels found in vascular smooth muscle, even in conditions where guanylate cyclase was inhibited by treatment with methylene blue[226]. Furthermore, NO• is known to inhibit NF-κB (nuclear factor κB) activation, a transcription factor key in both the innate and adaptative immune responses[227]. Activation of G-proteins, including the protooncogene p21ras, by NO• occurs by enhancement of nucleotide exchange, thereby increasing the ratio of GTP-bound forms to GDP-bound forms[228, 229]. It has been shown that cysteine 118 of p21ras is S-nitrosylated when NO• is present and this is key for the facilitation of guanine nucleotide exchange[230]. On the flip side of the coin, caspases, key apoptotic proteins and cysteine proteases, are reversibly inhibited by S-nitrosylation of their active site cysteine[231]. This means NO•, in addition to its countless other roles, also has the ability to regulate apoptosis. Finally, hemoglobin and the ryanodine receptor, a cardiac calcium-releasing channel, are found to be S-nitrosylated *in vivo* and this S-nitrosylation leads to changes in their functionality[232, 233]. The key with considering any new target of NO• is to consider whether these modifications can occur at physiologically relevant concentrations. Many *in vitro* experiments performed at high NO• levels can lead to more S-nitroscysteine than would be observed *in vivo*[212].

3. Roles of ROS/RNS in disease pathology

a. Cardiovascular diseases

ROS and RNS play crucial roles in signaling processes that go awry in cardiomyopathy and cardiovascular diseases. As a general rule of thumb, cardiovascular diseases are marked by ROS overproduction, but RNS formation can be either decreases or increased[234]. Angiotensin-converting enzyme (ACE) inhibitors and angiotensin receptor blockers (ARBs) are commonly used to treat heart failure as angiotensin II (ATII) has been shown to exacerbate the condition[235, 236]. This increase in ATII leads to a concurrent increase in NADH- and NADPH-driven superoxide production. The ATII-driven superoxide increase has been shown in vascular smooth muscle cells (VSMCs) and aortic adventitial fibroblasts[237, 238]. Thrombin, tumour necrosis factor-α (TNF-α), and platelet-derived growth factor (PDGF) have all been shown to also stimulated superoxide production in VSMCs[239]. The superoxide, and by extension hydrogen peroxide, produced by ATII expression, strongly activates mitogen-activated protein kinase (MAPK) family members (ERK1/2 and p38 MAPK), which are proteins that regulate growth, apoptosis, and stress responses[240, 241]. Atherosclerosis, or the build-up of cholesterols and fats (plaques) in arteries, can lead to blood clots and rabbit models of atherosclerosis have shown significantly elevated levels of superoxide[242-244]. A role of erroneous-produced superoxide has been defined in hypertension. Hypertensive rat models have shown that, in rats with elevated blood pressure, superoxide levels are high in arteries and veins[245]. In these rats, administering heparin-binding SOD, in other words SOD that localized to blood vessel walls, normalizes blood pressure[246].

b. Diabetes

Diabetes is tied to vascular complications and mitochondrial dysfunction in various tissues, such as skeletal muscle, heart, and lungs, to name a few[247, 248]. These observations are suggestive of a clear role of ROS/RNS in the progression of diabetic conditions. For example, it has been shown that type 2 diabetic patients have decreased oxygen consumption due to mitochondrial dysfunction (a decrease in complex I activity), increased ROS production, and a decrease in the levels of glutathione, a key antioxidant[249, 250]. Further evidence supporting the importance of reactive species for diabetes is that MitoQ, an antioxidant, is demonstrated to be beneficial for

the management of diabetes (e.g. diabetic mice show decreases in elevation of urinary albumin levels)[251].

c. Alzheimer's disease

Alzheimer's disease (AD) is a neurodegenerative disease, the most common type of dementia, characterized by elevated oxidative stress. Sporadic AD, in contrast to familial AD, tends to occur after 65 years of age and is associated with apolipoprotein E4 (APOE4) allele[252, 253]. The presence of this allele has been linked to a decrease in the activity of endogenous antioxidants, such as glutathione peroxidase and catalase[254]. Another hallmark of AD is senile plaques composed of amyloid beta (A*β*) peptides. A*β* peptide is formed by cleavage of amyloid precursor protein (APP) by *β*-secretase and *γ*-secretase[255]. The A*β* peptide associated with poor prognosis of AD is A*β* (1-42) and the presence of this peptide has been shown to induce oxidative stress both *in vitro* and *in vivo*[256, 257]. ROS formation has also been associated with other neurodegenerative diseases, including Parkinson's disease, Huntington's disease, and amyotrophic lateral sclerosis (ALS)[190].

d. Amyotrophic lateral sclerosis (ALS)

Amyotrophic lateral sclerosis (ALS) is a neurodegenerative disease where motor neurons are progressively lost in the brain and in the spiral cord, ultimately leading to death within 2-5 years of diagnosis[258, 259]. SOD1 mutations were first identified in patients with familial ALS in 1993 by the Rosen and collegeaues[260]. Because these SOD1 mutations were commonly found in exons, the initial hypothesis was that these cases of familial ALS resulted from the dysfunction of SOD1[261]. However, with more research, the relationship between SOD1 mutations and ALS has only gotten more complicated. It became clear that a hallmark of ALS was not SOD1 protein dysfunction per say, but aggregates of misfolded SOD1 that are found in glial cells of the nervous system[262, 263]. The exact mechanism of how these protein aggregates lead to motor neuron death remains to be elucidated.

e. Cancer development

ROS-mediated DNA damage is a generally accepted trigger of cancer development[264]. Studies in humans support that oxidative DNA damage is a carcinogenic factor[265]. When ROS causes

mutation, such as G to T transversions, in genes that function as oncogenes or tumour suppressor genes, initiation of cancer or increased progression of a pre-established cancer can occur[266, 267]. Note, the most frequent mutations in p53 tumours are G to T transversions[268, 269]. Combine these known cancer-causing mutations with the facts that human tumour cells are produce large bursts of ROS, specifically hydrogen peroxide, and oxidative DNA alterations are found in cancerous tissues, this is suggestive that ROS plays a central role in cancers[270, 271]. Let us examine the straightforward example of cancer initiation. Cigarette smoke results in an accumulation of 8-hydroxydeoxyguanosine (8-OHdG) in the lungs. 8-OHdG levels in cigarette smokers are up to 3-fold higher than non-smokers[272].

4. Superoxide dismutases

a. History

Superoxide dismutase (SOD) was discovered over a half a century ago, in 1969, by Joe M. McCord and Irwin Fridovich, at Duke University[273]. McCord and Fridovich purified a previously unidentified enzyme, termed superoxide dismutase, from bovine erythrocytes. This enzyme was shown to inhibit the reduction of cytochrome c by superoxide ($O_2^{\bullet-}$). The newly discovered superoxide dismutase had a unique ultraviolet absorption spectrum very similar to that of other copper-containing proteins that had been previously isolated but had no known enzymatic activity, notably hemocuprein (bovine)[274] and erythrocuprein (human)[275]. Most importantly, when hemocuprein and erythrocuprein were assayed for superoxide dismutase activity, the units of SOD activity per milligram (mg) were similar between hemocuprein, erythrocuprein, and the newly discovered SOD (~3000 units/mg). At the time, a unit of superoxide dismutase activity was defined as the amount of the enzyme required to reduce the rate of cytochrome c reduction by 50%[273]. Developing an assay for superoxide dismutase activity was only possible because, in 1968, McCord and Fridovich proved that the reduction of cytochrome c was is accomplished by the production of superoxide by xanthine oxidase[276].

SODs have evolved on, at least, three separate and independent instances, indicating that there is intense evolutionary pressure for defences against superoxide and/or products formed as a result of the presence of superoxide (i.e. peroxynitrite)[277]. The three occasions of SOD

evolution are represented by the three families of SOD enzymes known to exist. These families are defined by the metal used for their catabolic function – Fe or Mn, Cu or Zn, and Ni[278].

The first family likely to evolve would be the Fe- or Mn-containing SODs. This is because as the switch to an oxygenic atmosphere was occurring billions of years ago, the oceans still remained anoxic with high sulfur (S) contents[279]. In these conditions, metal solubility is the opposite of that observed today – iron (Fe), nickel (Ni), and manganese (Mn) dissolved and zinc (Zn) and copper (Cu) precipitate and became biologically inert[280]. These environmental conditions made key components, such as Fe, of some of the first enzymes, notably SOD, abundantly available[281]. Another reason to believe Fe-SODs evolved first is that they are one of the most common SODs in both aerobic and anaerobic bacteria[282, 283]. FeSODs were discovered by Yost and Fridovich in 1973[282].

CuZn SODs are hypothesized to be the most modern SOD family. This is for two reasons: 1) the bioavailability of Cu and Zn increases as atmospheric and oceanic O_2 levels increase[280], and 2) while CuZn SODs are highly abundant in animals and plants, there are found only at low levels in bacteria and are not found in archaea or protists[284-286]. An interesting note on CuZn SODs is that they share little structural homology with Fe/MnSODs[287]. CuZn SODs are homodimers of eight-strand beta barrel monomers, whereas Fe/Mn SODs are homodimers of monomers that have a C-terminal three-strand beta sheet surrounded by alpha helices and a N-terminal domain that is alpha-helical[288]. The fact that these enzymes, which both catalyze the dismutation of superoxide, accomplish their role with diverse structures fully solidifies the idea that Fe/MnSODs and CuZn SODs evolved independently of one another. CuZn SODs were discovered by Fridovich and McCord in 1969[273].

The last family of SODs to discuss is NiSODs. NiSODs are typically found in marine bacteria and algae[289, 290]. Little is known about this family of SODs as they were discovered in 1996[290]. However, just like CuZnSOD and Fe/MnSOD, NiSOD does not seem to be at all structurally to the other SOD families. Its structure is not dependent on Ni coordination as CuZnSOD and Fe/MnSOD are both dependent on the coordination of their metal to function[291]. In the case of SOD1, Cu^{2+} is associated to the active site by four histidines – His46, His48, His63, and His120. Nitrogen atoms in these histidines bind the copper ion[292]. Also significant, most mammalian cells do not rely on

the simple diffusion of copper to ensure its insertion to the SOD1 active site. Instead, a copper chaperone (CCS) expedites the process[293]. CCS docks onto a disulfide reduced form of SOD1 and remains inactive until exposed to superoxide, whereby the disulfide bond in SOD1 is isomerized and in the process, copper is transferred to SOD1[294]. SOD1 also bind Zn^{2+} in its active site through His63. His71, His80, and Asp83[292].

Since the identification of SOD by McCord and Fridovich, further evidence has been published to show that SODs are the primary line of defense against superoxide. In mammals, for example, SOD1 is one of the most abundant enzymes, with a cellular concentration estimated between 10-40μM[285, 295]. In mice, SOD1 its 34th most abundant protein in the whole organism, out of 17,698 proteins[296].

b. Function

Superoxide dismutases (SODs) are the enzymes responsible for the catalytic conversion of superoxide ($O_2^{\bullet-}$) to hydrogen peroxide (H_2O_2) and oxygen (O_2) [297, 298]. These enzymes are the only known defence against superoxide formation and accumulation[299]. SODs, in physiological conditions, allow for dismutation of superoxide to occur ~10^4 times faster than if left to occur spontaneously[300].

c. Mechanism

Superoxide dismutases must have a finely tuned mechanism because the difference between molecular oxygen and superoxide is only one electron. SODs are known as an enzyme with high specificity and efficiency[301]. In 2009, high resolution images of SOD in *Alvinella pompeiana*, an eukaryotic thermophile, helped to more concretely nail down the mechanism of SOD dismutation of superoxide into hydrogen peroxide[302]. Historically speaking, there has been a debate between two proposed mechanisms of SOD activity – the inner sphere model and the outer sphere model[303, 304]. The inner sphere mechanism of electron transfer suggests that a bond is established to keep reactants together during their transition state. In contrast, the outer sphere model of electron transfer proposes that no such bond exists, and reactants merely interact via weak electronic coupling[300]. The images of *Alvinelle pompeiana* SOD show geometrical constraints that favour the use of an inner sphere mechanism to achieve electron transfer[303].

Before any electrons are transferred, molecular oxygen is recognized electrostatically and guided into the active site of SOD[305]. The arrangement of positively charged residues in SODs encourages superoxide-SOD interaction[306]. These highly conserved residues, such as Lysine 134 and Arginine 141, create a strong positively charged catalytic site for the negatively charged superoxide to bind[307]. The presence of positively charged residues is very important for the interaction of superoxide with SODs because, at physiological pH, SOD carries a net negative charge[308]. Interestingly, neutralization of the charge of Arg141 in bovine SOD1 with phenylglyoxal caused a 90% reduction in SOD activity[309]. Furthermore, the structure of SOD allows for steric selection of superoxide as its preferred reactant, over other anions such as phosphate and diatomic species of similar size such as nitric oxide[303].

Once superoxide is successfully guided into the active site of the enzyme, it binds to cupric copper (Cu^{2+}). Upon superoxide binding, Cu^{2+} is reduced to cuprous copper (Cu^{1+}) and superoxide is oxidized to O_2. As a result of the reduction of copper, the bond between copper and histidine (His63), termed the histidine bridge, is broken. This leaves a histidine that has been protonated[310]. Protonation is the addition of a proton, typically via the hydrogen cation (H^+). Next, His63 donates a proton and Cu^{1+} donates an electron to the second superoxide molecule involved in the dismutation reaction. This superoxide is reduced to hydrogen peroxide and copper binding is restored to His63 as Cu^{1+} is converted to Cu^{2+}[303].

To clearly illustrate the superoxide dismutase reaction, with a copper/zinc cofactor, the associated chemical equations (broken into half reactions) are:

1. Cu^{2+}-SOD + $O_2^{\bullet-}$ → Cu^{1+}-SOD + O_2 (copper reduction and superoxide oxidation)
2. Cu^{1+}-SOD + $O_2^{\bullet-}$ + $2H^+$ → Cu^{2+}-SOD + H_2O_2 (superoxide reduction and copper oxidation)

Studies in 1974, using pulse radiolysis and electron paramagnetic resonance, were the first to show that CuZnSOD copper alternates between +1 and +2 oxidation states during its activities[311].

Note, that SOD1, the type of superoxide dismutase altered throughout this thesis, has several amino acid residues key to its functionality. The structure of SOD1 has been of great interest due to its high level of stability, rapid rate of reaction, and extreme specificity in selection of its reactants (i.e. superoxide). In 1992, the first crystal structures of SOD1 were published and

gave immense insight into how SOD accomplishes such feats (Figure 7)[312]. Key insight from these crystal structures revealed that the copper-binding site of SOD1 is formed by four histidine residues, each of which are key of holding copper in the active site of the enzyme[313]. These four histidines (His46, His48, His63, and His120) coordinately bind copper[312]. Arginine 143 is considered one of the most important residues of SOD1 for its dismutase activity. The arginine helps to facilitate diffusion of superoxide into the active site of the enzyme. Substitution of Arg143 to alanine, in other words substitution of a positively charged amino acid with a more neutrally charged amino acid, leads to a 10-fold decrease in the rate of superoxide dismutation. Furthermore, substitution of Arg143 to aspartate, a negatively charged amino acid, leads to a 100-fold decrease in superoxide dismutase activity[314].

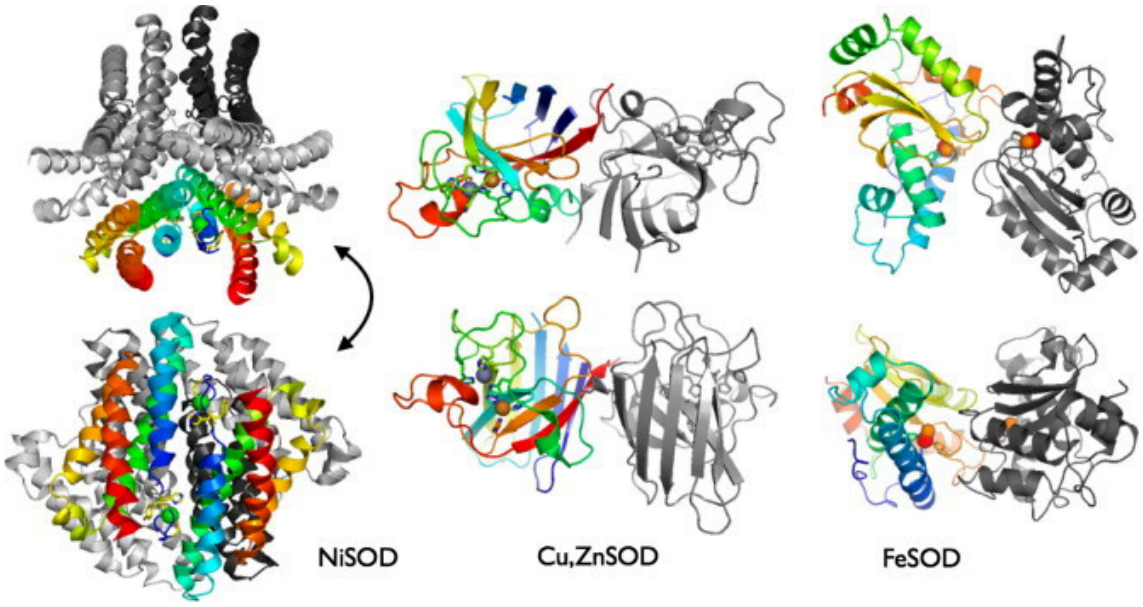

Figure 7: SOD1 crystal structure.
This figure illustrates the comparative structures of the three families of superoxide dismutases (SOD). For FeSOD and Cu/ZnSOD, the coloured portion represents one monomer and for NiSOD, the coloured portion represents two monomers. The second-row image for each family is the structure in the first row rotated 90° around a horizontal axis. This means that the portion of the structure shown on the top of the first-row image is now out of view and at the back in the second-row image. Cu/ZnSOD and Mn or FeSOD are homodimers, whereas NiSOD are homohexamers. Cu/ZnSOD monomers are flattened 8-strand β-barrels. Mn or FeSOD monomers are alpha helices in the N-terminal domain and 3- strand β-sheets surrounded by alpha helices in the C-terminal domain. Finally, NiSOD monomers are 4 helix bundles. These families of SODs

differ in many ways – the metal ion required for function, their protein folding, and their quaternary structure (e.g. dimer, hexamer, etc.) (Miller 2011).

d. Isoforms

SODs are classified based on their metal co-factor: nickel SOD (NiSOD), iron SOD (FeSOD), manganese SOD (MnSOD), and copper-zinc SOD (CuZnSOD[292]. Further classification of SODs is based on their localization within cells.

In mammals, there are three SOD isoforms (Figure 8). The cytoplasmic isoform, SOD1, is a CuZnSOD. SOD1, while found mainly in the cytoplasm, has also been shown to be expressed in the nucleus, lysosomes, peroxisomes, and mitochondrial intermembrane space[295, 315, 316]. SOD2 is a MnSOD and localizes to the mitochondrial matrix[317]. In the mitochondrial electron transport chain, complex I (NADH-Q oxidoreductase) releases superoxide almost solely to the mitochondrial matrix; however, complex III (succinate-Q reductase) produces superoxide that is let into both the mitochondrial matrix and to the mitochondrial inner membrane space[318]. As a result, superoxide produced at both complex I and complex III become the substrate for SOD2, but SOD1 is necessary to manage the superoxide released by complex III into the inner membrane space[319]. Finally, SOD3, a CuZnSOD, is secreted to the extracellular space and is often tethered to the plasma membrane of cells via interactions with fibulin-5, collagen, and heparin sulfate proteoglycan[320-322].

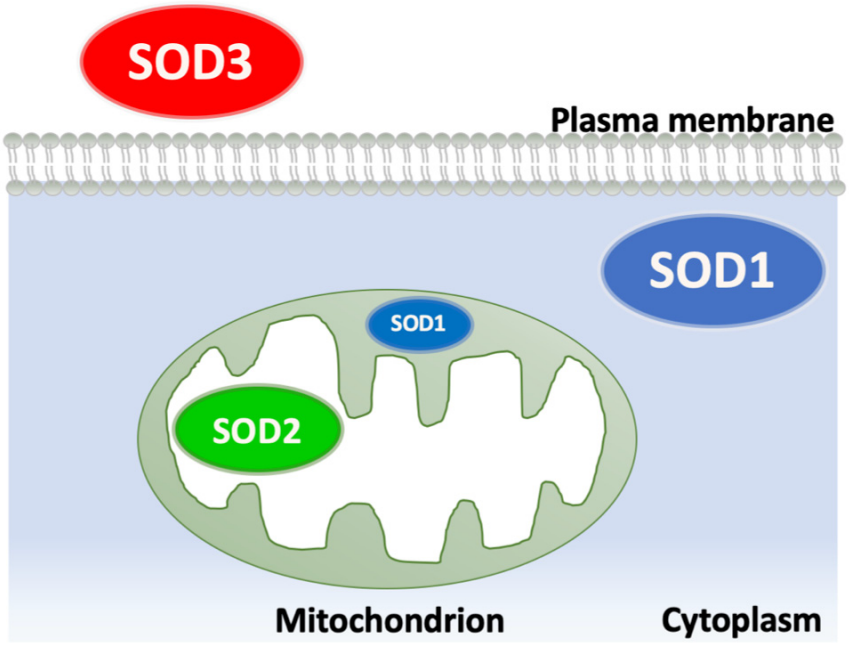

Figure 8: Mammalian isoforms of superoxide dismutase (SOD).
Superoxide dismutases (SODs) catalyze the dismutation of superoxide ($O_2^{\bullet -}$) to hydrogen peroxide (H_2O_2). In mammals, there are 3 SOD isoforms. SOD1 is the most abundant, responsible for about 80% of SOD activity, and is found in the cytoplasm and intermembrane space of the mitochondria. SOD2 is found in the mitochondria. SOD3 is found in the extracellular space, often tethered to the plasma membrane.

Superoxide dismutases (SODs) are one of the most abundant proteins in vertebrates. SOD1 is the most abundant out of the three isoforms. Cellular concentrations of SOD are surprisingly high, estimated to be 10-40μM[285]. While SOD1 and SOD2 are expressed in most cells and/or organs, high expression of SOD3 is found in select tissues, such as blood vessels, lungs, kidneys, and heart[323-326].

5. Nitric oxide synthases (NOS)

a. History

In 1987, the fact that perfusate from arteries or veins and nitric oxide caused a similar relaxation of an endothelium-stripped artery or vein heavily suggested that mammalian cells have a method to synthesize nitric oxide. However, at that time, this was merely a hypothesis. In 1988, it was uncovered that murine macrophages involved in immune response somehow convert L-arginine to L-citrulline and $NO^{\bullet}$, in a NADPH-dependent manner. These findings were especially

interesting because if the macrophages were not immuno-stimulated by either interferon γ or *Escherichia coli* lipopolysaccharide, no component of the "supernatant" that converted L-arginine to NO• could be found[327]. Finally, Mayer and colleagues showed, in 1989, that endothelial cells have a calcium-dependent cytosolic enzyme that is capable of converting L-arginine, proved to be the precursor of nitric oxide by Moncada in 1988, into what they termed, at the time, an activator of sGC[328]. Concurrently, another lab isolated a soluble enzyme for the rat forebrain that seemed to also catalyze the conversion of L-arginine into NO•[329].

Even though many papers in the late 1980s postulated the existence of an enzyme responsible for nitric oxide synthesis, it was not until 1990 that the first nitric oxide synthase was isolated from rat cerebella[330]. In this study, initial attempts to purify the proposed enzyme responsible for nitric oxide synthesis showed that the unknown substance resulting in the enzymatic activity bound to diethylaminoethyl (DEAE) columns. This substance could be eluted using 1M NaCl, but if gradient elution with NaCl was attempted, there was no enzymatic activity to be found. The researchers thought this may be because gradient elution separates an important co-factor for the enzyme, whereas elution with 1M NaCl keeps the co-factor and enzyme together. At this time, there were studies that suggested that nitric oxide formation required Ca^{2+} so Bredt and Synder hypothesized that adding calmodulin, a calcium-binding protein, to the DEAE elution fractions could restore NO synthesis and this is what occurred[328, 330]. This enzyme, isolated from the brain, was the first identified isoform of nitric oxide synthase (NOS) and is called neuronal NOS (nNOS) or NOS1.

Subsequently, the two other known NOS isoforms – inducible NOS (iNOS) and endothelial NOS (eNOS) – were isolated and characterized in 1991. iNOS or NOS2 was purified from macrophages and eNOS or NOS3 was purified from bovine aortic endothelial cells[331, 332].

b. Function

Nitric oxide is an unconventional signalling molecule, as it is a gas and is the smallest known signalling molecule[333]. Nitric oxide synthases (NOS) are the only known endogenous source of NO•[201]. NOS are an enzymatic family defined by the ability to produce NO• during the conversion of L-arginine to citrulline[334]. All NOS isoforms require the following – L-arginine, O_2, nicotinamide adenine dinucleotide phosphate (NADPH), flavin adenine dinucleotide (FAD), flavin

mononucleotide (FMN), and (6R-)5,6,7,8-tetrahydrobiopterin (BH_4)[335]. All NOS also have the ability to bind calmodulin, a calcium-binding protein, and require heme for successful $NO^{\bullet}$ synthesis[336, 337].

c. Mechanism

Nitric oxide synthase (NOS) has gained much less attention than the countless physiological roles of nitric oxide, but it is important not to lose sight of this enzyme as it is the enzyme responsible for nitric oxide production. Similar to the complexities of nitric oxide itself, NOS is also a fascinating enzyme. The reaction catalyzed by NOS is a 5-electron oxidation. All oxidation events occur on the nitrogen, resulting in the formation of nitric oxide and no change to the oxidation state of the guanidine carbon (marked with red dot in Figure 9)[335]. These oxidation events require both NADPH and O_2[338]. The formation of $NO^{\bullet}$ by NOS occurs via a two-step process[339]. First, L-arginine is converted to N-hydroxyl-L-arginine. Second, this N-hydroxyl-L-arginine is converted to $NO^{\bullet}$ and L-citrulline[340, 341]. Interestingly, it has never been conclusively shown which isomer of citrulline is formed, but it is assumed that L-citrulline rather than R-citrulline is formed[335]. Both reactions that lead to the conversion of L-arginine to L-citrulline are referred to as monooxygenation reactions, or the insertion of a single atom of oxygen that is taken from molecular oxygen[342, 343]. The intermediate, N-hydroxyl-L-arginine, remains bound to the active site before the second monooxygenation reaction occurs[344]. The heme present in all NOS isoforms is essential for these oxidation events; however, the exact catalytic mechanism has yet to be elucidated[345].

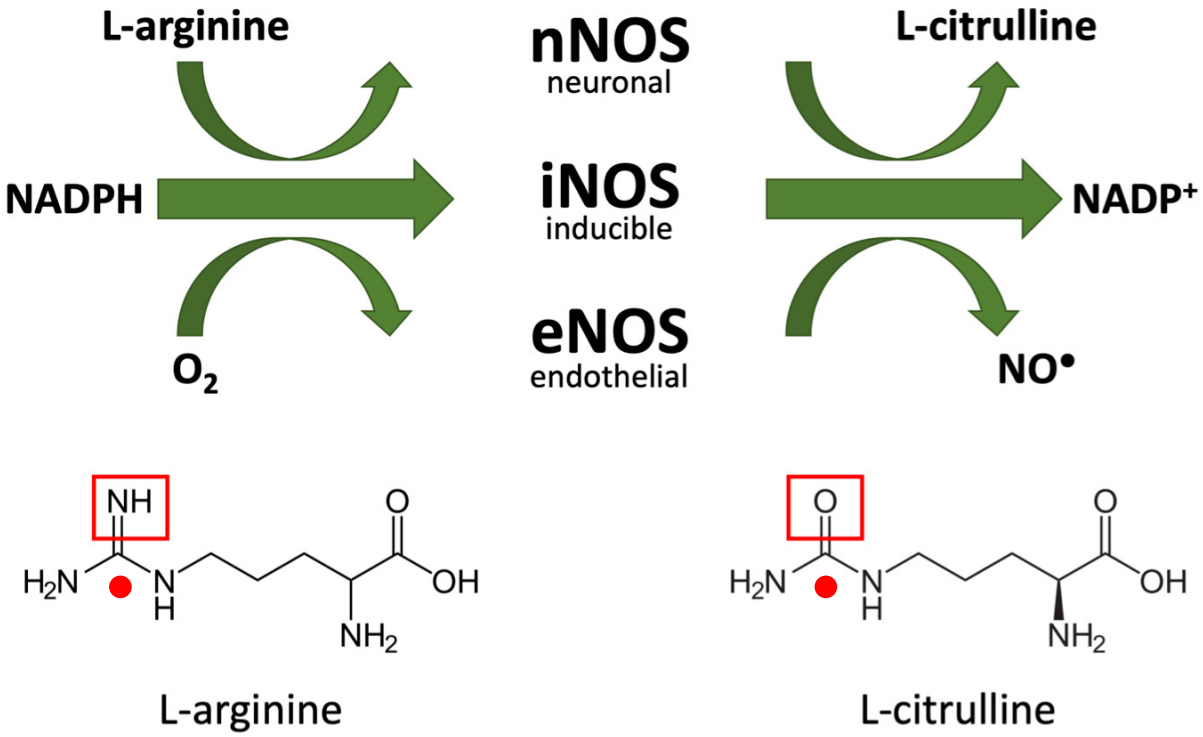

Figure 9: Formation of nitric oxide (NO•) by nitric oxide synthases (NOS).
Nitric oxide (NO•) is synthesized by nitric oxide synthases (NOS). All NOS convert L-arginine to L-citrulline and in the process produce NO•. There are three NOS isoforms. The constitutively expressed isoforms, neuronal NOS (nNOS/NOS1) and endothelial NOS (eNOS/NOS3), are calcium (Ca^{2+})-sensitive, whereas inducible NOS (iNOS/NOS2) is Ca^{2+}-independent. The NO• they generate is a small, hydrophobic molecule that can traverse cellular membranes and signals through soluble guanylate cyclases (sGC). NO• signalling is involved in physiological processes, such as vasodilation, neurotransmission, and the immune response. The red box indicates the difference between L-arginine and L-citrulline, with L-arginine having an amine group off its guanidine carbon (indicated by red dot) and L-citrulline having a carbonyl group off its guanidine carbon.

Mammalian NOS has two domains key for NO• formation – an oxygenase domain, consisting of a heme and a binding site for (6R)-5,6,7,8-tetrahydrobiopterin (BH_4), and a reductase domain that is related to cytochrome P450 reductase through structure, sequence, and function[346]. The reductase domain of NOS is where FMN (flavin mononucleotide) and FAD (flavin adenine dinucleotide) bind[347]. The FMN binding domain is linked to the oxygenase domain of NOS by ~30 amino acid polypeptide segment and this forms the binding site for calmodulin

(CaM)[330]. Even though all NOS isoforms are not considered calmodulin-sensitive, they do all bind calmodulin, more on this later. Mammalian NOS differ from NOS of other organisms, for example, bacterial NOS do not have a reductase domain, but the regions where important cofactors bind are well conserved[348, 349]. The flow of electrons through the NOS enzyme begins with the transfer of electrons from NADPH to FAD in the reductase domain[350]. This leads to the formation of a FAD hydroquinone, which then transfers electrons to FMN[351]. FMN proceeds to pass electrons, one-by-one, to the heme in the oxygenase domain[352]. Calmodulin aids in this electron transfer between FMN and the heme, acting as a switch[353]. A conformational change is required to allow FMN to transfer an electron to the heme in the oxygenase domain and this conformational change is triggered by calmodulin binding, although the mechanism by which this occurs is unknown[354]. After electrons have been transferred to the heme in the oxygenase domain, then the two monooxygenation events occur in this domain leading to the conversion of L-arginine to citrulline and the formation of nitric oxide[355]. Beyond this point, the mechanism is poorly defined[345].

d. Isoforms

Isoforms of NOS were initially characterized by order of identification and the tissue they were initially isolated from[335]. In mammals, there are three defined NOS isoforms, which will be discussed here. Note, alternative gene splicing is known to lead to the formation of additional versions of NOS in mammals[356]. The three major isoforms are – neuronal NOS (nNOS/NOS1), inducible NOS (iNOS/NOS2), and endothelial NOS (eNOS/NOS3)[340]. There are three major distinctions between the NOS isoforms – their localization, their physiological roles, and their calcium-sensitivity. Neuronal NOS, while it has been identified in tissues other than the brain, is expressed in highest concentration in neurons of the central nervous system[355]. Inducible NOS is found to be most abundant in activated macrophages. And finally, endothelial NOS, as the name implies, is more abundant in the vascular endothelium, but also localizes to other cell types, such as neurons in the brain and kidney cells[357-360].

Just like the localization of NOS, there are clearly delineated physiological roles for each NOS isoform, but there is skepticism in the field as to whether these distinct roles assigned to specific NOS isoforms are in fact overlapping. nNOS is said to be essential for both inter- and

intra-cellular signaling in the brain, the mediation of N-methyl-D-aspartate (NMDA) receptor glutamate responses, and neurotransmission in noradrenergic, noncholinergic nerves[361]. iNOS is the one of the keys to inflammatory and immune responses. It is therefore implicated in defense against pathogens and tumour development. iNOS has also been shown to mediate the sepsis response. Finally, eNOS is the producer of that endothelial-derived relaxing factor and is also heavily involved in inhibition of platelet aggregation, inhibition of leukocyte adhesion, and suppression of smooth muscle cell proliferation[362].

Classically, NOS1 (nNOS) and NOS3 (eNOS) are considered to constitutively expressed and NOS2 (iNOS) deemed to have inducible expression[363, 364]. However, recently it appears as if under the right circumstances, all three isoforms can show both constitutive and inducible expression. The reason for this classical viewpoint on expression of NOS comes from each isoforms' relationship with calmodulin and Ca^{2+}. In NOS enzymes, calmodulin is used to increase the rapidity of electron transfer from NADPH to the NOS heme[365]. nNOS and eNOS are regarded as Ca^{2+}-sensitive isoforms, whereas iNOS expression is considered independent of Ca^{2+} concentration. This difference in calcium sensitivity arises from structural differences in the calmodulin-binding domains of the NOS isoforms[334]. Note, the calmodulin-binding domain of iNOS alone is not sufficient for Ca^{2+} independent activity. This was shown when calmodulin-binding sequences of nNOS and eNOS were replaced with the calmodulin-binding sequence of iNOS and those chimeric nNOS and eNOS isoforms still remained calcium-dependent[366]. iNOS expression is inducible because its function is not regulated by Ca^{2+} concentration, and thereby regulation of iNOS must occur on a different level, in this case both transcriptional and post-transcriptionally. Transcription factors, such as NF-κB and STAT-1α, have been shown to regulate the iNOS promoter and be essential for the induction of iNOS expression[367].

When Ca^{2+} levels increase, there is an increase in the binding of Ca^{2+} to calmodulin. Calmodulin binds Ca^{2+} via 2 EF hands that connect its 2 globular domains[368]. This Ca^{2+} binding event causes a conformational change in calmodulin, exposes hydrophobic areas, that makes it more readily able to bind to and regulate certain proteins, examples of which are NOSs[369]. More evidence in support of the requirement of calmodulin for NOS function, calmodulin antagonists

(calmidazolium and trifluoperazine) inhibit $NO^{\bullet}$ formation in rat brains, neuroblastoma cells (N1E-115), and endothelial cells[336].

6. The reaction of superoxide and nitric oxide

a. Peroxynitrite

Peroxynitrite is formed by the reaction of superoxide with nitric oxide. It is a reaction of two free radicals with each other. When radical-radical coupling occurs, it is usually diffusion-controlled, because this unique reaction is both kinetically and thermodynamically favourable[370]. The reaction is so favourable because two unpaired electrons form one new chemical bond. In physiological settings, there are many possible radical combinations, but many occur rarely because of low steady-state levels of precursors and competing reactions limit the circumstances in which radical-radical combinations can occur[371]. In this sense, the reaction of superoxide with nitric oxide is different. Both superoxide and nitric oxide are readily available, as superoxide is produced at high level (in mice, ~0.66nmol $O_2^{\bullet-}$/min/mg protein) and nitric oxide is generated enzymatically by NOS and is a commonly used signaling molecule[372, 373]. Therefore, if not controlled by other mechanisms, peroxynitrite formation can be formed extremely easily. In fact, the reaction of superoxide with nitric oxide was first considered to be a mechanism of $NO^{\bullet}$ inactivation[374].

Peroxynitrite is both a strong oxidant and a strong nitrating agent. The rate of peroxynitrite (PN) formation (rate constant $k \sim 6.6 \times 10^9\ M^{-1}sec^{-1}$) is three times faster than the rate at which Cu/Zn SODs quench superoxide (rate constant $k \sim 2.5 \times 10^9\ M^{-1}sec^{-1}$)[375]. In fact, $NO^{\bullet}$ is the only biologically synthesized molecule that can outcompete SODs for reaction with superoxide[376]. PN formation is toxic to cells because it oxidizes thiols, iron/sulfur centers, heme groups, zinc fingers, methionine and cysteine, as well as nitrates tyrosine[377]. These modifications have been associated with diseases including Parkinson's, Alzheimer's, heart disease, atherosclerosis, and cancer[4].

PN can easily cross membranes but does have a short half-life (~10ms). Even with this short half-life, it can interact with targets in adjacent cells (1-2 cell diameters). Oxidation by PN can occur directly, via one- or two-electron transfers, or indirectly, by the reaction of PN with

carbon dioxide to form other highly reactive radicals ($CO_3^{\bullet-}$ and $NO_2^{\bullet}$) or the homolysis of peroxynitrous acid (ONOOH) into $OH^{\bullet}$ and $NO_2^{\bullet}$[377]. Homolysis is the breaking of a bond between electrons, in which the electrons are distributed evenly to the resulting products. Another way to put it is that electrons in the electron pair move as independent entities[378]. PN also readily leads to the nitration of tyrosine residues[379]. 3-nitrotyrosine (3-NT, the addition of $-NO_2$ to tyrosine) is a protein modification commonly attributed to peroxynitrite and is generally accepted as a biomarker for endogenous peroxynitrite activity[380].

PN was first identified as a biologically relevant oxidant in 1990. It was shown that PN is a more important source of the hydroxyl radical than the Fenton reaction or the Haber-Weiss reaction (reactions of Fe^{2+} and H_2O_2)[381, 382]. PN is unexpectedly stable considering that it is a strong oxidant that readily reacts with electron-rich groups. The surprising stability of PN results from its ability to fold into a *cis*-conformation that localizes its negative charge over the entirety of the molecule[383]. PN can be further stabilized by the formation of hydrogen bonds with water[384]. The stability of PN makes is especially influential in biological contexts.

b. Regulation of physiological processes by peroxynitrite

The discovery of the ability of PN to nitrate tyrosine quickly opened the possibility that PN modifications could be a way to modulate cell signally that relies on tyrosine phosphorylation[385]. This seems likely but there is evidence that shows that the presence of PN can both inhibit and promote phosphotyrosine signalling[386-388]. Interestingly, many of the presumptive PN signalling functions are implicated in inflammation. For example, NFκB, a key transcription factor that activates inflammatory and antiapoptotic genes, can be activated by PN. Here in Montréal, Filep and colleagues have shown that PN potently activates NFκB, which goes on to stimulate the secretion of interleukin-8 (IL-8). This leads to the amplification of neutrophil-dependent responses to inflammation[389]. PN's effect on NFκB, much like any other proposed PN signalling functions, is not universally accepted, however. Newer studies have shown that perhaps PN suppresses NFκB activation. Mass spectrometry showed that this inactivation was caused by nitration of Tyr-66 and Tyr-152 of the p65 family member[390].

Phagocytes (macrophages and neutrophils) harness PN during immune response by engulfing bacteria and releasing reactive species in a characteristic respiratory burst. This respiratory burst is marked by increased superoxide formation by NADPH oxidases and increased $NO^{\bullet}$ formation by iNOS, and thereby increased PN[391-393]. Additionally, activated macrophages' ability to kill bacteria is dependent on the presence of PN[393]. This same respiratory burst can also be observed in chronic and damaging inflammatory responses, such as traumatic brain injury[394].

c. Damage associated with peroxynitrite formation

DNA damage

Oxidative and nitration damage from PN can affect proteins, DNA, and lipids. These modifications can inactivate structural proteins, enzymes key for metabolism, and ionic pumps. This PN-related damage results in the disruption of cell membranes, the breaking of nucleic acids, the dysfunction of cellular processes, and the induction of both apoptosis and necrosis[395]. A pathway that is often focused on as a central mechanism for PN-dependent cytotoxicity is the activation of poly (ADP-ribose) polymerase (PARP). Activation of PARP occurs in response to DNA damage and can trigger cell death as it leads to depletion of NAD+ levels and a slowdown of the electron transport chain and glycolysis, leading to a depletion of ATP[396].

The activation of PARP *in vivo* requires DNA single-strand breaks[397]. Breaks in DNA can be caused by various free radicals, but studies have shown that PN is in fact the key oxidant for triggering *in vivo* formation of DNA breaks[398]. Peroxynitrite is particularly damaging, because unlike the hydroxyl radical, generally considered to be a highly damaging oxidant, it can cross cell membranes and it can enter the nucleus[399]. Once in the nucleus, PN can induce oxidative modifications to the sugar-phosphate backbone and to DNA bases[400]. Guanine is, by far, the nitrogenous base most often modified by PN. This is due to its low reduction potential (it is more likely to lose an electron than a base with a higher reduction potential)[401]. Guanine oxidation by PN yields 8-oxoguanine. 8-oxoguanine can also further react with PN to form cyanuric acid and oxazolone. These modifications of guanine result in guanine fragmentation, leading to mutagenesis and carcinogenesis[402]. Furthermore, PN can nitrate guanine bases, resulting in the formation of 8-nitro-guanine. The presence of 8-nitro-guanine results in abasic sites. These abasic

sites can be cleaved *in vivo* by endonucleases eventually giving rise to DNA single-strand breaks[401]. Additionally, PN alters the sugar-phosphate backbone of DNA by removing an atom of hydrogen from deoxyribose. This also leads to the formation of a DNA break because the loss of a hydrogen atom opens the sugar ring structure[400]. PARP activation, a result of peroxynitrite-mediated single stranded DNA break formation, is key for peroxynitrite-mediated cell death. Pharmacological inhibition or genetic inactivation of PARP-1 attenuates peroxynitrite-mediated cell death[403, 404].

Lipid peroxidation

Another key contributor to peroxynitrite-mediated cell death is lipid peroxidation, specifically in cell membranes, liposomes, and lipoproteins[405]. Peroxynitrite triggers lipid peroxidation by extracting a hydrogen from polyunsaturated fatty acids (PUFA). When PUFA loses a hydrogen, this can result in lipid hydroperoxyradicals and these radicals go on to attack a neighbouring PUFA, propagating the degeneration of a lipid membrane[405, 406]. Degeneration of lipid membranes leads to changes in both membrane permeability and membrane fluidity[407]. The peroxidation of lipids by PN plays a prominent role in demyelination as PN can initiate peroxidation of myelin lipids[408]. PN can also oxidize low-density lipoproteins (LDL)[409]. LDL that is modified by PN can lead to accumulation of oxidized cholesteryl esters, an early event in atherogenesis (the formation of plaques in arteries)[410, 411]. Additional interactions of membrane lipids with PN can result in the formation of nitrated lipids[412].

Reaction with transition metal centers

PN, as probably noted by now, reacts with most biological materials. However, out of all its possible reactions, the fastest known reaction for PN is with transition metal centers[413]. Because of PN's high reactivity with transition metal centers, PN can easily modify proteins with heme prosthetic groups. Proteins with heme include, but are not limited to, hemoglobin, myoglobin, and cytochrome c[414-416]. PN oxidizes ferrous (Fe^{2+}) heme to ferric (Fe^{3+}) heme. Modification of heme by PN is a way to inactivate NOS. This could potentially serve as a feedback mechanism for iNOS in inflammatory conditions[417]. PN can also inactivate enzymes via reaction with iron-sulfur

centers, such as in the case of the mitochondrial aconitase[187]. Zinc-sulfur motifs can also be oxidized by PN, such as in the case of eNOS[418].

Oxidation of thiols

PN can also change protein function and structure by reactions with several amino acids. Cysteine has a reactive thiol that can be oxidized by PN[419, 420]. When PN reacts with a thiol, this results in sulfenic acid (-RSOH) and then sulfenic acid can go on to react with a secondary thiol to form disulfide (-RSSR)[421]. The reaction of PN with thiols can also generate thiyl radicals ($RS^{\bullet}$).Thiyl radicals are capable of promoting oxygen-dependent radical formation[422]. Furthermore, PN can form S-nitrosothiols. It is unclear if S-nitrosylation occurs via a direct mechanism or via the formation of thiyl radicals by PN and subsequent reaction of $NO^{\bullet}$ with the thiyl radical[423, 424]. Either way, S-nitrosothiols has been implicated in mitochondrial dysfunction and PN-mediated vasodilation[425, 426].

PN-dependent formation of sulfenic acid and disulfide on cysteine thiols has been shown to inactivate many enzymes, specifically enzymes central to energy generation such as glyceraldehyde-3-phosphate dehydrogenase, creatine kinase, complex I of the ETC (NADH dehydrogenase), complex II of the ETC (succinate dehydrogenase), complex III of the ETC (cytochrome c reductase), and complex V of the ETC (ATP synthase)[427-430]. All of these enzymes can be inactivated by PN-mediated tyrosine nitration (more on this below). The presence of multiple vulnerable residues to PN-dependent modifications suggests that these enzymes are especially susceptible targets of PN. Oxidation of cysteines also is responsible for the inactivation of protein tyrosine phosphatases (PTP), specifically PTPs with CXXXXXR active-site sequences. This inactivation of PTPs results in a boost phosphotyrosine-dependent signaling cascades *in vivo*[431]. PN can also oxidize thiols that are not protein bound, like reduced glutathione (GSH). GSH is an endogenous scavenger of ROS[432]. There is sensitivity to PN can be predicted by intracellular GSH concentration[433, 434]. GSH depletion has been proposed as a key step in the development of many neurodegenerative diseases, such as Parkinson's and amyotrophic lateral sclerosis (ALS)[435, 436].

There are a few instances of PN-mediated cysteine oxidation that result in enzymatic activation. This is illustrated by matrix metalloproteinases (MMPs). MMP activation has been linked PN

toxicity in heart disease and stroke[437-439]. proMMPs are activated after thiol oxidation of the proenzyme's autoinhibitory domain[440]. Another illustration of activation driven by PN-mediated cysteine oxidation is the activation of src kinase *hck* that is found in erythrocytes. This leads to an increase in tyrosine-dependent signal cascades in erythrocytes[441].

Tyrosine nitration

3-nitrotyrosine (3-NT) is commonly used as a marker for PN[442]. Tyrosine nitration is the addition of a nitro (-NO_2) group to a hydroxyl (-OH) group found on the aromatic ring of tyrosine. This is a covalent protein modification[443]. Nitration of tyrosine residues changes protein function, structure, and catalytic activity and is considered to be characteristic of PN toxicity[444]. 3-NT is formed by a radical mechanism. First, hydrogen is removed from tyrosine, leading to the formation of a tyrosyl radical. Second, this tyrosyl radical combines with $NO_2^{\bullet}$ (a radical that results from PN homolysis) and a 3-NT residue remains. It is also possible for 2 tyrosyl radicals to combine, forming dityrosine, a competing reaction during 3-NT formation[376, 445]. Beckman et al. and Ischiropoulos et al. were the first to show that PN results in tyrosine nitration *in vitro* and propose the idea that this nitration may also occur *in vivo*[446-449]. Levels of tyrosine nitration *in vivo* and under normal conditions appear to be low with about 1 to 5 3-NT per 10,000 tyrosine resides (100-500µmol/mol)[450, 451]. Although 3-NT is the most well-accepted biological marker of a reactive species, there are still some questions concerning whether there are alternative mechanisms, other than PN, by which 3-NT can be formed[452, 453]. Proteomic analyses have further confirmed that tyrosine nitration is highly selective and limited to a select few tyrosine residues[454-456]. There are known characteristics that make a tyrosine especially susceptible to nitration. Is tyrosine's aromatic ring on the protein surface? Where is the loop structure of tyrosine located? Are there neighbouring negatively charged amino acids? Are there proximal cysteines[457]?

3-NT formation is sped up in the presence of transition metals, meaning that metalloproteins such as SOD may help mediate PN tyrosine nitration[379]. Over the years, it has been suggested that 3-NT is a better marker of nitrative stress, rather than PN formation[458]. However, looking at the available data, it quickly becomes clear that this is too broad of a

generalization and that 3-NT levels are quite specific to the amount of PN. Incubating $NO^{\bullet}$ alone with proteins, tissues, and cells does not result in significant 3-NT formation[459].

Nitrotyrosine formation has been associated with at least 50 human diseases and 80 animal-modeled conditions *in vivo* (Table 1)[460]. The list of nitrated proteins and associated pathologies keeps growing. It is important to remember that increased 3-NT, and therefore increased PN formation, does not necessarily indicate a pathological role of PN in disease, but rather that it is indicative that an increase in PN formation occurs at some point in the disease progression. Interestingly, the mitochondrial SOD was the first protein that was shown to be nitrated *in vivo*. Nitration of Tyr-34 causes complete inactivation of this SOD isoform[461]. This inactivation of any SOD isoform results in lower levels of superoxide dismutation and favours higher PN formation. Nitration of mitochondrial SOD has been found *in vivo* in rodents and humans. Figure 10 highlights the interaction between nitric oxide, superoxide, and peroxynitrite[462-466].

Table 1: Nitrotyrosine formation in humans and mice
Adapted from Greenacre and Ischiropoulos, 2009.

System	Species	Disease/Condition	Location of nitrotyrosine expression	References
Central nervous system	*Human*	*AIDS dementia complex*	Frontal cortical neurons, vascular wall	464, 467-480
		ALS sporadic and familial	Spinal cord, SOD2 isolated from cerebrospinal fluid, Neurofilament L, neurofilament aggregates, motor neurons (both the cell body and axon), astrocytes, vascular wall	
		Alzheimer's disease	Hippocampus, neocortex, ventricular cerebrospinal fluid, hippocampal neurons, neurofibrillary tangles	
		Multiple sclerosis	Monocytes, macrophages, hypertrophic astrocytes, areas of demyelination	
		Parkinson's disease	Core of Lewy bodies in melanized neurons, amorphous deposits associated with degenerating neurons	
		Parkinson's disease, Pick's disease, Diffuse Lewy body disease, Alzheimer's disease	Microglia, endothelial cells, degenerating neurons, neuritic sprouts	
		Progressive supranuclear palsy	Astrocytes, oligodendrocytes, neurons, endothelial cells	
		Stroke	Neutrophils and blood vessels of cerebral infarct	
	Mice	β-Amyloid induced neurotoxicity in the cerebral cortex	Cerebral cortex	481-493
		ALS mice that express the Cu/Zn SOD mutation – G37R	Ventral horn neurons, Neurofilament L, Schwann cell cytoskeletal proteins	
		ALS mice that express the Cu/Zn SOD mutation – G93A	Spinal cord astrocytes and motor neurons, cerebral cortex, pyramidal cells of hippocampus	

		Apo-E deficient mice	Cerebral cortex, hippocampus, brainstem, cerebellum	
		Cerebral I/R	Vascular wall of pre-infarct region of cerebral cortex	
		Inflammatory demyelination and allergic encephalomyelitis	Spinal cord, macrophages, membrane of T-lymphocytes, cytosol of astrocytes, glial cells	
		Ischemic stroke	Cerebral neurons and endothelial cells of infarcted region	
		Malonate neurotoxicity	Striatum	
		Methamphetamine-induced neurotoxicity	Striatum	
		MPTP (1-methyl-4-phenyl-1,2,3,6-tetrahydropyridine) model of Parkinson's disease	Midbrain brain homogenates, Tyrosine hydroxylase	
		Transgenic Huntington's disease model	Cerebral cortical neurons	
		Traumatic brain injury	Cytoplasm and dendritic processes of degenerating cortical neurons	
Eyes	*Human*	Glaucoma	Optic nerve heads	[494]
Cardiovascular system	*Human*	Atherosclerosis	Plasma & aortic lesion LDL, necrotic core of plaque, sub-intimal fatty streaks, macrophages, foam cells, smooth muscle cells, endothelial cells	[409, 459, 495-503]
		Cardiac allograft rejection	Macrophages and adjacent myocytes from endomyocardium	
		Coronary bypass graft	Plasma	
		Exercise intolerance in chronic heart failure	Skeletal muscle	
		Myocarditis	Endocardium, myocardium, coronary vascular endothelial cells, smooth muscle cells	
		Preeclampsia	Placental villous vessels, villous stroma, cytotrophoblasts, endothelial cells of maternal blood vessels	
		Transplant coronary artery disease	Macrophages, smooth muscle cells	
	Mice	Atherosclerosis in LDL receptor -/- mice	Macrophages, foam cells, smooth muscle cells	[504, 505]
		Autoimmune myocarditis	Myocardiocytes, macrophages	
Respiratory system	*Human*	Acute lung injury	Lung interstitium, alveolar epithelial cells, proteinaceous alveolar exudate, macrophages, neutrophils, vascular endothelial cells, sub-endothelial cells	[506-515]
		Acute respiratory distress syndrome	Plasma ceruloplasmin, transferrin, α_1-protease inhibitor, α_1-antichymotrypsin, β-chain fibrinogen, alveolar epithelial cells, capillary endothelial cells, broncholavage fluid	
		Asthma	Airway epithelial cells, macrophages, neutrophils, eosinophils, vascular endothelial cells, smooth muscle cells, lung parenchyma	
		Bronchopulmonary dysplasia in premature infants	Plasma	
		Cigarette smokers	Plasma	
		Idiopathic pulmonary fibrosis	Airway and alveolar epithelial cells, macrophages, neutrophils, vascular endothelium and smooth muscle	
		Infant respiratory failure	Airway biopsy homogenate	
		Neonatal pneumonia	Alveolar exudate	
		Obliterative bronchiolitis (lung transplants)	Epithelial cells, inflammatory cells, endothelial cells	
		Perennial nasal allergy	Nasal mucosa	

	Mice	Carrageenan induced pleurisy	Alveolar macrophages, airway epithelial cells	516-522
		Herpes simplex virus-1 induced pneumonia	Lung inflammatory cells	
		Hyperoxia	Lung structural proteins	
		Influenza induced pneumonia	Alveolar macrophages, neutrophils	
		Interstitial pneumonia	Alveolar macrophages	
		LPS induced acute lung injury	Large airway and alveolar epithelial cells, alveolar proteinaceous exudate, macrophages, vascular cells	
		$NO^{\bullet}$ inhalation	Lung macrophages	
Gastrointestinal tract	*Human*	Celiac disease	Plasma, small intestinal crypt enterocytes (intestinal absorption cells)	523-532
		Colon carcinoma	Neutrophils, tissue mononuclear cells, tumour cells, surrounding macrophages and fibroblasts	
		Gastric cancer	Epithelial cells, inflammatory cells, extracellular matrix	
		Gastric ulcer (associated with Helicobacter pylori)	Active ulcer margins, epithelial cells, lamina propria	
		Helicobacter pylori gastritis	Epithelial cells, inflammatory cells, extracellular matrix	
		Inflammatory bowel disease	Colonic epithelium, lamina propria, macrophages, neutrophils	
		Necrotizing enterocolitis	Enterocytes in apical villi	
		Oesophageal squamous cell carcinoma	Tumour cells, lymphocytes, macrophages	
		Pancreatic carcinoma	Tumour homogenates, c-Src tyrosine kinase	
		Ulcerative colitis	Epithelial cells, lamina propria	
	Mice	Autoimmune diabetes	Pancreatic islet β-cells, macrophages	533-535
		Colitis	Inflammatory cells, necrotic epithelial cells, mucosa, submucosa	
		Splanchnic artery occlusion shock	Mononuclear cells of necrotic ileum	
Hepatic system	*Human*	Cholangiocarcinoma	Malignant bilary epithelial cells	536, 537
		Chronic hepatitis	Hepatocytes, Kupffer cells	
	Mice	LPS induced hepatic injury	Hepatocytes around blood vessels	538, 539
		Acetaminophen/paracetamol	Centrilobular hepatocytes	
Renal system	*Human*	Chronic renal failure with septic shock	Plasma	463, 540-542
		Diabetic nephropathy	Proximal and distal tubules, thin limb of loop of Henle, collecting ducts	
		Renal allograft rejection	Tubular epithelial cells, SOD2	
		Uremic patients on peritoneal dialysis	Peritoneal biopsies	
	Mice	Acute renal ischemia in osteopontin KO mice	Kidney homogenate	543-545
		Sickle cell disease	Tubular epithelial cells, vascular wall, kidney homogenate	
Joints	*Human*	Hip replacement	Pseudosynovial interface membrane, CD68+ macrophages and neighbouring cells	546, 547
		Rheumatoid arthritis	Serum, synovial fluid	
	Mice	Collagen induced arthritis	Inflamed joint, paw extracts	548
Reproductive system	*Human*	Chorioamnionitis and placental abruption	Placenta	549

Skeletal muscle	*Human*	Inclusion-body myositis	Vacuolated skeletal muscle fibers, paired helical filaments, vacuoles	550
Skin	*Human*	Anaphylactoid purpura	Skin lesion neutrophils	551-553
		Malignant melanoma	Melanocytes, small blood vessels	
		Systemic sclerosis	Skin endothelial cells of superficial microvessels	
	Mice	Chronic ultraviolet B exposure	Skin homogenate	554, 555
		Skin papilloma	Dermal tissue	
Immune system	*Human*	Systemic lupus erythematosus	Serum	556, 557
		Granuloma	Granuloma epitheloid and multinucleated giant cells, endothelial cells	
	Mice	Irradiation following bone marrow transplantation	Bronchoalveolar lavage fluid	558, 559
		Lymphoma	Spleen and lymph node macrophages and surrounding cells	

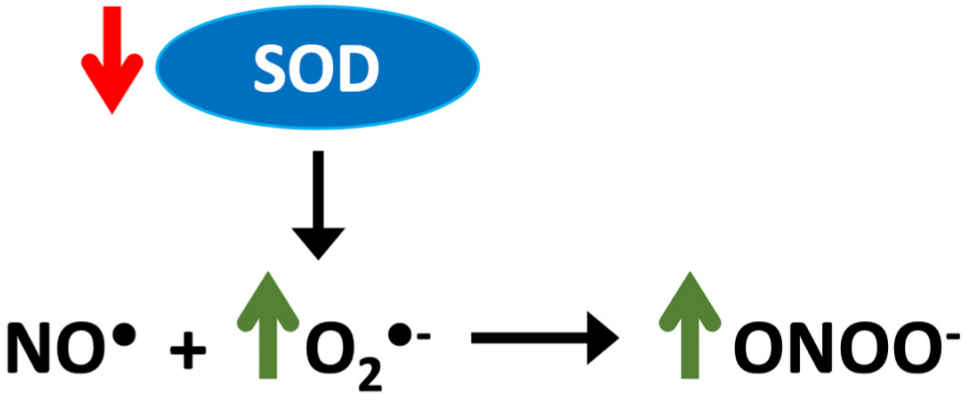

Figure 10: Decreased SOD expression and its effect on superoxide, nitric oxide, and peroxynitrite levels.
Superoxide dismutases (SODs) are responsible for the dismutation of superoxide ($O_2^{\bullet -}$) to hydrogen peroxide (H_2O_2). Mice or cells with lower SOD activity have higher concentrations of superoxide within the cell. Higher concentrations of superoxide provide favourable conditions for peroxynitrite ($ONOO^-$) generation by increasing the likelihood that a given nitric oxide ($NO^{\bullet}$) molecule is in close proximity with superoxide. Peroxynitrite (PN) formation ultimately leads to cell death. In addition to the direct toxic effects of peroxynitrite formation, the reaction of nitric oxide with superoxide also lowers the amount of nitric oxide available for signalling.

Tryptophan, methionine, and histidine oxidation

PN can directly oxidize methionine, leading to the formation of methionine sulfoxide and on occasion ethylene and dimethyldisulfide[413]. PN-mediated methionine oxidation is reversible and

this reversal involves methionine sulfoxide reductase. Reduced methionine sulfoxide reductase expression is associated with Alzheimer's development[560]. PN also oxidized tryptophan forming *N*-formylkynurenine, oxindole, hydropyrroloindole, and nitrotryptophan[561]. The relevance of tryptophan oxidation *in vivo* still remains to be elucidated. Lastly, PN oxidized histidine yielding a histidinyl radical. The oxidation of histidine by PN can lead to loss of CuZnSOD activity[562].

7. Cell work studying SODs and NOSs

a. Cells studying SOD

In vitro, the effects of losing different *Sod* isoforms seems to be the reverse of the effects of losing these genes *in vivo*. Mouse embryonic fibroblasts (MEFs) isolated from *Sod1*$^{-/-}$ mice quickly die days after isolation, whereas MEFs from *Sod2*$^{-/-}$ mice and equivalent *Sod2*$^{-/-}$ human cells can proliferate normally, despite their altered mitochondrial function[563-565]. Huang et al. show that *Sod1*$^{-/-}$ mouse embryonic fibroblasts (MEFs) have, on average, 4 to 10 times more apoptotic cells (labeled by biotinylated dNTP with terminal transferase (TdT)) than *Sod1*$^{+/+}$ MEFs. After only 48 hours in culture, culture plates of *Sod1*$^{-/-}$ MEFs were mostly remnants of apoptotic cells and healthy cells were rare[5]. In contrast, *Sod1*$^{-/-}$ mice are alive, with a mean lifespan of 20.8 months[17]. As will be seen later in this thesis, Sod*1*$^{loxP/loxP}$ MEFs (inducible *Sod1* knockout) were isolated to help understand how the severe phenotype associated with loss of *Sod1* expression *in vitro* relates to the mild phenotype observed *in vivo*. As *Sod3*$^{-/-}$ MEFs have not been well studied and the question of their viability in cell culture will also be addressed in this thesis.

b. Cells studying NOS

$NO^{\bullet}$ is a signalling molecule that has a presumptive role in modulation of neurogenesis in adults. Interestingly, proliferation of neural stem cells increases in nNOS-deficient cells. This seems to go against the assumption that nNOS-derived $NO^{\bullet}$ leads to neurogenesis, as when nNOS is lost, neural stem cell proliferation actually increases. These cells lacking nNOS, importantly, did not show compensatory upregulation of other NOS isoforms. It is however possible, that in neural cells, other NOS isoforms, whose expression were untouched, are the source of $NO^{\bullet}$ that is responsible for adult neurogenesis[566].

There is a well-establish murine lung endothelial cell (MLEC) model that lacks eNOS expression. These cells also have no nNOS and iNOS expression, as detected via Western blotting. But importantly, just like the NOS knockout mice and other cell types lacking NOS expression, these cells remain alive. eNOS knockout cells and wild-type cells exhibit very similar morphology, form a contact-inhibited monolayer of cells, and have nearly identical growth characteristics[567].

With regards to eNOS, it has also been shown that vascular smooth muscle cells (SMCs) proliferation is dependent on its expression, however all these experiments were done using NO-donors (e.g. sodium nitroprusside) or cGMP analogues (e.g. 8-Br-cGMP) rather than altering eNOS expression itself[568, 569]. An interesting cellular experiment involving alterations in NOS expression involves exogenous eNOS expression in SMCs. Adding eNOS gene expression to a site of injury in a SMC monolayer leads to inhibition of SMC migration to the injury site and therefore "wound healing." This lack of SMC migration to an injury site as a result of increased eNOS expression occurs due to the inhibition of matrix metalloproteinase (MMP) activity[570]. MMPs facilitate cell migration[571].

8. Mouse models studying SODs NOSs

a. Mouse models studying SOD

As previously discussed, there are three mammalian SOD isoforms. Numerous mouse models have been made to elucidate the impacts of altering SOD activity. These mouse models are valuable tools to study ROS metabolism. While *Sod1*$^{-/-}$ and *Sod3*$^{-/-}$ mice are alive, albeit with mild phenotypes, loss of *Sod2* (*Sod2*$^{-/-}$ mice) is lethal (Table 2).

Table 2: Sod knockout mouse models and their phenotypes.
From our review Wang, Branicky, Noë, and Hekimi, 2018.

Gene	Type of mutation	Genotype	Phenotype	Oxidative stress	References
Sod1	Germline mutation	*Sod1*$^{-/-}$	grossly normal, increased incidence of hepatocarcinogenesis, distal motor axonopathy, locomotor defects, reduction in hind limb skeletal muscle mass and strength, acceleration of age-dependent skeletal muscle atrophy, hearing loss, delayed wound healing, accelerated age-related macular degeneration, a decrease in motivational behavior, impaired olfactory sexual signaling, lower fertility, increase in cellular senescence, higher levels of circulating cytokines, and a ~30% decrease in lifespan	extensive oxidative damage in the cytoplasm	17, 572-582

		Sod1$^{+/-}$	viable, fertile and grossly normal, increased vulnerability to facial nerve axotomy	Not determined	576
Sod2	Germline mutation	*Sod2*$^{-/-}$	die within 21 days after birth with cardiomyopathy, fatty liver, neurodegeneration, metabolic acidosis, anemia, increased susceptibility to oxygen toxicity, mitochondrial dysfunction, inhibition of ETC and TCA enzymes	accumulation of oxidative DNA damage	583-587
		Sod2$^{+/-}$	phenotypically normal, normal lifespan, increased cancer incidence over lifespan, decreased respiratory function	accelerated accumulation of oxidative damage	95, 583, 584, 588
	Conditional KO	Heart and skeletal muscle (MCK-Cre;*Sod2*$^{fl/fl}$)	growth retardation, cardiac myopathy, reduced lifespan with a median life span of 15.4 ± 4.0 weeks, abnormal mitochondrial structure, loss of respiratory enzyme activities, reduced ATP production	elevated mitochondrial ROS and oxidative damage in muscle tissues	589
		Skeletal muscle (HSA–Cre;*Sod2*$^{fl/fl}$)	normal spontaneous motor activity and muscle strength, but reduced exercise activity, loss of enzymatic activity for mitochondrial respiratory chain complexes (especially complex II), reduced ATP production	elevated mitochondrial ROS and an increase in oxidative DNA damage in the skeletal muscle	590
		Type IIB skeletal muscle fibers (*TnIFastCre;Sod2*$^{fl/fl}$)	decreased mitochondrial function, reduced complex II activity, reduced ATP production, decreased aconitase activity, impaired exercise capacity	elevated mitochondrial oxidative stress and oxidative damage in the skeletal muscle	591, 592
		Liver (Alb-Cre; *Sod2*$^{fl/fl}$)	no detected phenotype	No elevation of lipid peroxidation in the liver	593
		Liver (α-fetoprotein-Cre, *Sod2*$^{fl/fl}$)	phenotypically normal, decreased liver to body weight ratio, sign of hepatocyte injury, increased likelihood of tumor formation in a chemically induced liver carcinogenesis model	elevated oxidative damage in the liver	594, 595
		Kidney (Ksp1.3/Cre; *Sod2*$^{fl/fl}$)	phenotypically normal, mild renal damage and normal lifespan	Increased oxidative stress (tyrosine nitration)	596
		cells of the neurogenic lineage mostly in the brain (nestin-Cre*;Sod2*$^{fl/fl}$)	die by 25 days of age, growth retardation, spongiform neurodegeneration, loss of mitochondrial complex II activity	higher intracellular superoxide levels and oxidative damage in the brain	597, 598
		Hematopoietic stem cells (vav-iCre*;Sod2*$^{fl/fl}$)	Impaired red blood cell development, systematic redistribution of iron, heme synthetic defect	an increase in superoxide in hematopoietic organs	599
		Postnatal motor neuron (VAChT-Cre*;Sod2*$^{fl/fl}$)	No altered function in motor neurons, but accelerated disorganization of distal nerve axons following injury	no signs of oxidative damage in animals up to 1 year after birth	600
		Connective tissue (Col1α2-Cre; *Sod2*$^{fl/fl}$)	weight loss, skin atrophy, kyphosis, muscle degeneration and a reduced life span	Not determined	601
		Mammary gland (MMTV-cre*;Sod2*$^{fl/fl}$)	post-natal KO: no gross abnormalities		602
		T cells (Lck-Cre*;Sod2*$^{fl/fl}$)	Increased apoptosis, and aberrant T cell development and function	elevated superoxide in the T-cell population	603
		Gastric parietal cells (Atp4b-Cre*;Sod2*$^{fl/fl}$)	Mitochondrial dysfunction and increased apoptosis in the gastric mucosa of the parietal cell	increased gastric mucosal oxidative stress	604
Sod3	Germline mutation	*Sod3*$^{-/-}$	phenotypically normal under normal conditions, reduced survival time under high oxygen tension, exaggerated response to induced hypertension	higher level of vascular superoxide	605, 606
	Inducible conditional KO	Global (*Tg*$^{cre/esr}$*;Sod3*$^{fl/fl}$)	lung damage, die shortly after induction of *Sod3* KO	increase in lung superoxide	607
		Vascular smooth muscle cells (Tg$^{cre/SMMHC}$; *Sod3*$^{fl/fl}$)	normal blood pressure, no augmented response to angiotensin II-induced hypertension	increased vascular superoxide and reduced vascular NO levels	608
		Circumventricular organs (*Sod3*$^{fl/fl}$ + intracerebroventricular injection of Cre adenovirus)	an elevation of blood pressure, hypertensive response to angiotensin II	increased vascular superoxide production, T-cell activation	609

Phenotypes associated with loss of Sod1

Ting-Ting Huang, under the supervision of Charles Epstein at UCSF, was the first to generate *Sod1*$^{-/-}$ mice, published in 1997. These *Sod1*$^{-/-}$ mice have a deletion of exon 3 and 4 of the *Sod1* gene, resulting in a shortened *Sod1* allele where exon 1, 2, and 5 are spliced together[17]. Most studies in the Epstein lab focused on embryonic fibroblasts isolated from the animals; however, when Huang opened her own lab at Stanford, she began to study the phenotypes of *Sod1*$^{-/-}$ mice. She was the first to report the reduced lifespan of *Sod1*$^{-/-}$ mice and showed that over 50% of *Sod1*$^{-/-}$ mice had abnormal livers (56% in female mice, 79% in male mice). Abnormal livers were characterized by visible nodules on the liver surface, large outgrowths from the liver, and elevated liver weight to body weight ratios. Furthermore, all *Sod1*$^{-/-}$ livers showed hepatocyte injury beginning at 16 months of age. Hepatocyte injury is identified by the presence of enlarged hepatocytes with swollen nuclei. In contrast, age-matched *Sod*$^{+/+}$ mice had normal hepatocytes and normal liver appearance. The livers of *Sod1*$^{-/-}$ mice were said to have: "widespread oxidative damage" measured by aconitase activity, protein oxidation, lipid peroxidation, and oxidative DNA damage[17].

Soon after the study of *Sod1*$^{-/-}$ mice began, it was evident that both male and female *Sod1*$^{-/-}$ mice have reduced fertility. In males, male genitals and accessory organs are significantly smaller than wild-type controls. Additionally, the fertilization rate of wild-type oocytes by *Sod1*$^{-/-}$ sperm was significantly lower than the fertilization rate of wild-type oocytes by *Sod1*$^{+/+}$ sperm, due to the inability of *Sod1*$^{-/-}$ sperm to penetrate the oocyte's zona pellucida and a time-dependent decrease of *Sod1*$^{-/-}$ motility[610]. In females, if *Sod1*$^{-/-}$ mice managed to get pregnant (measured over a 6-month period), their average brood size 2.7 offspring/litter or 0.23 offspring/month. Ovaries from these mice are smaller and, while primary follicles appear normal, there are few large antral follicles when compared to controls. It was also found that infertile female *Sod1*$^{-/-}$ mice have decreased expression of the follicle stimulating hormone and activin receptor type II[580].

The Van Remmen lab has acutely focused on the muscle phenotypes of *Sod1*$^{-/-}$ mice. *Sod1*$^{-/-}$ mice have significantly less muscle mass than wild-type mice beginning at 3-4 months of age[6]. By 8-12 months of age, *Sod1*$^{-/-}$ mice have decreases in muscle mass that mimic changes seen in

25-30 month old wild-type mice (Figure11a)[611]. Age-related loss of muscle mass is termed sarcopenia, meaning *Sod1*$^{-/-}$ mice have accelerated and more dramatic sarcopenia than their wild-type controls. Decreases in muscle mass are seen in all muscle types, except the soleus (muscle in calves, runs between knee and heel)[6]. In addition to loss of muscle, *Sod1*$^{-/-}$ mice also showed a decrease in muscle function, measured by ability to generate isometric contractile force (the generation of muscle tension without changes in muscle length or joint angle)[612]. This decrease in contractile force was accompanied by reductions in rotarod performance[6], wheel running[6], treadmill endurance[613], and grip strength (Figure11b-d). It is believed that sarcopenia, or muscle loss, in *Sod1*$^{-/-}$ mice is due to less innervation of the muscle by motor neurons. Motor neuron innervation is necessary for maintenance of muscle size, structure, and function[614]. This could possibly be due to low $NO^{\bullet}$, as a result of low NOS, affecting neural development. *Sod1*$^{-/-}$ mice show changes in neuromuscular junctions (NMJs) structure including acetylcholine receptor (AChR) cluster fragmentation, NMJ deterioration, and degeneration and retraction of motor neurons[615]. The structure 18-month-old *Sod1*$^{-/-}$ mice NMJs was comparable with that of 30-month-old wild type mice[611]. Interestingly, mice lacking *Sod1* solely in skeletal muscles (mSod1 KO mice) show a 30% increase in muscle mass compared to WT controls[616].

The body mass of *Sod1*$^{-/-}$ mice is lower than that of wild type mice over the course of their lifespan[617]. The reduction in body weight (~17% in females and ~20% in males) was first seen at 5 months of age and continued to be observed until about 20 months of age (Figure 12a-b)[6]. It is important to note that decrease in muscle tissue specifically seems to be responsible for the age-related decrease in body mass of *Sod1*$^{-/-}$ mice. Heart and brain mass of *Sod1*$^{-/-}$ mice remained grossly unchanged, and, intriguingly, liver, spleen, kidney, and lung mass all increased even though the total body mass of these mice decreased. Only changes in skeletal muscle mass accounted for the changes in total body mass of *Sod1*$^{-/-}$ mice (Figure 12c)[618].

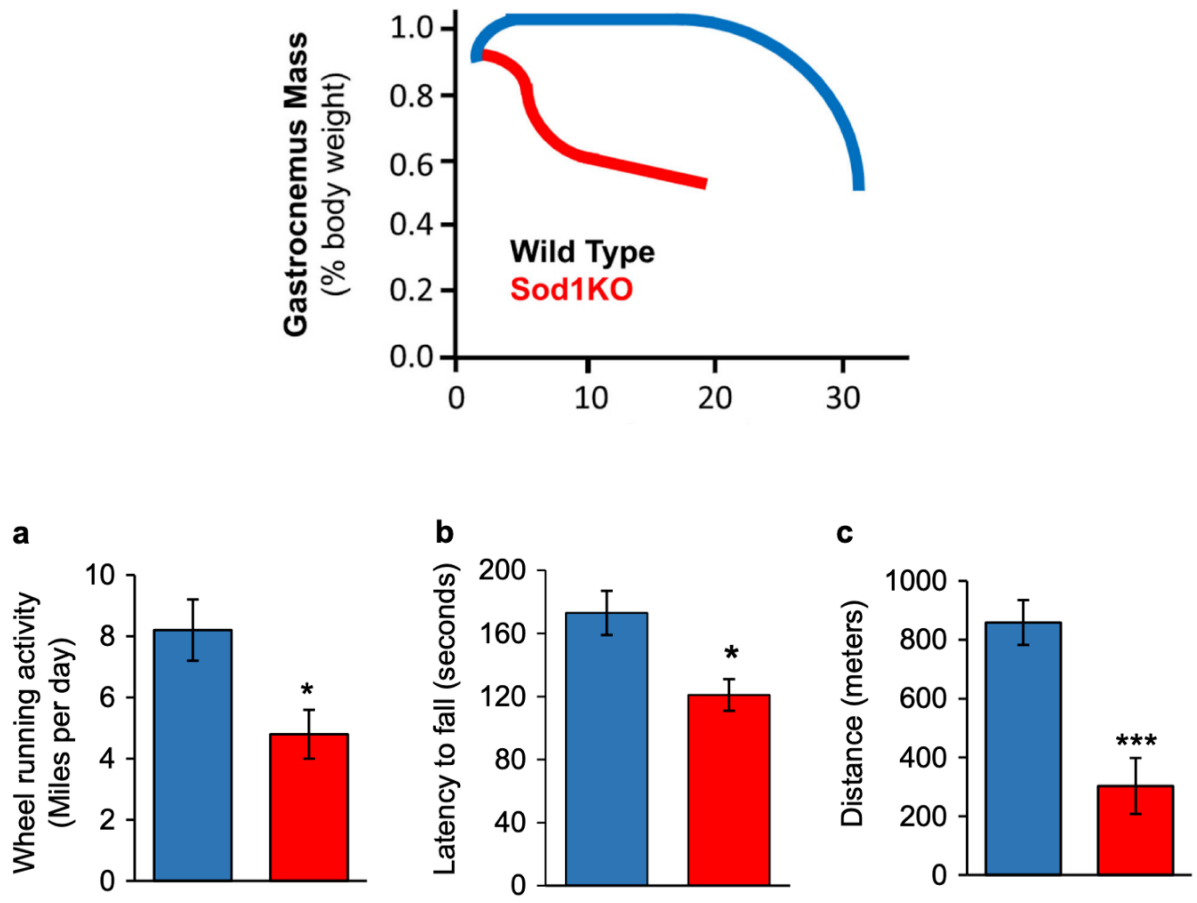

Figure 11: Sarcopenia in *Sod1*$^{-/-}$ mice.
a) The mass of the gastrocnemius (muscle in back of lower leg, just below the knee) plotted relative to lifespan of WT and *Sod1*$^{-/-}$ mice. The mass of the gastrocnemius in *Sod1*$^{-/-}$ mice is significantly decreased, so much so that the mass of *Sod1*$^{-/-}$ mice gastrocnemius at 8-12 months of age is similar to the mass of WT gastrocnemius at 25-30 months of age. b-d) Voluntary wheel running, rotarod performance, and endurance on a treadmill are all significantly decreased in *Sod1*$^{-/-}$ mice. b) WT and *Sod1*$^{-/-}$ mice were each housed in individual cages with wheels that they could willing choose to run on. The wheels had zero resistance. The running distance shown is the average distance per day over a 16-week period. c) The rotarod performance indicates the time, in seconds, before the mouse falls off the rotarod. d) Treadmill endurance signifies the distance, in meters, that the mice could run for until exhaustion (Deepa et al., 2019; Deepa et al., 2017).

a

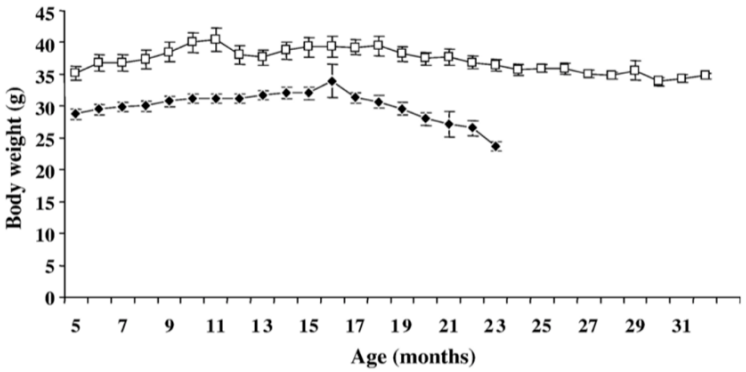

b

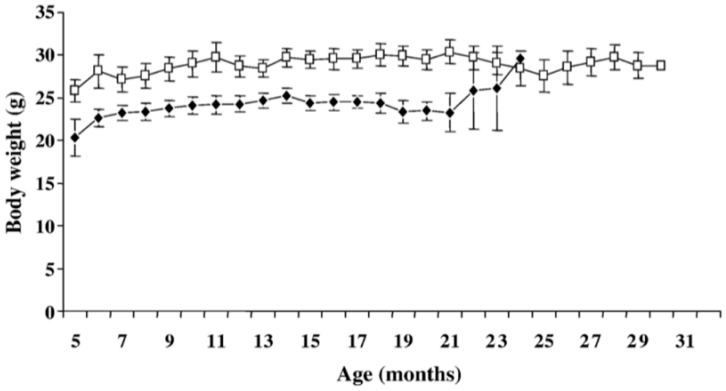

c

TABLE 1. COMPARISON OF TISSUE WEIGHTS FROM *SOD1*$^{-/-}$ AND *WT* (*SOD1*$^{+/+}$) MICE

Tissue	WT (Sod1$^{+/+}$)	Sod1$^{-/-}$
BW (g)	32 ± 1.2	30.7 ± 1.4
AT (mg)	50.1 ± 1.7	41.7 ± 1.1[a]
EDL (mg)	11.4 ± 0.8	11.9 ± 0.7
GTN (mg)	172.5 ± 4.6	120.7 ± 7.6[a]
SOL (mg)	9.6 ± 1.2	10.6 ± 0.4
Liver (g)	1.77 ± 0.1	1.85 ± 0.2
Spleen (mg)	119.4 ± 22.6	173.4 ± 27.3
Kidney (mg)	238 ± 26.6	276.5 ± 39.7
Heart (mg)	177.7 ± 7.8	190.9 ± 32.7
Lung (mg)	179.7 ± 26.1	215.3 ± 35.3
Brain (mg)	440 ± 33	445.3 ± 38.4

Figure 12: Decrease in skeletal muscle mass accounts for decrease in body mass of *Sod1*$^{-/-}$ mice.

a-b) Absence of *Sod1* in mice decreases body weight of both male (a) and female (b) mice. c) Comparison of tissue weights between WT mice and *Sod1*$^{-/-}$ mice shows that decrease in skeletal muscle mass is responsible for the overall decreased in body mass of *Sod1*$^{-/-}$ mice. Some tissue weight in *Sod1*$^{-/-}$ mice actually increase, such as the liver, spleen, kidney, heart, and lungs. The weight of *Sod1*$^{-/-}$ brains remains unchanged compared to WT. (Muller et al., 2006; Sakellariou et al., 2018).

Note, the mice used in the Van Remmen studies differ from the mice originally made by Ting-Ting Huang. While both are mice that lack *Sod1* expression, the mice in the muscle studies were originally generated by Russell M. Lebovitz in 1998 and lack exons 1 and 2 of the *Sod1* gene, rather than exons 3 and 4 as in the Huang mice[580]. In this thesis, the Lebovitz mice are used as well as they are readily available via The Jackson Laboratory. In addition to the phenotypes discussed above, these mice have also shown delayed wound healing, hearing loss, increase in cellular senescence, denervation, motor axonopathy, macular degeneration, impaired motivational behavior, and impaired olfactory sexual signaling[578, 619-625]. This highlights just how many processes *Sod1* is involved in and makes it all the more shocking that these mice without SOD1 expression are alive and appear, to the untrained eye at least, relatively normal.

Lethality associated with loss of Sod2

Although loss of a single copy of *Sod2* (*Sod2*$^{+/-}$ mice) produces no obvious pathologies, loss of both copies of *Sod2* (*Sod2*$^{-/-}$ mice), if successfully born, die within 20 days[626]. *Sod2*$^{+/-}$ mice display an increased incidence of cancer in old age, higher oxidative damage, increased susceptibility to oxidative stress, premature apoptotic initiation, and perturbations of mitochondrial function, yet somehow have a lifespan resembling that of wild-type mice[95, 627-630]. In the same realm of thought, studies show that increasing SOD2 expression leads to a marked reduction in mitochondrial superoxide levels, less of an age-associated increase in oxidative damage, and improved mitochondrial function at geriatric ages[631-633]. Importantly, despite these changes, increased SOD2 expression had little to no effect on lifespan[632].

To further study how loss of *Sod2* leads to premature death in mice and what is the requirement for SOD2 *in vivo*, various conditional knockout have been created. Of these knockouts, the loss of *Sod2* in cardiac and skeletal muscles appears to be the most detrimental[589]. Early death is seen in conditional knockout mice in both cardiac/skeletal muscle and the brain. Note, loss of *Sod2* in the brain appears to mimic whole body *Sod2* knockout as these mice survive only 3-4 weeks after birth. This suggests that neurons are particularly sensitive to loss of mitochondrial superoxide dismutase activity and therefore elevated mitochondrial superoxide levels[634].

The physiological processes that are affected by the loss of mitochondrial SOD activity and how these alterations lead to death remains to be uncovered. This is further complicated because superoxide itself is not particularly reactive, if compared to other reactive species found in organisms, and the toxicity associated with increased superoxide levels is most likely a result of transformation of superoxide into other reactive species rather than by superoxide-caused oxidative damage[635]. The most well-known direct target of superoxide, iron-sulfur clusters found in proteins. This may be extremely relevant in a mitochondrial setting as most of the mitochondrial respiratory chain proteins (e.g. succinate dehydrogenase) and citric acid cycle enzymes (e.g. aconitase) have Fe-S clusters in their active sites. Both the mitochondrial respiratory chain and the Krebs cycle are key for energy generation in the cell. The influence of superoxide on some of these enzymes, such as aconitase, is so well-established that they can be used as a sensitive indicator of steady-state superoxide levels. When superoxide levels are high, as they are in *Sod2*$^{-/-}$ mice, aconitase activity is greatly diminished[636]. Another consideration necessary to understand the lethality of *Sod2* loss is that superoxide, especially when in excess and without the control of SOD activity, readily reacts with nitric oxide. The reaction of superoxide with nitric oxide leads to peroxynitrite formation, a damaging oxidant in of itself, but also leads to decreased nitric oxide bioavailability. Nitric oxide, while noted as a potent inhibitor of cytochrome oxidase, is also a significant regulator of oxygen consumption. Peroxynitrite, like nitric oxide, is an inhibitor of mitochondrial complexes, but unlike nitric oxide that causes selective, rapid, and reversible inhibition of the electron transport chain, peroxynitrite causes irreversible and non-selective inhibition of a vast array of mitochondrial components[637]. Inhibition of the mitochondrial electron transport chain further increase oxidative stress and alters energy production of cells.

Phenotypes associated with loss of Sod3

Sod3$^{-/-}$ mice, more so than mice lacking another other isoform of *Sod*, develop normally and are healthy for the bulk of their adult lives[605]. However, when not under normal conditions, one can uncover the impact of the loss of extracellular SOD activity on a mouse's ability to respond to stressors. When under high oxygen pressure conditions (>99% oxygen, 8 litres/minute), *Sod3*$^{-/-}$ mice have a significantly reduced lifespan compared to that of wild-type mice in the same

stressful conditions. These mice, which lack extracellular SOD activity, also develop lung edema when housed under high oxygen pressure. The mice lacking SOD3 survived ~91 hours post oxygen exposure, whereas mice with SOD3 expression survived ~121 hours. The death of these oxygen-exposed, SOD3 null mice is caused by lung edema[605]. Loss of SOD3 expression is also known to exasperate angiotensin-induced hypertension. This worsening of hypertension caused by loss of *Sod3* is likely due to a decreased in NO• bioavailability[638]. Lungs and blood vessels seem to be some of the most affected tissues by *Sod3* loss. This is not surprising as high SOD3 expression has been shown in these tissues[322]. Interestingly, in contrast to germline knockout *Sod3* mice, inducible knockout *Sod3* mice leads to severe lung injury and these mice die within 7 days of the induction of *Sod3* knockout[639]. This remarkable difference between the survival of germline *Sod3* knockout mice and inducible adult-onset *Sod3* knockout mice indicates that there are compensatory mechanisms or developmental adaptations at play in germline *Sod3* knockout mice that allow for survival and a relatively normal phenotype.

b. Mouse models studying NOS

NO• is known to be involved in various physiological processing ranging from neurotransmission to vasodilation. Mouse models lacking each isoform of NOS have been key to investigate the specific roles of NO• derived from each isoform. Of note from single NOS knockout mice, is that NOS activity and nitric oxide production are well-preserved[640]. Because NOS activity is grossly unaltered in single NOS knockout mice, this makes it more difficult to unravel the distinct roles of each NOS isoform as the possibility of NOSs compensating for one another is quite strong.

Some surprising findings have come from studies of mice lacking NOS isoforms (Figure 13). While eNOS knockout mice (*Nos3*$^{-/-}$ mice) do show increased risk of cardiovascular disease and its anti-arteriosclerotic role is well-established, these mice do not develop atherosclerotic lesions[641]. Another shocking finding is that triple n/i/eNOS null mice are viable and although their survival and fertility is significantly reduced, mice completely lacking any NOS activity can live for up to 10 months[642]. The creation and study of triple knockout NOS mice also confirmed the role of NOS in various physiological processes, as these mice exhibit phenotypes of the metabolic, renal, respiratory, bone, and cardiovascular systems. However, the question does still remain, how do these physiological processes function at a high enough level to sustain life without the

production of NO• for signaling. This raises the possibility that all regulation provided by ROS and RNS is simply fine-tuning, rather than obligatory regulation. ROS and RNS may make the system better, but not be essential for the system to function.

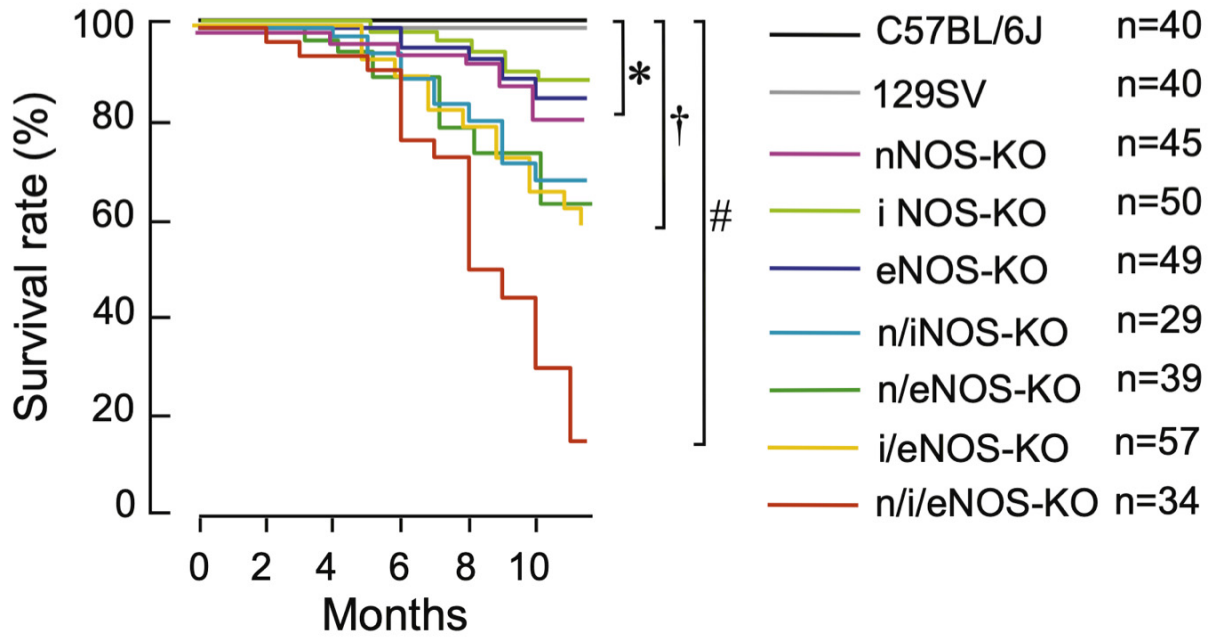

Figure 13: Mice lacking all three NOS isoforms are alive.
Nitric oxide is a pervasive mammalian signaling molecule, involved in vasodilation, neurotransmission, and immune responses. Surprisingly, mice lacking all three NOS isoforms are alive and can even live as long as 11 months. At 11 months of age, 100% of the wild-type mice survived and 15% of the triple knockout NOS mice survived. The survival rate of mice lacking NOS isoforms gets progressively worse as the number of NOS genes disrupted increases. This to say that single NOS knockouts live longer than double NOS knockouts that live longer than triple NOS knockouts. 55% of the mice lacking all NOS isoforms death was caused by myocardial infarction and this study was the first to show that loss of NOS expression is linked to the development of myocardial infarction. The wild-type mice in this study were C57BL/6J. n is the number of mice for each group. *, †, and # indicate that $P < 0.05$ (Tsutsui et al., 2015).

Triple KO NOS mice are hypertensive, but this hypertension is comparable to the hypertension seen in *(e)Nos3*$^{-/-}$ mice[640]. This suggests that hypertension in these mice is caused by a diminished level of endothelium-derived NO•. The heart rate of triple KO NOS mice is significantly lowered (bradycardia), but also to an extent that is comparable with *Nos3*$^{-/-}$ mice, once again indicative that the bradycardia phenotype is mostly due to deletion of the eNOS gene[643]. These mice that lack all NOS expression helped to reveal that, perhaps unexpectedly, all

three NOS isoforms play a role in the regulation and formation of vascular lesions[644]. Spontaneous vascular lesion formation was only noted in triple KO NOS mice, not eNOS KO mice. Spontaneous accumulation of lipids was also only noted in triple KO NOS mice, perhaps thanks to the high diffusion distance of $NO^{\bullet}$[645].

At the 11-month time point, only 15% of triple NOS KO mice survived, whereas all wild-type mice were still alive. The survival rate of mice lacking NOS isoforms progressively worsens as the number of NOS isoforms disrupted increases. This to say that single NOS KO mice survive longer than double NOS KO mice that survive longer than the triple NOS KO mice. Post-mortem examination of triple KO NOS mice showed that 55% of these mice died from myocardial infarction[645]. Interestingly, beginning at 5 months of age, triple NOS KO mice and eNOS KO mice, but not nNOS KO or iNOS KO mice, show left ventricular hypertrophy, cardiac myocyte hypertrophy, and elevated mass of the left ventricle. This hypertrophy was much more significant in triple NOS KO mice than eNOS KO mice. Also noted at 5 months of age in triple NOS KO mice was significant left ventricle diastolic dysfunction. This was evaluated using echocardiograph E/A wave ratio.[646]. The E/A wave ratio is used as an indicator of function of the heart's left ventricle., The E wave measures the velocity of blood flow in early diastole and the A wave measures the velocity of blood flow in late diastole. The blood flow during the E wave is caused by ventricular relaxation, whereas the blood flow during the A wave is caused by atrial contraction[647]. These studies of diastolic dysfunction in triple NOS KO mice were the first to demonstrate *in vivo* that NOS have a central role in the pathology of diastolic heart failure. Furthermore, arterial responses to acetylcholine (endothelium-derived hyperpolarization) reduced as the number of NOS isoforms disrupted increased. However, function of the vascular smooth muscle was conserved in all mice lacking NOS activity[648].

Another finding in these mice was that both triple NOS KO mice and eNOS KO mice showed evidence of phenotypes of metabolic syndrome. These phenotypes include hypertension, obesity, impaired glucose tolerance, insulin resistance, and hypertriglycemia[645]. It has also been shown that renal lesion formation is greatly accelerated in response to chronic unilateral ureteral obstruction in triple NOS KO mice, indicating that NOSs play a vital role in renoprotection[649]. Finally, bone mineral density and bone thickness were both significantly

elevated in triple NOS KO mice, but not in any single NOS KO mice[650]. This is indicative of a key role of NOSs in regulation of bone homeostasis.

In closing, triple NOS KO mice, especially, highlight the various roles of NOS in the pathology of countless physiological dysfunctions and thereby significance of $NO^{\bullet}$ as both a signaling molecule and essential regulator.

9. Thesis Rationale

This thesis aims to better understand the distinct phenotypes observed upon loss of SOD1 expression *in vitro* and *in vivo*. As highlighted earlier, when SOD1 expression is lost *in vitro* (*Sod1*$^{-/-}$), the cells rapidly undergo apoptosis; however, when SOD1 expression is lost *in vivo*, the mice can survive for up to ~25 months. How is it possible that cells isolated from these animals cannot last in culture, but the animals themselves can survive? To unravel this conundrum, we used a conditional *Sod1* knockout model. Inducible knockouts allow us to bypass any possible developmental adaptations that germline knockout models may have and that could explain their survival. As you will be shown in later chapters, the inducible *Sod1* knockout mice (*Sod1*$^{loxP/loxP}$) die within weeks of the loss of SOD1 expression, in distinct contrast to their germline knockout counterparts. This is highly suggestive that there are developmental adaptations that are important to allow *Sod1*$^{-/-}$ mice to survive. Attempting to rescue the phenotypes of the inducible knockout mice is a way we can determine what allows the germline knockout mice to survive. This is somewhat the opposite of the more usual approach. . Conditional models are typically made after seeing that loss of the expression of a particular gene results in a severe phenotype (e.g. loss of viability). In this case, conditional models tend to knockout the gene of interest in particular tissues to uncover where the loss of the gene is most significant to the phenotype seen in germline knockouts. This thesis highlights the prospect of using conditional mouse models differently, to uncover why mice that we expect not to survive do, in fact, survive with relatively mild phenotypes.

CHAPTER 2: CONSEQUENCES OF THE LOSS OF THE CYTOPLASMIC SUPEROXIDE DISMUTASE SOD1 ON CELLULAR PHYSIOLOGY

1. Abstract

Superoxide dismutases (SODs) are one of the most abundant proteins in vertebrates, responsible for the dismutation of superoxide to hydrogen peroxide. It is a key element of the antioxidant machinery endogenous to aerobic organisms. In fact, in mice, SOD1 is the 34th most abundant protein in the whole organism, out of 17,698 proteins[296]. Keeping oxidative stress under control is a crucial element of various metabolic diseases and, possibly, aging. The difficulty for cells and tissues arises because reactive oxygen species (ROS) and reactive nitrogen species (RNS) are both crucial signaling molecules and potentially toxic. For example, nitric oxide ($NO^{\bullet}$) fulfills indispensable signaling functions in the vasculature, the immune system, and in neurotransmission[213-215]. Similarly, hydrogen peroxide (H_2O_2) is a widespread modulator of signal transduction pathways[651]. Here, we create a new tool for studying ROS/RNS metabolism, a line of mouse embryonic fibroblasts which can survive without any detectable SOD expression. These cells thrive in the presence of nitric oxide synthase (NOS) inhibitors and a peroxynitrite decomposition catalyst, indicating that peroxynitrite, rather than superoxide per se, is the molecule SODs defend against. Our study highlights that superoxide is not an inherently damaging molecules in the absence of $NO^{\bullet}$, in contrast to what was previously thought.

2. Introduction

Superoxide dismutases (SOD) are the first line of defence against the formation of reactive oxygen species. The importance of SODs is highlighted by the fact that the vast majority of aerobic organisms, and interestingly some anaerobic organisms such as the obligate anaerobe bacteria *Clostridium perfringens*, express at least one SOD isoform[652]. SODs accelerate the dismutation of superoxide ($O_2^{\bullet-}$), or the breakdown of $O_2^{\bullet-}$ to hydrogen peroxide (H_2O_2) and molecular oxygen (O_2) ($O_2^{\bullet-} + 2H^+ \rightarrow H_2O_2 + O_2$) (Figure 14)[3]. Beyond that, by controlling superoxide, SODs also control the concentrations of other reactive species that can be generated when superoxide is abundant, such as hydrogen peroxide and peroxynitrite ($ONOO^-$). The dismutation of superoxide via SODs is extremely efficient. The reaction occurs at ~2 x 10^9 $M^{-1}s^{-1}$. or approximately 10^4 times faster than spontaneous dismutation of superoxide[653]. Note, the reaction of superoxide with nitric oxide, yielding the damaging peroxynitrite, occurs three times

faster than SOD dismutation (6.7 x 10^9 $M^{-1}s^{-1}$), because $O_2^{\bullet-}$ and $NO^{\bullet}$ are both radicals with unpaired electrons in their outer orbitals[128].

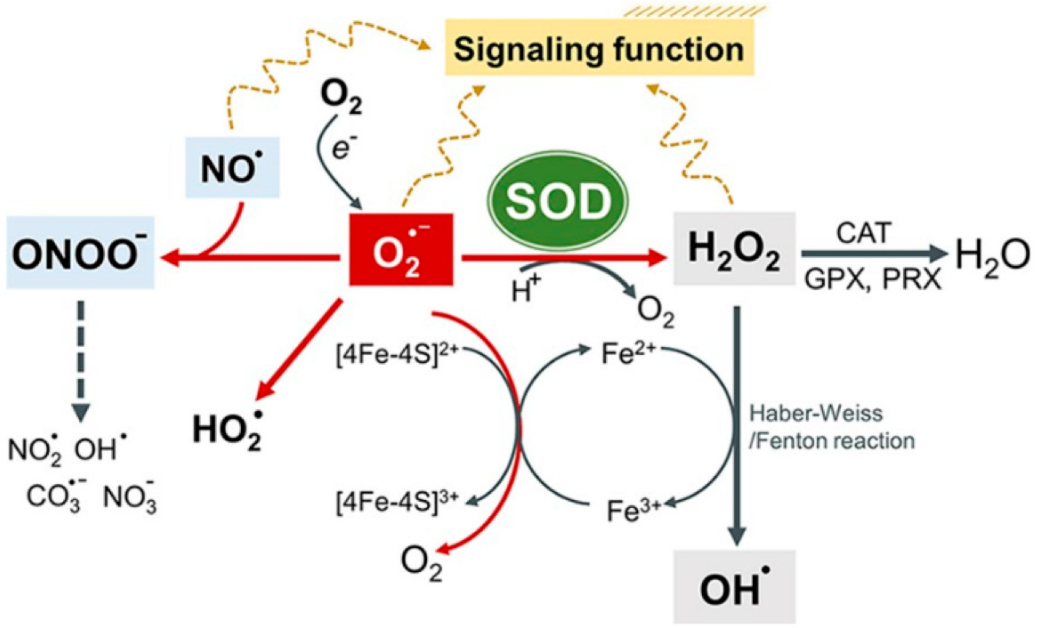

Figure 14: Reactions of superoxide
Dismutation of superoxide ($O_2^{\bullet-}$) by superoxide dismutases (SOD) generates hydrogen peroxide (H_2O_2) and molecular oxygen (O_2). From there, catalases (CAT), glutathione peroxidases (GPx), and peroxiredoxins (PRX) can convert H_2O_2 to water. It is also possible for H_2O_2 to react with metals, such as iron, to generate a more reactive ROS, the hydroxyl radical ($OH^{\bullet}$). The reaction of H_2O_2 with a redox-active metal is termed the Fenton/Haber-Weiss reaction. Prior to SOD dismutation, superoxide can also react with nitric oxide ($NO^{\bullet}$) to produce peroxynitrite ($ONOO^-$). Peroxynitrite is known to lead to cell death, but its decomposition can also yield highly oxidizing molecules including $NO_2^{\bullet}$, $OH^{\bullet}$, $CO_3^{\bullet-}$, and the stable $NO_3^{\bullet-}$. Due to the formation of peroxynitrite, elevated levels of superoxide ultimately have the ability to decrease nitric oxide bioavailability and thereby peroxynitrite toxicity. Finally, $O_2^{\bullet-}$) itself can reduce ferric (Fe^{3+}) to ferrous (Fe^{2+}) iron in essential iron-sulfur centres of proteins. This causes enzymatic inactivation and loss of Fe^{2+} from these proteins. This Fe^{2+} can then further fuel Fenton chemistry. The protonation of $O_2^{\bullet-}$ can also from the hydroperoxyl radical ($HO_2^{\bullet}$) (Wang et al., 2018).

Superoxide is both a by-product of metabolic processes (e.g. mitochondrial respiration) and the intended product of enzymes dedicated to superoxide formation (e.g. NADPH oxidases) (Figure 15)[319]. Reactive species, such as superoxide and its derivatives, are essential for signalling, despite being potentially toxic. These oxygen-containing compounds are involved in cell

proliferation, migration, and differentiation, and pathogen defence amongst other cellular processes[60, 654, 655]. Since superoxide does not readily cross cell membranes and is short-lived, it is thought to act locally to where it is produced. However, hydrogen peroxide, produced as a result of superoxide dismutation, is more stable, uncharged, and freely able to pass through cell membranes, qualities making it an extremely versatile signaling molecule[319, 656]. SOD isoforms are found in distinct subcellular compartments, highlighting how changes in SOD activity can lead to H_2O_2 concentration gradients and activation of specific redox-sensitive pathways.

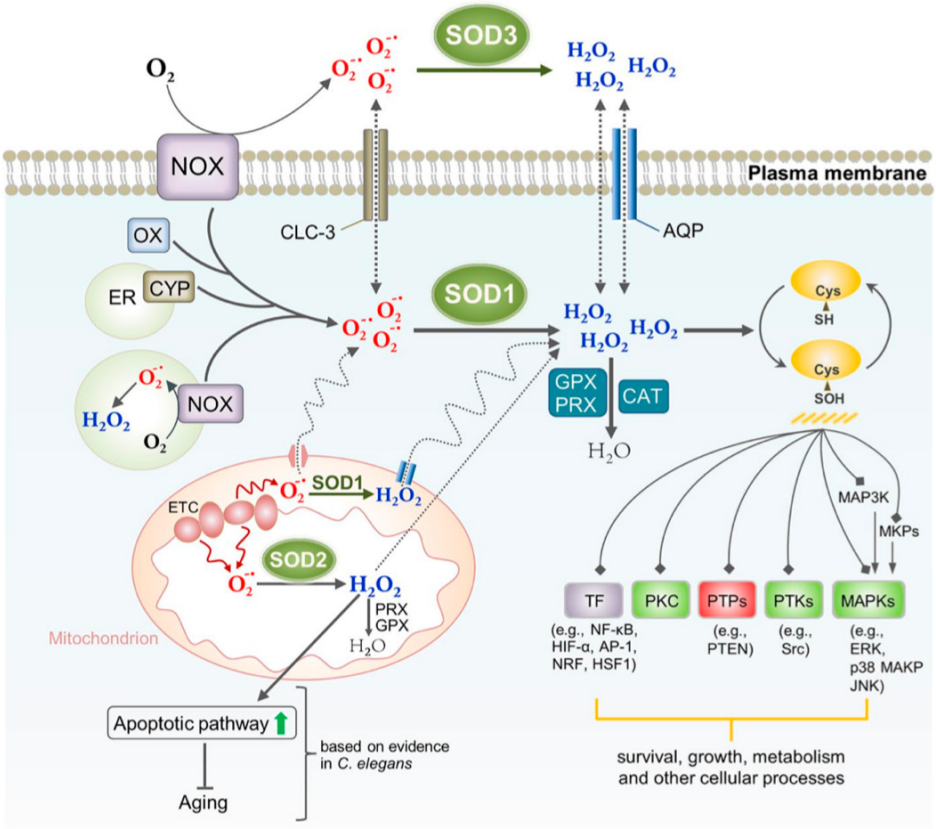

Figure 15: SOD-dependent mammalian ROS signaling
In mammals, numerous processes lead to superoxide ($O_2^{\bullet-}$) formation including, but not limited to, the mitochondrial electron transport chain (ETC), NADPH oxidases (NOX), cytosolic xanthine oxidase (OX), and cytochrome P450-monooxygenases (CYP) in the endoplasmic reticulum. NOX is a membrane-bound enzyme, found in the plasma membrane and in vesicle membranes and produces superoxide both intra- and extra-cellularly[657]. Extracellular $O_2^{\bullet-}$ has two methods of entering the cell – first via chloride channel-3 (CLC-3) or via conversation to H_2O_2 by SOD3, after which it can freely traverse into the cell using aquaporin channels (AQP) and go on to initiate cellular signalling[67, 658]. H_2O_2 has been the focus of ROS signalling studies as it is known to

oxidatively modify redox-sensitive cysteines in proteins and thereby alter protein function. Well-accepted targets of ROS signalling include protein phosphatases (PTP), nonreceptor protein tyrosine kinases (PTK), transcription factors (TF), mitogen-activated protein kinases (MAPK), and protein kinase C (PKC). Unlike H_2O_2, the signalling function of $O_2^{\bullet-}$ remains largely unknown. Additionally, compartmentalization of SOD expression is a key mechanism for spatial and temporal control of ROS homeostasis and therefore ROS signaling (Wang et al., 2018).

Surprisingly considering how ubiquitous SODs are in organisms, organisms can survive with low SOD expression, notably this has been well demonstrated in *C. elegans* that can live just as long as their wild-type controls, although lacking all of their five SOD isoforms[16]. Important for this chapter is the conundrum of *Sod1*$^{-/-}$ (germline knockout) mice and embryonic fibroblasts. Huang et al. show that *Sod1*$^{-/-}$ mouse embryonic fibroblasts (MEFs) have, on average, 4 to 10 times more apoptotic cells (labeled by biotinylated dNTP with terminal transferase (TdT)) than *Sod1*$^{+/+}$ MEFs. After only 48 hours in culture, culture plates of *Sod1*$^{-/-}$ MEFs were mostly remnants of apoptotic cells and healthy cells were rare (Figure 16)[5]. In contrast, *Sod1*$^{-/-}$ mice are alive, with a mean lifespan of 20.8 months[17]. To better investigate the mechanisms of cell death in mammalian cells lacking *Sod1 in vitro* and to understand how *Sod1*$^{-/-}$ mice are alive, we engineered a conditional (floxed) allele of *Sod1*, from which we derived *Sod1* KO MEFs by retroviral-mediated expression of *Cre* recombinase. Control of gene expression with inducible systems allows for both spatial and temporal regulation of a gene. This chapter characterizes inducible knockout *Sod1* cells in an attempt to shed light on the balance between the beneficial and harmful effects of reactive oxygen species in mammalian systems.

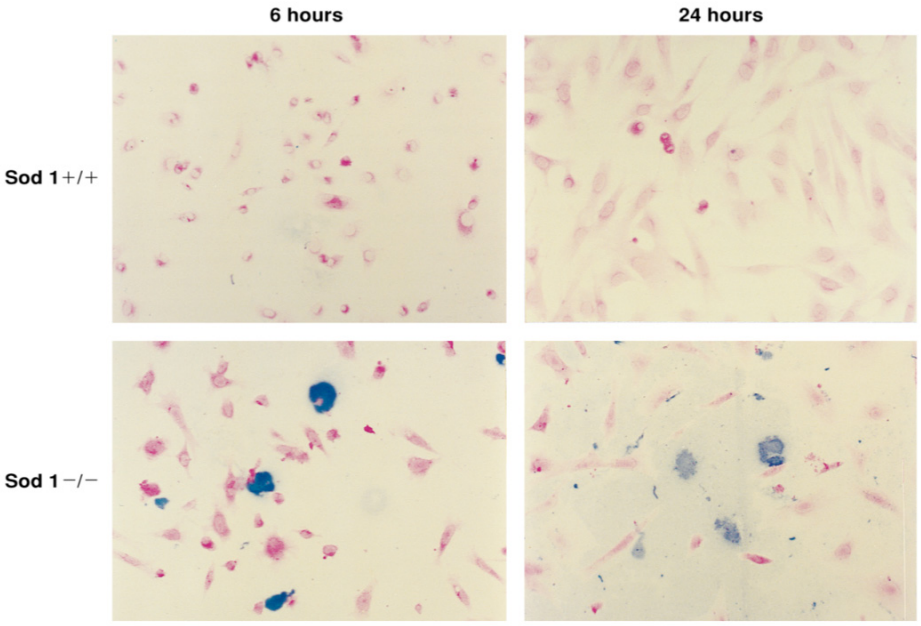

Figure 16: *Sod1*$^{-/-}$ mouse embryonic fibroblasts undergo apoptotic cell death
Cell death analysis of *Sod1*$^{+/+}$ and *Sod1*$^{-/-}$ MEFs. On average, *Sod1*$^{-/-}$ MEFs had 4 to 10 times more apoptotic cells (labeled by biotinylated dNTP with terminal transferase (TdT), blue) than *Sod1*$^{+/+}$ MEFs. By 48 hours, most of what remains on the plate is cellular debris (Huang et al., 1997).

3. Material and Methods

a. Reagents and chemicals

Dulbecco's Modified Eagle Medium (DMEM), fetal bovine serum (FBS), and cell culture phosphate buffer saline (PBS, 1x) was obtained from Wisent. Trypsin-EDTA (0.05% and 0.25%) were both obtained from Gibco. Lipofectamine 2000 and OptiMEM Reduced Serum Medium (no phenol red), used for transfections, were purchased from Invitrogen. All other reagents and chemicals, excluding L-NAME and FeTPPS, were purchased from Sigma-Aldrich. L-NAME and FeTPPS were both purchased from Cayman Chemicals.

b. Mice

Conditional *Sod1* knockout mice (*Sod1*$^{loxP/loxP}$) were generated in collaboration with InGenious Targeting Laboratory in Stony Brook, New York. Targeted iTL BA1 (C57BL/6 x 129/SvEv) hybrid embryonic stem cells were microinjected to C57BL/6 blastocysts. The target region of *Sod1*

includes exons 2 and 3, which contain 3 of the 4 essential copper binding sites for superoxide dismutase function. The resulting chimeras with the highest percentage of agouti coat colour were crossed with C57BL/6 FLP mice. These crosses were necessary to remove the Neomycin cassette. Agouti mice are grey in coloration, but each strand of fur is both partly yellow and partly black. Tail DNA from these mice was analyzed using PCR to ensure deletion of Neomycin cassette. Then, the resulting heterozygous mice were mated to C57BL/6 (wild type mice). The genotype of their offspring was also confirmed using PCR, as described below, to ensure the absence of both the Neomycin cassette and FLP transgene. These mice were then interbred to generate homozygous *Sod1*$^{loxP/loxP}$ mice. Mice with the inducible *KRas*^{LSL} allele has been previously described by Tuveson, et al. and can be obtained from The Jackson Laboratory. All mice were handled in accordance with recommendation of the Canadian Council on Animal Care and studies were conducted under an approved Animal Utilization Protocol (AUP). This protocol was approved by the animal Care and Use Committee of McGill University. The mice were house in the pathogen-free animal facility at McGill University (CMARC). All experimental mice were sacrificed using isoflurane (Baxter Corporation) as an anaesthetic, followed by cervical dislocation for euthanasia.

c. Genotyping and detection of *Sod1*^{loxP} allele

All mice were genotyped via PCR amplification of genomic DNA isolated from tails. ~1-2mm mouse tail clippings were boiled in 25mM NaOH, 0.2mM EDTA (Solution I) at 100°C for 20 minutes. Immediately after boiling, the DNA extraction reaction is neutralized with 40mM Tris-HCL pH 5.5 (Solution II). 60µL of both Solution I and II are used for DNA extraction from a single 1-2mm piece of tail. After the reaction is neutralized with Solution II, the tails should be spun down. The floxed *Sod1* allele was amplified using primer #1 (ALTLOX-forward): 5' - CTCCACAGGCAGTAGGACAA - 3' and primer #2 (ALTLOX-reverse): 5'- CAACACAACTGGTTCACCGC - 3'. The resulting wild-type product size is 496bp, whereas the loxP product size is 541bp. PCR reactions were performed using NEB's OneTaq DNA polymerase. Genotyping PCR program is: 95°C for 3 minutes (initial denaturation), 35 cycles of 95°C for 30 seconds, 60°C for 30 seconds, and 72°C for 60 seconds, followed by 72°C for 5 minutes (final extension), and hold amplified

products at 4°C. For mouse embryonic fibroblasts obtained from *Sod1*$^{loxP/loxP}$ mice, embryonic DNA extraction was performed using the QIAGEN DNeasy Blood & Tissue Kit and using their protocol for DNA extraction from animal tissues. To detect the recombined *Sod1*^{loxP} allele in genomic DNA isolated from mouse embryonic fibroblasts (MEFs) from the mice discussed above, different primers, but the same PCR program were used. The recombined *Sod1*^{loxP} allele was detected with primer #3 (NDEL2): 5'- GGG GCT TTA GTA AAG TAT GCC AGC TC - 3' and primer #4 (LOX1): 5'- CTC CAC AGG CAG TAG GAC AAA GG - 3'. The resulting band of a successfully excised allele of *Sod1* is 600bp. PCR products were visualized by gel electrophoresis on a 2% agarose (FroggaBio) gel at 120V until satisfactory resolution and band separation was reached (~30 minutes).

d. Genotyping and detection of *KRas*^{LSL} allele

All mice and the MEFs isolated from *KRas*^{LSL} mice were genotyped using the same protocol of DNA isolation as for *Sod1*$^{loxP/loxP}$. The *KRas*^{LSL} allele was amplified using primer #5 (KRasWT_F): 5' - GTCGACAAGCTCATGCGGG - 3', primer #6 (KRasG12D_F): 5' - CCATGGCTTGAGTAAGTCTGC - 3', and primer #7 (KRas_R): 5' - CGCAGACTGTAGAGCAGCC - 3'. The resulting bands are ~600bp for the LSL allele and ~507bp for the wild-type allele of *KRas*. Genotyping PCR program is: 95°C for 3 minutes (initial denaturation), 35 cycles of 95°C for 30 seconds, 60°C for 30 seconds, and 72°C for 60 seconds, followed by 72°C for 5 minutes (final extension), and hold amplified products at 4°C. PCR products were visualized by gel electrophoresis on a 2% agarose (FroggaBio) gel at 120V until satisfactory resolution and band separation was reached (~30 minutes).

e. Preparation of mouse embryonic fibroblasts

Sod1$^{loxP/loxP}$ males and females were placed together and the females were checked every morning for a copulation/vaginal plug (white in appearance). The morning a copulation plug is found is termed embryonic day 0.5 (E0.5) and the female with the plug is subsequently moved to a separate cage. The copulation plug indicates that a mating has occurred and the female in question could be pregnant. The method of mouse embryonic fibroblasts (MEFs) isolation is based on that described by Robertson and colleagues in 1987[659]. In short, embryos were removed

from pregnant females at E13.5 and placed into a dish with PBS. Embryos are first separated from their lining. In PBS, the head was removed from each embryo and reserved for genotyping. In addition to removal of the head, soft tissues, such as the liver (a bright red spot in the embryo) were removed. These tissues have the possibility of being further along in their differentiation than the remainder of the embryo. Next, each embryo was placed into a separate well of a 6-well plate and 500µL 0.25% trypsin. Embryos were then crushed using autoclaved scissors. After shearing, an additional 500µL 0.25% trypsin was added to each well and the embryos were incubated at 37°C for 20 minutes. 20 minutes later, cells were pipetted up and down in each well and then mixture was transferred, one well at a time, to separate plates containing 10mL DMEM (10% FBS, 1% antimycin A). These freshly isolated MEFs were incubated at 37°C overnight. The following day, the media on these plates was changed to remove any debris from MEF isolation process. Cells can then be cultured and expanded in DMEM (10% FBS, 1% antimycin A). *KRas*$^{LSL/+}$ MEFs were isolated using the same protocol as for the isolation of *Sod1*$^{loxP/loxP}$ MEFs.

f. Construction of retroviral vector and retroviral infection

The retroviral vector used to induce expression of Cre recombinase in mouse embryonic fibroblasts is a pBabe-Cre-Puro retroviral vector. It was constructed by subcloning the cDNA of Cre recombinase into EcoRI and SaII sites of a pBabe-Puro retroviral vector. To produce the retroviruses used in these experiments, PhoenixTM-Eco virus packaging cells, provided by Cedarlane Labs, were used. Separate plates of PhoenixTM-Eco cells, at 60-80% confluence, were transfected with either pBabe-Cre-Puro vector DNA or empty pBabe-Puro vector DNA, at a concentration of 20µg plasmid DNA/100mm pplate. All transfections were conducted using Lipofectamine 2000 (Invitrogen) and by following the manufacturer's protocol. 48-hours after the introduction of plasmid DNA to PhoenixTM-Eco cells, virus-containing media was taken, filtered, and placed on *Sod1*$^{loxP/loxP}$ mouse embryonic fibroblasts. This infection procedure of introducing virus-containing media onto MEFs was repeated for a total of three times – twice on the first day and then once on the second day. Infected MEFs were then incubated in puromycin-containing DMEM (10µg/mL) for two days. Puromycin selects for only cells that have been

infected and stably express the viral DNA. MEFs obtained after retroviral infection were always used at passage numbers below 12.

g. Cells and tissue culture

All cells were incubated at 37°C in 5% CO_2. Mouse embryonic fibroblasts were grown and maintained in Dulbecco's Modified Eagle's Medium (DMEM) supplemented with 10% fetal bovine serum (FBS) and 1% antimycin A. PhoenixTM-Eco cells are plated on poly-D-lysine (Sigma) coated plates prior to transfections. If cells are frozen, they are frozen in 70% DMEM, 20% FBS, and 10% DMSO.

h. Cell viability assays

For crystal violet assays, cells (1.5 x 10^4 cells/well for MEFs) were plated in 12-well dishes in triplicates. The day cells are seeded is termed day 1. Plates are then washed with PBS and fixed in 4% paraformaldehyde (Cedarlane) on each day where readings were to be taken. After cells were fixed, cells are stained with 0.5mL of 0.1% crystal violet (Sigma) per well and the crystal violet was allowed to sit on fixed cells for 30 minutes. Plates are then repeatedly rinsed with tap water to remove excess crystal violet dye and then left to air dry. Crystal violet is then extracted from each well using 1mL 10% acetic acid and 100µL of this mixture is transferred to a 96-well plate. Using a Bio-Tek PowerWave XS microplate reader/spectrophotometer, absorbance is read at 590nm. For AlamarBlue cell viability assays, also referred to as resazurin assays throughout this thesis, cells are seeded, in triplicates, at a concentration of 2.5 x 10^3 into 96-well plates. For rescue experiments, various different substances were added to growth media and then cell viability assays could be performed at any time point. After at least 3 days in culture (occasionally more), AlamarBlue assay was completed according to manufacturer's instructions. In short, on the day of cell viability readings, AlamarBlue reagent is diluted 100x in DMEM and 100µL of this mixture is added to each well. The 96-well plates are then incubated for at least 4 hours (can be incubated up to 24 hours) and absorbance is read using plate reader mentioned above. Absorbance of the AlamarBlue reagent is read at 570nm and an absorbance reading of 600nm is used as a reference wavelength.

i. Superoxide dismutase activity

Superoxide dismutase activity was measured, according to manufacturer's instructions, using the Superoxide Dismutase Assay Kit from Cayman Chemical.

j. Microscopy

For fluorescence microscopy, cells were plated onto glass coverslips in the bottom of each well of a 12-well plate. These coverslips had been coated with poly-D-lysine. After leaving cells to adhere to coverslips overnight, the fluorescent dye of choice is then introduced and incubated with cells according to manufacturer's instructions. The cells were then fixed for 10 minutes in 4% paraformaldehyde. After 10 minutes of fixation, coverslips are washed twice in PBS to ensure removal of any leftover fixative. The coverslips were then mounted on slides using Prolong Anti-Fade Reagent (Invitrogen) and imaging was done using an Olympus BX63 microscope. Live cell images, used to visually track cell growth, were taken on an Olympus CKX41 microscope.

k. Detection of apoptotic cells

Detection of apoptotic cells was achieved by use of a fluorogenic dye, CellEvent Caspase-3/7 Green Detection Reagent (ThermoFisher). The fluorescence of this substrate is only activated by caspase 3/7, caspases associated with activation of the apoptotic machinery of cells. To stain cells, 2 drops (2-8 μM) of the reagent are added per 1mL of DMEM culture media. The media containing the reagent was incubated with cells for 30 minutes at 37°C. After this, cells are preserved in 4% paraformaldehyde for 15 minutes. They are then washed in PBS 3 times, for 5 minutes each wash. Finally, coverslips containing now stained and fixed cells are mounted using Anti-Fade reagent. Using the Olympus BX63 microscope, a bright-field image is first taken to ensure there are cells on the slide and then cells are imaged using an appropriate filter set, the same used for FITC and Alexa Fluor 488 dye. The excitation/emission maxima for this reagent is 502/530nm. Cells that fluoresce green have caspase activation and therefore have begun the apoptotic cascade.

l. RNA preparation and qRT-PCR analysis

Total RNA was extracted from mouse embryonic fibroblasts using TRIzol reagent (Invitrogen). 1µg of extracted RNA was then reverse transcribed to cDNA according to manufacturer's instructions with use of the QuantiTect Reverse Transcription Kit (Qiagen). Next, RT-PCR was performed using Qiagen SYBR Green and CFX96TM Real-Time PCR Detection System and C1000TM Thermal Cycler (BioRad). Primers for *Sod1* mRNA were Sod1-forward: 5' - GGCCGTACAATGGTGGTCC - 3' and Sod1-reverse: 5' - TGGTTTGAGGGTAGCAGATGAG - 3'. Primers for *Sod2* mRNA were Sod2-forward: 5' - ACCGAGGAGAAGTACCACGA – 3' and Sod2-reverse: 5' AGCGGAATAAGGCCTGTTGT - 3'. Primers for the mRNA of the housekeeping gene (control) β-actin were forward 5' - GGAGCACCCTGTGCTGCTCA - 3' and reverse 5' -GGATTCCATACCCAAGAAGGAAGGC - 3'. Data was analyzed using the $\Delta\Delta$Ct method and CFX MaestroTM Software (Bio-Rad)[660].

m. Cell lysis and protein quantification

For western blots using protein isolated from mouse embryonic fibroblasts, cells were lysed using CellLytic™ M buffer (Sigma). Cells were scraped off confluent 100mm plates, spun down to collect cell pellet, and this pellet was suspended in 200 µL of cell lysis buffer and then rocked at 4°C for 30 minutes. Lysed cells were then centrifuged for 10 minutes at 13,000g in an accuSpin Micro R microcentrifuge (Fisher Scientific). The protein-containing supernatant was removed and quantified using Bio-Rad Protein Assay Dye, according to manufacturer's instructions.

n. Western blotting

Total cell lysate samples were loaded into 12% running gel/5% stacking gel SDS-PAGE gels. These gels were initially electrophoresed at 70V until the stacking gel was cleared, then 120V for the remainder of the running time, and finally transferred onto nitrocellulose membranes (Bio-Rad). Membranes were blocked in 5% milk-PBS for 2 hours and then exposed to primary antibody overnight at 4°C. All antibodies were diluted in 5% milk-PBS. The following antibodies were used: anti-SOD1 (ab16831; dilution 1:2000), anti-SOD2 (ab13533; dilution 1:5000), anti-SOD3 (ab83108; dilution 1:1000). Control antibodies were all diluted 1:2000. They were one of the following: GAPDH (2118S Cell Signaling Technology (CST)), α-tubulin (2144S CST), or β-actin

(4967S CST). The next day, primary antibody mixtures were removed, and membranes were washed 3 times in PBS-0.05% Tween 20 (Sigma). Membranes were then incubated for 2 hours with anti-rabbit IgG, horseradish peroxidase (HRP)-linked secondary antibody (7074S CST) and ultimately developed using the GE Healthcare ECL Plus Western Blotting Detection System. Protein band signals were visualized using AFP Manufacturing Mini-Med 90.

o. Statistical analysis

All statistical analyses were performed using Prism 8 (GraphPad Software) using either ANOVA or t-tests, as appropriate. All data is presented at mean ± standard error of the mean (SEM). A result is considered significant when the p-value is less than 0.05.

4. Results

a. Generation of mice with floxed *Sod1* allele for conditional knockout

Germline *Sod1* knockout (KO) mice (*Sod1*$^{-/-}$) live a moderately shortened lifespan (~2 years of age)[17]. But, germline deletion of *Sod1* slows the growth rate of mouse embryonic fibroblasts to 25% that of their wild-type controls[5]. Furthermore, PC12 (rat adrenal medulla) cells with downregulated *Sod1* (via antisense oligonucleotides) do not survive in culture[661]. With a goal of understanding how the severe phenotype associated with SOD1 deficiency *in vitro* relates to the mild phenotype observed *in vivo*, we generated, in collaboration with the Dankort lab and inGenious Targeting Laboratory, conditional *Sod1* knockout (KO) mice where exons 2 and 3 are flanked by loxP (Figure 17b). LoxP sites allow for targeted excision of a segment of DNA by Cre recombinase[662]. Mice homozygous for floxed alleles of *Sod1* are indistinguishable from their wild-type littermates and if no excision of *Sod1* is induced, they develop normally.

b. Generation of inducible *Sod1* knockout mouse embryonic fibroblasts (MEFs)

Next, I generated *Sod1* knockout mouse embryonic fibroblasts (MEFs) using retroviral-mediated expression of Cre recombinase (pBabe-Puro-Cre) in MEFs isolated from *Sod1*$^{loxP/loxP}$ mice. For control, I also infected the same MEF lines used for the experiments with an empty vector

(pBabe-Puro). This ensures that the infection itself and the selection of successfully infected cells with puromycin (Puro denotes the presence of a puromycin resistance gene in the vector notation) are not responsible for any observed phenotypes in cells that express Cre recombinase. Knockout of the floxed *Sod1* allele upon retroviral infection with the Cre-expressing retrovirus was analyzed both by PCR and RT-PCR amplification of the intact or recombined *Sod1* alleles and by western blot (Figure 17c, and 26). Collectively, these results confirmed that the change of the floxed *Sod1* allele into a form lacking exons 2 and 3 (the knockout form of the allele) was complete. Hereinafter, these cells will be referred to as $Sod1^{loxP/loxP}$ knockout (KO) cells. The cells transfected with an empty vector will be referred to as $Sod1^{loxP/loxP}$ control cells.

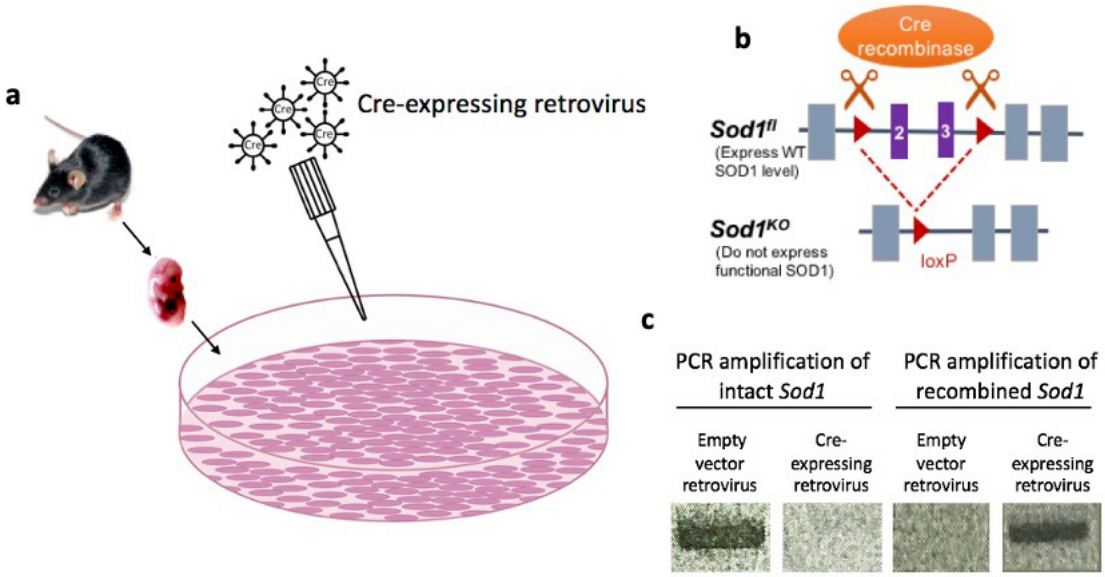

Figure 17: Generation of $Sod1^{loxP/loxP}$ knockout mouse embryonic fibroblasts.
a) Schematic of retroviral infection of mouse embryonic fibroblasts (MEFs) isolated from $Sod1^{loxP/loxP}$ mice. MEFs are express *Cre* recombinase due viral introduction of its DNA into cells. b) Upon expression of *Cre* recombinase, exons 2 and 3 are excised from *Sod1* to generate a stable recombinant *Sod1* lacking those exons. c) PCR amplification of intact *Sod1* and recombined *Sod1* confirms knockout of *Sod1* in $Sod1^{loxP/loxP}$ MEFs expressing *Cre* recombinase. Cells treated with empty-vector retrovirus showed a band for intact *Sod1* only and cells treated with Cre-containing retrovirus showed only a band for recombined *Sod1*.

c. Viability of inducible *Sod1* knockout MEFs

As expected, $Sod1^{loxP/loxP}$ KO MEFs undergo cell death, just like $Sod1^{-/-}$ MEFs (Figure 18)[563]. Cell viability was assessed by visual inspection of the cells by quantitative resazurin- and crystal violet-

based cell viability assays (Figure 19) [663]. These MEFs undergo apoptotic cell death shortly after *Sod1* excision by Cre recombinase, as confirmed by a caspase 3/7 detection assay (Figure 20). This assay takes advantage of a cell-permeable fluorogenic substrate that requires cleavage of a 4-amino acid peptide (DEVD) by activated caspases to reveal its fluorescent qualities. Upon cleavage of the DEVD peptide, the reagent can bind to DNA and brightly label apoptotic cells. Caspase activation is associated with stimulation of the apoptotic machinery[664]. If a cell produces green fluorescence, as seen in the majority of *Sod1*$^{loxP/loxP}$ KO MEFs, there is activation of its apoptotic machinery. If a cell does not fluoresce, as with *Sod1*$^{loxP/loxP}$ control cells, these are viable and actively dividing cells. Thus, we conclude that *Sod1*$^{loxP/loxP}$ KO MEFs are not viable and cannot proliferate *in vitro*.

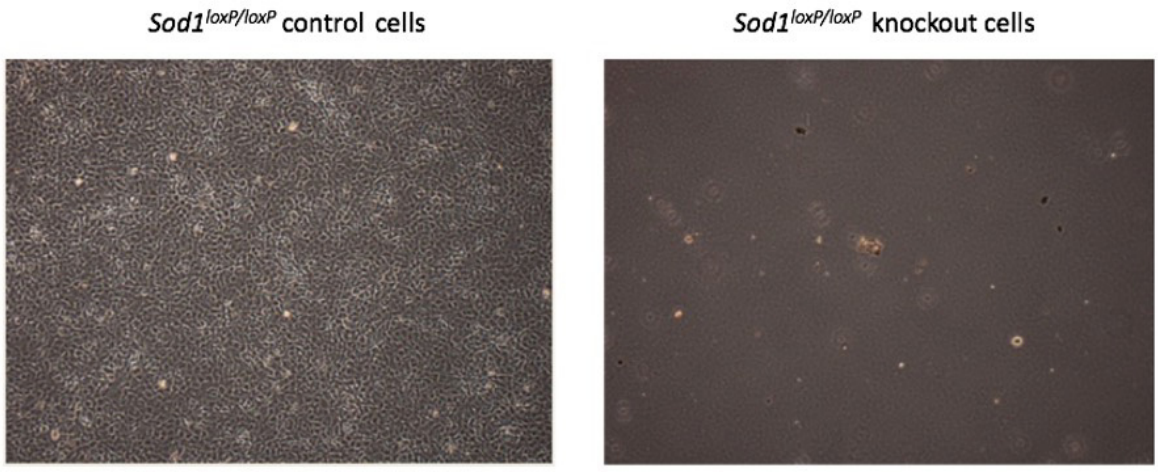

Figure 18: Induction of *Sod1* knockout in mouse embryonic fibroblasts leads to cell death.
Microscope mages comparing the viability of *Sod1*$^{loxP/loxP}$ KO MEFs to wild-type MEFs, 1.5 weeks post-transduction. *Sod1*$^{loxP/loxP}$ KO MEFs, unlike *Sod1*$^{loxP/loxP}$ control MEFs, fail to survive in culture.

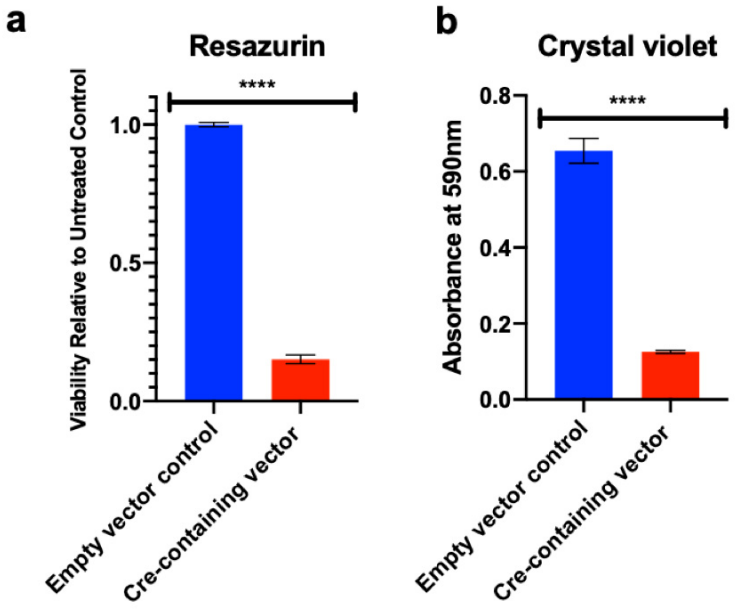

Figure 19: Viability of *Sod1*$^{loxP/loxP}$ knockout mouse embryonic fibroblasts.
Cell viability of *Sod1*$^{loxP/loxP}$ MEFs measured by a) resazurin assay and b) crystal violet. The resazurin assay is a colorimetric assay that measures the metabolic capability of cells. In other words, only live cells can reduce the non-fluorescent blue resazurin put on cell culture to the fluorescent red resorufin. The amount of resorufin created is directly proportional to the number of live cells. The crystal violet assay makes use of a blue dye to stain cells that are attached to cell culture plates. This assay assumes that non-adherent cells are cells undergoing cell death, which for mouse embryonic fibroblasts is true. The crystal violet stain binds to ribose-based molecules, such as nuclear DNA.

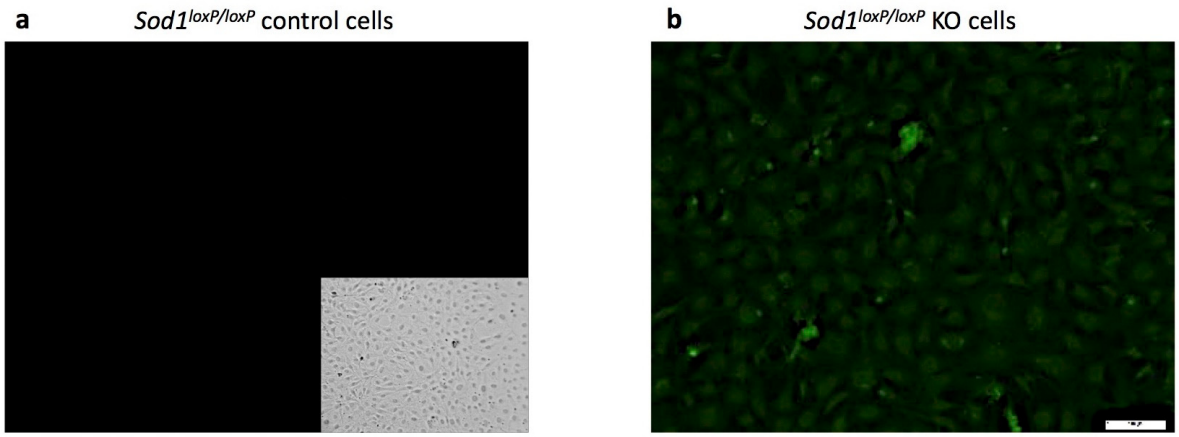

Figure 20: *Sod1*$^{-/-}$ mouse embryonic fibroblasts (MEFs) and *Sod1*$^{loxP/loxP}$ knockout MEFs both undergo apoptotic cell death.
Cell death analysis of *Sod1*$^{+/+-}$ and *Sod1*$^{-/-}$ MEFs showed that on average, *Sod1*$^{-/-}$ MEFs had 4 to 10 times more apoptotic cells (labeled by biotinylated dNTP with terminal transferase (TdT), blue) than *Sod1*$^{+/+}$ MEFs. By 48 hours, most of what remains on the plate is cellular debris (Huang et al., 1997). CellEvent Caspase 3/7 Green Detection Reagent was used to assess caspase activation in *Sod1*$^{loxP/loxP}$ control and knockout (KO) cells. This reagent is a fluorogenic substrate that is activated only by caspase 3 and 7. Caspases active in apoptotic cells cleave the DEVD peptide from the intrinsically non-fluorescent reagent. The DEVD peptide inhibits the ability of the dye to bind to DNA. Once cleaved, the dye can bind to DNA and yields a fluorogenic response. Fluorescence was detected using a fluorescent microscope. Caspase activation is associated with the stimulation of the apoptotic machinery. Caspases were activated in *Sod1*$^{loxP/loxP}$ KO cells, but not in *Sod1*$^{loxP/loxP}$ control cells.

d. Rescue inducible *Sod1* knockout MEFs by L-NAME

Next, I attempted various treatments to rescue the viability of *Sod1*$^{loxP/loxP}$ KO MEFs. As expected, the addition of reactive oxygen species, by means of hydrogen peroxide (H_2O_2) addition, did not increase cell viability (Figure 21b). We did not anticipate increasing the levels of ROS to improve the viability of *Sod1*$^{loxP/loxP}$ KO MEFs because loss of SOD1 already means increased ROS levels, albeit levels of superoxide, rather than hydrogen peroxide. The reason to attempt rescue with hydrogen peroxide is because with less superoxide dismutase, less superoxide is transformed to hydrogen peroxide, which, although a ROS molecule, is also a well-established signaling molecule. I also found that antioxidants, which hypothetically can quench the presumably increased levels of superoxide, such as ascorbic acid (vitamin C), had no effect on the survival of *Sod1* KO MEFs (Figure 21c). Similarly, when I treated *Sod1*$^{loxP/loxP}$ KO MEFs with ascorbate and iron simultaneously to yield hydroxyl radicals ($OH^{\bullet}$), a pro-oxidant, cell death was unaffected

(Figure 21d). And finally, in the list of unsuccessful rescue attempts, the divalent chelator, clioquinol, also failed to prolong the viability of *Sod1* KO MEFs (Figure 21e).

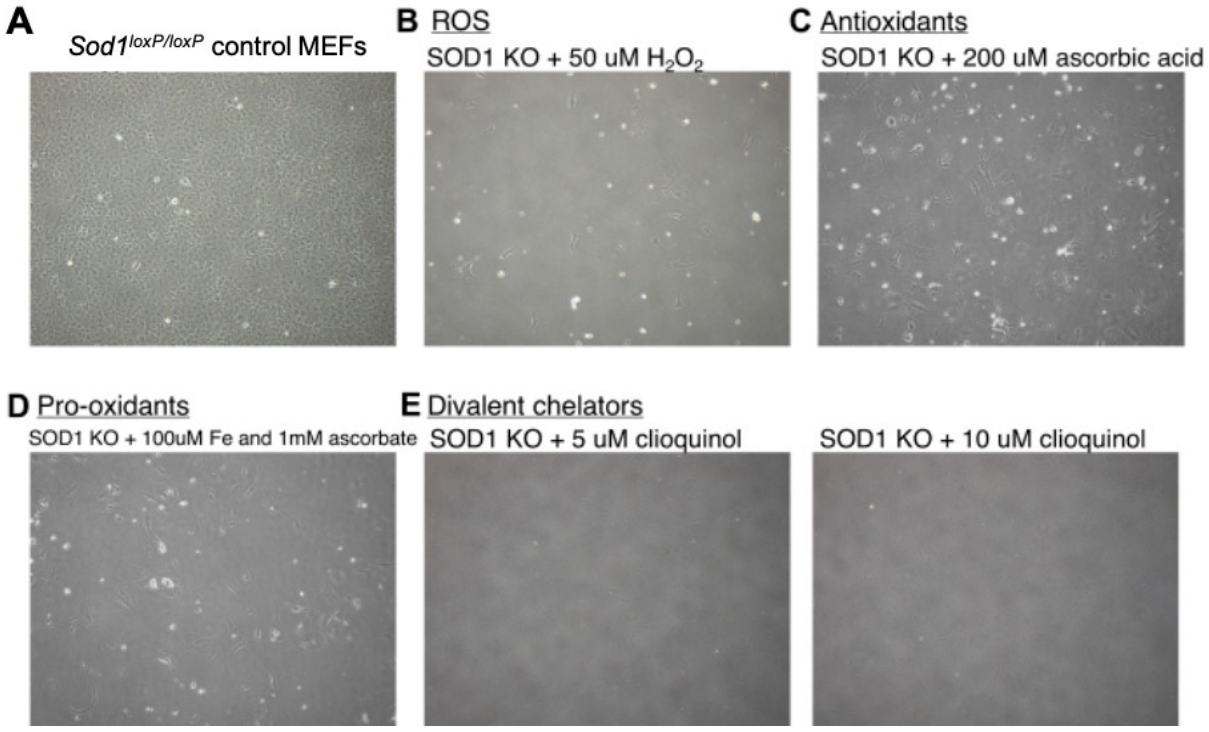

Figure 21: Unsuccessful rescue attempts for *Sod1*$^{loxP/loxP}$ KO MEFs.
Microscope images showing a) *Sod1*$^{loxP/loxP}$ control MEFs that thrive in culture. b) *Sod1*$^{loxP/loxP}$ KO MEFs cultured with hydrogen peroxide (H_2O_2), a reactive oxygen species (ROS), are not rescued c) *Sod1*$^{loxP/loxP}$ KO MEFs cultured in the presence of the antioxidant, ascorbic acid, are not rescued. d) *Sod1*$^{loxP/loxP}$ KO MEFs cultured in the presence of the hydroxide ion, a pro-oxidant formed from the reaction of iron (Fe^{2+}) with ascorbate, did not survive 1.5 weeks like control MEFs did. e) *Sod1*$^{loxP/loxP}$ KO MEFs cultured in the presence of the divalent chelator clioquinol were also not rescued.

Findings described in early literature indicated that the lethality associated with *Sod1* antisense knockdown in PC12 (rat adrenal medulla) cells was rescued by treatment with L-nitro-L-arginine methyl ester (L-NAME), a non-specific NOS inhibitor (Figure 22)[661]. I confirmed that L-NAME also rescues *Sod1*$^{loxP/loxP}$ KO MEFs (Figure 23). Likewise, I showed that 7-nitroindazole (7-NI), a nNOS-specific inhibitor, is effective for rescuing the viability of *Sod1*$^{loxP/loxP}$ KO MEFs (Figure 23). It can be concluded that nNOS is the pertinent NOS in MEFs.

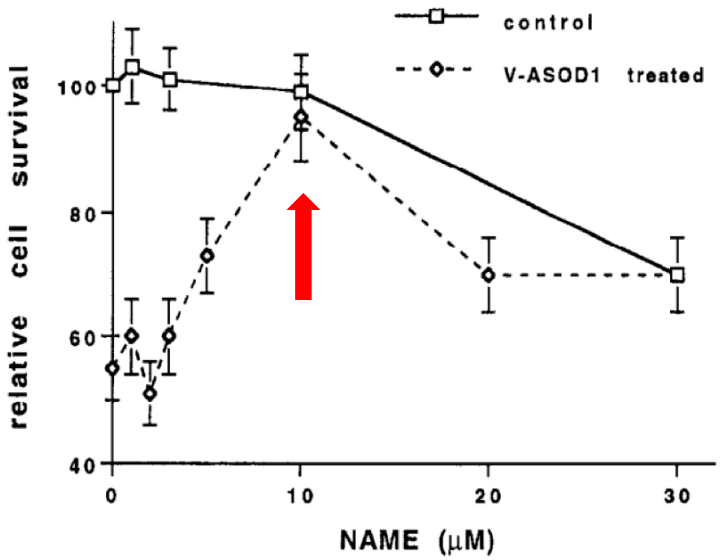

Figure 22: Downregulation of *Sod1* in rat adrenal medulla cells leads to cell death that can be rescued by a nitric oxide synthase inhibitor.
PC12 cells with low levels of SOD1, caused by downregulation of *Sod1* by exposure to an antisense oligonucleotide, undergo apoptotic cell death. This was the first finding to indicate that the reaction of superoxide with nitric oxide to form peroxynitrite could be responsible for this apoptotic cell death. Inhibitors of NO synthase (NOS), such as L-NAME (shown in the above figure), blocked cell death in this publication, whereas NO donors, compounds that stimulate the production of NO, accelerated cell death. In these experiments, cell viability was tracked by counting visible nuclei using a hemocytometer (Troy et al., 1996).

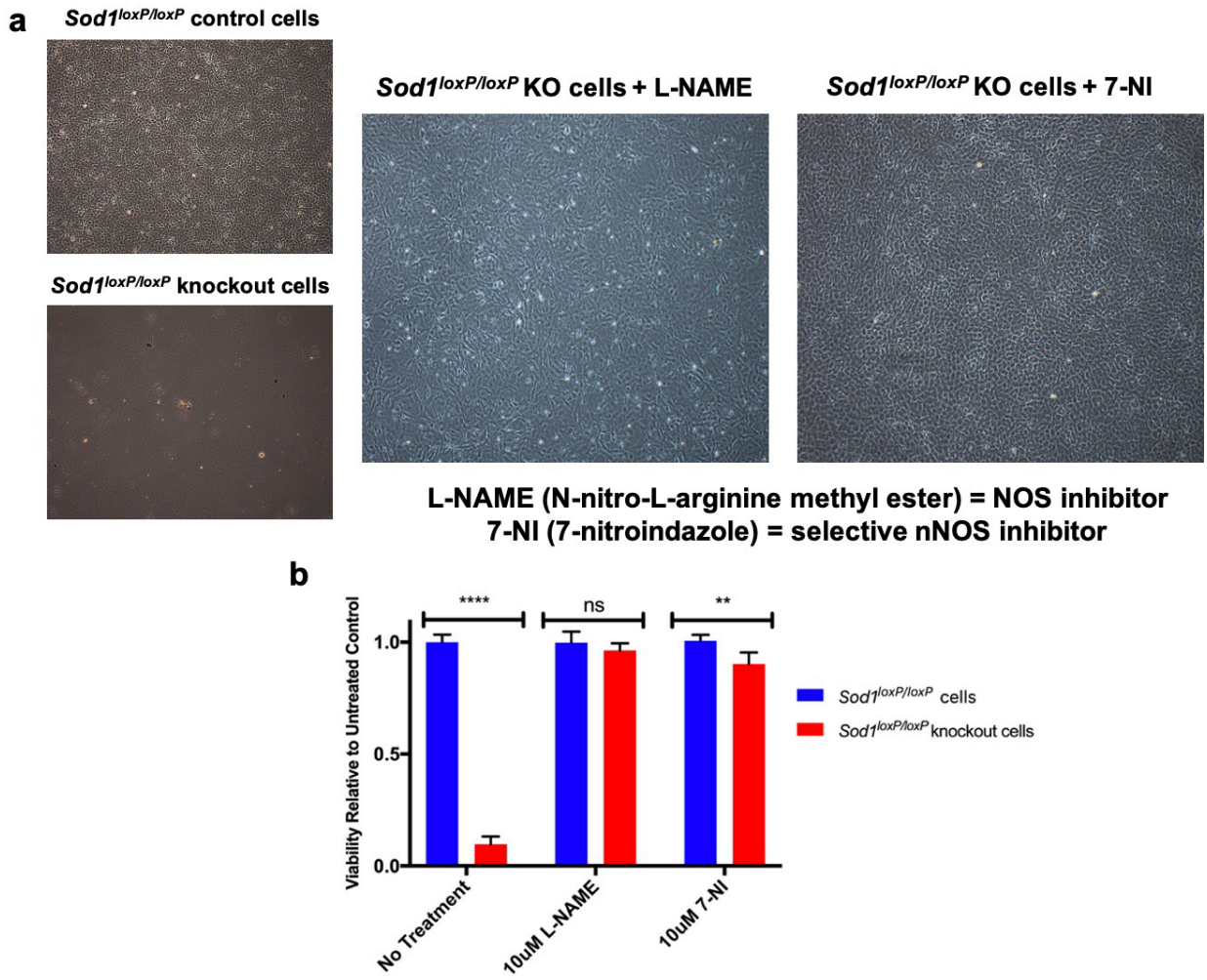

Figure 23: Nitric oxide synthase (NOS) inhibitors fully rescue viability of *Sod1*$^{loxP/loxP}$ knockout mouse embryonic fibroblasts.

L-NAME and 7-nitroindazole (7-NI) inhibit NOS. Inhibition of NOS leads to a reduced NO$^{\bullet}$ levels. NO$^{\bullet}$ spontaneously reacts with $O_2^{\bullet-}$ to form $ONOO^-$, a very toxic oxidant that causes cell death. With less NO$^{\bullet}$ to react with $O_2^{\bullet-}$, less $ONOO^-$ is formed. a) *Sod1*$^{loxP/loxP}$ KO MEFs cultured in the presence of 10 μM L-NAME, a nonselective NOS inhibitor, are successfully grown in culture for the same length of time as wild-type MEFs. 7-NI, a selective nNOS inhibitor, also rescues *Sod1*$^{loxP/loxP}$ KO MEFs. b) Cell viability assessed by visual inspection of the cells was confirmed by resazurin-based cell viability assays (and crystal violet, not shown).

As mentioned previously, NO$^{\bullet}$ spontaneously reacts with $O_2^{\bullet-}$ to form $ONOO^-$, a very toxic oxidant. *Sod1*$^{loxP/loxP}$ KO MEFs treated with 5,10,15,20-tetrakis-(4-sulfonatophenyl)-porphyrinato-Fe(III) (FeTPPS), a $ONOO^-$ decomposition catalyst, thrive like their *Sod1*$^{loxP/loxP}$ control cell

counterparts (Figure 24). The full rescue of *Sod1*$^{loxP/loxP}$ KO MEFs by FeTPPS indicates that $ONOO^-$ generation is the cause of cell death.

After observing that inducible *Sod1* KO MEFs die by apoptosis, by measuring caspase activation using the CellEvent Caspase 3/7 Green Detection Reagent, I also decided to attempt rescuing these cells with a caspase inhibitor (Figure 25). Carbobenzoxy-valyl-alanyl-aspartyl-[O-methyl]- fluoromethylketone (Z-VAD-FMK) is an irreversible caspase inhibitor that binds to the catalytic site of caspases thereby blocking their activity. Treatment with Z-VAD-FMK allows the cells to survive in culture as well as control cells, albeit with a depressed growth rate. This suggests that PN-induced cell death in *Sod1*$^{loxP/loxP}$ KO cells requires caspase activation, a crucial stage in apoptosis.

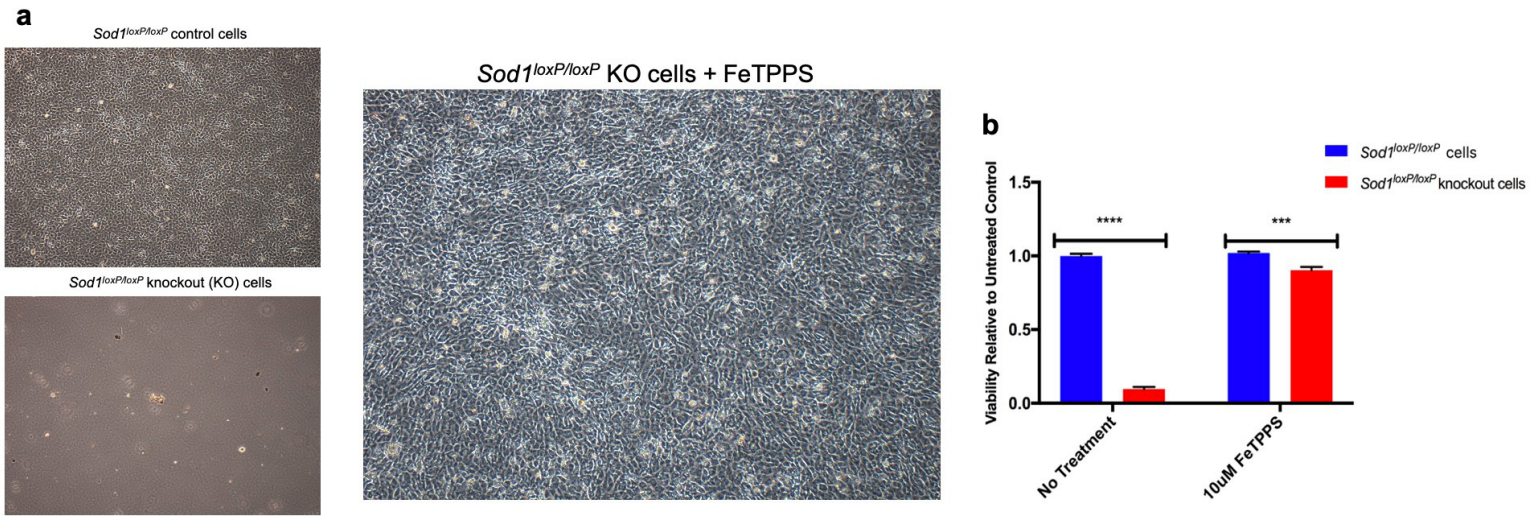

Figure 24: Peroxynitrite decomposition catalyst, FeTPPS, rescues *Sod1*$^{loxP/loxP}$ knockout MEFs. a) 5,10,15,20-tetrakis-(4-sulfonatophenyl)-porphyrinato-Fe(III) (FeTPPS), a peroxynitrite decomposition catalyst, increases the likelihood of isomerization of $ONOO^-$ to nitrate (NO_3^-). Nitrate is a harmless anion that is eliminated in the urine of mammals. FeTPPS rescues *Sod1*$^{loxP/loxP}$ knockout MEFs. These cells have a growth rate similar to that of control cells. b) Cell viability assessed by visual inspection of the cells was confirmed by resazurin-based cell viability assays (and crystal violet, not shown).

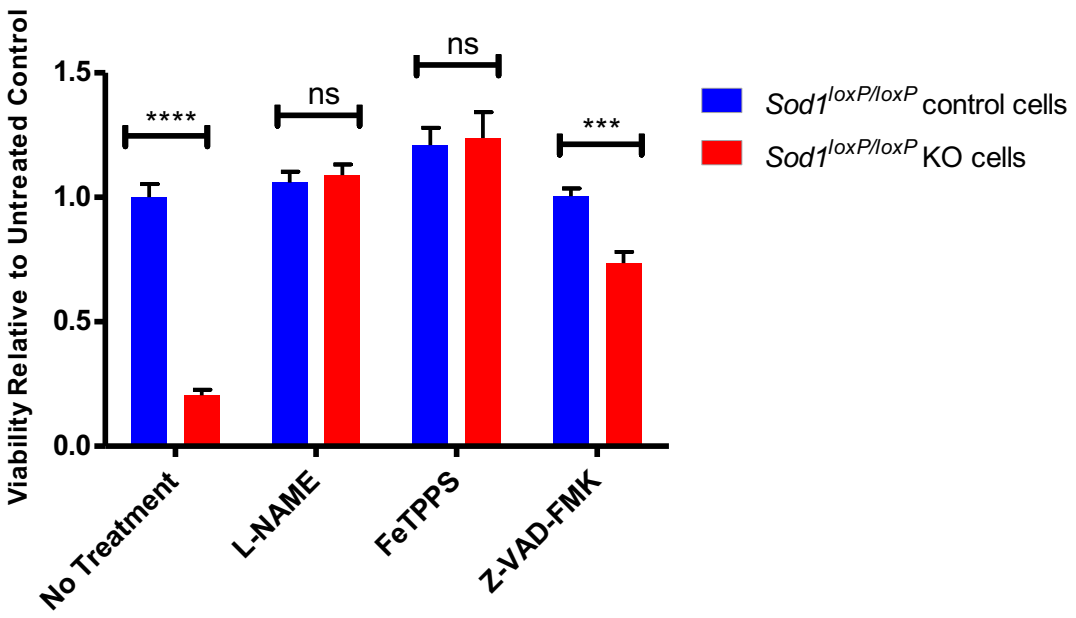

Figure 25: Resazurin cell viability assay on *Sod1*$^{loxP/loxP}$ cells.
Resazurin cell viability assays are based on the fact that nonfluorescent resazurin can only be reduced to fluorescent resorufin by dehydrogenases in viable, metabolically active cells. The absorbance of these cells is then measured using a spectrophotometer. The viability of *Sod1*$^{loxP/loxP}$ control cells and *Sod1*$^{loxP/loxP}$ knockout (KO) cells with no treatment (NT) is significantly different. Knockout cells do not survive beyond 1.5 weeks in culture, whereas control cells undergo normal cell division and can survive numerous weeks in culture. N-nitro-L-arginine methyl ester (L-NAME), a nitric oxide synthase inhibitor, rescues KO cells. The viability of L-NAME-treated KO cells resembles that of untreated control cells. 5,10,15,20-tetrakis-(4-sulfonatophenyl)-porphyrinato-Fe(III) (FeTPPS), a peroxynitrite (PN) decomposition catalyst, also restores the cell viability of KO cells. PN is formed from the reaction of superoxide with nitric oxide. Both KO and control cells treated with FeTPPS grow faster than untreated control cells. Carbobenzoxy-valyl-alanyl-aspartyl-[O-methyl]-fluoromethylketone (Z-VAD-FMK), a caspase inhibitor, partially rescues KO cells. KO cells treated with Z-VAD-FMK have a slower growth rate than control cells. Results are expressed as mean ± SEM. Two-way ANOVA with multiple comparisons: **** $p < 0.001$.

For all treatments, cell viability was assessed by visual inspection of the cells and by quantitative resazurin- and crystal violet-based cell viability assays[663]. The results suggest that SOD activity affects the bioavailability of $NO^{\bullet}$ by controlling the level of $O_2^{\bullet-}$ and thus the elimination of $NO^{\bullet}$ through $ONOO^-$ formation[376]. The intracellular concentrations of SODs are estimated to be very high. SOD concentrations must be so high to ensure low levels of residual

$O_2^{\bullet-}$ and $ONOO^-$ since the rate of $ONOO^-$ formation is three times faster than the rate at which SODs quench $O_2^{\bullet-}$ [375, 665].

e. Expression of SOD2 and SOD3 in inducible *Sod1* knockout MEFs

In *Sod1*$^{loxP/loxP}$ KO MEFs rescued by NOS inhibition, we expected that the loss of SOD1 would lead to a compensatory increase in the expression of the other two SOD isoforms. In contrast, shockingly, the expression of SOD2 and SOD3 is almost completely abolished in L-NAME treated *Sod1*$^{loxP/loxP}$ KO MEFs (Figure 26f). Moreover, these cells have dramatically low SOD activity and have impaired $O_2^{\bullet-}$ handling (Figure 27). At first, it seems hard to understand that these cells are fully viable and have a normal growth rate and appearance. The survival of the cells is in keeping with our hypothesis that it is not superoxide but peroxynitrite that is toxic. The absence of SOD2 and SOD3 likely does not increase peroxynitrite generation when $NO^{\bullet}$ levels are low, thanks to the L-NAME treatment.

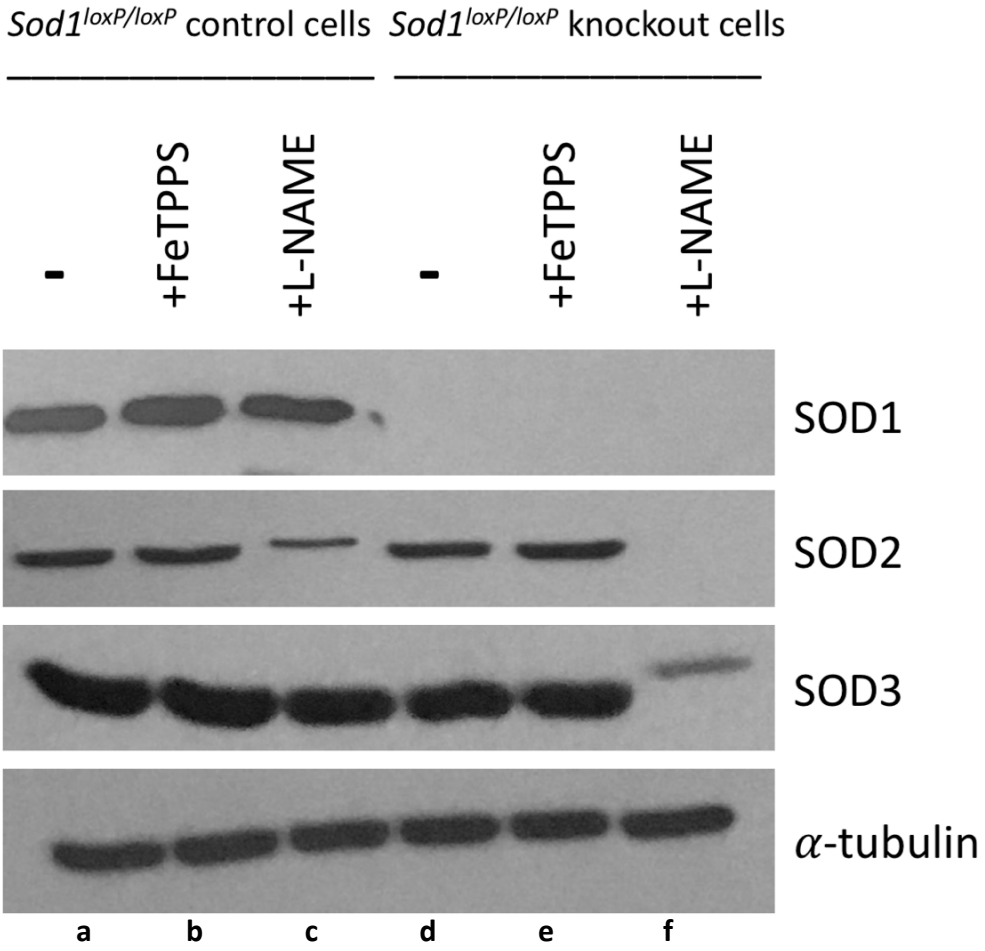

Figure 26: SOD levels in control cells and *Sod1*$^{loxP/loxP}$ knockout cells (before and after rescue).
Sod1$^{loxP/loxP}$ control cells are infected with an empty-vector retrovirus. *Sod1*$^{loxP/loxP}$ knockout cells are infected with a retrovirus containing *Cre* recombinase. *Cre* expression induces the excision of exons 2 and 3 of *Sod1*. a) Control cells with no treatments express all three isoforms of mammalian SODs. b) Levels of SOD expression in control cells are unaffected by treatment with FeTPPS. c) Treatment of control cells with L-NAME noticeably decreases the levels of SOD2 expression. d) KO cells with no treatments do not survive beyond 1.5 weeks in culture. *Sod1* KO cells lack SOD1 expression, as expected. However, when these cells are isolated immediately after infection and selection, they have SOD2 and SOD3 levels comparable to control cells. e) *Sod1* KO cells treated with FeTPPS have SOD2 and SOD3 levels comparable to control cells. f) *Sod1* KO cells treated with L-NAME show no SOD1 or SOD2 expression and little SOD3 expression.

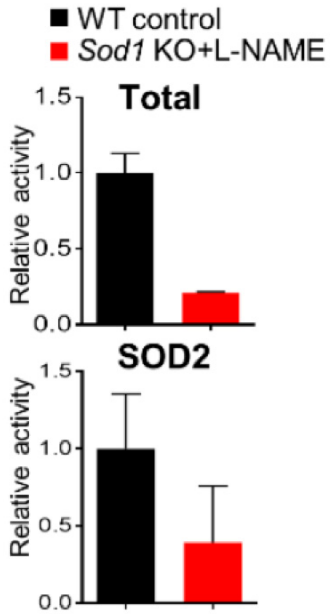

Figure 27: SOD activity in *Sod1* knockout MEFs.
The total SOD enzymatic activity and the mitochondrial SOD2 activity in *Sod1*$^{loxP/loxP}$ knockout cells rescued with L-NAME is dramatically decreased. This result is consistent with the loss of SOD expression observed in western blots.

Our current hypothesis of why SOD2 and SOD3 expression is abolished is the following: we surmise that L-NAME-rescued *Sod1*$^{loxP/loxP}$ KO MEFs have extremely low levels of $NO^{\bullet}$ due to two mechanisms – 1) the inhibition of NO formation and 2) the interaction of any remaining $NO^{\bullet}$ with the high levels of $O_2^{\bullet-}$ resulting from the absence of SOD1. Thus, very low levels of $NO^{\bullet}$ could be incompatible with SOD2/3 expression if $NO^{\bullet}$ is a sensitive positive regulator of their expression.

This conclusion is reinforced by the face that rescue with FeTPPS, a compound that catalyzes the decomposition of $ONOO^-$ but does not affect $NO^\bullet$ levels, does not change SOD2 or SOD3 expression (Figure 26d). Furthermore, when *Sod1*$^{loxP/loxP}$ control cells are treated with L-NAME, SOD2 expression is decreased (Figure 26c). This role of $NO^\bullet$ in the regulation of SOD expression has not previously been documented.

There is a positive correlation between the dose of L-NAME and the efficiency of *Sod1*$^{loxP/loxP}$ KO MEFs rescue (Figure 28a). The optimal dose of L-NAME to fully rescue *Sod1*$^{loxP/loxP}$ KO MEFs is 10μM. This allowed me to observe how increasing NOS inhibition affects SOD expression. Thus far, I have shown that SOD2 expression decreases with increasing doses of L-NAME (Figure 28b). These results strengthen our supposition that $NO^\bullet$ positively regulates SOD expression.

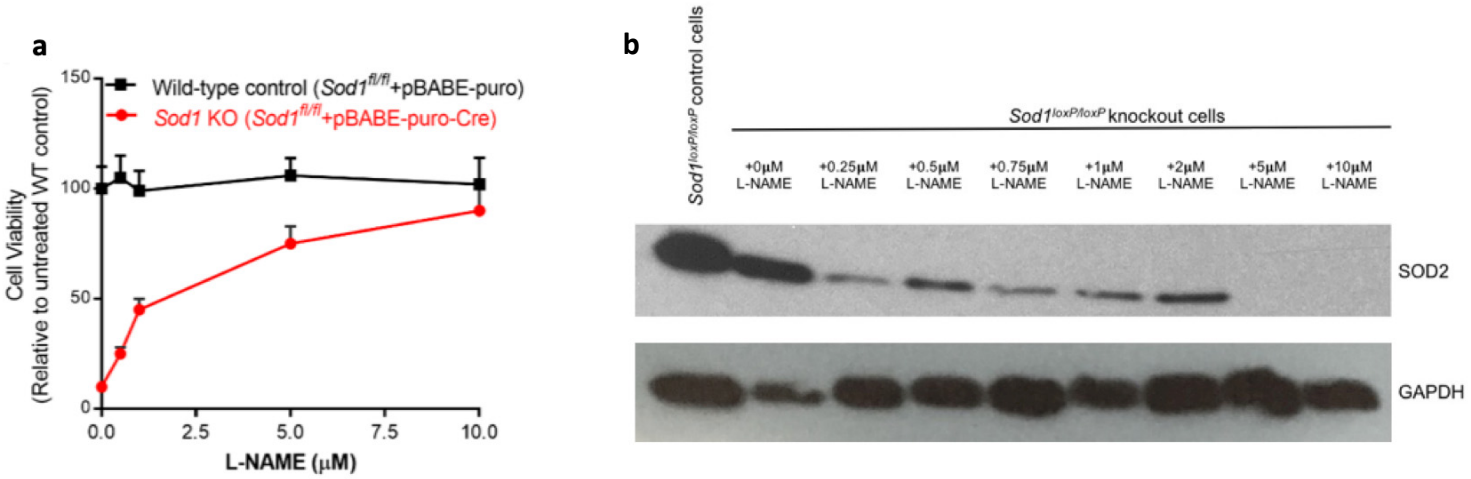

Figure 28: Dose-dependent effects of L-NAME on the survival of *Sod1*$^{loxP/loxP}$ knockout MEFs and SOD2 expression.
Cells were exposed to different doses of L-NAME immediately after the completion of infection with control or *Cre*-expressing virus. a) Cell viability was determined after 5 days of treatment. It is apparent that survival of *Sod1*$^{loxP/loxP}$ knockout cells is positively correlated to the dose of L-NAME. b) Cells were collected after 1 day of L-NAME treatment to ensure that in all treatment groups, most of the knockout cells were still alive. Expression of SOD decreases with increasing L-NAME doses.

f. The regulation of SOD expression is not transcriptional

We tested transcript levels of the recombined *Sod1* gene in L-NAME rescued *Sod1*$^{loxP/loxP}$ KO MEFs. The expression of the recombined gene, which makes a stable transcript, in knockout MEFs is equivalent to the expression of the intact *Sod1* gene in control cells (Figure 29c). These results provided preliminary evidence that perhaps the decrease of SOD expression observed when NO• levels are low is not transcriptional.

To further investigate, we checked the levels of *Sod2* transcript in L-NAME treated *Sod1*$^{loxP/loxP}$ KO MEFs where SOD2 and SOD3 are virtually undetectable. We found no change by qPCR in levels of *Sod2* transcript in the knockout cells (Figure 30). Once again, our observations support our assertion that NO• regulation of SOD is not via a transcriptional mechanism.

After our results showed that SOD regulation by NO• is not transcriptional, I evaluated past western blot results for any hints concerning SOD regulation. It became apparent that SOD may be regulated via post-translational modifications. In L-NAME treated *Sod1*$^{loxP/loxP}$ KO MEFs, SOD3 levels are dramatically decreased but more significantly, the remaining protein is heavier. An increase in molecular weight is observed by the upward shift of the protein in the gel (Figure 26e). This shift in molecular weight can also be seen in what remains of SOD2 expression in *Sod1*$^{loxP/loxP}$ control MEFs (Figure 26c). Post-translational modifications, or the covalent addition of functional groups to a protein, will increase the molecular weight [666]. At this time, the idea that SOD expression is regulated via post-translational modification is still very much a hypothesis. In our western blots, while we have seen an upward shift in SOD2 and SOD3 bands many times, it is not always the case. We have yet to work out the conditions under which this upward shift can be seen systemically.

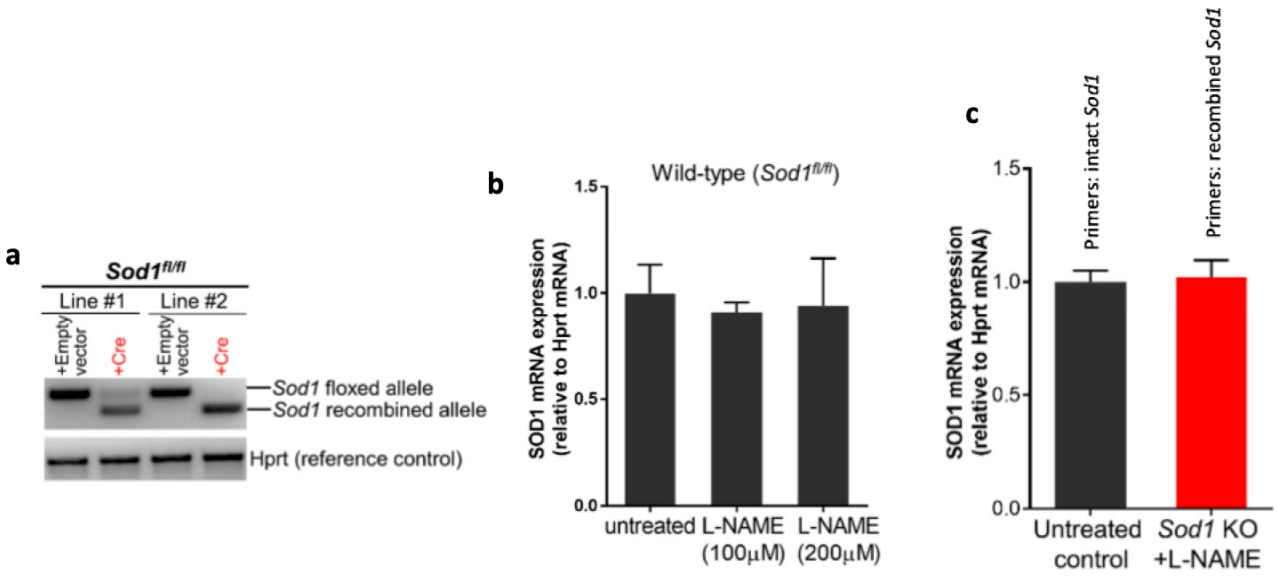

Figure 29: The effect of L-NAME treatment on *Sod1* mRNA expression.
a) RT-PCR analysis confirms the loss of *Sod1* expression from the floxed allele and the presence of a stable shorter transcript from the recombined locus in our *Sod1* KO MEFs. Shown here are agarose gel electrophoresis images of RT-PCR amplicons of *Sod1* and *Hprt* in total RNA extracts from *Sod1*$^{loxP/loxP}$ MEFs infected with empty viral vector (wild-type control) and *Cre*-expressing virus (KO). b) No change in *Sod1* mRNA expression in wild-type cells after treatment is observed. c) qRT-PCR analysis of *Sod1* mRNA expression in L-NAME treated *Sod1* KO MEFs related to untreated wild-type control cells shows that levels of intact *Sod1* expression in controls and recombined *Sod1* expression in KO cells are similar.

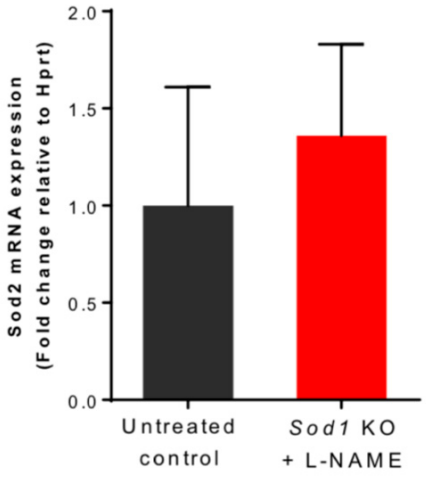

Figure 30: Relative *Sod2* mRNA expression level in L-NAME treated *Sod1* KO cells by qRT-PCR.
There is no change in the levels of *Sod2* transcript in *Sod1* KO MEFs relative to those seen in untreated control cells, measured by qRT-PCR. These results support our assertion that NO• regulation of SOD is not via a transcriptional mechanism.

g. Sensitivity of viable *Sod1* knockout MEFs (rescued with L-NAME) to paraquat ($O_2^{\bullet-}$ generator)

Inducible *Sod1* KO MEFs treated with L-NAME are alive and grow normally. Yet, they lack SOD1 completely, their levels of SOD2 and SOD3 fall below the level of detection of a western blot, and they have low superoxide dismutase enzymatic activity. It can therefore be assumed that these cells thrive with a greatly diminished ability to handle superoxide. To test this assumption, we used the superoxide generator, paraquat (PQ) to challenge these cells. We used a dosage of PQ (100μM) that almost entirely prevents the survival of control cells to challenge the rescued *Sod1* KO cells. Surprisingly, with the L-NAME treatment that allows survival of the inducible *Sod1* KO MEFs, these KO cells show even better survival than the control cells after exposure to PQ (Figure 31). Another fascinating observation is that while FeTPPS fully relieves the toxicity of PQ on control cells (cells with remaining SOD1 expression), it does not have the same effect on inducible *Sod1* KO cells (Figure 31).

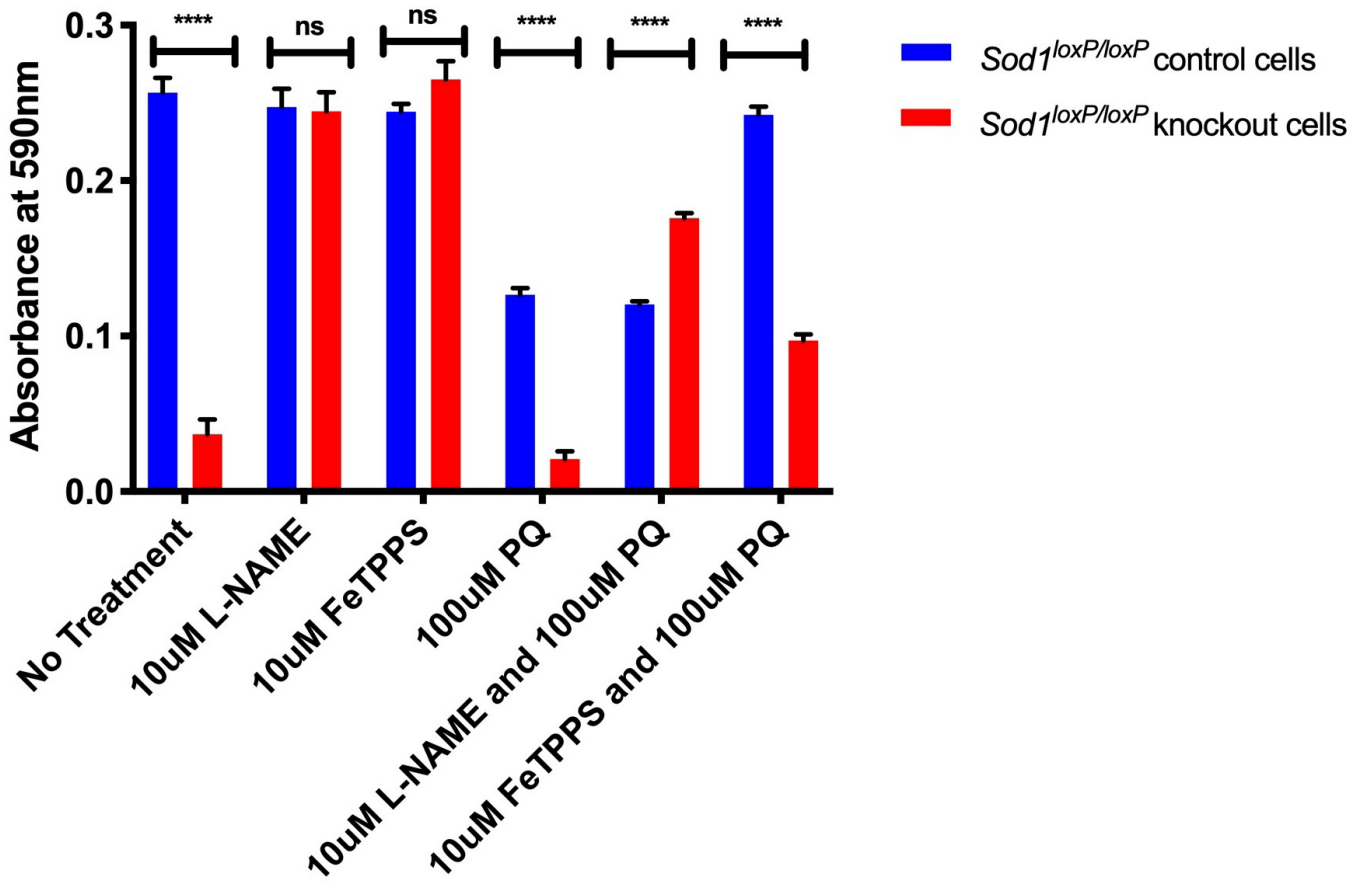

Figure 31: Paraquat (PQ) treatment on *Sod1*$^{loxP/loxP}$ mouse embryonic fibroblasts.
PQ generates $O_2^{\bullet-}$ in the mitochondria. *Sod1*$^{loxP/loxP}$ KO MEFs were hypersensitive to PQ compared to control cells. Treatment with FeTPPS fully relieves the toxicity of PQ on control cells, but not on *Sod1*$^{loxP/loxP}$ KO MEFs Treatment with L-NAME dramatically relieved the effect of PQ on *Sod1*$^{loxP/loxP}$ KO MEFs. A possible interpretation of these findings is that when the generation of $ONOO^-$ is reduced with L-NAME treatment, cells with less SOD activity are protected from PQ because they generate less H_2O_2. This implies that the toxicity of $O_2^{\bullet-}$ is much less problematic than that of H_2O_2.

One possible interpretation of these observations is that the toxicity of PQ, as a superoxide generator, is not directly due to the reactivity of superoxide itself, but rather to the combinatorial effect of peroxide toxicity and peroxynitrite toxicity. This is within the realm of possibility, as superoxide is 1) a negatively charged molecule that diffuses rather slowly, 2) is only moderately reactive by itself, 3) does not readily pass through cell membranes, and 4) is relatively short-lived, meaning that superoxide presumable acts only where it is produced[85, 129, 667].

In FeTPPS-rescued *Sod1* KO MEFs treated with PQ, the lack of SOD1 expression and the addition of PQ are both expected to lead to an increase in superoxide levels. This means there is more superoxide available to spontaneously react with nitric oxide to form peroxynitrite. FeTPPS, as a peroxynitrite decomposition catalyst, then helps to remove some of the deleterious peroxynitrite formed. However, FeTPPS-rescued *Sod1* KO MEFs treated with PQ will produce more peroxynitrite than their counterparts that are not treated with PQ, meaning there could be some residual peroxynitrite contributing to the deleterious effects of PQ on these cells. This affect may not be as prominent in L-NAME rescued *Sod1* KO MEFs treated with PQ, as nitric oxide expression is reduced in these cells, which prevents peroxynitrite from being produced in the first place. Additionally, the role of SODs is to catalyze the transformation of superoxide to hydrogen peroxide (H_2O_2), which can diffuse much greater distances than superoxide and can traverse cellular membranes[668]. Furthermore, the role of H_2O_2 in signal transduction is more common, at least based on current scientific knowledge, than superoxide[651]. *Sod1* KO MEFs rescued with L-NAME have very low superoxide dismutase activity and thus might produce much less H_2O_2 in response to PQ treatment. Consequently, one interpretation of our observations is that the well-known toxicity of PQ is more related to excess H_2O_2 production, rather than superoxide

formation, and that excess H_2O_2 can be deleterious through direct toxicity of macromolecules and disruption of signal transduction pathways. This interpretation also explains why PQ toxicity is not changed in FeTPPS-rescued *Sod1* KO MEFs. These MEFs still have SOD2 and SOD3 levels comparable to control cells, meaning they have much stronger remaining superoxide dismutase activity than their L-NAME counterparts, and therefore still produce higher levels of H_2O_2.

h. Sensitivity of viable *Sod1* knockout MEFs (rescued with L-NAME) to N-acetyl cysteine (antioxidant)

Inducible *Sod1* KO MEFs treated with L-NAME have very low SOD activity, suggesting that they have low levels of H_2O_2, as discussed above when considering the sensitivity of these cells to PQ. Note, however, that there are remaining sources of H_2O_2 in these cells, such as spontaneous superoxide dismutation, peroxisomes, and some NOX isoforms (e.g. NOX4)[669]. N-acetyl cysteine (NAC) functions as an antioxidant by introducing cysteine into cells, which stimulates the production of glutathione[670]. Glutathione, as discussed above, is the main antioxidant and redox regulator of the cell and numerous H_2O_2 detoxification mechanisms have been shown to depend on it[671]. Therefore, treatment of cells with NAC leads to a reduction in H_2O_2 levels. So, we treated control cells and inducible *Sod1* KO cells with NAC to see how these treatments would affect cell growth. Treatment of control cells with 5mM NAC did not impair cell growth. Similarly, simultaneous treatment of control cells with NAC and L-NAME did not inhibit growth and these cells survived and appeared normal. However, the addition of NAC to inducible *Sod1* KO cells, whose viability were previously maintained by L-NAME, resulted in a dramatic loss of viability (Figure 32).

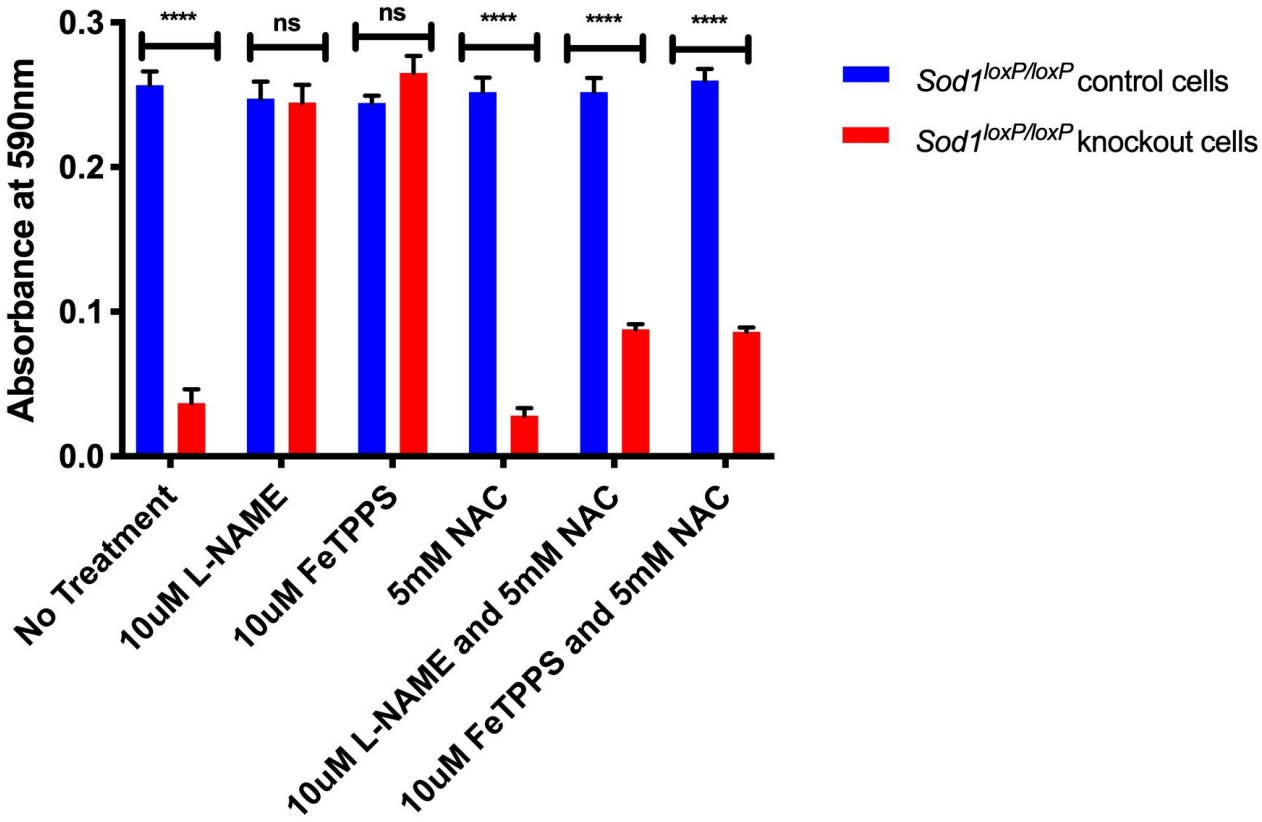

Figure 32: N-acetyl cysteine treatment on *Sod1*$^{loxP/loxP}$ mouse embryonic fibroblasts.
NAC is known for its antioxidant activity. This activity is due to its participation in the synthesis of glutathione. Glutathione helps lower H_2O_2 levels and repair ROS damage. Treatment with NAC does not significantly improve the survival of *Sod1*$^{loxP/loxP}$ KO MEFs that have been treated with L-NAME or FeTPPS. In fact, NAC almost completely eliminates the pro-survival effect of L-NAME and FeTPPS. Our current interpretation of these results is that the amounts of H_2O_2 needed for signalling are limiting when H_2O_2 is low due to the absence of SOD1.

The fact that inducible *Sod1* KO cells, formerly rescued with L-NAME, are killed by a normally non-toxic dose of NAC was surprising. One possible interpretation of this observation is that there are already low levels of H_2O_2 in L-NAME rescued inducible *Sod1* KO MEFs because of their very low superoxide dismutase activity, and NAC treatment further lowers these levels more, resulting in a deleterious disruption of signal transduction pathways that rely upon H_2O_2 as a messenger or modulator.

i. The sensitivity of KRas^{G12D} cells to nitric oxide donors

We also took another approach to study the consequences of changing levels of intracellular superoxide. *KRas* is part of a family of small GTPases and is one of the most frequently mutated genes in cancer[672, 673]. Mutated *KRas* cells produce more ROS than wild-type *KRas* cells[674, 675]. In cancer models, this increase in ROS has been shown to downregulate tumour suppressor genes, increase cell proliferation, and mutate DNA[674]. Thus, we wanted to see if the survival of mutant *KRas* cells are more sensitive to treatment with nitric oxide donors, due to a possible increase in peroxynitrite formation. We tested this idea in *KRas$^{lsl/+}$* mouse embryonic fibroblasts. These MEFs have a transcription stop signal flanked by loxP before the *KRas* mutant allele (lsl or lox-stop-lox). Upon retroviral presentation of Cre, the transcriptional stop codon is excised, allowing for the mutant allele (G12D) to be expressed[676]. For this experiment, we infected MEFs with an empty-vector retrovirus or a retrovirus containing Cre recombinase. Then, we treated all cells with diethylenetriamine-nitric oxide (DETA-NO), a nitric oxide donor. After three days of DETA-NO treatment, Cre-infected *KRas$^{lsl/+}$* MEFs were significantly more sensitive to treatment with DETA-NO than control MEFs (Figure 33).

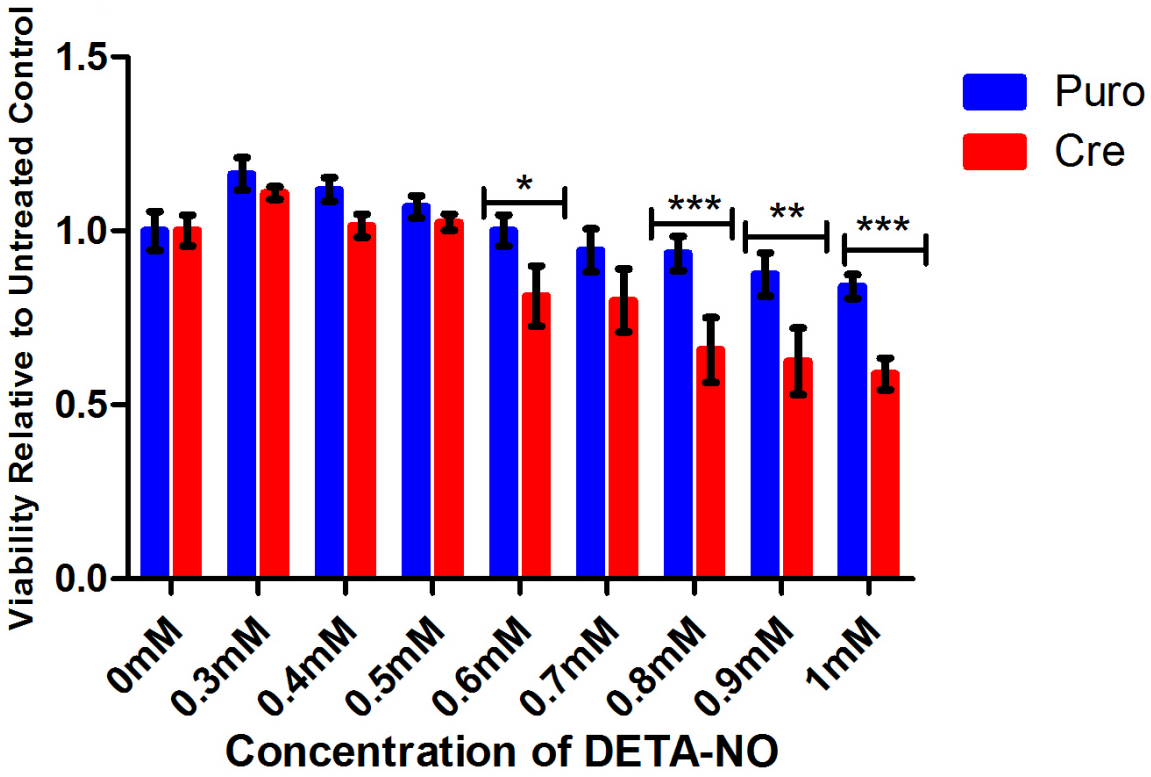

Figure 33: Sensitivity of *KRas$^{lsl/+}$* cells to nitric oxide donors.
Cre-infected *KRas$^{lsl/+}$* MEFs are significantly more sensitive to treatment with diethylenetriamine/nitric oxide adduct (DETA-NO) than Puro-infected *KRas$^{lsl/+}$* MEFs at concentrations higher than 0.6mM. Results are expressed as mean ± SEM. Two-way ANOVA with Bonferroni posttests: * $p < 0.05$, ** $p < 0.01$, *** $p < 0.001$.

5. Discussion

In this chapter, we describe the generation and characterization of mouse embryonic fibroblasts lacking expression of SOD1. Viability of these cells is restored by reducing peroxynitrite formation, using either nitric oxide synthase inhibitors or peroxynitrite decomposition catalysts. Surprisingly, when both SOD1 are lost and NOS function is hindered, expression of the two other mammalian isoforms of superoxide dismutase is also lost. We have also shown that *Sod1* KO cells that are rescued by NOS-inhibitor (with no SOD1 and undetectable SOD2 and SOD3) are not hypersensitive to the superoxide generator paraquat but are killed by the antioxidant N-acetylcysteine.

a. Rescued inducible *Sod1* KO MEFs are viable, despite lack of SOD expression

NOS inhibition, not low peroxynitrite, leads to low SOD2/3 expression in rescued inducible *Sod1* knockout MEFs. In L-NAME-rescued *Sod1* KO MEFs, we speculate that there is an extremely low level of nitric oxide thanks to the inhibition of NOS by L-NAME. L-NAME is a derivative of L-arginine, the precursor of nitric oxide formation by nitric oxide synthases[677]. This extremely low level of nitric oxide also corresponds with little to no expression of all three mammalian SOD isoforms. Loss of superoxide dismutase expression is not seen in cells rescued with FeTPPS and this further validates our conclusion that a threshold level of nitric oxide is required to maintain superoxide dismutase expression. In FeTPPS rescued $Sod1^{loxP/loxP}$ KO cells, there is only one pathway removing nitric oxide, the excess formation of peroxynitrite due to increased reactions of superoxide with nitric oxide. But, in L-NAME rescued $Sod1^{loxP/loxP}$ KO cells, there are two pathways removing nitric oxide from the cell, the formation of peroxynitrite and the overall decrease in nitric oxide due to the inhibition of nitric oxide synthases by L-NAME itself.

It is quite surprising that cells that have little to no SOD expression are viable. It suggests that these mouse embryonic fibroblasts can tolerate relatively high levels of superoxide. The question then becomes, if cells can tolerate high levels of superoxide, why are SODs necessary? SOD expression is conserved in vertebrates, invertebrates, aerobes, and some anaerobes and these enzymes are some of the most abundant in mammals, indicating that their function is likely significant. These results thus suggest that superoxide dismutases are not important to prevent the formation of superoxide per se, but rather to control the levels of peroxynitrite made in the cell. We show that if we intervene to reduce nitric oxide levels in cells with already high peroxynitrite levels (L-NAME rescued *Sod1* KO MEFs), these MEFs can survive and survive with little SOD expression, suggesting that when peroxynitrite is not being produced, there is no longer much reason for SOD expression.

Several questions remain at this time and present a line of inquiry for future studies. At this time, we do not know the mechanism by which $NO^{\bullet}$ impacts the expression of superoxide dismutases. It is important to further investigate this mechanism because the observed phenomenon is so dramatic *in vitro* that it is reasonable to postulate that it corresponds to an equally important *in vivo* mechanism of superoxide dismutase expression as well. Our preliminary

data suggests that the regulation of SOD2 and SOD3 expression is not post-transcriptional and may be post-translational. We showed that the transcript levels of *Sod2* are unaffected in L-NAME rescued *Sod1* KO MEFs, yet when we look at SOD2 protein expression in these same cells, there is no SOD2 expression. Furthermore, we also found a suggestion, in our western blots looking at SOD2 and SOD3 expression, of SODs being degraded in response to low levels of $NO^{\bullet}$. This is represented by an upward shift in SOD2 and SOD3 bands. Thus, we will probe to discover the mechanism of SOD degradation. It is possible that a post-translational modification, such as the addition of ubiquitin or ubiquitin-like (e.g. SUMO), leads to the altered molecular weight bands of SOD2 and SOD3. Other mechanisms of SOD degradation to explore would be covalent protein modifications known to contribute to protein degradation, such as phosphorylation and whether protease inhibitors, both broad-spectrum and mitochondrial-specific (e.g. MG132 and velcade) interfere with loss of SOD2 and SOD3 expression.

Additionally, the best documented method of nitric oxide signaling is via soluble guanylate cyclases (sGC). Binding of $NO^{\bullet}$ to the prosthetic heme of sGC activates its ability to synthesize cGMP, an intracellular messenger that can go on to activate various enzymes, most notably cGMP protein kinases (PKG, of which there are two mammalian isoforms)[678]. There are pharmacological inhibitors available that inhibit sGC and cGMP kinase. These inhibitors would allow us to investigate if nitric oxide signalling is necessary for SOD expression or if the interaction between SOD and nitric oxide is more direct (e.g. a nitrosative modification of SOD)[679, 680]. If any of these inhibitors impact SOD expression, it is indicative that the regulation of SOD is via a $NO^{\bullet}$ signalling pathway, rather than by $NO^{\bullet}$ itself. If regulation of SOD is through a $NO^{\bullet}$ signalling pathway and inhibitors of downstream elements of this pathway also impact SOD expression, this would represent a helpful tool to study the regulation of SOD, without needing to use NOS inhibitors such as L-NAME and potentially even in the absence of high superoxide levels (if the inhibitor also impacts SOD2 and SOD3 expression in wild-type cells). If these inhibitors have no effect, it is possible that SOD regulation occurs through non-canonical, yet well-documented, methods of $NO^{\bullet}$ signalling[681].

b. Inducible *Sod1* knockout MEFs are a new tool to understand ROS/RNS metabolism

Superoxide dismutases are essential to protect against the formation of peroxynitrite, not the formation of superoxide. This is evident because cells without any detectable superoxide dismutase expression (L-NAME rescued *Sod1*$^{loxP/loxP}$ KO MEFs) are viable. These cells, although alive, have changes in their levels of reactive species ($O_2^{\bullet-}$, H_2O_2, $NO^{\bullet}$, $ONOO^-$, and the GSSG/GSH ratio) and thereby most likely in the molecular damage that they produce. To further understand ROS/RNS metabolism, it will be useful to score the reactive species levels in both *Sod1* inducible KO cells and control cells, treated with NOS inhibitors and $NO^{\bullet}$ donors. There are both direct and indirect measures for reactive species, including: 1) ROS-sensitive dyes, such as MitoSox and DCF-DA, to visualize and quantify levels of ROS in living cells and their mitochondria, 2) Amplex Red assay to determine H_2O_2 levels in cells and mitochondria, 3) scoring of ROS modification to cellular components (e.g. activity of Fe-S cluster enzymes, protein carbonyls, isoprostanes, and 8-OHdG), 4) scoring $NO^{\bullet}$ by measuring nitrite accumulation (Griess reagent) and imaging with the fluorescent probe DAF-FM, 5) assessing $ONOO^-$ levels indirectly by measuring 3-nitrotyrosine, and 6) assaying GSSG/GSH ratio using a well-established kit.

Comparison of the concentration of reactive species and oxidative/nitrosative damage will further confirm the physiological differences between cells rescued with either L-NAME or FeTPPS. For example, L-NAME treated cells that have lost most of their SOD2 and SOD3 expression should show more damage to mitochondrial Fe-S clusters (e.g. aconitase, due to higher superoxide levels) and low GSSG/GSH ratio (because of much lower hydrogen peroxide production) in comparison to FeTPPS treated cells that have normal levels of SOD2 and SOD3.

We also observed paradoxical sensitivity of L-NAME rescued inducible *Sod1* knockout cells to pro-oxidants and antioxidants. Despite the loss of SOD1/2/3 expression in these cells, they are no more or less sensitive than control cells to PQ, a pro-oxidant. We believe that this suggests that PQ's normally observed harmful effects are more a result of H_2O_2 toxicity, rather than $O_2^{\bullet-}$ toxicity. Furthermore, L-NAME rescued inducible *Sod1* knockout cells are killed by low dose of NAC (5mM) and we believe this may be due to insufficient H_2O_2 to support necessary signalling transduction pathways. It is possible to delve deeper into these observations by using already

available tools to measure oxidative damage, such as measurements of H_2O_2 levels with Amplex Red, damage to Fe-S clusters, and the GSSG/GSH ratio.

Another clear question to address with this new tool, our inducible *Sod1* knockout cells, is how reactive species levels impact signal transduction. To gain insight, we can establish how known targets of ROS signaling are affected by altered levels of reactive species, as seen in our cells. For example, the oxidation state of PTEN (a redox-sensitive phosphatase) and the activation of MAPKs (ERKs, JNKs, p38 MAPKs) are known to be modulated by changes in ROS levels[682, 683]. The activation of MAPKs is also known to respond to changes in intracellular nitric oxide levels[684]. Recent work has shown that PTEN is inactivated by oxidation of its active site cysteine by H_2O_2, so one would expect to see less PTEN activity (i.e. phosphorylation status of its downstream effectors, such as PI3K and AKT, or decrease in measured phosphatase ability) in conditions of high H_2O_2[685, 686]. Examining how ROS levels impact signal transduction in our inducible *Sod1* KO cells seems as a validation to any results found from measuring indicators of oxidative damage, as many of these measures simply account for all ROS present. Exploring the activity of ROS-sensitive transcription factors, such as NFκB and HIF-1α, by determining the expression levels of their target genes, would also provide valuable insight as to the redox state of the cells[687, 688].

Finally, as the importance of $NO^{\bullet}$ and H_2O_2 in signaling is well documented, viable L-NAME and FeTPPS treated *Sod1*$^{loxP/loxP}$ knockout cells provide us with a unique opportunity to uncover not only how cells can manage dramatic changes in reactive signaling molecules, but also how cells can survive with major changes in the production of these molecules, that at toxic levels, are expected to severely alter macromolecules (e.g. nucleic acids and proteins).

After these striking *in vitro* results, we used the insight we gained to move onto the potential applications of L-NAME treatment in both inducible and germline knockout *Sod1* mice. While it is clear that our *in vitro* findings can lead to more cell work, we chose to prioritize characterizing the effects of L-NAME *in vivo*. Before addressing the further open questions in cells, we want to do more work to ensure the reproducibility of these results, including in other cell types, and confirm the best protocol for the production of inducible *Sod1* knockout mouse embryonic fibroblasts.

CHAPTER 3: ADULT-ONSET LOSS OF SOD1 IS LETHAL DUE TO PEROXYNITRITE DAMAGE TO SKELETAL MUSCLES

1. Abstract

SOD1 is one of the most abundant proteins in mammalian cells and carries out ~90% of total cellular superoxide dismutase activity[689]. Loss of *Sod1 in vitro* is lethal, meaning cells are unable to grow and die by apoptosis. It is therefore surprising that homozygous germline knockout mice (*Sod1*$^{-/-}$) display only a relatively mild phenotype, producing animals that are fertile and live up to two years[17]. To investigate this observation further, we created a mouse model with adult-onset global knockout of *Sod1*, by combining a floxed *Sod1* allele with a globally expressed tamoxifen-sensitive *Cre* recombinase-expressing transgene (CAG-CreER^{T2}). Tamoxifen treatment in these mice does indeed cause the loss of SOD1 in the heart, skeletal muscle, lungs, brain, and kidney. SOD1 expression remains in the liver as tamoxifen is metabolized in the liver. The health of these mice declines rapidly after tamoxifen injections and they die within three weeks of the loss of *Sod1*. Pathology of adult-onset *Sod1* knockout mice showed that most organs (heart, brain, kidney, and liver) are unaffected in adult-onset *Sod1* knockout mice. But loss of *Sod1* in young adult mice leads to acute degeneration of skeletal muscles. The knockout phenotype, viability of the mice and skeletal muscle degradation, can be rescued by intraperitoneal injections of L-nitro-L-arginine methyl ester (L-NAME), a nitric oxide synthase (NOS) inhibitor. These results indicate that germline knockout *Sod1*$^{-/-}$ mice have a developmental adaptation, perhaps in nitric oxide handling, that allow them to survive. Our preliminary findings are that these mice have changes in their blood composition and lower nNOS expression, specifically in muscle tissues. Overall, our study presents the first mammalian model of inducible global *Sod1* knockout and provides new insights into the strategies for handling reactive oxygen and nitrogen species, specifically superoxide, nitric oxide, and peroxynitrite.

2. Introduction

a. Superoxide dismutases

Superoxide dismutases (SODs) are one of the most abundant proteins in vertebrates. In mice, SOD1 is the 34th most abundant protein in the whole organism, out of 17,698 proteins[296]. The first SOD was discovered over half a century ago, in 1969, by Fridovich and McCord. They

demonstrated that hemocuprein (the future SOD1), a blue-copper protein isolated from bovine erythrocytes, competitively inhibits the reduction of cytochrome c by xanthine oxidase[273]. Xanthine oxidase produces superoxide ($O_2^{\bullet -}$)[276]. All SODs catalyze the dismutation of superoxide ($O_2^{\bullet -}$) to hydrogen peroxide (H_2O_2)[128]. In mammals, there are 3 SOD isoforms – SOD1 in the cytoplasm and mitochondrial intermembrane space, SOD2 in the mitochondria, and SOD3 in the extracellular space[315, 690, 691].

Historically, the existence of SOD enzymes was key evidence supporting the oxidative stress theory of aging, because of their abundance and because they are highly conserved and found in all kingdoms of life[288, 295]. The oxidative stress theory of aging states that organisms age due to accumulated damage from reactive species and has since been greatly debated[11, 692]. For example, our lab showed that SODs, the only enzymatic defence against superoxide, are dispensable for normal lifespan in *C. elegans*[16]. Furthermore, mice lacking superoxide dismutase 1 (SOD1) are alive, albeit with a reduced lifespan, with *Sod1*$^{-/-}$ mice having mean lifespan of 20.8 months, compared to 29.8 months in *Sod1*$^{+/+}$ mice[17]. Phenotypes of *Sod1*$^{-/-}$ mice include reduced body weight[617], sarcopenia (muscle loss)[611], reduced physical activity and endurance[693], increased incidence of liver tumours[17], reduced fertility[694], and various accelerated aging phenotypes such as hearing loss, skin thinning, and cataracts[621, 695-697].

Germline knockout *Sod1*$^{-/-}$ mice were first generated in 1997[5]. These *Sod1*$^{-/-}$ mice have a deletion of exon 3 and 4 of the *Sod1* gene, resulting in a shortened *Sod1* gene, in which exon 1, 2, and 5 are spliced together[17]. Then, in 1998, Russell M. Lebovitz generated another mouse that lacked *Sod1* expression, but these mice lack exons 1 and 2, rather than exons 3 and 4 as in the Huang mice[580]. The Van Remmen lab, using the Lebovitz mice, went to focus specifically on the muscle phenotypes of these mice. Germline knockout *Sod1*$^{-/-}$ mice have significantly less muscle mass than wild-type mice beginning at 3-4 months of age[6]. By 8-12 months of age, *Sod1*$^{-/-}$ mice show decreased muscle mass that mimics changes seen in 25-30 months old wild-type mice[611]. In addition to loss of muscle, *Sod1*$^{-/-}$ mice also showed a decrease in muscle function, measured by diminished ability to generate isometric contractile force (the generation of muscle tension without changes in muscle length or joint angle) and reductions in rotarod performance, wheel running, treadmill endurance, and grip strength[6, 612, 613]. It is believed that sarcopenia, or muscle

loss, in *Sod1*$^{-/-}$ mice is due to less innervation of the muscle by motor neurons. Motor neuron innervation is necessary for maintenance of muscle size, structure, and function[614].

The body mass of *Sod1*$^{-/-}$ mice is lower than that of wild type mice[617]. The reduction in body weight (~17% in females and ~20% in males) was first seen at 5 months of age and continued to be observed until about 20 months of age[6]. It is important to note that decrease in muscle tissue specifically seems to be responsible for the age-related decrease in body mass of *Sod1*$^{-/-}$ mice[618]. Note, in our lab, for any experiments using germline knockout *Sod1*$^{-/-}$ mice, we use the Lebovitz mice which are available via The Jackson Laboratory.

The goal of this project is to better understand how *Sod1*$^{-/-}$ mice can lack *Sod1* and still be alive as SODs are the sole defense against superoxide formation, typically considered to be a damaging reactive oxygen species (ROS) and has been implicated in disease development and aging.

b. Cre-loxP system

Most site-specific recombinases fall into two families – tyrosine recombinases and serine recombinases[698]. Cre recombinases, along with flipase (Flp) and D6 specific recombinase (Dre), are tyrosine site-specific recombinases[662]. Initiation of recombination by tyrosine recombinases occurs when one strand of double-stranded DNA is cleaved by the nucleophilic tyrosine of these recombinases. This leads to the creation of DNA-protein phosphotyrosine covalent linkages at 3' DNA ends and free hydroxyl groups at 5' DNA ends[699]. Proper recombination requires a cleavage event at two sites. Next, the free 5' hydroxyl attacks the 3' phosphotyrosine at the other cleavage site, forming a Holliday junction. A Holliday junction is a cross-shaped structure where 2 double-stranded DNA molecules are separated into 4 separate strands to aid in exchange of genetic material[700]. This structure allows the second strand of each DNA duplex to be attacked, leading to resolution of the Holliday junction, release of the tyrosine recombinase enzyme, and completion of the DNA recombination event[701]. Cre recombinases specifically recognize loxP (locus of x-over, P1) sites[702]. loxP sites are 34 base pair (bp) sequences consisting of two inverted and palindromic repeats (13bp each) and an 8bp core sequence – 5'-ATAACTTCGTATANNNTANNNTATACGAAGTTAT - 3' (N = any nitrogenous base)[662].

The Cre-loxP system is a powerful tool as it allows for temporal and spatial control of gene expression. In a tamoxifen-inducible Cre-loxP system, as used for the experiments in this chapter, the Cre recombinase protein has been fused with an estrogen receptor (CreER) that contains a mutated ligand binding domain that only binds tamoxifen[703, 704]. When CreER is in the cytoplasm, it normally binds heat shock protein 90 (HSP90), preventing nuclear translocation. Upon tamoxifen binding, this CreER recombinase is then free to translocate to the nucleus and effect genetic modifications[705].

c. Elimination of nitric oxide from the body

The reaction of nitric oxide ($NO^{\bullet}$) with hemoglobin (Hb) is one of the main sinks of nitric oxide in the body. The physiological significance of this reaction was established when $NO^{\bullet}$ was established as the endothelial-derived relaxing factor. In mammals, $NO^{\bullet}$ is eliminated by binding to hemoglobin (Hb)[706, 707]. Hemoglobin can bind oxygen when its iron heme is ferrous (Fe^{2+}), leading to the formation of oxyhemoglobin (oxyHb). When the iron heme of hemoglobin is ferric (Fe^{3+}), oxygen can no longer bind and methemoglobin (metHb) is formed. The dioxygenation reaction, or the reaction responsible for the sequestration of $NO^{\bullet}$, is when oxyHb reacts with $NO^{\bullet}$ leading to the formation of metHb and nitrate ($Fe^{2+}O_2Hb + NO^{\bullet} \rightarrow Fe^{3+}Hb + NO_3^-$) (Figure 34)[708]. This reaction occurs at a rate of 6-8 x 10^7 M^{-1} s^{-1} and is limited merely by the rate of diffusion of $NO^{\bullet}$ to the heme. It has even been suggested that one of the advantages for Hb compartmentalization in red blood cells (RBCs) is that it ensures that there is not excessive scavenging of $NO^{\bullet}$[709]. $NO^{\bullet}$ has an incredibly high affinity (K_d (dissociation constant) = 10^{-11} M) for the ferrous heme of hemoglobin[710].

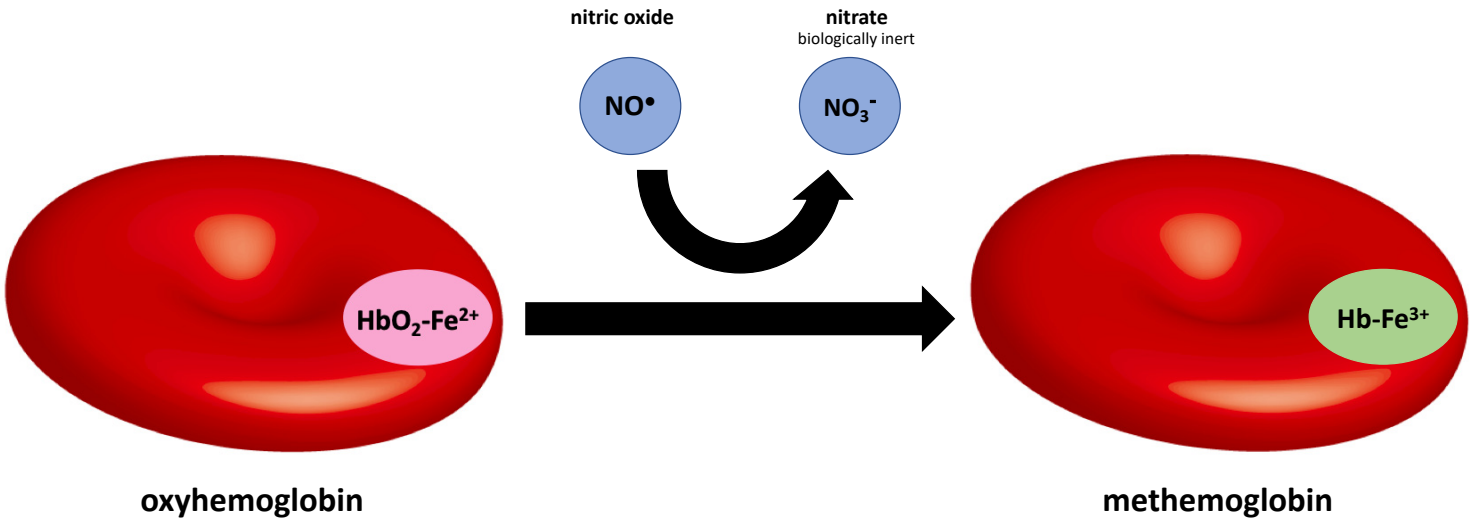

Figure 34: The dioxygenation reaction of hemoglobin and nitric oxide.
The reaction of nitric oxide (NO•) with hemoglobin (Hb) is one of the main sinks of nitric oxide in the body. The physiological significance of this reaction was established when NO• was established as the endothelial-derived relaxing factor. NO is quickly inactivated by oxyhemoglobin. Hemoglobin can bind oxygen when its iron heme is ferrous (Fe^{2+}), leading to the formation of oxyhemoglobin (oxyHb). When the iron heme of hemoglobin is ferric (Fe^{3+}), oxygen can no longer bind and methemoglobin (metHb) is formed. The dioxygenation reaction, or the reaction responsible for the sequestration of NO•, is when oxyHb reacts with NO• leading to the formation of metHb and nitrate.

3. Materials and Methods

a. Reagents and chemicals

All reagents and chemicals in this study were purchased from Sigma-Aldrich or Cayman Chemical, unless otherwise noted, and were of molecular biology grade or higher.

b. Mice

Conditional *Sod1* knockout mice (*Sod1*$^{loxP/loxP}$) were generated in collaboration with InGenious Targeting Laboratory in Stony Brook, New York. Targeted iTL BA1 (C57BL/6 x 129/SvEv) hybrid embryonic stem cells were microinjected to C57BL/6 blastocysts. The target region of *Sod1* includes exons 2 and 3, which contain 3 of the 4 essential copper binding sites for superoxide

dismutase function. The resulting chimeras with the highest percentage of agouti coat colour were crossed with C57BL/6 FLP mice. These crosses were necessary to remove the Neomycin cassette. Agouti mice are grey in coloration, but each strand of fur is both partly yellow and partly black. Tail DNA from these mice was analyzed using PCR to ensure deletion of Neomycin cassette. Then, the resulting heterozygous mice were mated to C57BL/6 (wild type mice). The genotype of their offspring was also confirmed using PCR, as described below, to ensure the absence of both the Neomycin cassette and FLP transgene. These mice were then interbred to generate homozygous *Sod1*$^{loxP/loxP}$ mice. Mice with the *CAG-CreER*^{T2} recombinase were obtained from The Jackson Laboratory. With these two mouse lines, *CAG-CreER*^{T2}; *Sod1*$^{loxP/loxP}$ mice were generated. In brief, *Sod1*$^{loxP/loxP}$ mice were bred with *CAG-CreER*^{T2} mice, resulting in mice that carry *CAG-CreER*^{T2} and were heterozygous for *Sod1*^{loxP}. The heterozygous mice were then intercrossed to generate mice harbouring both homozygous floxed *Sod1* and *CAG-CreER*^{T2} recombinase. All mice examined in this study had a hybrid 129/Sv ×C57BL/6 background and were handled in accordance with recommendation of the Canadian Council on Animal Care and studies were conducted under an approved Animal Utilization Protocol (AUP). This protocol was approved by the animal Care and Use Committee of McGill University. The mice were house in the pathogen-free animal facility at McGill University (CMARC). All experimental mice were sacrificed using isoflurane (Baxter Corporation) as an anaesthetic, followed by cervical dislocation for euthanasia.

c. Genotyping of mice

All mice were genotyped via PCR amplification of genomic DNA isolated from tails. ~1-2mm mouse tail clippings were boiled in 25mM NaOH, 0.2mM EDTA (Solution I) at 100°C for 20 minutes. Immediately after boiling, the DNA extraction reaction is neutralized with 40mM Tris-HCL pH 5.5 (Solution II). 60µL of both Solution I and II are used for DNA extraction from a single 1-2mm piece of tail. After the reaction is neutralized with Solution II, the tails should be spun down. The floxed *Sod1* allele was amplified using primer #1 (ALTLOX-forward): 5’ - CTCCACAGGCAGTAGGACAA - 3’ and primer #2 (ALTLOX-reverse): 5’ - CAACACAACTGGTTCACCGC - 3’. The resulting wild-type product size is 496bp, whereas the loxP product size is 541bp. PCR reactions were performed using NEB’s OneTaq DNA polymerase. Genotyping PCR program is:

95°C for 3 minutes (initial denaturation), 35 cycles of 95°C for 30 seconds, 60°C for 30 seconds, and 72°C for 60 seconds, followed by 72°C for 5 minutes (final extension), and hold amplified products at 4°C. For mouse embryonic fibroblasts obtained from *Sod1*$^{loxP/loxP}$ mice, embryonic DNA extraction was performed using the QIAGEN DNeasy Blood & Tissue Kit and using their protocol for DNA extraction from animal tissues. The recombined *Sod1*^{loxP} allele was detected with primer #3 (NDEL2): 5'- GGG GCT TTA GTA AAG TAT GCC AGC TC - 3' and primer #4 (LOX1): 5'- CTC CAC AGG CAG TAG GAC AAA GG - 3'. The resulting band of a successfully excised allele of *Sod1* is 600bp. To detect AlbCre, the primers were as follows: primer #8 (Cre-forward): 5' - GCCAGCTAAACATGCTTCATC - 3' and primer #9 (Cre-reverse): 5' - ATTGCCCCTGTTTCACTATCC - 3' and, once again, the same PCR program, detailed above, was used. PCR products were visualized by gel electrophoresis on a 2% agarose (FroggaBio) gel at 120V until satisfactory resolution and band separation was reached (~30 minutes). Genotyping protocol is based on that previously described by the Hekimi lab[711].

d. Intraperitoneal injections

To induce the excision of floxed *Sod1* alleles, *CAG-CreER*^{T2}; *Sod1*$^{loxP/loxP}$ mice, between the age of 12 to 15 weeks, were intraperitoneally injected, every other day for a total of 10 days, with tamoxifen (7mg tamoxifen/kg mouse body weight). Injected tamoxifen solution was prepared at a concentration of 15mg/mL in sterilized corn oil. Litter siblings of tamoxifen-injected mice were injected with corn oil only, as a vehicle control. If mice were also receiving L-NAME or FeTPPS injection, these injections began on off days of tamoxifen or corn oil injections and then continued every other day for a total of three months. Injected L-NAME solution was prepared in saline at a concentration of 20mg/mL and intraperitoneally injected mice received 7mg/kg L-NAME each injection. There were three concentrations of FeTPPS attempted in mice – 5mg/mL, 10mg/mL, and 15mg/mL. Both L-NAME and FeTPPS were acquired from Cayman Chemical. Mice only injected with tamoxifen or corn oil were sacrificed the day after the completion of their intraperitoneal injections. Mice that also received L-NAME or FeTPPS injections, in conjunction with corn oil or tamoxifen, were sacrificed the day after the completion of their L-NAME or FeTPPS injections.

e. Protein extraction and quantification from mouse tissue

Immediately following sacrifice of mouse, the organs of interest were dissected out of the animal. The organs dissected were the heart, brain, lungs, liver, kidneys, and various leg muscles. Organs were stored in Axygen Scientific 2mL, flat bottomed Microcentrifuge Tubes (MCT-200C) at -80°C until extraction of protein. Organ samples were thawed on ice and cold 200-400μL RIPA buffer was added. The RIPA buffer is composed of: 150mM NaCl, 50mM Tris-HCl pH 7.4, 1% NP-40, 0.5% Na-deoxycholate, 0.1% SDS, and 2mM EDTA. Prior to use, 1 tablet of cOmplete Mini per every 10mL RIPA buffer is dissolved. The cOmplete Mini tablet (Roche) is a protease inhibitor tablet. This tablet inhibits a range of serine and cysteine proteases and helps defend protein lysates against degradation. The organ and RIPA buffer were homogenized for 15 seconds using the OMNI International Tissue Master 125 Watt Lab Homogenizer with 7mm probe. Homogenized samples were then spun down in a microcentrifuge for 15 minutes at 4°C, at 13,000rpm. The protein-containing supernatant was reserved and stored in a separate microcentrifuge tube at -80°C until quantification. Protein lysates were quantified using the Pierce BCA Protein Assay (Thermo Scientific), according to manufacturer's instructions.

f. Western blotting

Total organ lysate samples were loaded into 12% running gel/5% stacking gel SDS-PAGE gels. These gels were initially electrophoresed at 70V until the stacking gel was cleared, then 120V for the remainder of the running time, and finally transferred onto nitrocellulose membranes (Bio-Rad). Membranes were blocked in 5% milk-PBS for 2 hours and then exposed to primary antibody overnight at 4°C. All antibodies were diluted in 5% milk-PBS. The following antibodies were used: anti-SOD1 (ab16831; dilution 1:2000), anti-SOD2 (ab13533; dilution 1:5000), anti-SOD3 (ab83108; dilution 1:1000), anti-eNOS (ab76198; dilution 1:500), anti-nNOS (ab76067; dilution 1:1000), and anti-iNOS (ab15323; dilution 1:250). Control antibodies were all diluted 1:2000. They were one of the following: GAPDH (2118S Cell Signaling Technology (CST)), α-tubulin (2144S CST), or β-actin (4967S CST). The next day, primary antibody mixtures were removed, and membranes were washed 3 times in PBS-0.05% Tween 20 (Sigma). Membranes were then

incubated for 2 hours with anti-rabbit or anti-mouse IgG, horseradish peroxidase (HRP)-linked secondary antibody (7074S and 7076S CST) and ultimately developed using the GE Healthcare ECL Plus Western Blotting Detection System. Protein band signals were visualized using AFP Manufacturing Mini-Med 90.

g. Tissue processing and pathology

Mice were anaesthetized using isoflurane (Baxter Corporation), during which mice were perfused with phosphate-buffered saline (PBS) via injection in the right ventricle of their heart. After, organs of interest (heart, lungs, liver, kidney, leg muscles, aorta, and brain) were dissected and washed in PBS. Extracted organs were then rocked at 4°C overnight in Zn^{2+} formalin. The next day, organs were removed from formalin and sequentially dehydrated in 30%, 50%, and finally 70% ethanol. Organs gently rocked in each concentration of ethanol for at least 1 hour. Organs were then embedded in paraffin by the Histology Core Facility at McGill or by Charles River Laboratories. After paraffin embedding, organs were sectioned (5µm) and mounted onto Fisher Superfrost Glass Slides. Initial histopathology and interpretation were performed by Charles River Laboratories and then with guidance, further analysis of the provided slides was performed (e.g. acquisition of microscope images).

h. Hematoxylin and Eosin

Paraffin embedded tissue sections were de-paraffinized and rehydrated in xylenes, followed by decreasing ethanol concentrations (100%, 95%, 70% diluted in distilled water) and finally distilled water. All of these steps were completed using a Varistain^{TM} Gemini ES Automated Slide Stainer. In running distilled water, nuclei were stained in 100% hematoxylin and then counterstained with eosin. Next, tissue sections were once again dehydrated using increasing ethanol concentrations (70%, 95%, 100%) and xylene. Finally, slides were mounted using Acrytol Mounting Media (Leica Biosystems) and cover slipped.

i. Immunohistochemistry

Paraffin embedded tissue sections were de-paraffinized and rehydrated in xylenes, followed by decreasing ethanol concentrations (100%, 95%, 70% diluted in distilled water) and finally distilled water. For the purposes of immunohistochemistry (IHC), all slides were hand dunked. Next, antigen retrieval was accomplished by pressure cooking slides for 10 minutes in 10mM sodium citrate pH 6.0. Slides were allowed to cool to room temperature and then washed in distilled water followed by PBS. One by one, slides were placed onto a humidity chamber and tissue sections were outlined using a PAP pen to create a hydrophobic barrier. From there, tissue sections were blocked with 2% BSA dissolved in PBS for half an hour and then incubated with primary antibody overnight at 4°C. Primary antibodies used were: anti-SOD1 (ab16831; dilution 1:5000) and anti-3-nitrotyrosine (ab110282; dilution 1:5000). After primary antibody incubation, slides were washed with dH_2O and PBS-T. Immediately following the washes, slides were treated with 0.3% hydrogen peroxide for 20 minutes. This is done to block endogenous peroxidases. Next, slides are incubated with secondary biotinylated antibodies (in 2% BSA) for 1 hour. Tissue sections are then incubated with Vectastain avidin-biotin complex kit (Vector laboratories). Finally, antigens are revealed with DAB substrate to allow visualization. Slides are once again dehydrated in increasing ethanol concentrations (70%, 95%, and 100%) followed by xylenes and are mounted using Acrytol Mounting Media (Leica Biosystems).

j. Microscopy

For both hematoxylin and eosin staining and immunohistochemistry, prepared slides were imaged using the automated upright microscope Leica DM4000B and Olympus CellSens imaging technology to aid in digital image acquisition and processing. Images were taken using brightfield and using either 20x or 40x magnification.

k. Tail vein lactate measurements

Tail vein blood lactate measurements were taken with the Lactate Plus handheld blood lactate meter (Nova Biomedical). These measurements were taken for a week after the completion of

tamoxifen or corn oil injections and then immediately before sacrifice. Adapted from Lønbro et al., one drop of tail vein blood was collected onto the disposable lactate analysis strips, provided by Nova Biomedical with the lactate meter[712]. To collect blood sample, the tail of each mouse was punctured with a razor blade and a drop of blood was allowed to drop onto lactate strip. Vein puncture is the preferred method of tail vein blood collection for lactate measurements. All animals were acclimated prior before tamoxifen and corn oil injections began to the blood sampling procedure.

l. Urea assay

To assess urea excretion, an indicator of kidney function, the Urea Nitrogen (BUN) Colorimetric Detection Kit from Arbor Assays was used[713]. Urine was collected from each mouse immediately after sacrifice. Once urinating, a 200µl single channel pipette was used to collect urine and urine was stored in a microcentrifuge tube at -80°C until urea measurements could be made. The urea content of this urine was determined according to manufacturer instructions. This is a colorimetric assay.

m. Bloodwork

Blood was collected via cardiac puncture from mice anesthetized with 5% isoflurane. Cardiac puncture is a technique that allows for up to 1mL of blood collection from a mouse. After blood samples were taken from the heart (ventricle on the left side of mouse chest), mouse was sacrificed immediately, and organs were removed for western blotting. Blood gently inverted in 1.3mL microtubes coated with K3 EDTA (Sarstedt) to prevent coagulation. A complete blood panel was performed each blood sample by the Comparative Medicine and Animal Resources Centre (CMARC) at McGill University.

n. Statistics

All statistical analyses were performed using Prism 8 (GraphPad Software) using either ANOVA or t-tests, as appropriate. All data is presented at mean ± standard error of the mean (SEM). A result is considered significant when the p-value is less than 0.05.

4. Results

a. Construction of a mouse strain combining a floxed *Sod1* allele and a broadly expressed tamoxifen (TM)-inducible *Cre* transgene

Although germline *Sod1*$^{-/-}$ mice are viable, MEFs isolated from these mice die. Therefore, it is likely that the survival of germline *Sod1* KO mice is the result of a developmental adaptation to the absence of SOD1. If this is true, adult-onset loss of SOD1, as can be obtained with TM-inducible CRE, would have a much more severe phenotype (Figure 35).

Adult-onset global *Sod1* knockout mice were generated by two breeding steps. First, we crossbred floxed *Sod1*$^{loxP/loxP}$ mice (previously described in chapter 2 and used to generated mouse embryonic fibroblasts) with CAG-CreER^{T2} mice[714]. CAG-CreER^{T2} mice ubiquitously express the fusion protein, Cre recombinase-ER^{T2}, a version of Cre recombinase that is only active when the synthetic estrogen analogues, tamoxifen, is present[714]. The resulting progeny from these breedings, CAG-CreER^{T2}; *Sod1*$^{loxP/loxP}$ mice, were then treated with tamoxifen to induce the excision of exons 2 and 3 from *Sod1*, yielding no detectable SOD1 protein.

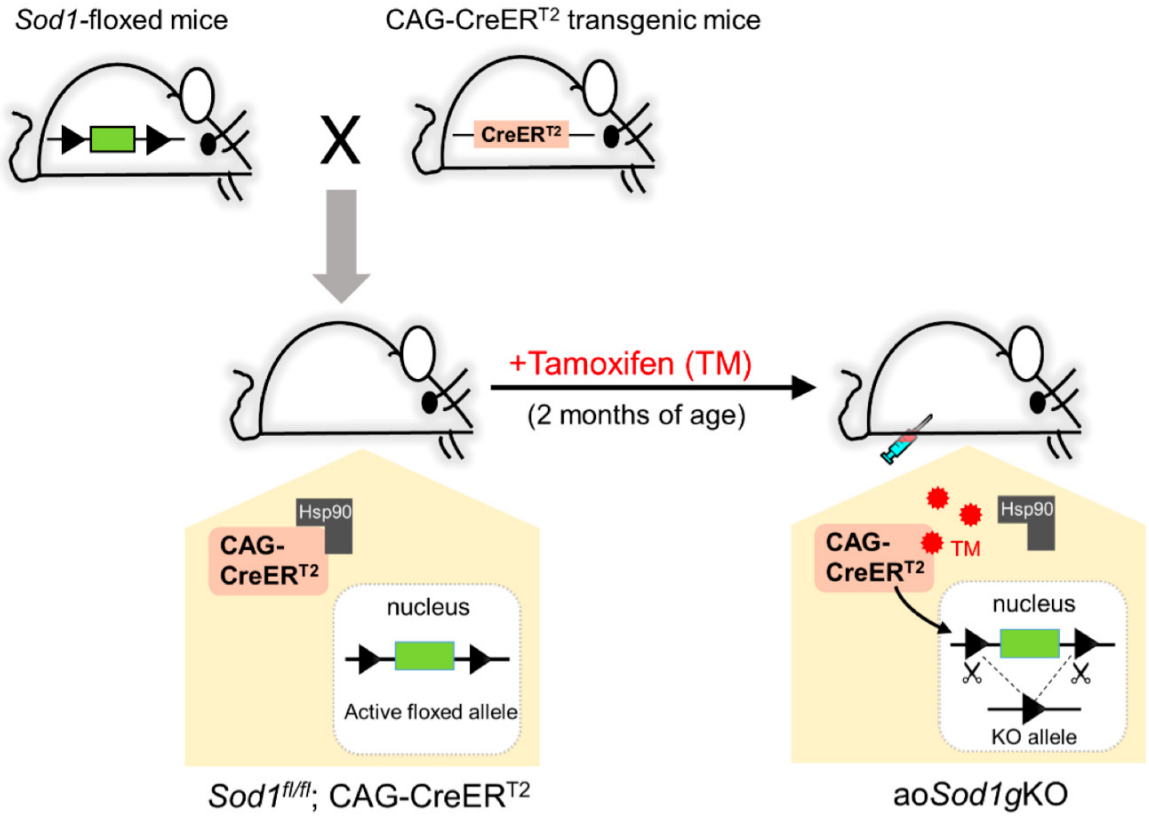

Figure 35: Schematic describing the steps involved in the generation of adult-onset *Sod1* global knockout mice.

Sod1$^{loxP/loxP}$ mice are crossed with mice containing the CAG-CreER^{T2} transgene. CAG-CreER^{T2} is an inducible version of *Cre*-recombinase. It is engineered to be activated by tamoxifen (TM). In CAG-CreER^{T2}, the inducible *Cre*-recombinase is under the control of a ubiquitous chimeric promoter of the cytomegalovirus immediate-early enhancer and chicken β-actin promoter/enhancer (CAG). Without TM, the fusion protein CreER^{T2} is inactive while being confined to the cytoplasm in a complex with heat shock protein 90 (Hsp90). Untreated *Sod1*$^{loxP/lox}$*; CAG-CreER*^{T2} mice express wild-type SOD1 at endogenous levels. Following intraperitoneal (IP) administration of TM, TM releases CreER^{T2} from Hsp90. CreER^{T2} can then translocate to the nucleus, where it is able to catalyze recombination between loxP sites.

b. Adult-onset global *Sod1* knockout mice die within three weeks of *Sod1* excision and are rescued by L-NAME treatment

We developed an inducible mouse model to understand how *Sod1*$^{-/-}$ mice can lack *Sod1*, which is responsible for up to 80% of superoxide dismutase activity, yet still be alive[715]. We use a *Cre-lox* system to control *Sod1* expression. These mice contain a floxed *Sod1* allele (*Sod1*$^{loxP/loxP}$) and a

transgene expressing a tamoxifen (TM)-sensitive *Cre* recombinase under an ubiquitous promoter (CAG)[716]. When the mice are treated with TM, *Cre* recombinase is translocated to the nucleus where it can splice out exons in the *Sod1* gene, leading to KO. Tamoxifen is used to induce knockout of *Sod1*. From a stock solution of 15mg tamoxifen/mL of corn oil, the mice receive 10 intraperitoneal (IP) injections, every other day (10μL/gram). Tamoxifen treatment successfully knocks out SOD1 expression (Figure 36) and within 3 weeks of the deletion of *Sod1*, the health of the mice quickly declines (weight loss, scruffy coat, hunched) and they die (Figure 37a-c). Furthermore, L-NAME IP injections (20mg/mL injected 10μL/gram, dissolved in saline), beginning on the off-days of tamoxifen injections and continued every other day for two months, successfully rescued the adult onset *Sod1* knockout mice. Instead of adult onset *Sod1* knockout mice dying no later than 3 weeks after loss of *Sod1*, mice treated with L-NAME are still alive and well, appearing healthy (well-groomed and energetic), after receiving L-NAME injections for 2 months (Figure 38a-c). Also note, the loss of SOD1 expression and treatment with L-NAME does not affect SOD2 and SOD3 expression levels, unlike in the cell work shown in the previous chapter (Figure A1).

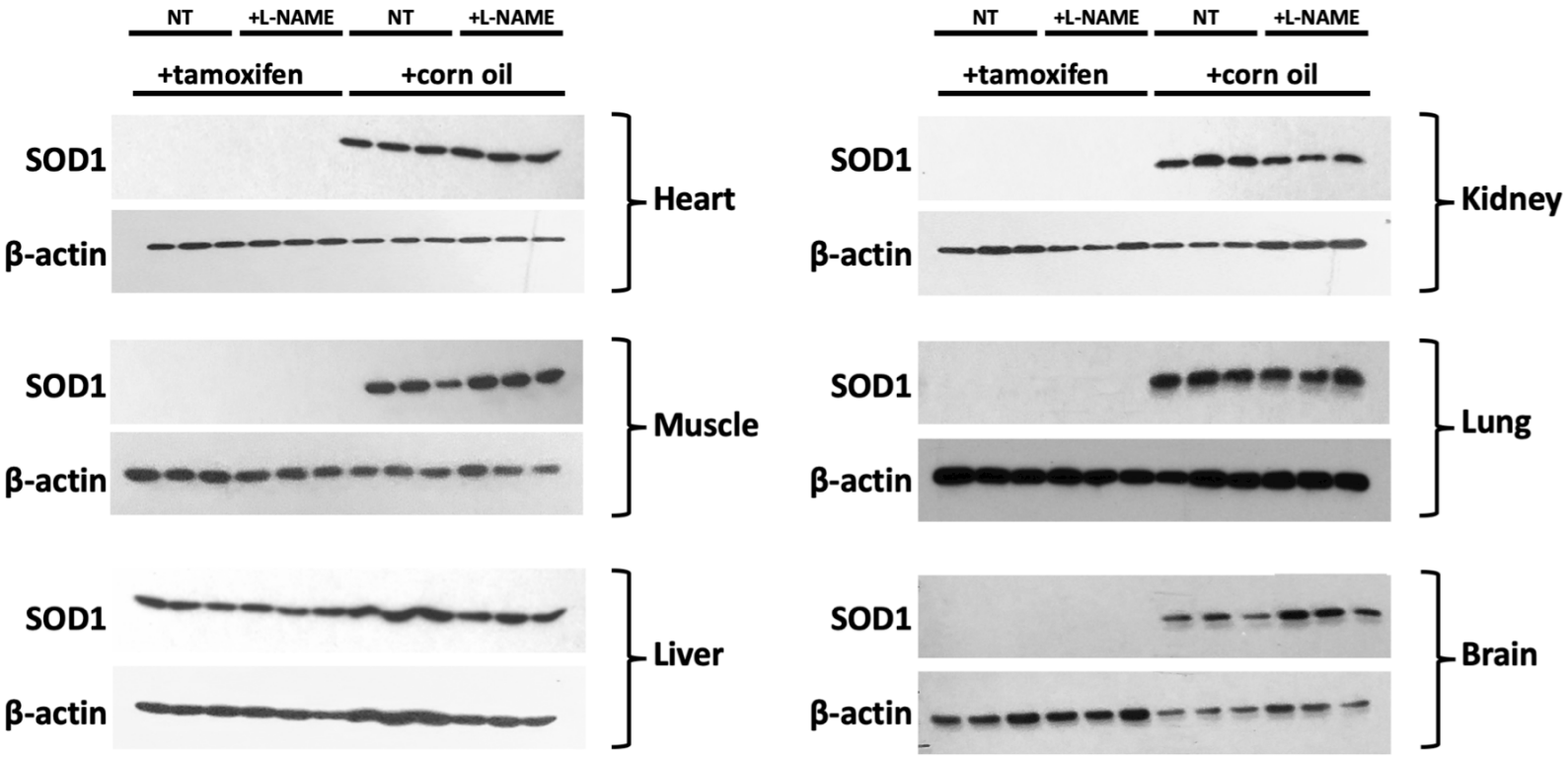

Figure 36: Tamoxifen successfully knockouts SOD1 in *Sod1$^{loxP/loxP}$* mice.
SOD1 expression is absent in the heart, muscle, kidney, lung and brain of all tamoxifen treated mice. The levels of SOD1 were analyzed 2 months after the completion of tamoxifen/corn oil intraperitoneal injections for all groups except the "tamoxifen only" mice since these mice die within three weeks of the completion of tamoxifen injections. Samples are taken for the tamoxifen only group at endpoint (approximately 2-3 weeks after the completion of tamoxifen injections) and all other samples are taken 2 months after the completion of corn oil/tamoxifen injections. During the 2 months following tamoxifen or corn oil injections, the mice in the L-NAME treated groups received intraperitoneal L-NAME injections every other day. The L-NAME is dissolved in saline at a concentration of 20mg/mL. NT stands for no treatments, meaning these mice received no further injections, other than the corn oil or tamoxifen injections.

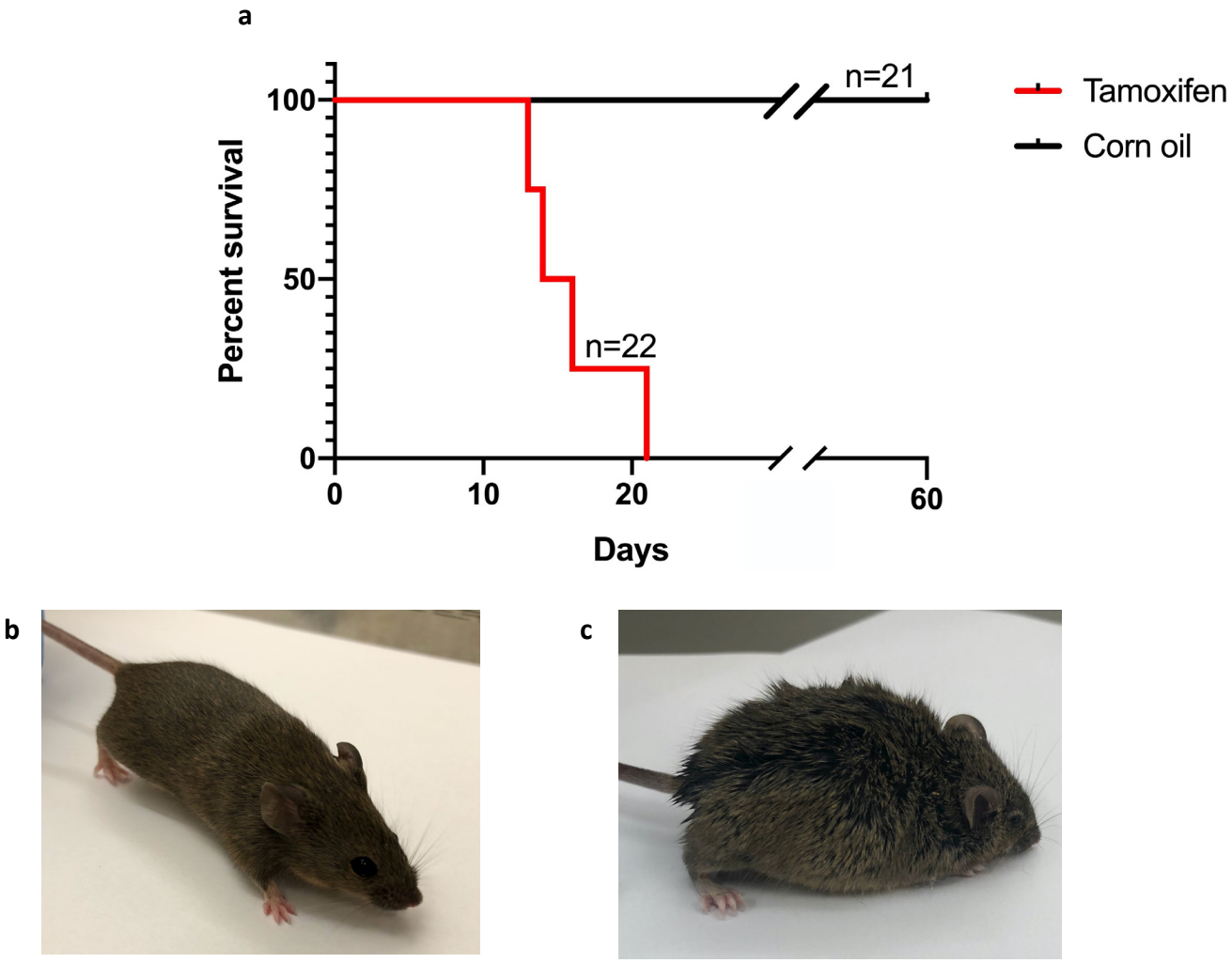

Figure 37: Adult onset *Sod1* knockout mice degenerate and die quickly.
a) Survival curve of control mice (*Sod1*$^{loxP/loxP}$ mice that received 10 intraperitoneal injections of corn oil, the vehicle used for tamoxifen) relative to the survival curve of tamoxifen treated *Sod1*$^{loxP/loxP}$ mice (adult onset *Sod1* knockout mice). Mice that lose *Sod1* expression as adults quickly die after the completion of tamoxifen injection, which induce the knockout. n=21 for corn oil group and n=22 for tamoxifen only group and the mice represent a collection of 6 individual experiments. b) Image of a control mouse (corn oil) and c) image of an adult onset *Sod1* knockout mouse (tamoxifen).

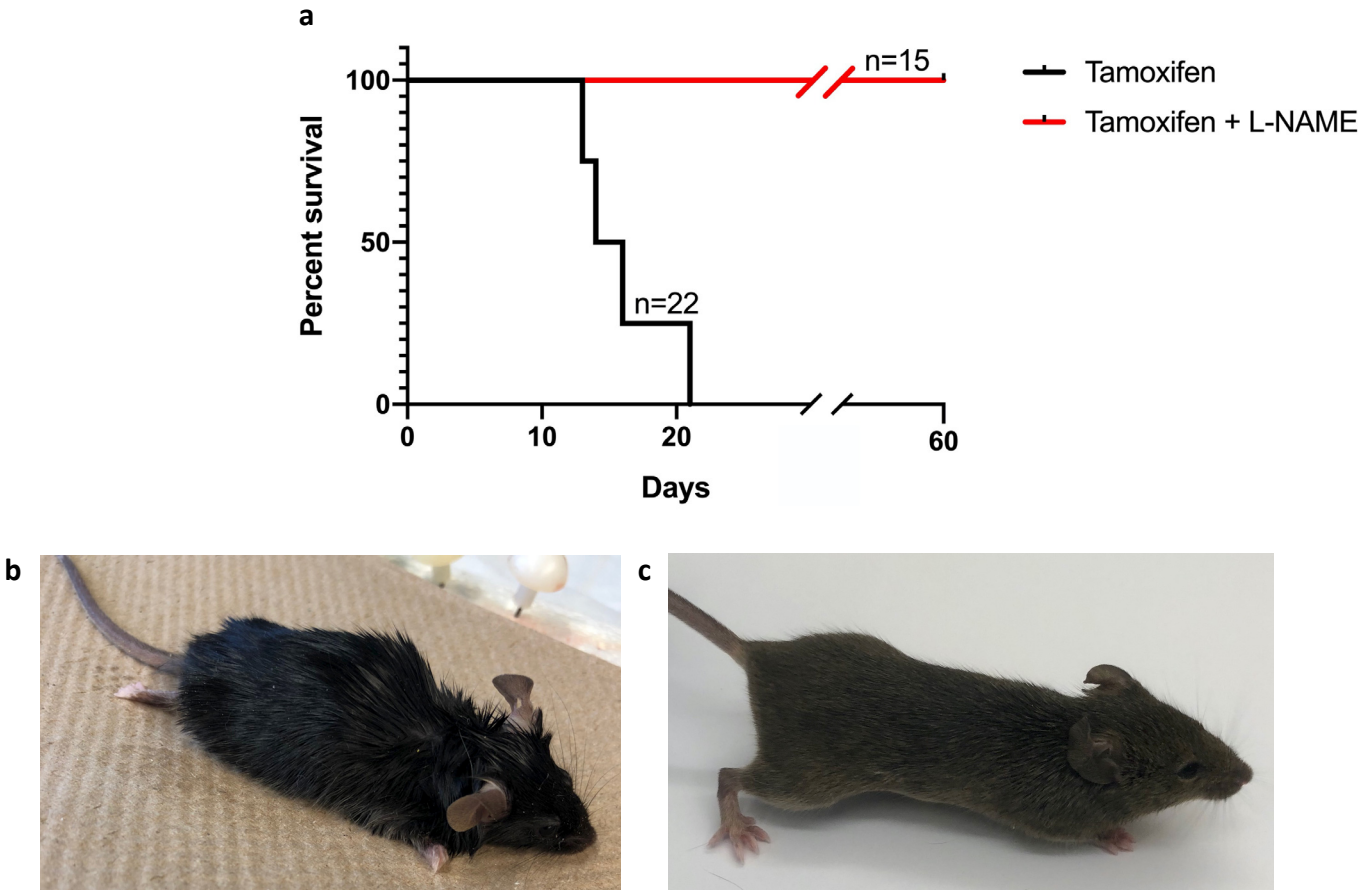

Figure 38: Adult onset *Sod1* knockout mice are rescued by L-NAME treatment.
a) Survival curve of tamoxifen treated *Sod1*$^{loxP/loxP}$ mice (adult onset *Sod1* knockout mice) relative to the survival curve of adult onset *Sod1* knockout mice that also received L-NAME injections. Mice that lose *Sod1* expression as adults quickly die after the completion of tamoxifen injection. But mice that receive L-NAME injections in combination with tamoxifen injections survive for the 2 months post tamoxifen injections that L-NAME injections are given. n= 22 for tamoxifen group and n=15 for the tamoxifen + L-NAME group. b) Image of an adult onset *Sod1* knockout mouse (tamoxifen) and c) image of a L-NAME treated adult onset *Sod1* knockout mouse (tamoxifen + L-NAME).

c. Dying adult-onset global *Sod1* knockout mice show signs of muscle atrophy and degradation

To uncover how adult-onset global *Sod1* knockout mice are dying, we sent formalin-fixed, paraffin-embedded mouse organs, specifically heart, muscle, brain, liver, and kidney, to Charles River Laboratories for trained pathologists to analyze. We sent samples from 12 mice – 3 that only received corn oil IP injections, 3 that received both corn oil and L-NAME IP injections, 3 that

only received tamoxifen IP injections, and 3 that received tamoxifen and L-NAME IP injections. Pathology showed that most organs (heart, brain, kidney, and liver) are unaffected in adult-onset *Sod1* knockout mice. They identified signs of muscle degradation in skeletal muscles of mice lacking *Sod1* and from there we went on to analyze tissue sections and procure images of these afflicted muscles. From there, we analyzed further muscle sections for similar signs of muscle degeneration and found that loss of *Sod1* in young adult mice clearly leads to acute degeneration of skeletal muscles (Figure 39 and 40). Signs of skeletal muscle degeneration include nuclear clumps, swollen/fragmented muscle fibers, macrophage infiltration, and dystrophic mineralization[717]. Immunohistochemistry for SOD1 confirmed that SOD1 was, in fact, lost in skeletal muscles that show signs of muscle degeneration (Figure 41). Even better, L-NAME rescued adult-onset *Sod1* knockout mice have skeletal muscles that resemble normal, healthy skeletal muscles (Figure 42 and A2).

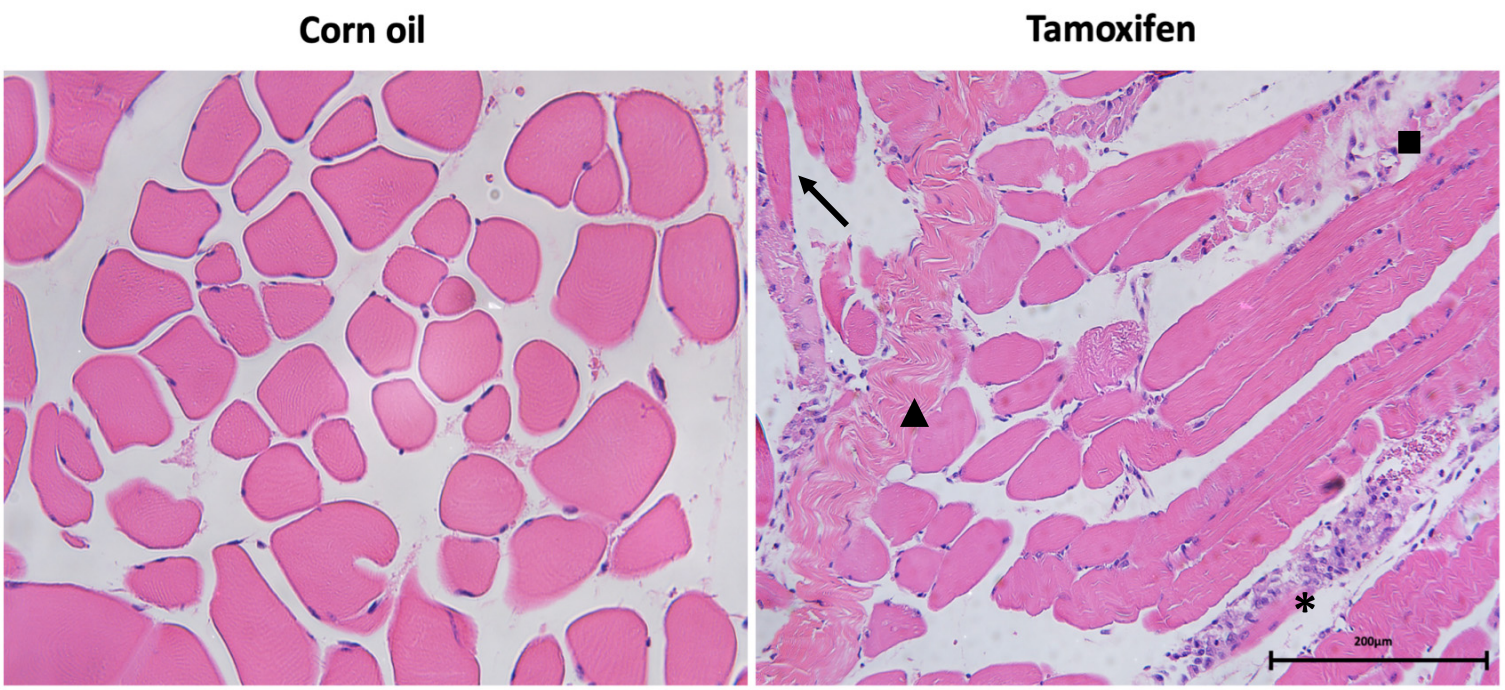

Figure 39: Loss of Sod1 in young adults leads to acute skeletal muscle degeneration.
Adult onset *Sod1* knockout mice (tamoxifen injected) show signs of muscle degeneration. There are little to no signs of muscle degeneration in mice that still have SOD1 expression (corn oil injected). * indicates an example of phagocytosis seen in degenerating muscle, characterized by clusters of nuclei seemingly without associated cellular structure. Macrophage infiltration is key for phagocytosis of debris associated with muscle degeneration. Arrow indicates swollen myofibers, yet another sign of muscle degeneration. Triangle indicates fragmented muscle fibers. Square indicates hyalinized muscle fibers, or tissue that is degenerating into a translucent glass-like state. All images are longitudinal cross-sections of muscle tissues. Degenerating myofibers can be displaced, enlarged, and fragmented, therefore are not always cut exactly perpendicularly as can be easily done in healthy muscle tissue.

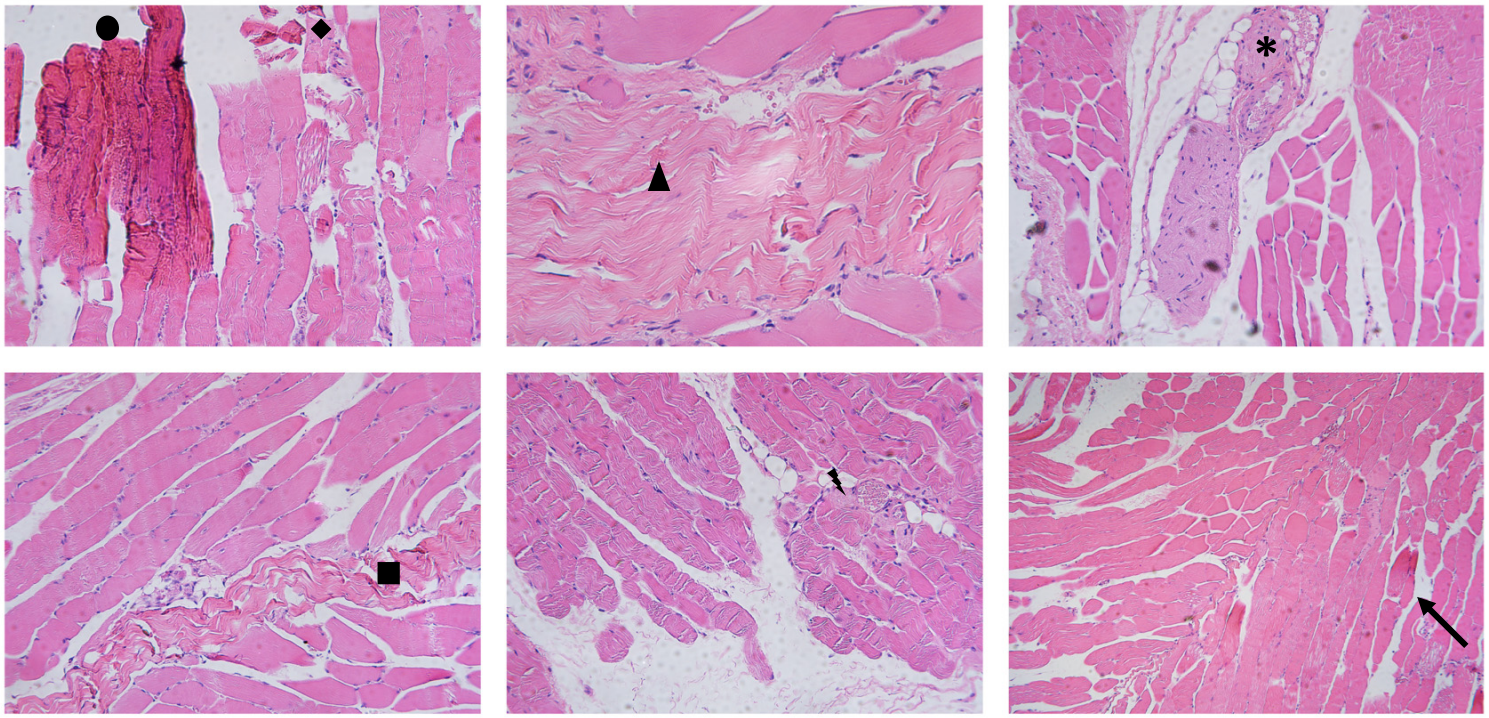

Figure 40: Further examples of muscle degeneration in adult onset *Sod1* knockout mice.
Other images of muscle degeneration seen in adult onset *Sod1* knockout mice. Top left image shows more signs of muscle degeneration - the juxtaposition of hypereosinphilic and hypoeosinphilic muscle fibers, indicated by a circle, and dystrophic calcification (calcification that occurs during the degeneration of necrotic tissue), indicated by a diamond. Triangle in the top middle image indicates fragmented muscle fibers. In the top right image, * indicates phagocytosis of severely degenerated muscle tissue. In the bottom left image, the box marks fragmented and partly hyalinized muscle fiber that loses striations. This is accompanied by early infiltration of macrophages. Lightning bolt in the bottom middle image marks rounded fiber with internal nucleus and cytoplasmic vacuoles, another sign of muscle degeneration. And, the bottom right image has many examples of swollen myofibers, indicated by an arrow.

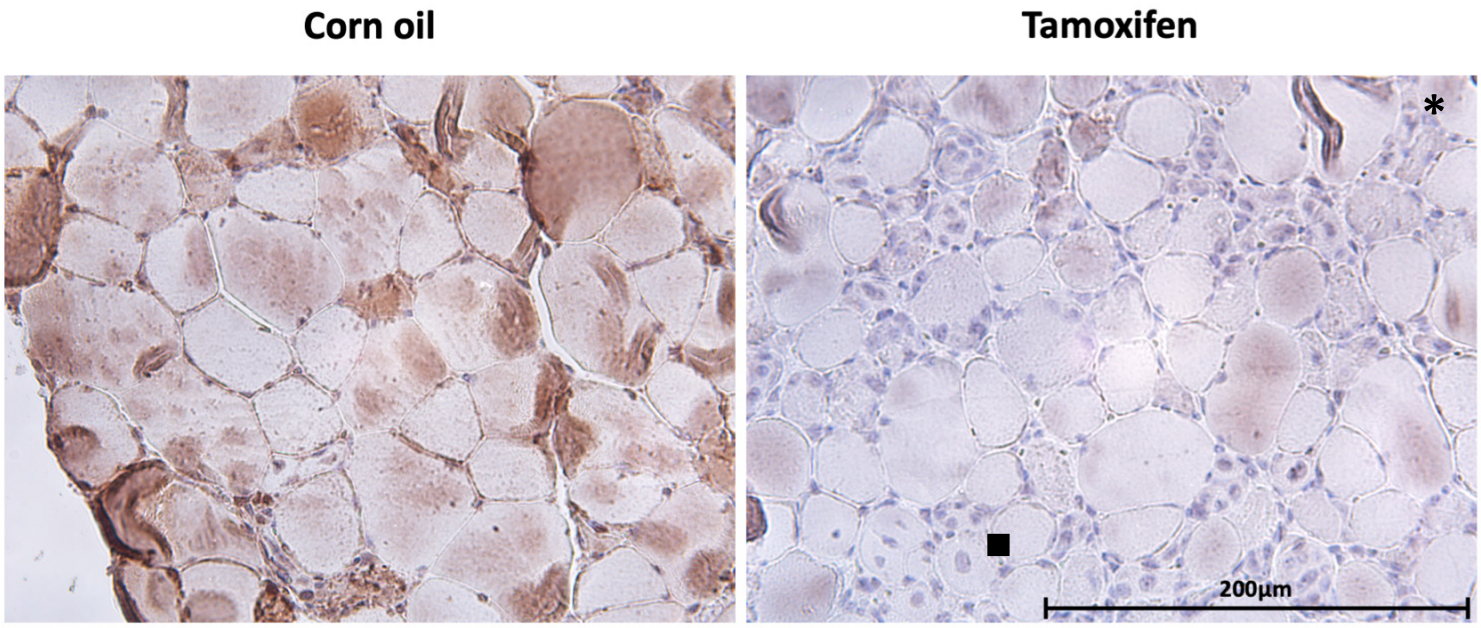

Figure 41: SOD1 is lost in degenerating skeletal muscle.
Immunohistochemistry further confirms that SOD1 expression is lost in skeletal muscle of mice that received tamoxifen injections. Blue staining is hematoxylin and the brown staining results from SOD1 antibody (ab16831). Tissues were removed at sacrifice, fixed in formalin for 24 hours, and then embedded with paraffin. Tissue sections were sliced on a microtome and mounted on Fisherbrand™ Superfrost™ Plus Microscope Slides. Superfrost slides have undergo a special treatment process that electrostatically adheres tissue sections to the slide without the need for extra adhesives or protein coatings. For immunohistology study, the sections were incubated with sodium citrate (10mM, pH 6.0, pressure cooked for 10 minutes) for antigen retrieval. Blocking for non-specific binding was achieved by 30 minutes incubation in 2% BSA. Slides were subsequently incubation with primary antibody against SOD1 overnight at 4°C. Next, the slides were incubated with biotinylated secondary antibody and avidin-biotin-peroxidase from Vectastain ABC kit according to manufacturer's instructions. Binding of ABC was visualized by incubation with diaminobenzidine. Finally, the nuclei were counterstained with hematoxylin. Staining revealed, once again, that adult onset *Sod1* knockout mice show signs of muscle degenerations, in this case, nuclear clumps. Nuclear clumps are nuclei that are detached from their normal location and found in the center of the cell. Centrally located nuclei are a sign of muscle atrophy and degeneration. The most obvious signs of muscle degeneration seen are phagocytosis (*) and centrally located nuclei/nuclear clumps (square).

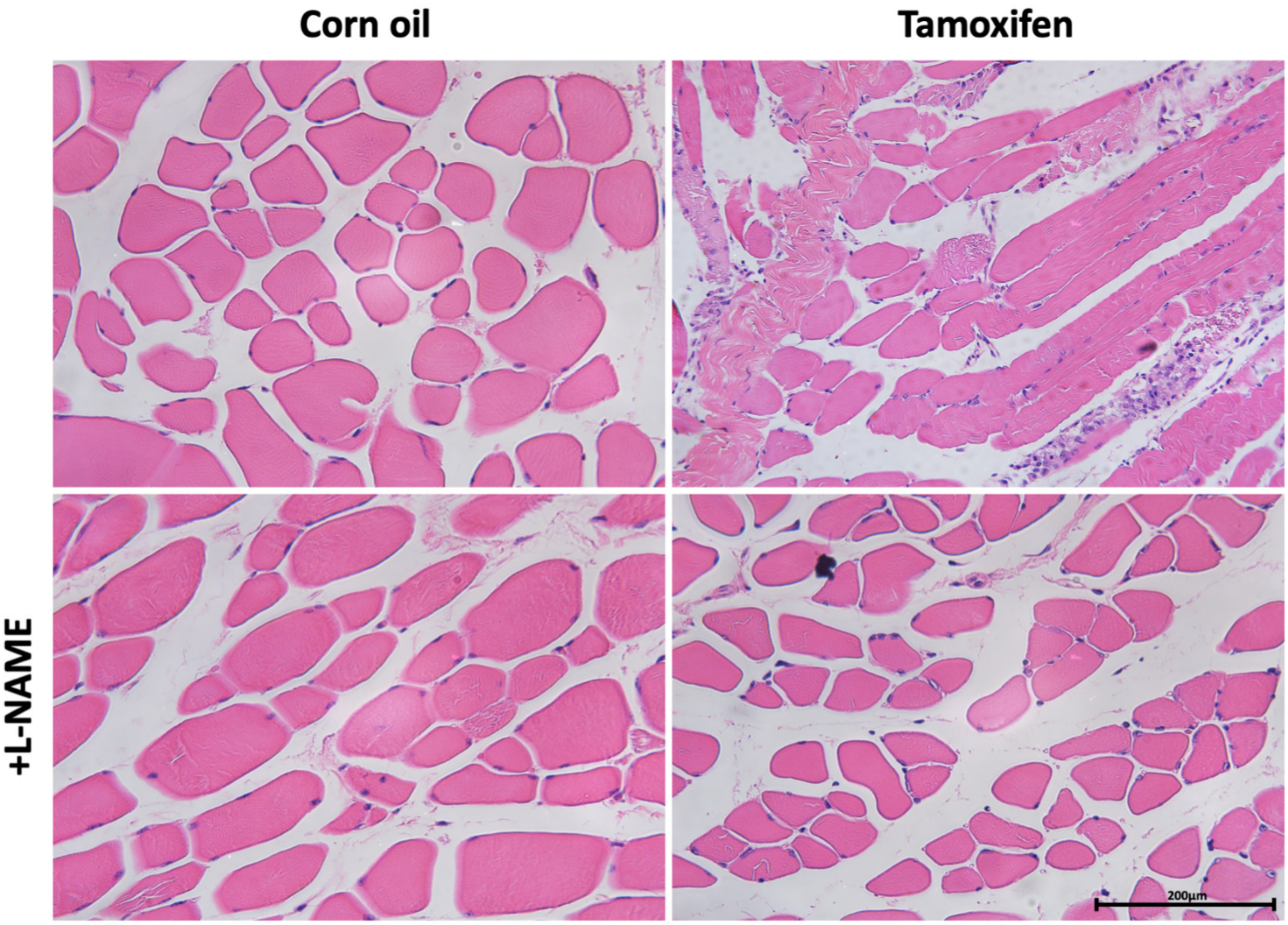

Figure 42: L-NAME rescued adult onset *Sod1* knockout mice have healthy skeletal muscles. Pathology of skeletal muscles shows muscle degeneration in adult onset *Sod1* knockout mice. Skeletal muscle pathology is seen by H&E (hematoxylin & eosin) staining. Hematoxylin stains the nuclei blue and eosin stains the extracellular matrix and cytoplasm pink. This is not observed in adult onset *Sod1* knockout mice rescued with L-NAME. The skeletal muscles of L-NAME rescued adult onset *Sod1* knockout mice resemble skeletal muscles of healthy mice (e.g. corn oil injected mice). Also note, L-NAME does not appear to alone affect skeletal muscles (see mice treated with simultaneously corn oil and L-NAME.

Elevated lactate (>3mmol/L) is an indicator of mitochondrial dysfunction and the presence of high levels of reactive oxygen species (ROS) [718, 719]. Lactate is a sign that the tissues are relying on the glycolysis for energy production, rather than the mitochondrial electron transport chain (ETC), because of damage, including possibly ROS damage, to the ETC. [720]. To check lactate levels in these mice, I tracked lactate levels using a lactate blood meter and test strips from Nova Biomedical. I measured lactate levels in adult-onset global *Sod1* knockout mice every other day for the first week of injections and then at endpoint. Lactate levels are significantly elevated and the elevation of lactate in tail vein blood appears to worsen as the condition of the mice worsen (Figure 43).

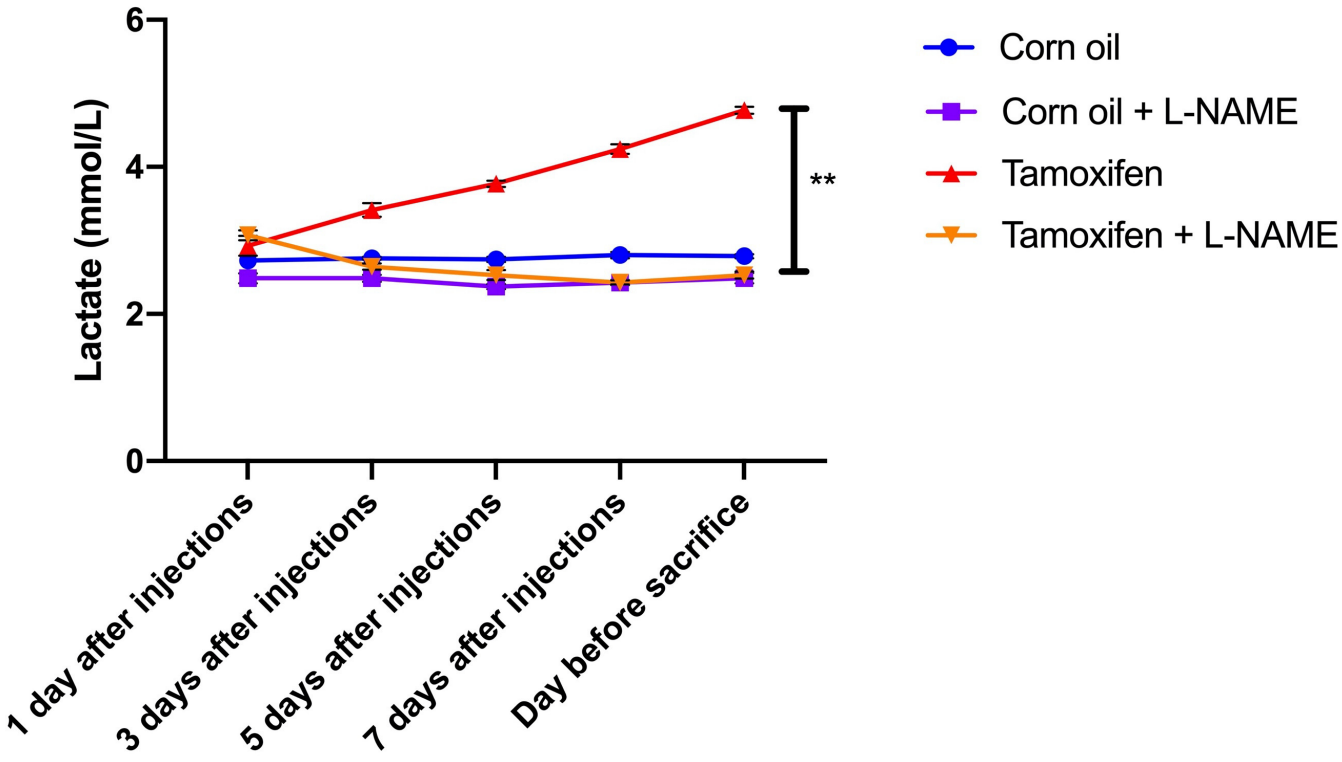

Figure 43: Adult onset *Sod1* knockout mice have elevated lactate levels.
Elevated lactate levels are most commonly caused by tissue hypoperfusion and are a sign of elevated reactive oxygen species (ROS). Lactate is produced as a result of glycolysis. Glycolysis becomes the primary method of ATP production when there is damage to the mitochondrial electron transport chain (ETC). Damage to the ETC is associated with ROS production. Adult onset *Sod1* knockout mice (tamoxifen) have significantly elevated lactate levels, compared to both control (corn oil) groups and L-NAME rescued adult onset *Sod1* knockout mice (tamoxifen + L-NAME). n=7 for all 4 groups of mice. Error bars indicate SEM. ** $p \leq 0.01$ (t-test).

As adult-onset *Sod1* knockout mice worsen, their body weight dramatically decreases (Figure 44) and there are changes in their breathing patterns by visual observation. Due to these observations and the rapid degeneration of hindlimb skeletal muscles, we hypothesize that the muscles involved in eating, drinking, and breathing may be compromised as well.

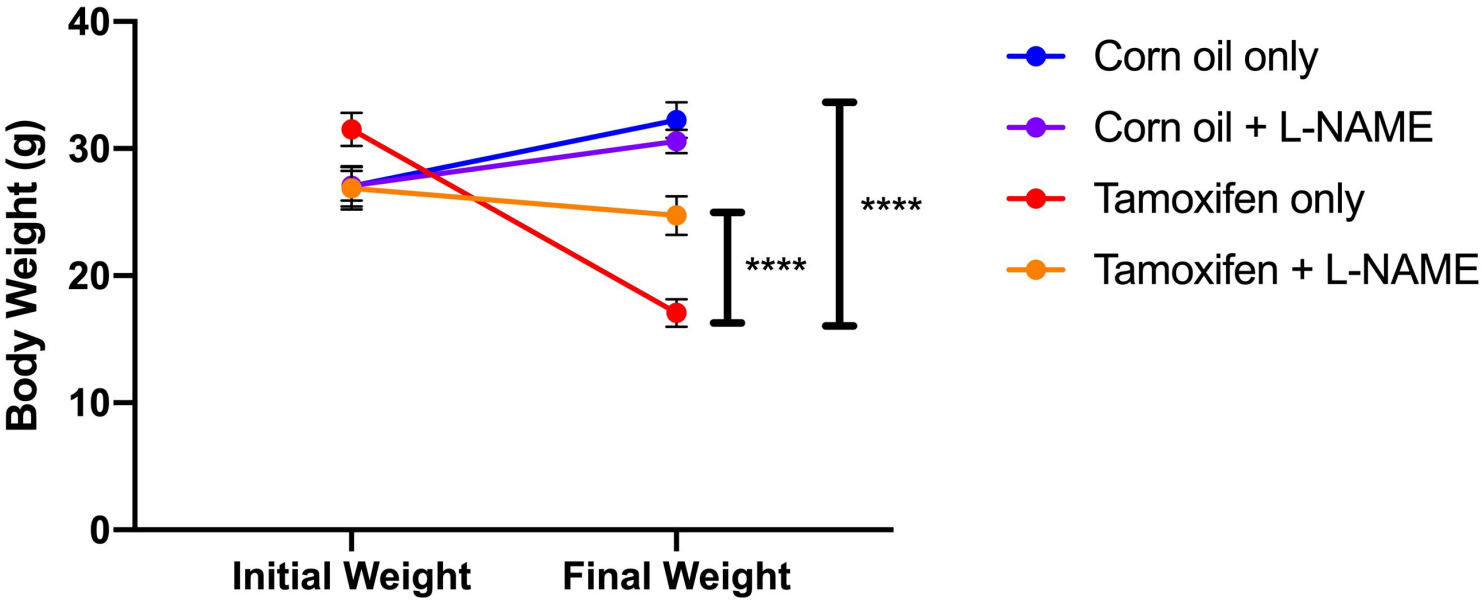

Figure 44: Body weight of adult onset *Sod1* knockout mice.
Body weights in adult-onset *Sod1* knockout mice. Initial weights of the mice were measured the day prior to beginning treatments. The animals were intraperitoneally injected with corn oil or tamoxifen 10 times, every other day. The animals receiving L-NAME intraperitoneal injections received the first injection the day after the first corn oil/tamoxifen injection, and then received a L-NAME injection every other day until 2 months after the completion of corn oil/tamoxifen injections. The body weights of both corn oil-treated (control) groups gained weight, whereas the body weights of both tamoxifen-treated (adult-onset *Sod1* knockout) groups lost weight. The tamoxifen only group lost weight much more rapidly than the tamoxifen + L-NAME group.). n=12 for all groups of mice, except the tamoxifen group where n=18. Error bars indicate SEM. **** $p \leq 0.0001$ (t-test).

d. Peroxynitrite in adult-onset global *Sod1* knockout mice

We hypothesize that the degenerating muscles of adult-onset global *Sod1* knockout mice show increased protein damage from peroxynitrite, formed as a result of the reaction of excess $O_2^{\bullet-}$ and $NO^{\bullet}$. While this hypothesis is supported by the fact that L-NAME treatment fully prevents muscle degeneration in adult-onset *Sod1* knockout mice, we would like more direct evidence that peroxynitrite formation is involved. 3-nitrotyrosine (3-NT, the addition of $-NO_2$ to tyrosine) is a protein modification commonly attributed to peroxynitrite and is generally accepted as a biomarker for endogenous peroxynitrite activity[380]. Analysis of peroxynitrite levels in muscle by immunohistochemistry (IHC) suggests that adult-onset *Sod1* knockout mice with degenerating muscles do have higher peroxynitrite levels than both the control mice and adult-onset *Sod1* knockout mice rescued with L-NAME (Figure 45). It is also noteworthy that the highest 3-NT levels correspond to the areas of significant muscle degeneration, specifically, in Figure 45, nuclear clumps and macrophage infiltration. This is not entirely surprising as it has been shown that skeletal muscle from germline *Sod1*$^{-/-}$ mice have increased 3-NT[721]. However, the fact the skeletal muscle phenotype of adult onset *Sod1*$^{-/-}$ mice also show this elevation of 3-NT is a good indicator that muscle degradation, although more rapid, may be occurring by a similar mechanism. Furthermore, any previous study that looked at 3-NT levels in germline *Sod1*$^{-/-}$ mice observed these levels only by western blot. IHC provides us with new insight of where increases in peroxynitrite are important for muscle maintenance.

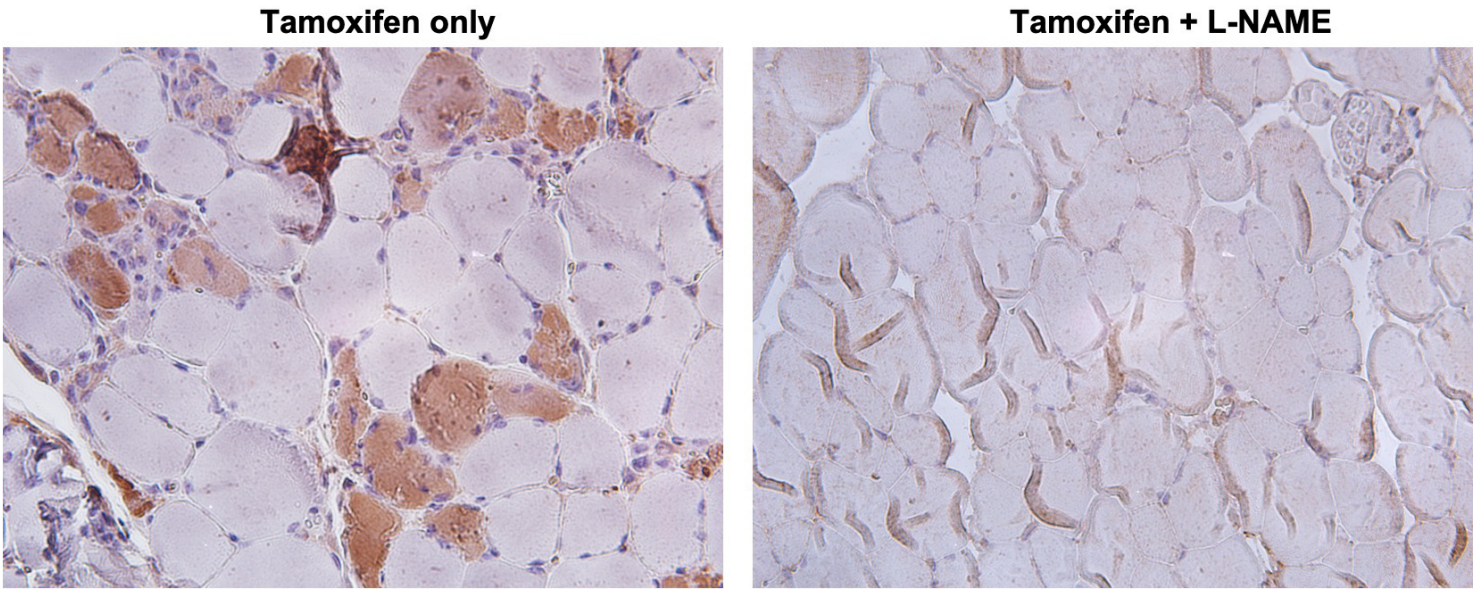

Figure 45: Peroxynitrite in skeletal muscles of adult onset Sod1 knockout mice.
Immunohistochemistry for 3-nitrotyrosine (3-NT), a biomarker of peroxynitrite, shows elevated 3-NT levels in adult onset *Sod1* knockout, compared to L-NAME rescued adult onset *Sod1* knockout mice and corn oil injected control mice. Blue staining is hematoxylin and brown staining results from binding of 3-NT antibody. The above figure compares 3-NT staining in not-rescued adult-onset *Sod1* knockout mice (tamoxifen only) to 3-NT staining in L-NAME rescued adult-onset *Sod1* knockout mice (tamoxifen + L-NAME). In addition to seeing an elevated level of 3-NT staining in the tamoxifen only mice to the L-NAME rescued tamoxifen mice, there are also indications of muscle degradation in the tamoxifen only image, specifically nuclear clumps (aggregates of nuclei) and macrophage infiltration.

e. Heart, brain, liver, and kidney are unaffected by loss of *Sod1*

Paraffin-embedded organs, other than skeletal muscles, were also analyzed. The heart and brain showed no morphological changes, assessed with H&E (hematoxylin and eosin) staining, when *Sod1* expression was lost (Figures 46 and 47). This was both unexpected and somewhat expected. The fact that germline *Sod1* knockout mice (*Sod1*$^{-/-}$) live for approximately 24 months suggests that the major organs can thrive without *Sod1.* But our inducible *Sod1* KO mice (*Sod1*$^{loxP/loxP}$) die within three weeks of the completion of their tamoxifen injections and in mice that quickly deteriorate, one would expect damage to major organs, such as the heart. Furthermore, *Sod1* is one of the most abundant proteins in mice and it still remains surprising that the majority of the mouse's organs can remain undamaged in mice that lack *Sod1* and that die as a result of this loss

of gene expression. Note, while the liver and kidneys showed no morphological changes as a result of *Sod1* loss, these organs in all treatment groups (corn oil alone, corn oil + L-NAME, tamoxifen alone, and tamoxifen + L-NAME) showed evidence of damage that is characteristic of receiving continuous intraperitoneal injections for consecutive months (Figure 48 and 49)[722]. Mild kidney damage, in all groups, was also evident from elevated blood urea nitrogen (BUN) levels. This data is not included in the thesis as the elevated BUN levels are a result of continuous intraperitoneal injections, rather than the loss of *Sod1*.

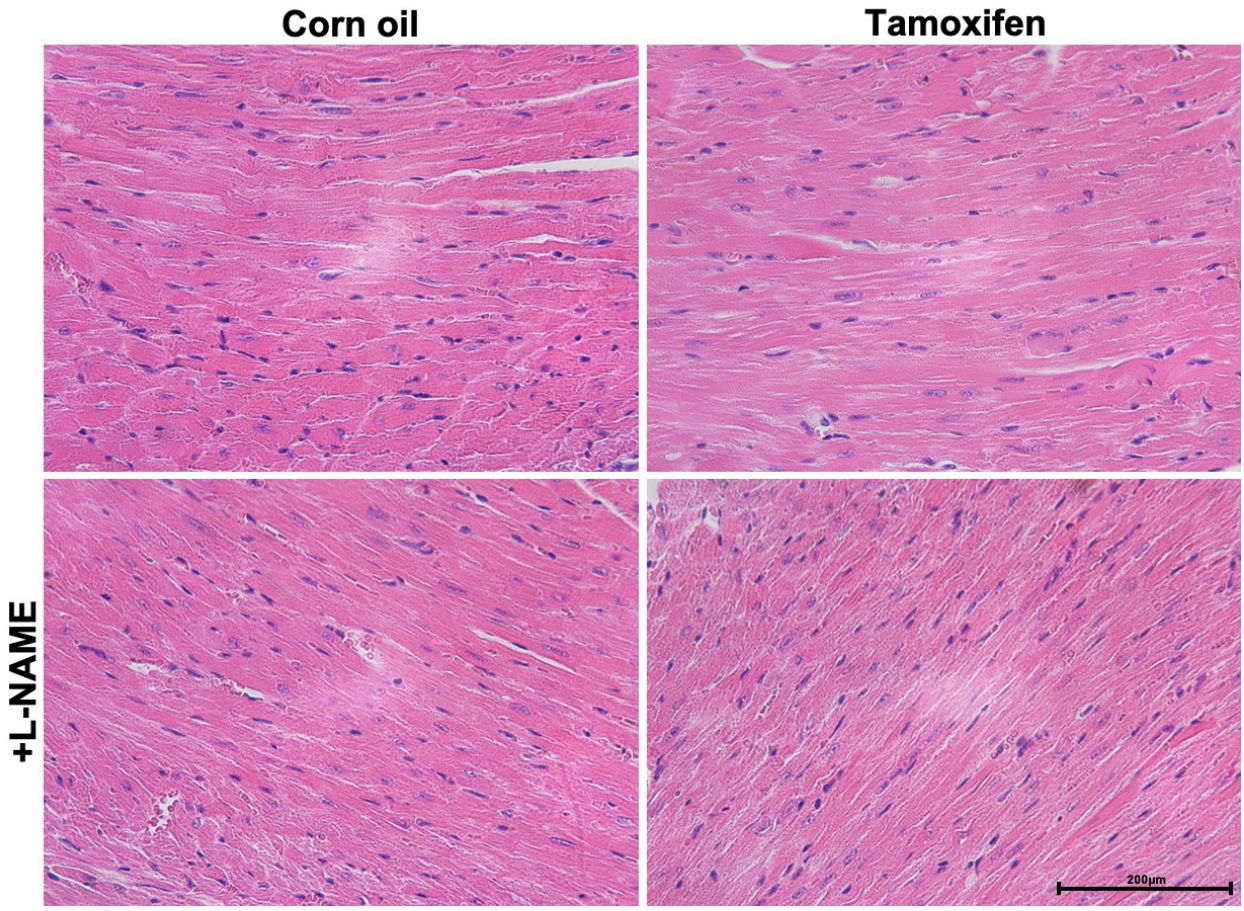

Figure 46: Loss of *Sod1* does not alter the morphology of cardiac muscles.
Pathology of cardiac muscles (heart) shows no morphological changes in adult onset *Sod1* knockout mice when compared to control mice (corn oil only). Cardiac muscle pathology is visualized by H&E (hematoxylin & eosin) staining. Hematoxylin stains the nuclei blue and eosin stains the extracellular matrix and cytoplasm pink. The cardiac muscles of tamoxifen-only adult onset *Sod1* knockout mice and L-NAME-rescued adult onset *Sod1* knockout mice resemble cardiac muscles of healthy mice. Also note, L-NAME does not appear to alone affect cardiac muscles (see mice treated with simultaneously corn oil and L-NAME).

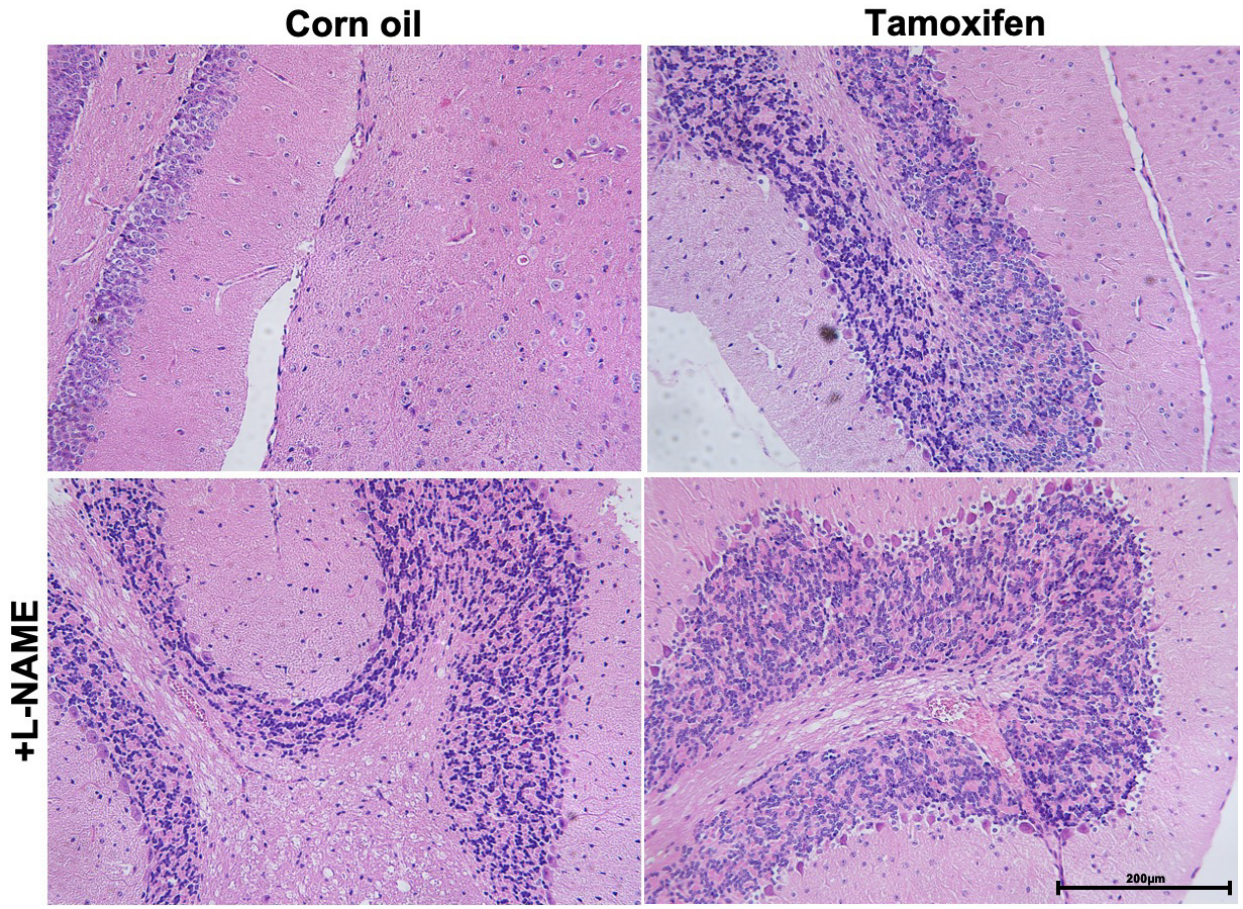

Figure 47: Loss of *Sod1* causes no morphological changes in the brain.
Pathology of the brain shows no morphological changes in adult onset *Sod1* knockout mice when compared to control mice (corn oil only). Brain morphology is visualized by H&E (hematoxylin & eosin) staining. Hematoxylin stains the nuclei blue and eosin stains the extracellular matrix and cytoplasm pink. The brains of tamoxifen-only adult onset *Sod1* knockout mice and L-NAME-rescued adult onset *Sod1* knockout mice resemble brains of healthy mice. Also note, L-NAME does not appear to alone affect brain morphology (see mice treated with simultaneously corn oil and L-NAME).

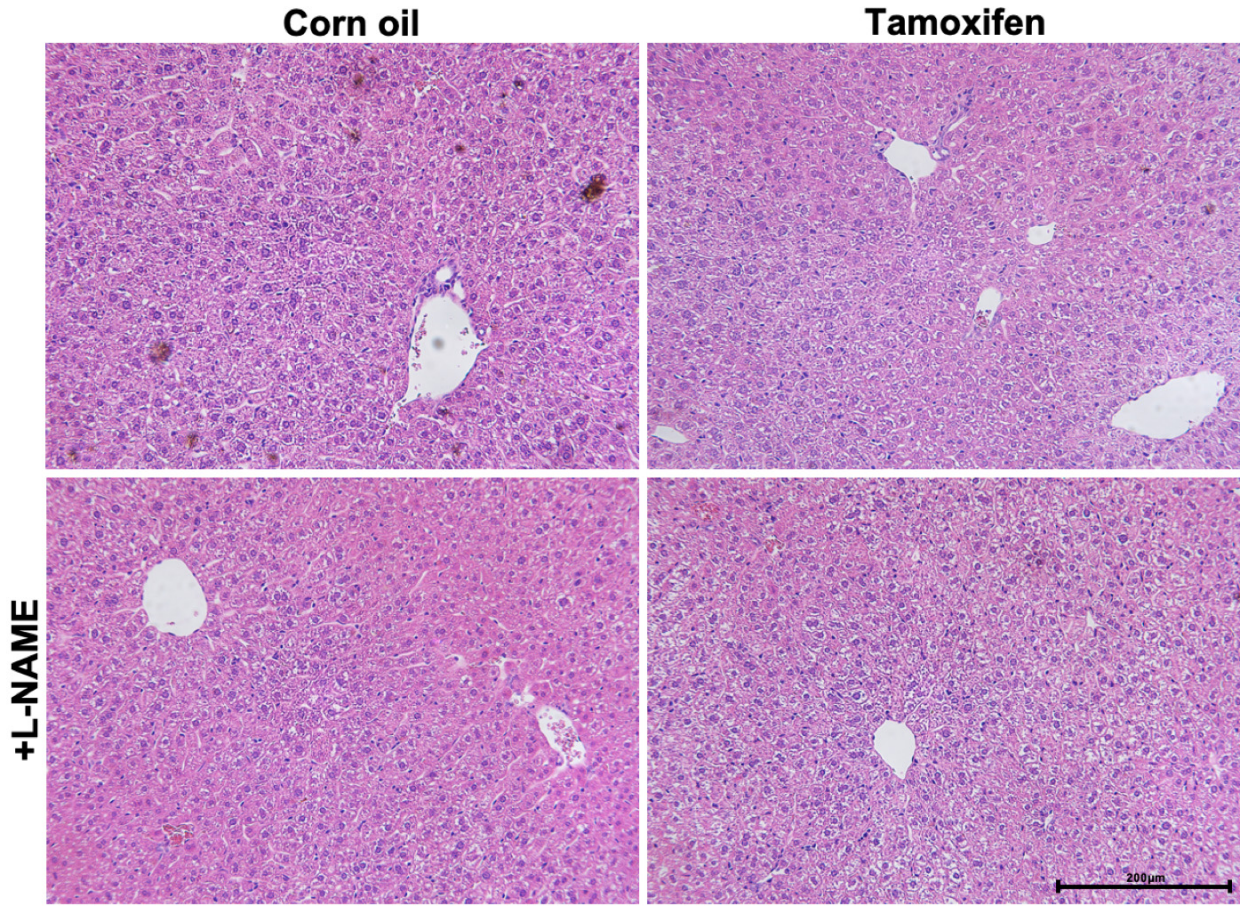

Figure 48: Morphological changes in liver of mice lacking *Sod1* are a result of continuous intraperitoneal injections.

Any morphological changes observed in the liver are not a result of the loss of *Sod1*, but rather a result of continuous intraperitoneal injections of corn oil, tamoxifen, and L-NAME for months. In fact, *Sod1* is not lost in the liver as tamoxifen is metabolized in the liver. Histological assessment of the liver was performed on tissues fixed in zinc-formalin at 4°C, followed by sequential dehydration to a final concentration of 70% ethanol. Next, tissues were paraffin-embedded, sectioned, and stained with hematoxylin and eosin to visualize nuclei and extracellular matrix/cytoplasm, respectively. Liver sections were initially assessed by a trained pathologist and the abnormality seen in all liver samples, for each experimental group, was mild necrosis. This is a result of drug metabolism in the liver and tissue damage from intraperitoneal injections.

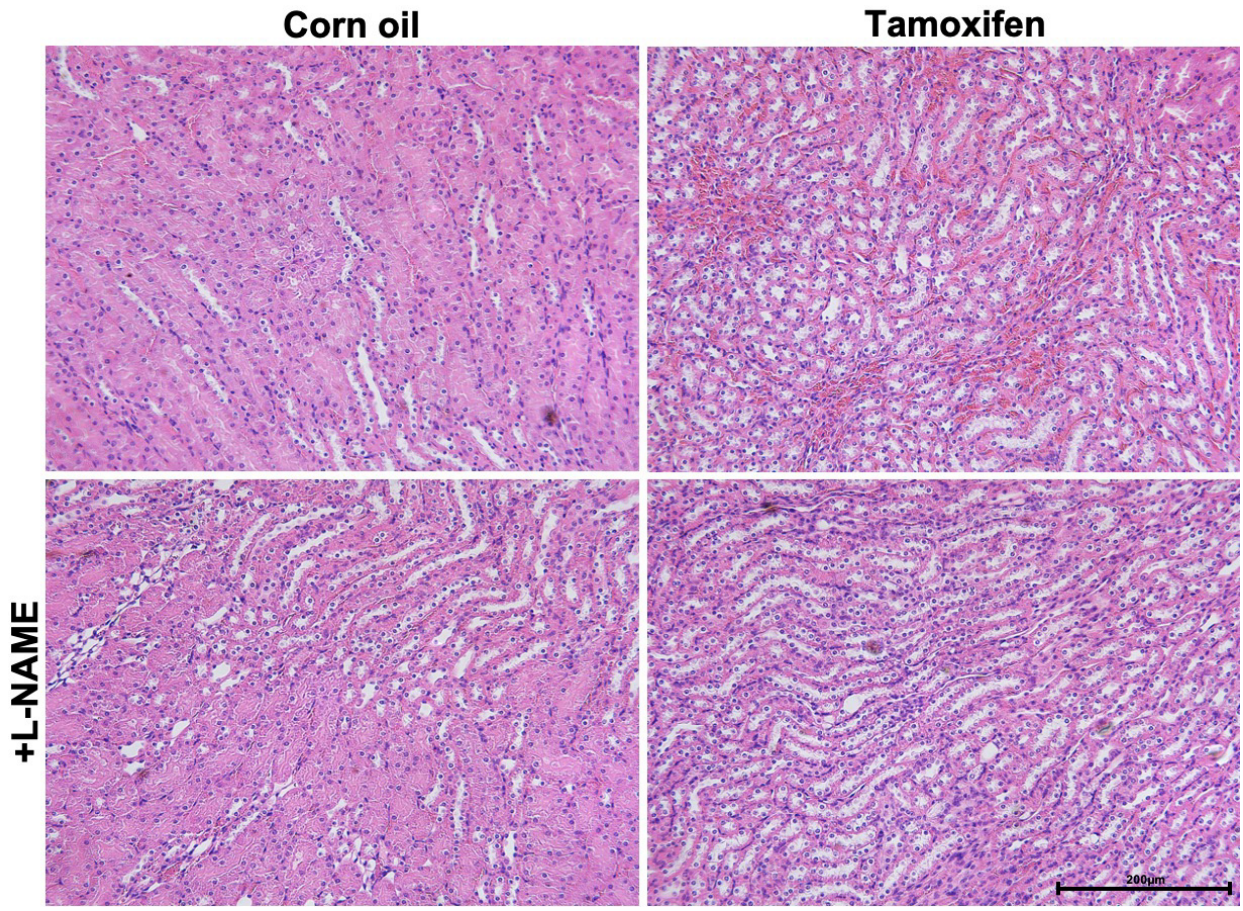

Figure 49: Changes in kidney morphology in inducible *Sod1* knockout mice result from continuous intraperitoneal injections.

Any morphological changes to the kidneys, were observed in all 4 experimental groups, indicating that the changes were a result of intraperitoneal injections, not the loss of *Sod1* expression. Histological assessment of the kidneys was performed on tissues fixed in zinc-formalin at 4°C, followed by sequential dehydration to a final concentration of 70% ethanol. Next, tissues were paraffin-embedded, sectioned, and stained with hematoxylin and eosin to visualize nuclei and extracellular matrix/cytoplasm, respectively. Kidney sections were initially assessed by a trained pathologist and the gross abnormality seen in all kidney samples, for each experimental group, was acute kidney injury resulting from repetitive intraperitoneal injections. This damage likely occurs because kidneys are the major organ responsible for toxin filtration[723].

f. Developmental adaptations in germline *Sod1* knockout mice

The fact that adult-onset inducible *Sod1* knockout mice rapidly die after the loss of *Sod1* expression, yet somehow germline *Sod1* knockout mice, also lacking *Sod1* expression but since the beginning of their development, have a mean lifespan of 20.8 months was surprising[17]. This suggests that *Sod1* germline KO mice have developmental adaptation(s) that enable these mice to survive without *Sod1,* the principal defense against superoxide formation. To uncover what adaptation(s) allow $Sod1^{-/-}$ mice to survive, we were guided by the result that L-NAME rescues adult-onset *Sod1* knockout mice. It suggests that $NO^{\bullet}$ handling may be altered to allow $Sod1^{-/-}$ mice to survive.

First, we examined NOS expression in $Sod1^{+/+}$, $Sod1^{+/-}$ and $Sod1^{-/-}$ mice. L-NAME rescues inducible *Sod1* KO mice by inhibiting NOS. Decreasing NOS expression would also lead to a decrease in $NO^{\bullet}$ available to react with superoxide and thereby less peroxynitrite. Furthermore, since skeletal muscle degradation was found in dying inducible *Sod1* KO mice, perhaps this change in NOS expression in germling *Sod1* KO mice would occur in the skeletal muscle. I evaluated the expression levels of all three NOS isoforms in skeletal and cardiac muscles (Figure 50 and A3). The only significant change of NOS expression seen between the $Sod1^{+/+}$ and $Sod1^{-/-}$ mice was a decrease in nNOS expression in the skeletal muscle of both $Sod1^{+/-}$ and $Sod1^{-/-}$ mice. Although we only observe a decrease in expression of a single NOS isoform, the localization of the activity might be crucial and sufficient to reduce the levels of peroxynitrite formed so they are not lethal.

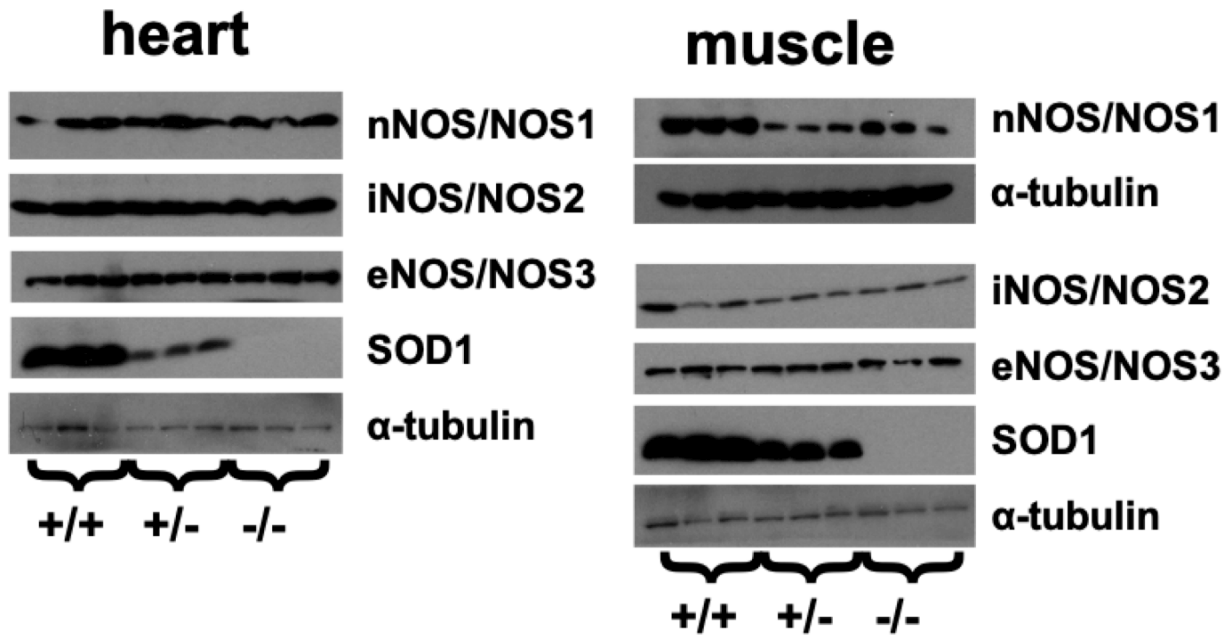

Figure 50: NOS expression in *Sod1* germline knockout mice
In heart, expression of all three nitric oxide synthase (NOS) isoforms remains unchanged between the three genotypes examined - $Sod1^{+/+}$, $Sod1^{+/-}$ and $Sod1^{-/-}$ mice. However, in the muscle, inducible NOS and endothelial NOS levels remain the same regardless of *Sod1* expression, but neuronal NOS levels seem to have significantly decreased in both the heterozygous and homozygous *Sod1* knockout mice. The genotypes of the mice were confirmed by PCR and SOD1 western blotting. It is evident that $Sod1^{+/-}$ mice have a lower level of SOD1 expression than $Sod1^{+/+}$ mice. It is also evident that $Sod1^{-/-}$ mice have no residual SOD1 expression, as expected. The protein lysates were collected from samples from littermates.

Another mechanism to modulate nitric oxide levels, and therefore peroxynitrite levels, is to alter the bioavailability of hemoglobin. Oxyhemoglobin is a sink for nitric oxide. In the absence of superoxide dismutase expression, modulation of nitric oxide levels is the only other way to affect the amounts of peroxynitrite formed. This is because superoxide dismutases are the only known mechanism from breaking down superoxide and when not present, superoxide levels cannot be easily lowered. The simplest ways to change the bioavailability of oxyhemoglobin would be by increasing the hematocrit, the proportion of red blood cells relative to the liquid, or plasma, component of blood, or by increasing the hemoglobin in the blood overall or in a red blood cell itself.

To see if the composition of the blood is altered in germline *Sod1* knockout mice, we performed cardiac blood draws on mice with the three genotypes of interest (*Sod1*$^{+/+}$, *Sod1*$^{+/-}$ and *Sod1*$^{-/-}$) and then did a complete blood count (CBC) for each sample of blood collected. CBC is a group of blood measurements that collectively provide insight into the composition of the blood – red blood cells, white blood cells, plasma, and hemoglobin[724]. These analyses identified significant changes in five measurements – red blood cell (RBC) count, hematocrit, hemoglobin, mean corpuscular volume (MCV), and mean corpuscular hemoglobin (MCH).

Overall, the red blood cell count, the hematocrit, and the hemoglobin are all significantly lower in the *Sod1*$^{-/-}$ mice (Figure 51-53). This is rather surprising as it is the opposite of what we expected to see, either no change at all or an increase in one or all of these measurements. This is based on the notion that hemoglobin is a sink for nitric oxide. We expect peroxynitrite levels to be managed in germline *Sod1*$^{-/-}$ mice to allow these mice to survive and one way to do so would be to increase nitric oxide binding to hemoglobin by either increasing hemoglobin directly or by making hemoglobin more readily available.

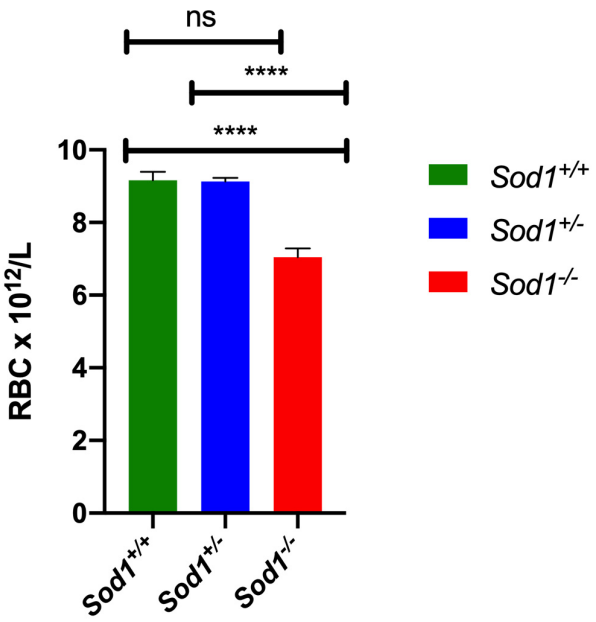

Figure 51: Red blood cells (RBC) of *Sod1* germline knockout mice
The comparative number of red blood cells per liter of blood for the three genotypes examined - *Sod1*$^{+/+}$, *Sod1*$^{+/-}$ and *Sod1*$^{-/-}$ mice. Blood was taken from the heart and processed the same day.

Sod1$^{-/-}$ mice have significantly less RBCs per liter than their wild-type and heterozygous littermates. Error bars indicate SEM. n = 7 for all groups of mice. **** $p \leq 0.0001$.

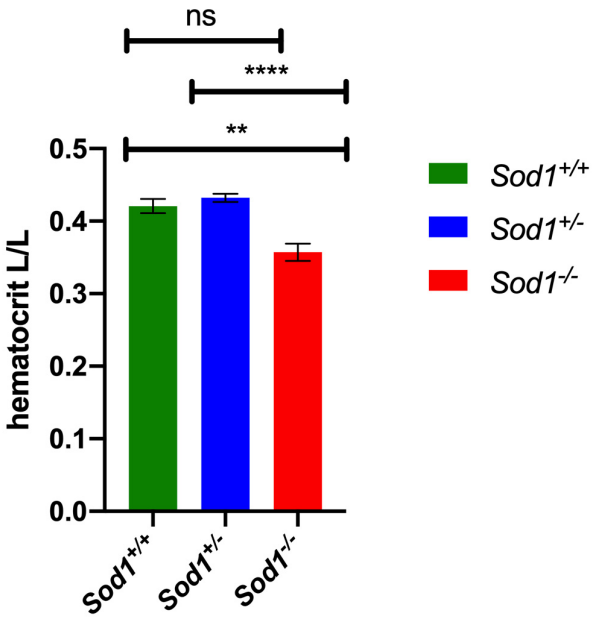

Figure 52: Hematocrit of *Sod1* germline knockout mice
The comparison of hematocrit for the three genotypes examined - *Sod1*$^{+/+}$, *Sod1*$^{+/-}$ and *Sod1*$^{-/-}$ mice. Blood was taken from the heart and processed the same day. *Sod1*$^{-/-}$ mice have a significantly lower hematocrit than their wild-type and heterozygous littermates. Error bars indicate SEM. n = 7 for all groups of mice. ** $p \leq 0.01$ and **** $p \leq 0.0001$.

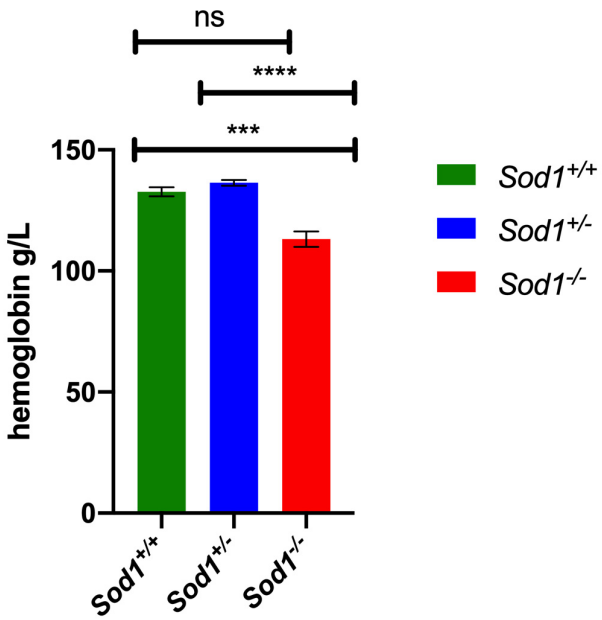

Figure 53: Hemoglobin of *Sod1* germline knockout mice
The comparison of hemoglobin for the three genotypes examined - *Sod1*$^{+/+}$, *Sod1*$^{+/-}$ and *Sod1*$^{-/-}$ mice. Blood was taken from the heart and processed the same day. *Sod1*$^{-/-}$ mice have a significantly lower hemoglobin concentration than their wild-type and heterozygous littermates. Error bars indicate SEM. n = 7 for all groups of mice. *** $p \leq 0.001$ and **** $p \leq 0.0001$.

The other two measurements where we observed significant differences were the MCV and MCH. MCV is a measure that indicates the average size and volume of a red blood cell. Mice, in general, have much smaller RBCs compared to other mammals, with a normal MCV being 45-55 femtoliters (fL, 10^{-15}L). MCH is a measure of the average amount of hemoglobin per red blood cell and a normal MCH for a mouse is considered ~16.7 picograms (pg)[725, 726]. Both MCV and MCH values increased in *Sod1*$^{-/-}$ mice (Figure 54 and 55).

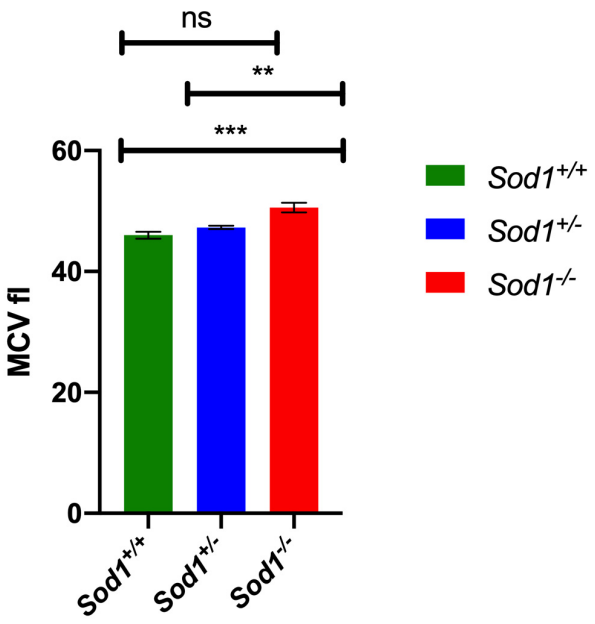

Figure 54: Mean corpuscular volume (MCV) of *Sod1* germline knockout mice
The comparison of the mean corpuscular volume of the three genotypes examined - *Sod1*$^{+/+}$, *Sod1*$^{+/-}$ and *Sod1*$^{-/-}$ mice. Blood was taken from the heart and processed the same day. The MCV of *Sod1*$^{-/-}$ mice is elevated compared to that of their wild-type and heterozygous littermates. Error bars indicate SEM. n = 7 for all groups of mice. ** $p \leq 0.01$ and *** $p \leq 0.001$.

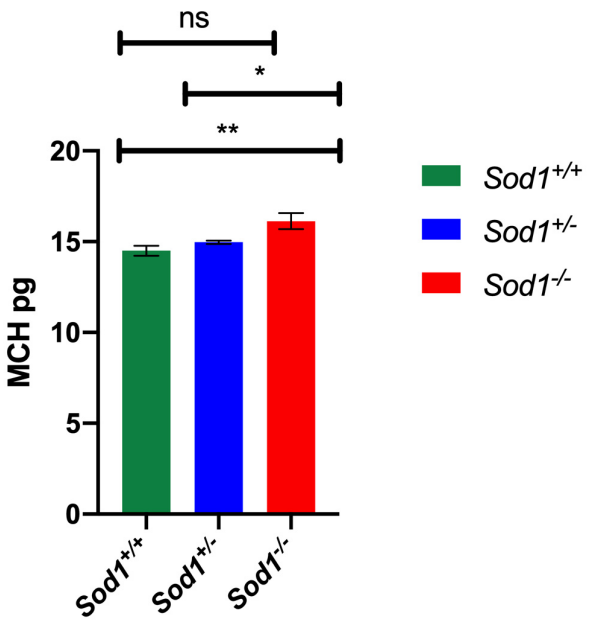

Figure 55: Mean corpuscular hemoglobin (MCH) of *Sod1* germline knockout mice
The comparison of the mean corpuscular hemoglobin of the three genotypes examined - *Sod1*$^{+/+}$, *Sod1*$^{+/-}$ and *Sod1*$^{-/-}$ mice. Blood was taken from the heart and processed the same day. The MCH of *Sod1*$^{-/-}$ mice is elevated compared to that of their wild-type and heterozygous littermates. Error bars indicate SEM. n = 7 for all groups of mice. * $p \leq 0.05$ and ** $p \leq 0.01$.

Taken together, germline *Sod1* knockout mice have lower nNOS expression in their skeletal muscles, less red blood cells and overall hemoglobin, but interestingly a higher concentration of hemoglobin per red blood cell. Perhaps, with a higher concentration of hemoglobin per cell, even if the concentration of hemoglobin overall is lower not higher, this is sufficient to quench enough nitric oxide when combined with lower nNOS expression in the skeletal muscles. Another possibility is the larger blood cells move more slowly through capillaries and therefore there's more time for hemoglobin to interact with nitric oxide. Or, the larger blood cell size allows hemoglobin to be closer to the capillary walls, where nitric oxide is produced. The skeletal muscles are the only organ we observed degeneration and damage in as a result of *Sod1* loss in adult onset inducible *Sod1* knockout mice.

It is clear that more, yet unknown, adaptations must collaborate with the changes we have identified to lead to germline *Sod1* knockout mice that survive almost two years. Without SOD1, the organism needs to strike a balance between the need for $NO^{\bullet}$ and the deleterious effects of peroxynitrite formation. The particular balance struck could be quite subtle, meaning low nNOS

and low hemoglobin, although they seem counterintuitive, may be necessary to ensure both survival and proper signalling. Additional changes to those observed could be changes in blood flow may also need to accompany the changes in blood composition to attain the phenotypes we observe. Altering the speed of blood flow, like changes to hematocrit and hemoglobin, would similarly affect the availability of red blood cells and thus hemoglobin to quench nitric oxide. In principle, a way to study the balance of $NO^{\bullet}$ needed in germline *Sod1*$^{-/-}$ mice is to treat them with L-NAME. L-NAME could be either deleterious, if $NO^{\bullet}$ levels become too low, or beneficial, if these mice would benefit from an even more dramatic decrease in peroxynitrite formation. It would also be intriguing to see if blood transfusions, from wild-type mice, and erythropoietin (EPO) treatment alter the survival of germline *Sod1*$^{-/-}$ mice, as we did observe changes to the blood composition of germline *Sod1*$^{-/-}$ mice that may be key for their survival.

5. Discussion

We have described the generation and characterization of adult-onset whole-body *Sod1* knockout mice. These mice are born with normal *Sod1* expression and, at approximately 12-15 weeks of age, tamoxifen injections begin, leading to translocation of *Cre* recombinase to the nucleus and successful excision of *Sod1* leading to its loss of expression. These mice are the first inducible model for whole-body *Sod1* knockout in a mammalian model organism.

a. L-NAME rescues the lethality of *Sod1* loss and skeletal muscle degradation in adult onset *Sod1* knockout mice

Loss of *Sod1* in adult mice leads to rapid death. This is unlike their germline counterparts, mice that proceed through development without *Sod1* and are readily able to survive. The loss of *Sod1* as an adult can be rescued, however, by treatment with a nitric oxide synthase (NOS) inhibitor, L-NAME. L-NAME treatment of inducible *Sod1* KO mice not only restored their viability, but it also improved the skeletal muscle degradation we observed in dying mice. The skeletal muscles appear to be the only organ severely affected in dying inducible *Sod1* KO mice. Their skeletal muscles display distinct signs of muscle necrosis and degeneration, such as the juxtaposition of hypereosinphilic and hypoeosinphilic muscle fibers, dystrophic calcification, fragmented muscle

fibers, phagocytosis of muscle fibers, hyalinization, infiltration of fibers by macrophages, and round muscle fibers with internal nuclei and cytoplasmic vacuoles[727]. In L-NAME rescued inducible *Sod1* KO mice, their muscles no longer show signs of degradation and resemble healthy, normal skeletal muscles.

There remain several open questions that can be address with our inducible *Sod1* KO mouse model. As we see an association between an increase in peroxynitrite expression and indicators of muscle degeneration in dying mice, it would be intriguing to see if FeTPPS, the peroxynitrite decomposition catalyst that rescues $Sod1^{loxP/loxP}$ KO MEFs, can result in a similar rescue in these mice as treatment with L-NAME does. We focused on L-NAME for our initial experiments as it is a much easier drug to deliver to mice, both intraperitoneally and in drinking water. FeTPPS is only ever used for a maximum of three intraperitoneal injections, but, in our case, we would need to inject continually for months as both superoxide and nitric oxide continue to be produced in these mice[728]. In the same line of thought, it would be beneficial to see if L-NAME rescue is also effective when L-NAME is delivered via drinking water, rather than intraperitoneally. L-NAME delivery via drinking water would allow aging of these mice to see if they can survive as long as $Sod1^{-/-}$ mice. Although we successfully deliver L-NAME to our mice for two months without any negative L-NAME dependent phenotypic effects, it is known that long-term L-NAME treatment can damage the blood-brain barrier and lead to arteriosclerotic lesions and changes in heart structure[729-731]. In addition to L-NAME, there are several other NOS inhibitors that can be tested for their rescue effects on adult onset *Sod1* KO mice. 7-NI is an intriguing candidate, as it is a neuronal NOS specific inhibitor, was shown to rescue $Sod1^{loxP/loxP}$ KO MEFs, and nNOS expression is reduced in the skeletal muscle of $Sod1^{-/-}$ mice that survive.

Furthermore, $Sod1^{-/-}$ mice display accelerated sarcopenia, or aged-related loss of skeletal muscle strength and mass[611]. We show that inducible *Sod1* KO mice have similar, albeit much more rapid, muscle degeneration and wasting, but it would be insightful to also measure their muscle strength. Measuring the muscle strength of inducible *Sod1* KO mice would help us further understand how similar the muscle phenotype of $Sod1^{loxP/loxP}$ mice is to that of $Sod1^{-/-}$ mice. In mice, there are numerous well-established methods to measure skeletal muscle performance.

These include, but are not limited to, treadmill exhaustion test, wheel running, rotorod, whole-limb grip strength assay[693, 732].

Finally, as adult-onset *Sod1* knockout mice worsen, their body weight dramatically decreases and there are changes in their breathing patterns by visual observation. Due to these observations and the rapid degeneration of hindlimb skeletal muscles, we hypothesize that muscles other than hindlimb skeletal muscles may be compromised, specifically muscles involved in eating, drinking, and breathing. Jaw muscles such as the superficial masseter muscles and muscles key for breathing such as the diaphragm are possible candidates that could help further explain the rapid decline of these mice[733, 734].

b. Lessons from *Sod1*$^{loxP/loxP}$ and *Sod1*$^{-/-}$ mice and mouse embryonic fibroblasts

To date, there is no clear understanding of the great phenotypic difference between *Sod1*$^{-/-}$ mice, that can survive almost two years, and their mouse embryonic fibroblasts, where most cells die within 48 hours in culture. An understanding of NO$^{\bullet}$ and peroxynitrite formation in the phenotype of *Sod1*$^{loxP/loxP}$ cells and mice help to begin to explain why *Sod1*$^{-/-}$ MEFs have a more severe phenotype than *Sod1*$^{-/-}$ mice and why adult onset *Sod1* knockout mice die quickly after the loss of *Sod1* expression but their germline counterparts survive for years. Here, we show that NO$^{\bullet}$ is essential for understanding the toxicity associated with *Sod1* loss.

NO$^{\bullet}$ is a small hydrophobic molecule that can easily traverse cellular membranes and signals through activation of soluble guanylate cyclases (sGC)[735]. NO$^{\bullet}$ signaling is key for physiological processes, such as vasodilation, neurotransmission, and the immune response[170, 736, 737]. Nitric oxide synthases, of which there are 3 isoforms (neuronal NOS, inducible NOS, and endothelial NOS), synthesize NO$^{\bullet}$[735]. However, NO$^{\bullet}$ also readily reacts with superoxide, to form peroxynitrite, a molecule that is highly toxic. Peroxynitrite ($ONOO^{-}$), although it is not a radical as its radical precursors are, it is a stronger oxidant than both nitric oxide and superoxide and its formation is highly favoured as it is formed by the reaction of two radicals to form a non-radical[738]. Peroxynitrite is known to interact with critical biomolecules via direct, such as DNA, proteins, and lipids. It can directly target these molecules with one- or two-electron oxidations or it can alter these molecules by radical-mediated mechanisms, as the presence of peroxynitrite

is known to contribute to the formation of radicals like the carbonate radical ($CO3^{\bullet-}$) via a reaction with carbon dioxide[412]. We show that peroxynitrite is associated with muscle degradation and dying mice in the adult onset *Sod1* KO mouse model. Informed by this, we began to investigate possible developmental adaptations in germline *Sod1* KO mice. Mice that lack *Sod1* have little way to modulate superoxide levels, but modulation of nitric oxide levels is still possible. With this thought in mind, we decided to look at the two main ways to alter levels of nitric oxide: 1) changing the expression of NOS, the only known *in vivo* source of $NO^{\bullet}$ and 2) changing the bioavailability of oxyhemoglobin, a pathway of $NO^{\bullet}$ elimination from the body[706]. These possible developmental adaptations are only the simplest answers and it is likely that germline *Sod1* KO mice survive as a result of a combination of biomolecular alterations.

Germline *Sod1* KO mice showed decreased nNOS expression in skeletal muscles, less red blood cells but a higher level of hemoglobin per red blood cell. This suggests that perhaps the combination of lower nNOS solely in skeletal muscles with a higher percentage of hemoglobin per RBC is sufficient to allow these mice to survive, but, more likely, various other developmental adaptations are present in these mice and we have just begun to uncover the first few. This opens the question of what other developmental adaptations could occur in these mice to allow them to survive. In addition to changes in blood composition, it is also worth looking at the rates of blood flow in these mice, as this would also impact the bioavailability of oxyhemoglobin. The rate of blood flow can be measured using Laser-Doppler flowmetry (LDF). LDF is a well-established, non-invasive method of measuring blood flow in tissues. The general principle of LDF is that most photons can readily travel through tissue, but a small fraction of these photons are scattered back towards the light probe as a result of hitting moving red blood cells[739]. It is also possible that developmental adaptations that allow germline *Sod1* KO mice to survive are independent of $NO^{\bullet}$ production and elimination. For example, we know that muscle wasting is a problem in these animals but occurs at a much slower rate than in our inducible KO mice. Perhaps the slower rate of muscle wasting and degeneration is a result of improved muscle repair mechanisms, rather than less damage resulting from peroxynitrite formation. Skeletal muscle repair is highly dependent on satellite cells, that are located next to myofibers[740]. These satellite cells are mitotically inactive in adult skeletal muscle, but upon muscle damage can quickly enter the cell

cycle and form proliferating myoblasts that go one to form multinucleated myotubes[741]. It is known that the number of satellite cells differs between species, developmental stages, types of myofibers, and most importantly muscles. For instance, there are 2- to 4-fold more satellite cells in the soleus (located in the back of the lower leg and is an important flexor muscle of the ankle) muscle than in the tibialis anterior or extensor digitorum longus (both found at the front of the leg, tibalis anterior on top of the extensor digitorum longus) muscles[742, 743]. Therefore, it is conceivable that germline *Sod1* KO mice may have increased numbers of satellite cells in their skeletal muscles, both during development and during adulthood. Such an increase in satellite cells would improve the efficiency of skeletal muscle repair. In fact, 88% of satellite cells in humans are within 21µm of a capillary, blood vessels that connect arteries to veins, quite interesting considering that $NO^{\bullet}$ signalling is prominent in the vasculature[744, 745].

Finally, there is yet another way to see if $NO^{\bullet}$ is of as great of importance in germline *Sod1* KO mice as it is in adult onset inducible *Sod1* KO mice. It would be insightful to treat the germline *Sod1* KO mice with L-NAME, the compound used to rescue the inducible *Sod1* KO mice, and see if this treatment further improves their muscle phenotype. Following the same line of thought, we could also create mice that lack both *Sod1* and one, or multiple, *Nos* genes, as we know that *Nos* are dispensable[642].

In conclusion, comparing the phenotypes of germline and inducible *Sod1* knockout mice and cells can help us elucidate mechanisms that are essential for mouse survival, especially in conditions of elevated oxidative stress. Altering $NO^{\bullet}$ production and elimination seems to make a difference in both models, but is not the complete story, particularly in the germline model. These findings can be essential to develop potential treatments for diseases that involve dysfunctional superoxide dismutases.

CHAPTER 4: GENERAL DISCUSSION

In this thesis, the Cre-loxP system for conditional gene targeting is used to provide insight into the disagreement between *in vitro* and *in vivo* phenotypes that result from *Sod1* loss. An inducible *Sod1* global knockout mouse line was created that had not been studied before. The use of the Cre-loxP system in this mouse allows for temporal control of *Sod1* deletion.

1. The SOD conundrum

Superoxide dismutases (SOD) are the first, and only known, line of defence against superoxide ($O_2^{\bullet-}$). SODs are one of the most abundant proteins in vertebrates and are found in all aerobic organisms. This is a good indicator of their importance. But why are SODs important? Is it simply for preventing the potential harmful effects of superoxide itself or is there more to it? Superoxide is not considered to be a particularly strong oxidizing agent, but it has been shown to be potentially toxic. For example, it can oxidize iron-sulfur clusters in proteins resulting in loss of their catalytic iron and their enzymatic activity, as seen in Krebs cycle proteins and aconitase[117, 125]. However, our results suggest that one of the focus of the need for SODs is somewhere else. Our work suggests that the most important reaction to consider is the reaction of superoxide with nitric oxide to form peroxynitrite ($ONOO^-$). After all, peroxynitrite is a much stronger oxidizing agent and its decomposition can result in the formation of other very reactive molecules, such as $OH^{\bullet}$, $NO2^{\bullet}$, and $CO3^{\bullet-}$[97, 746]. Additionally, free radicals react with one another at diffusion-controlled rates, meaning very quickly[747]. This reaction of superoxide with nitric oxide is therefore both thermodynamically and kinetically favoured as the formation of this new chemical bond results in the elimination of the unpaired elections[371]. All this to highlight that SODs, in addition to being the only enzyme that interacts with superoxide, are also the only enzymes that can prevent dangerously high peroxynitrite levels. This thesis shows that the management of peroxynitrite levels is the most acute role of SODs in mammals.

Since the creation of germline *Sod1* knockout mice in 1997, it has been unclear why these mice are able to survive for ~2 years, but mouse embryonic fibroblasts isolated from these mice die within 48 hours in culture[5]. One of the most interesting findings on this dilemma was that growth retardation and cell death of *Sod1*$^{-/-}$ MEFs was partially rescued in hypoxic (2% O_2) conditions and this continued the theory that superoxide alone was responsible for the death of

these cells. But how does that reconcile with the fact that mice lacking *Sod1* are still alive[563]. In efforts to unravel this mystery, we designed an inducible *Sod1* knockout mice strain, of which we studied both the mice themselves and embryonic fibroblasts. We show that cells can somehow survive with little to no SOD expression and activity. Indeed, L-NAME treated *Sod1*$^{loxP/loxP}$ knockout cells not only lacked SOD1, but the SOD2 and SOD3 expression seemingly disappeared. It is likely that this is a phenomenon specific to *in vitro* conditions, but nonetheless we show that in the absence of $NO^{\bullet}$, *in vitro* mammalian cells can survive well without SOD. This is much like what was shown by our lab in *C. elegans. C. elegans* do not produce $NO^{\bullet}$ and can survive, with a lifespan similar to wild-type worms, without any of their 5 SOD isoforms[16, 748]. Likely because superoxide toxicity is not a major problem thanks to the absence of $NO^{\bullet}$ formation in these organisms. All these results together suggest that superoxide by itself is not very toxic, but rather peroxynitrite, formed via the reaction of superoxide with nitric oxide, is responsible for many of the toxic effects historically attributed to superoxide formation. Additionally, we show that L-NAME-treated wild-type cells are still sensitive to paraquat treatment and this is likely a result of hydrogen peroxide toxicity, as more superoxide is converted to hydrogen peroxide by SODs, or because paraquat leads to superoxide formation in specific locations where damage is particularly detrimental (e.g. complex I of the mitochondrial electron transport chain).

Furthermore, we show that adult onset *Sod1* knockout mice die rapidly after the loss of SOD1 expression. This was surprising as their germline knockout counterparts can survive for up to 2 years. Our observation rather deepened the mystery of how germline *Sod1*$^{-/-}$ mice survive much more profound. Adult onset *Sod1* knockout mice seemingly die of muscle wasting/degradation and rapid weight loss. The phenotype of adult onset *Sod1* knockout mice mimics the loss of muscle seen in germline *Sod1*$^{-/-}$ mice, just at a much more rapid pace[693]. The lifespan and muscle degeneration of adult onset *Sod1* knockout mice was rescued with L-NAME, a nitric oxide synthase inhibitor. The L-NAME treatment mice can thus thrive with an elevated level of superoxide, simply because we prevent the formation of the truly damaging compound, peroxynitrite in muscles. These results suggest that germline *Sod1*$^{-/-}$ mice must have developmental adaptations that allow them to deal with elevated peroxynitrite levels in muscles or that allow them to prevent peroxynitrite formation in muscles.

The ability of mice lacking *Sod1*, both germline and adult-onset knockouts, to survive provides another piece of evidence that challenges the oxidative stress theory of aging. The oxidative stress theory of aging proposes that organisms age due to an accumulation of damage produced by reactive oxygen species[749]. The very existence of SODs was a key piece of evidence used to support this theory as they are both highly conserved and incredibly abundant enzymes[750]

2. Sod1 and skeletal muscles

In skeletal muscles, 65-85% of superoxide dismutase activity occurs in the cytosol (SOD1) and the remaining 15-35% of superoxide dismutase activity is located in mitochondria (SOD1 and SOD2)[751]. Superoxide dismutase activity is higher in type I (slow-twitch) muscle fibers than in type II (fast-twitch) muscle fibers[752]. This difference in SOD activity is thought to be due to the fact that slow-twitch muscle fibers have two- to three-times more mitochondria, a source of superoxide, than fast-twitch muscle fibers[753]. SOD activity in skeletal muscles has also been shown to be influenced by exercise, which increases levels of both SOD1 and SOD2[752]. Superoxide is produced at various sites in skeletal muscles, but mitochondria are often said to be the primary source of superoxide in muscle fibers[754].

Germline *Sod1*$^{-/-}$ knockout mice are a model of sarcopenia, or aged-related muscle loss and degeneration[613]. Sarcopenia is observed in aging humans, who show a 30-40% reduction in skeletal muscle. This sarcopenia is generally accepted as the main cause of frailty in the elderly[755]. Larkin et al. showed in germline *Sod1*$^{-/-}$ knockout mice that the reduction in muscle function, measured by grip strength, rotarod, wheel running, and treadmill running, is a result of, at least partially, to loss of innervation in muscles[612]. Furthermore, the Van Remmen lab showed that germline *Sod1*$^{-/-}$ knockout mice, as a result of this denervation, have deterioration of their neuromuscular junction (NMJs) characterized by acetylcholine receptor cluster fragmentation and degenerating or retracting motor neurons[611]. Interestingly, expression of *Sod1* in the neurons of germline *Sod1*$^{-/-}$ knockout mice was sufficient to prevent the accelerated sarcopenia of these mice, but neuronal specific reduction of *Sod1* and muscle specific deletion of *Sod1* were both not sufficient to mimic the sarcopenia phenotype seen in whole-body germline *Sod1*$^{-/-}$ knockout

mice[611, 756]. Based on our findings, we show that germline *Sod1*$^{-/-}$ knockout mice have systemic adaptations such as changes to blood composition and possible other factors that affect NOS expression in the muscle. While these adaptations do not prevent eventual damage, they delay this damage as compared to adult-onset *Sod1*$^{loxP/loxP}$ knockout mice and help germline *Sod1*$^{-/-}$ knockout mice survive for as long as they do.

Interestingly, muscle atrophy is seen in mouse models of amyotrophic lateral sclerosis (ALS), a disease characterized by the progressive loss of motor neurons, induced by SOD1^{G93A} expression[258, 757]. Note, it is not fully understood how this mutation in *Sod1* results in neuronal degeneration and eventual death. The mutant form of *Sod1* is expressed at high levels and it has been proposed that aggregation of mutant SOD1 leads to mitochondrial damage that results in muscle atrophy and loss of motor neurons[758, 759].

3. Nitric oxide and skeletal muscles

The role of nitric oxide in skeletal muscles has been explored after it was shown that all NOS isoforms are expressed in mammalian skeletal muscles[760]. The location and time of expression of NOS isoforms in skeletal muscle is highly dependent on age, innervation of muscle, function or activity of muscle group, inflammatory response, and muscle fiber type (e.g. slow- and fast-twitch muscles)[761]. In 1977, identification of guanylate cyclase activity in skeletal muscle was the first indication that nitric oxide signaling may be pivotal in muscle[211]. Remember, soluble guanylate cyclase is primarily activated by binding of nitric oxide to the enzyme's heme group. Even more striking evidence of the involvement of NO$^{\bullet}$ signaling in muscle function came when it was shown that nNOS and cGMP colocalize near the sarcolemma of muscle fibers[762]. cGMP activation led to the inhibition of muscle force production. This study was the first evidence of a functional link between NO$^{\bullet}$, cGMP, and muscle activity[763]. From this point, skeletal muscle NOS activity has been implicated in altered mitochondrial respiration, calcium homeostasis, contractility, injury response, and glucose uptake[764-768].

Interestingly, we observed that a reduction in nNOS was one of the developmental adaptations that allow germline *Sod1*$^{-/-}$ mice to survive. This corresponds with existing literature that shows that a redistribution/elevation of nNOS contributes to muscle fiber degradation in

dystrophic muscle in Duchenne muscular dystrophy[769]. Note, in rodents, nNOS is primarily expressed in type II (fast-twitch) muscle fibers and not type I (slow-twitch) muscle fibers. Fast-twitch muscle fibers are have higher NOS activity than slow-twitch muscle fibers[762]. However, in humans, nNOS appears to be expressed in similar amounts in both type I and type II muscle fibers[770]. Furthermore, in normal skeletal muscles, nNOS expression is enriched at neuromuscular junctions (NMJ) and seems to be implicated in the proper development of NMJs from embryonic muscle cells[771, 772]. The reduction in nNOS we observe in germline *Sod1*$^{-/-}$ mice could therefore explain the previously described degeneration of NMJs in the skeletal muscle and the general denervation of the muscle of these mice.

4. A new perspective on superoxide and nitric oxide

Loss of *Sod1* in adult-onset knockout mice results in low levels of superoxide dismutation, rapid skeletal muscle degeneration, and ultimately death. However, these mice live with intraperitoneal injections of L-NAME, a nitric oxide synthase inhibitor. Plus, L-NAME treatment prevents the skeletal muscle degradation. This highlights that the main function of SOD1 *in* vivo is to control peroxynitrite in skeletal muscles. Peroxynitrite, as mentioned previously, is formed by the spontaneous reaction of superoxide with nitric oxide. SODs are one of the most abundant proteins in mammals and perhaps this high concentration is required to compete with nitric oxide for superoxide. This is a shift from the classic viewpoint that SODs prevent damage from superoxide. Rather, we show that SODs, via regulation of superoxide levels, prevent peroxynitrite formation and that, when peroxynitrite cannot be formed as well, superoxide is not all that toxic.

In 2000, it was shown as mice that lack each NOS, pair-wise combinations, and even all three NOS are alive, albeit with a shorter lifespan and phenotypes such as increased incidence of myocardial infraction and renal disease[642]. The fact that mice can survive without any endogenous source of $NO^{\bullet}$ is shocking, as $NO^{\bullet}$ is a pivotal signalling molecule involved in neurotransmission, vasodilation, immune response, and much more[678]. This was the first evidence to support the idea that low $NO^{\bullet}$ is easily tolerated by animals. This thesis validates idea that $NO^{\bullet}$ is not necessarily required for survival, but later in life, phenotypes arise due to this lack of $NO^{\bullet}$. This is highlighted by the fact that L-NAME treated adult-onset *Sod1* knockout mice

survive even though $NO^{\bullet}$ levels are low as a result of treatment with a NOS inhibitor and residual peroxynitrite formed.

This thesis also provides another piece of support to the growing body of evidence that illustrates that the oxidative stress theory of aging is not the entire story. The oxidative stress theory of aging proposes that organisms age due to an accumulation of reactive oxygen species, which are inherently damaging[749]. SODs were a key piece of evidence used to support this theory as they are both highly conserved and incredibly abundant enzymes[750]. But, just as the work showing that *C. elegans* can survive without all 5 *sod* isoforms challenges this theory, so does the work presented in this thesis. For example, adult-onset *Sod1* knockout mice survive, with a still elevated level of superoxide, simply because we prevent the truly damaging compound, peroxynitrite, from being formed. Of note here is that superoxide levels still remain elevated in these mice, yet, with L-NAME treatment, survive. Similarly, if superoxide was central to aging, as it has been argued, cells that lack SOD expression should not be able to survive under any conditions, yet in this thesis, they do.

5. Evolutionary perspective

A look at the evolutionary timeline of SOD and NOS can provide insight into the observation in my thesis. Superoxide dismutases are thought to have appeared prior to Great Oxidation Event (GOD) that occurred ~2.4 billion years ago[278, 773]. The GOE was a simultaneous increased in both oceanic and atmospheric oxygen concentration in the atmosphere[1]. While the accepted start of the GOE is ~2.4 billion years ago, there is evidence to suggest the oxygen levels began to increase in cells almost 300 million years prior to this event. This is possible because oxidative photosynthesis predates the GOE and is key to the evolution of an oxygen-rich atmosphere[774]. Interestingly, nitric oxide synthases in animals evolved much later, around 800 million years ago[775]. But, nitric oxide signaling can be traced back to ~3.5 billion years ago, as $NO^{\bullet}$ can be produced by events such as volcanic eruptions and lighting in the early atmosphere of the Earth[776]. So how can we reconcile this evolutionary perspective with what we observe about the interactions between superoxide and nitric oxide today?

Perhaps, at first, the presence of SOD was for a signaling purpose. We have shown that without sufficient levels of hydrogen peroxide, the main by-product of superoxide dismutation, cells cannot survive (*Sod1*$^{loxP/loxP}$ knockout cells treated with L-NAME and NAC). This would be why *C. elegans* that do not produce nitric oxide still have SOD. But as nitric oxide levels began to increase as mammals could synthesize their own nitric oxide, the main purpose of SOD had to adapt. This is because of the paradox of nitric oxide expression – low levels are useful for signaling but higher levels can be damaging as nitric oxide can cause damage itself and higher levels of peroxynitrite are made. One way to allow more nitric oxide, without the damaging effects of peroxynitrite formation, is to express SOD at such a high level that it can out-compete $NO^{\bullet}$. This is only one possible interpretation that allows us to fit in our results to an evolutionary perspective.

6. Clinical applications

Changes in the level of SOD expression or activity have been identified in various diseases. These diseases include common age-dependent conditions, such as cardiovascular disease, neurodegenerative diseases, and cancer. The most extensively studied connection between SOD and a pathological condition is SOD's involvement in amyotrophic lateral sclerosis (ALS). ALS is a neurodegenerative disease that affects motor neurons. The onset of ALS is variable but in most cases occurs in patients 50 years and older[777]. In 1993, the first mutations in SOD1 were found in patients with familial ALS[260]. In the years since, over 170 SOD1 mutations have been found in both familial and sporadic cases of ALS[778, 779]. SOD1 mutations seem to contribute to the progression of ALS, not necessarily due to the gain or loss of superoxide dismutase function, but rather the accumulation of an altered form of SOD1. However, the mechanism of how SOD1 mutations contribute to ALS motor neuron death remains to be elucidated[129].

SODs, and more specifically the oxidative stress that can result from diminished superoxide dismutase activity, have also been implicated in the pathology of cancers. High reactive oxygen and nitrogen species can serve both a potential causal and propagative role in cancer development and progression. Elevated ROS levels favour DNA mutations that can play a causative role in tumorigenesis. The majority of ROS DNA mutations are G→T transversions and

if these mutations occur in oncogenes or tumour suppressor genes, both initiation and progression of cancer can result[780, 781]. The resulting cancer cells have elevated levels of ROS that would be toxic to normal cells, but elevated ROS can promote tumour growth and maintenance as a result of genomic instability and altered cell metabolism[782]. For example, mutations in oncogenes such as KRAS and MYC have been shown to be associated with elevated levels of mitochondrial ROS[783]. This ROS can then go on to activate the PI3K/AKT signalling pathway that can stimulate cell proliferation, cell mobility, and metabolic changes[686, 784]. Another example of elevated ROS level aiding cancer cell maintenance is the ability of ROS to stimulate HIF1α and thereby activate NRF2. This aberrant activation of NRF2, a transcription factor, can stimulate angiogenesis and cell proliferation and promote adaptations to hypoxia[785-787].

Likewise, cancer cells have also shown changes in expression of endogenous antioxidants, such as alterations in SOD2 expression[788]. Reported changes to antioxidant expression in cancer cells vary, although perhaps this is not surprising as many of the studies are on different types of cancer and cancer at various stages of progression. Interestingly, with regards to SOD2 expression, one of the interpretations is that SOD2 levels may be kept low to foster an environment of high oxidative stress at tumour initiation, but SOD2 activity may be increased later on in tumour progression, leading to increased mitochondrial H_2O_2 and increased activation of angiogenic and oncogenic pathways[129].

Altered SOD expression or activity has also been implicated in cardiovascular diseases. It was rather unexpected when, in 1997, Tribble et al. showed that mice overexpressing SOD1 have more atherosclerotic lesions than control mice[789]. Atherosclerosis is plaque formation in arteries, or the buildup of fats and cholesterol[790]. It has been proposed that excessive SOD activity actually enhances oxidative injury as SOD1 overexpression generates higher amounts of H_2O_2 that can promote the formation of proatherogenic compounds like hydroxyl radicals and metal-containing reactive species[128]. Interestingly, loss of SOD function can also stimulate vascular disease. Both superoxide and peroxynitrite can lead to mitochondrial dysfunction, which in turn results in increases in mitochondrial ROS. This mitochondrial ROS can then activate NADPH oxidase, leading to further ROS production. Increased superoxide severely impacts the levels of nitric oxide, due to the reaction of superoxide and nitric oxide to form peroxynitrite[791]. Loss of

nitric oxide and increases in peroxynitrite can result in vascular inflammation and remodeling that alter vascular tone, increase vascular permeability, and can stimulate platelet aggregation[792, 793]. Finally, SOD3 seems to play a key role in the vasculature, as patients with coronary artery disease has significantly decreased levels of SOD3[128].

Taken together, as SODs are the only known enzyme to act directly on superoxide, these enzymes are unique in their ability to control the levels of ROS and RNS. This means that considering how to mimic the functions of SOD or reduce the downstream reactions of superoxide in diseases where SOD activity is diminished has high therapeutic potential. In this thesis, L-NAME has been shown to both reduce the level of peroxynitrite formed in adult-onset *Sod1* knockout mice and to be effective in rescuing their viability and skeletal muscle degeneration. As L-NAME is a NOS inhibitor, perhaps altering $NO^{\bullet}$ levels can be useful as a treatment in neurodegenerative diseases, cancer, and cardiovascular diseases[794-797]. For example, in Chapter 2, I show that cells that express a mutant allele of *KRas*, a common mutation in cancer known to increase levels of ROS, are more vulnerable to treatment with $NO^{\bullet}$ donors, supposedly because increases in $NO^{\bullet}$ levels result in further production of peroxynitrite, which is damaging to cells. One could see this having broader applications in lung cancer for example, where *KRas* is often mutated. Perhaps patients could inhale a low level of $NO^{\bullet}$, which would lead to increased peroxynitrite formation in cancer cells specifically and cancer cell death. Furthermore, in cardiovascular diseases where increased superoxide can severely hinder $NO^{\bullet}$ levels, treatment with a NOS inhibitor, such as L-NAME, may not be the way to go and it may too severely diminish $NO^{\bullet}$ levels. But, if cardiovascular diseases result as a combination of reduced $NO^{\bullet}$ levels and increased peroxynitrite formation, treatment with a peroxynitrite decomposition catalyst, such as FeTPPS, may be sufficient. Overall, this thesis shows the reaction of superoxide with nitric oxide is central to various processes throughout the body and should be considered when developing new therapeutics.

APPENDIX

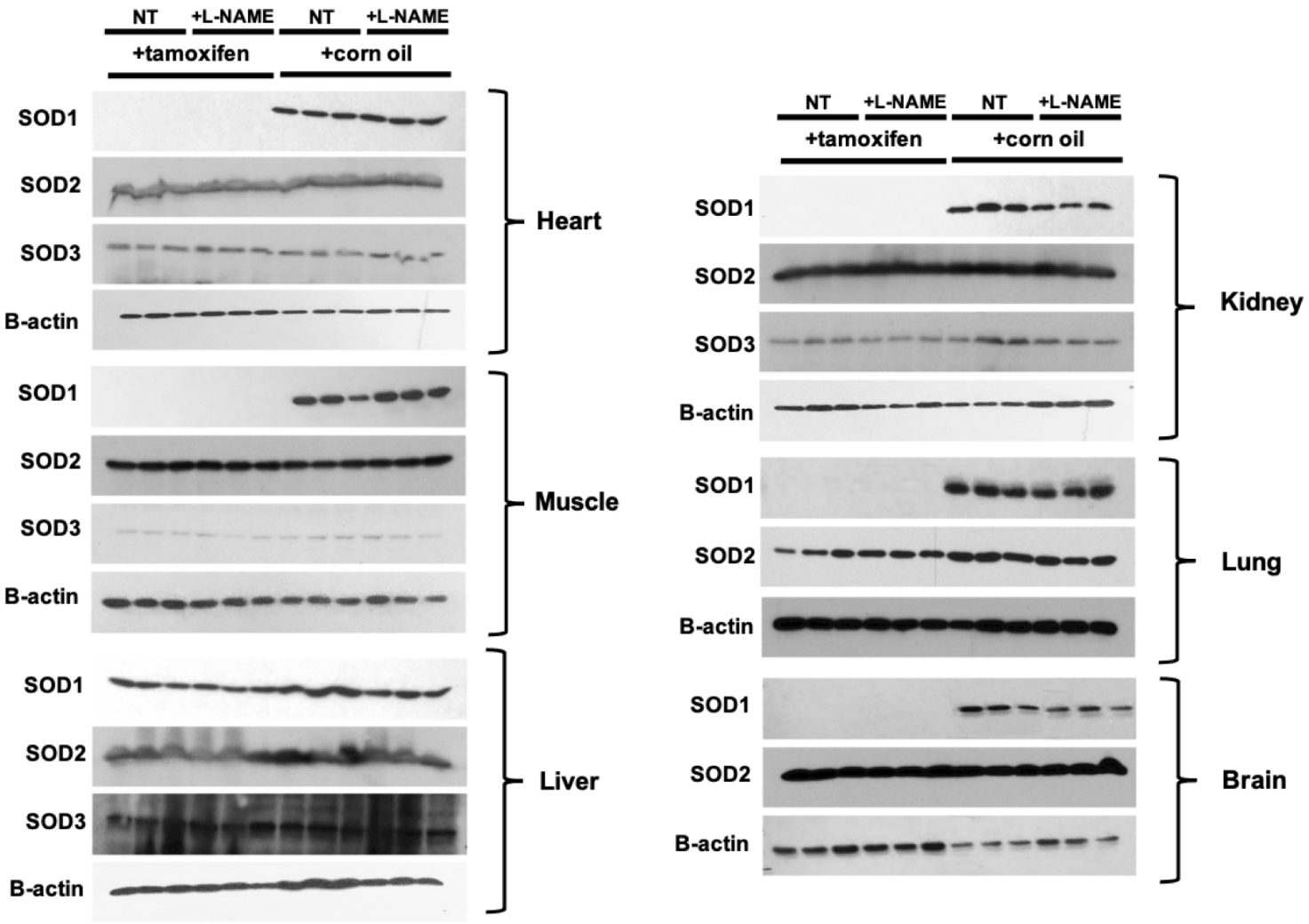

Figure A1: SOD expression in adult-onset Sod1 knockout mice

SOD1 expression is absent in all tamoxifen treated mice, however SOD2 and SOD3 expression remains unchanged. SOD1 expression remains in the liver despite tamoxifen treatment as tamoxifen is metabolized in the liver. SOD expression levels were analyzed 2 months after the completion of tamoxifen or corn oil intraperitoneal injections. The tamoxifen only mice samples were analyzed at approximately 2-3 weeks post injections since these mice die within 3 weeks of the completion of tamoxifen injections from loss of SOD1 expression. During the 2 months following tamoxifen or corn oil injections, mice in the L-NAME groups receive intraperitoneal L-NAME injections every other day.

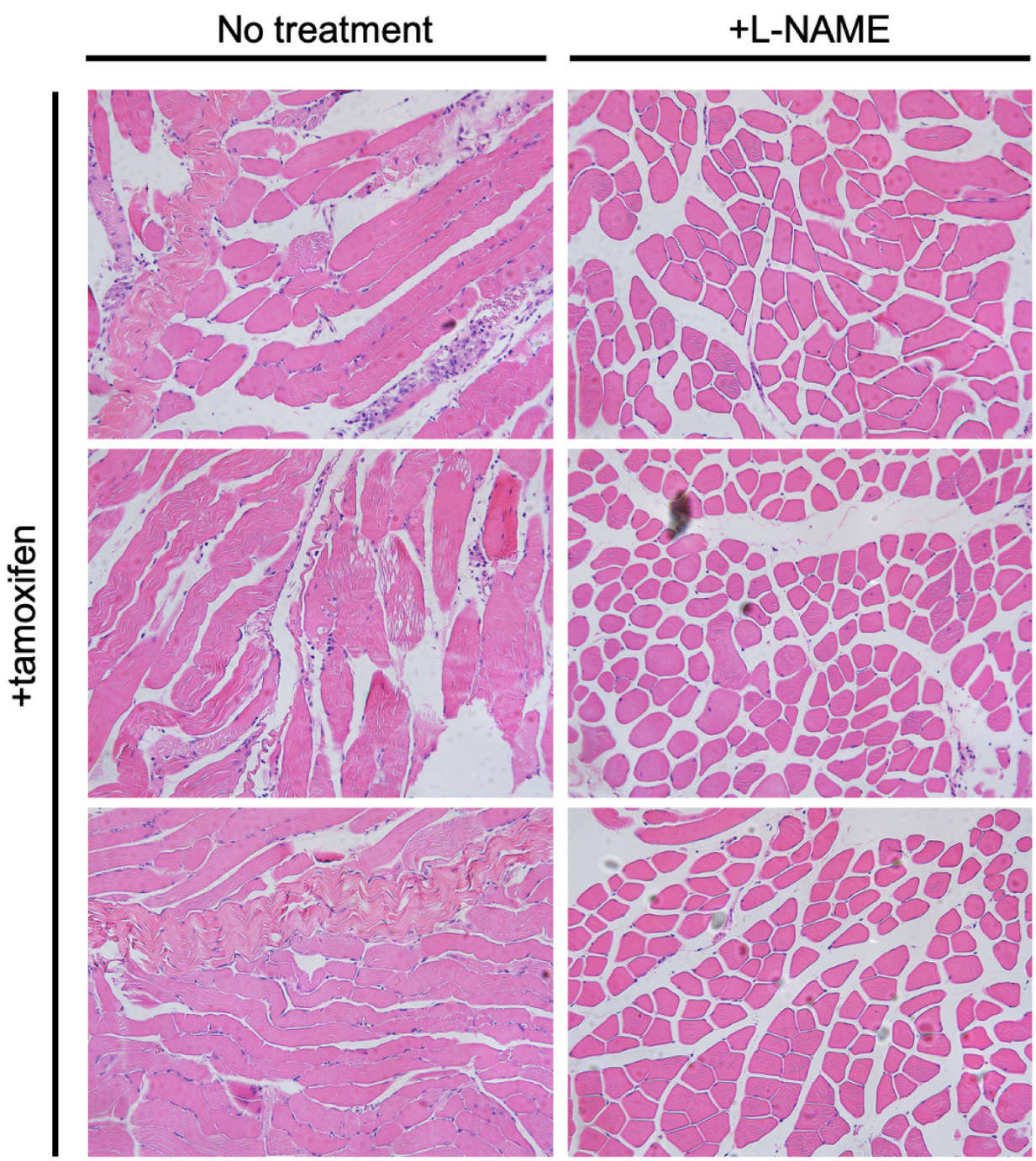

Figure A2: Replicates of L-NAME rescued adult-onset *Sod1* knockout skeletal muscles
Skeletal muscle pathology examined using H&E (hematoxylin & eosin) staining. Hematoxylin stains the nuclei blue and eosin stains the cytoplasm and extracellular matrix pink. Pathology of skeletal muscles shows muscle degradation in adult-onset *Sod1* knockout mice (+tamoxifen only). There are no signs of muscle degradation in adult-onset *Sod1* knockout mice that received intraperitoneal injections of L-NAME, a NOS inhibitor. Here, the three separate images for each group come from different mice.

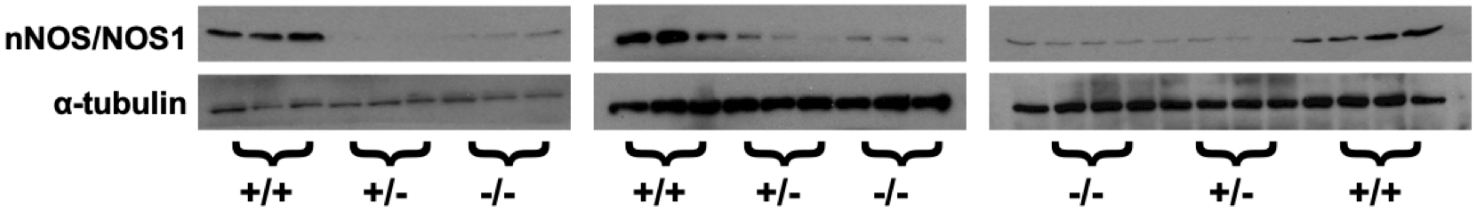

Figure A3: Replicates of reduction in nNOS expression in *Sod1* germline knockout mice
Comparison of nNOS (neuronal NOS) expression in skeletal muscle of mice with varying degrees of *Sod1* expression. The three genotypes examined were $Sod1^{+/+}$, $Sod1^{+/-}$ and $Sod1^{-/-}$. Each lane is a skeletal muscle protein lysate sample from a different mouse (n = 10). $Sod1^{+/+}$ mice have higher nNOS expression than their $Sod1^{+/-}$ and $Sod1^{-/-}$ counterparts. Each western blot compares littermates. The genotypes of the mice were confirmed by PCR and SOD1 western blotting (not shown).

Literature Cited

1. Case, A.J. On the Origin of Superoxide Dismutase: An Evolutionary Perspective of Superoxide-Mediated Redox Signaling. *Antioxidants (Basel)* **6** (2017).
2. Tally, F.P., Goldin, B.R., Jacobus, N.V. & Gorbach, S.L. Superoxide dismutase in anaerobic bacteria of clinical significance. *Infection and immunity* **16**, 20-25 (1977).
3. Fridovich, I. Superoxide anion radical (O2-.), superoxide dismutases, and related matters. *J Biol Chem* **272**, 18515-18517 (1997).
4. Pacher, P., Beckman, J.S. & Liaudet, L. Nitric oxide and peroxynitrite in health and disease. *Physiological Reviews* **87**, 315-424 (2007).
5. Huang, T.-T. *et al.* Superoxide-Mediated Cytotoxicity in Superoxide Dismutase-Deficient Fetal Fibroblasts. *Archives of Biochemistry and Biophysics* **344**, 424-432 (1997).
6. Muller, F.L. *et al.* Absence of CuZn superoxide dismutase leads to elevated oxidative stress and acceleration of age-dependent skeletal muscle atrophy. *FRB Free Radical Biology and Medicine* **40**, 1993-2004 (2006).
7. Larkins, N.J. Free radical biology and pathology. *Journal of Equine Veterinary Science* **19**, 84-85 (1999).
8. Phaniendra, A., Jestadi, D.B. & Periyasamy, L. Free radicals: properties, sources, targets, and their implication in various diseases. *Indian J Clin Biochem* **30**, 11-26 (2015).
9. Commoner, B., Townsend, J. & Pake, G.E. Free Radicals in Biological Materials. *Nature* **174**, 689-691 (1954).
10. Al'tshuler, S.A. & Kozyrev, B.M. *Electron paramagnetic resonance*. (Academic Press, New York; 1964).
11. Harman, D. Aging: A Theory Based on Free Radical and Radiation Chemistry. *Journal of Gerontology* **11**, 298-300 (1956).
12. Harman, D. The Free Radical Theory of Aging. *Antioxidants and Redox Signaling* **5**, 557-561 (2003).
13. Harman, D. Aging: Prospects for further increases in the functional life span. *AGE* **17**, 119-146 (1994).
14. Harman, D. Aging and disease: extending functional life span. *Ann N Y Acad Sci* **786**, 321-336 (1996).
15. Lapointe, J. & Hekimi, S. When a theory of aging ages badly. *Cell Mol Life Sci* **67**, 1-8 (2010).
16. Van Raamsdonk, J.M. & Hekimi, S. Superoxide dismutase is dispensable for normal animal lifespan. *Proceedings of the National Academy of Sciences of the United States of America* **109**, 5785-5790 (2012).
17. Elchuri, S. *et al.* CuZnSOD deficiency leads to persistent and widespread oxidative damage and hepatocarcinogenesis later in life. *Oncogene* **24**, 367-380 (2005).
18. Balaban, R.S., Nemoto, S. & Finkel, T. Mitochondria, oxidants, and aging. *Cell* **120**, 483-495 (2005).
19. Korshunov, S.S., Skulachev, V.P. & Starkov, A.A. High protonic potential actuates a mechanism of production of reactive oxygen species in mitochondria. *FEBS Letters* **416**, 15-18 (1997).

20. Murphy, M.P. How mitochondria produce reactive oxygen species. *Biochem J* **417**, 1-13 (2009).
21. Zhao, R.-Z., Jiang, S., Zhang, L. & Yu, Z.-B. Mitochondrial electron transport chain, ROS generation and uncoupling (Review). *Int J Mol Med* **44**, 3-15 (2019).
22. Cadenas, E. & Davies, K.J. Mitochondrial free radical generation, oxidative stress, and aging. *Free Radical Biology and Medicine* **29**, 222-230 (2000).
23. Loschen, G., Flohe, L. & Chance, B. Respiratory chain linked H(2)O(2) production in pigeon heart mitochondria. *FEBS Lett* **18**, 261-264 (1971).
24. Loschen, G., Azzi, A., Richter, C. & Flohé, L. Superoxide radicals as precursors of mitochondrial hydrogen peroxide. *FEBS letters* **42**, 68-72 (1974).
25. Weisiger, R.A. & Fridovich, I. Superoxide dismutase organelle specificity. *Journal of Biological Chemistry* **248**, 3582-3592 (1973).
26. Sawyer, D.T. & Valentine, J.S. How super is superoxide? *Accounts of Chemical Research* **14**, 393-400 (1981).
27. Fridovich, I. Oxygen: How do we stand it? *Medical principles and practice : international journal of the Kuwait University, Health Science Centre* **22** (2012).
28. Turrens, J.F. Mitochondrial formation of reactive oxygen species. *The Journal of physiology* **552**, 335-344 (2003).
29. Muller, F. The nature and mechanism of superoxide production by the electron transport chain: Its relevance to aging. *J Am Aging Assoc* **23**, 227-253 (2000).
30. Brand, M.D. The sites and topology of mitochondrial superoxide production. *Experimental gerontology* **45**, 466-472 (2010).
31. Mimaki, M., Wang, X., McKenzie, M., Thorburn, D.R. & Ryan, M.T. Understanding mitochondrial complex I assembly in health and disease. *Biochimica et Biophysica Acta (BBA) - Bioenergetics* **1817**, 851-862 (2012).
32. Skulachev, V.P. *Membrane bioenergetics*. (Springer-Verlag, Berlin ;; 1988).
33. Zorova, L.D. *et al.* Mitochondrial membrane potential. *Anal Biochem* **552**, 50-59 (2018).
34. Cadenas, E., Boveris, A., Ragan, C.I. & Stoppani, A.O. Production of superoxide radicals and hydrogen peroxide by NADH-ubiquinone reductase and ubiquinol-cytochrome c reductase from beef-heart mitochondria. *Archives of biochemistry and biophysics* **180**, 248-257 (1977).
35. Alhasan, R. & Njus, D. The epinephrine assay for superoxide: Why dopamine does not work. *Anal Biochem* **381**, 142-147 (2008).
36. Boveris, A., Oshino, N. & Chance, B. The cellular production of hydrogen peroxide. *Biochem J* **128**, 617-630 (1972).
37. Gupta, R.C. & Milatovic, D. Chapter 23 - Insecticides, in *Biomarkers in Toxicology*. (ed. R.C. Gupta) 389-407 (Academic Press, Boston; 2014).
38. Kushnareva, Y., Murphy, A.N. & Andreyev, A. Complex I-mediated reactive oxygen species generation: modulation by cytochrome c and NAD(P)+ oxidation-reduction state. *The Biochemical journal* **368**, 545-553 (2002).
39. Liu, Y., Fiskum, G. & Schubert, D. Generation of reactive oxygen species by the mitochondrial electron transport chain. *J Neurochem* **80**, 780-787 (2002).

40. Takeshige, K. & Minakami, S. NADH- and NADPH-dependent formation of superoxide anions by bovine heart submitochondrial particles and NADH-ubiquinone reductase preparation. *Biochem J* **180**, 129-135 (1979).
41. Genova, M.L. *et al.* The site of production of superoxide radical in mitochondrial Complex I is not a bound ubisemiquinone but presumably iron-sulfur cluster N2. *FEBS Lett* **505**, 364-368 (2001).
42. Bleier, L. & Dröse, S. Superoxide generation by complex III: From mechanistic rationales to functional consequences. *Biochimica et Biophysica Acta (BBA) - Bioenergetics* **1827**, 1320-1331 (2013).
43. Rich, P.R. & Bonner, W.D. The sites of superoxide anion generation in higher plant mitochondria. *Archives of Biochemistry and Biophysics* **188**, 206-213 (1978).
44. Andreyev, A.Y., Kushnareva, Y.E. & Starkov, A. Mitochondrial metabolism of reactive oxygen species. *Biochemistry (Moscow)* **70**, 200-214 (2005).
45. Trumpower, B.L. The protonmotive Q cycle. Energy transduction by coupling of proton translocation to electron transfer by the cytochrome bc1 complex. *J Biol Chem* **265**, 11409-11412 (1990).
46. Crofts, A.R. *et al.* Mechanism of ubiquinol oxidation by the bc(1) complex: different domains of the quinol binding pocket and their role in the mechanism and binding of inhibitors. *Biochemistry* **38**, 15807-15826 (1999).
47. Battelli, M.G., Polito, L., Bortolotti, M. & Bolognesi, A. Xanthine Oxidoreductase-Derived Reactive Species: Physiological and Pathological Effects. *Oxidative medicine and cellular longevity* **2016**, 3527579-3527579 (2016).
48. Maiuolo, J., Oppedisano, F., Gratteri, S., Muscoli, C. & Mollace, V. Regulation of uric acid metabolism and excretion. *International Journal of Cardiology* **213**, 8-14 (2016).
49. Cantu-Medellin, N. & Kelley, E.E. Xanthine oxidoreductase-catalyzed reactive species generation: a process in critical need of reevaluation. *Redox biology* **1**, 353-358 (2013).
50. Xu, P., LaVallee, P. & Hoidal, J.R. Repressed expression of the human xanthine oxidoreductase gene E-box and TATA-like elements restrict ground state transcriptional activity. *Journal of Biological Chemistry* **275**, 5918-5926 (2000).
51. Harrison, R. Structure and function of xanthine oxidoreductase: where are we now? *Free Radical Biology and Medicine* **33**, 774-797 (2002).
52. Godber, B.L., Doel, J.J., Durgan, J., Eisenthal, R. & Harrison, R. A new route to peroxynitrite: a role for xanthine oxidoreductase. *FEBS letters* **475**, 93-96 (2000).
53. McDonnell, A.M. & Dang, C.H. Basic review of the cytochrome p450 system. *J Adv Pract Oncol* **4**, 263-268 (2013).
54. Zangar, R.C., Davydov, D.R. & Verma, S. Mechanisms that regulate production of reactive oxygen species by cytochrome P450. *Toxicology and Applied Pharmacology* **199**, 316-331 (2004).
55. Park, S.-H., Wiwi, C.A. & Waxman, D.J. Signalling cross-talk between hepatocyte nuclear factor 4α and growth-hormone-activated STAT5b. *Biochemical Journal* **397**, 159-168 (2006).
56. Cai, Z. Monoamine oxidase inhibitors: promising therapeutic agents for Alzheimer's disease. *Mol Med Rep* **9**, 1533-1541 (2014).

57. De Colibus, L. *et al.* Three-dimensional structure of human monoamine oxidase A (MAO A): Relation to the structures of rat MAO A and human MAO B. *Proceedings of the National Academy of Sciences of the United States of America* **102**, 12684-12689 (2005).
58. Edmondson, D.E., Mattevi, A., Binda, C., Li, M. & Hubalek, F. in Current Medicinal Chemistry, Vol. 11 1983-1993 (2004).
59. Maggiorani, D. *et al.* Monoamine Oxidases, Oxidative Stress, and Altered Mitochondrial Dynamics in Cardiac Ageing. *Oxidative medicine and cellular longevity* **2017**, 3017947-3017947 (2017).
60. Cross, A.R. & Segal, A.W. The NADPH oxidase of professional phagocytes—prototype of the NOX electron transport chain systems. *Biochimica et Biophysica Acta (BBA)-Bioenergetics* **1657**, 1-22 (2004).
61. Nguyen, G.T., Green, E.R. & Mecsas, J. Neutrophils to the ROScue: Mechanisms of NADPH Oxidase Activation and Bacterial Resistance. *Frontiers in Cellular and Infection Microbiology* **7** (2017).
62. Greenberg, S. & Grinstein, S. Phagocytosis and innate immunity. *Current opinion in immunology* **14**, 136-145 (2002).
63. Baldridge, C.W.C.C.W. The extra respiration of phagocytosis. *Am. J. Physiol.* **103**, 235-236 (1933).
64. Sbarra A.J, A.A.J. The biochemical basis of phagocytosis. I. Metabolic changes during the ingestion of particles by polymorphonuclear leukocytes. *Journal of Biological Chemistry* **234**, 1355-1362 (1959).
65. Leto, T.L. & Geiszt, M. Role of Nox family NADPH oxidases in host defense. *Antioxid Redox Signal* **8**, 1549-1561 (2006).
66. Ameziane-El-Hassani, R. *et al.* Dual oxidase-2 has an intrinsic Ca2+-dependent H2O2-generating activity. *J Biol Chem* **280**, 30046-30054 (2005).
67. Brown, D.I. & Griendling, K.K. Nox proteins in signal transduction. *Free radical biology & medicine* **47**, 1239-1253 (2009).
68. Krause, K.H. Tissue distribution and putative physiological function of NOX family NADPH oxidases. *Jpn J Infect Dis* **57**, S28-29 (2004).
69. Cave, A.C. *et al.* NADPH oxidases in cardiovascular health and disease. *Antioxid Redox Signal* **8**, 691-728 (2006).
70. Milenkovic, M. *et al.* Duox expression and related H2O2 measurement in mouse thyroid: onset in embryonic development and regulation by TSH in adult. *J Endocrinol* **192**, 615-626 (2007).
71. Fruehauf, J.P. & Meyskens, F.L. Reactive oxygen species: a breath of life or death? *Clinical Cancer Research* **13**, 789-794 (2007).
72. Kim, C.-M., Kim, J.-Y. & Kim, J.-H. Cytosolic phospholipase A 2, lipoxygenase metabolites, and reactive oxygen species. *BMB reports* **41**, 555-559 (2008).
73. Cho, K.-J., Seo, J.-M. & Kim, J.-H. Bioactive lipoxygenase metabolites stimulation of NADPH oxidases and reactive oxygen species. *Mol Cells* **32**, 1-5 (2011).
74. De Duve, C. Functions of microbodies (peroxisomes). *J. Cell Biol.* **27**, 25A-26A (1965).
75. De Duve, C. & Baudhuin, P. Peroxisomes (microbodies and related particles). *Physiological reviews* **46**, 323-357 (1966).

76. Kunau, W.-H., Dommes, V. & Schulz, H. β-Oxidation of fatty acids in mitochondria, peroxisomes, and bacteria: A century of continued progress. *Progress in Lipid Research* **34**, 267-342 (1995).
77. Antonenkov, V.D., Grunau, S., Ohlmeier, S. & Hiltunen, J.K. Peroxisomes are oxidative organelles. *Antioxidants & redox signaling* **13**, 525-537 (2010).
78. Fransen, M., Nordgren, M., Wang, B. & Apanasets, O. Role of peroxisomes in ROS/RNS-metabolism: Implications for human disease. *Biochimica et Biophysica Acta (BBA) - Molecular Basis of Disease* **1822**, 1363-1373 (2012).
79. Pauling, L. THE NATURE OF THE CHEMICAL BOND. APPLICATION OF RESULTS OBTAINED FROM THE QUANTUM MECHANICS AND FROM A THEORY OF PARAMAGNETIC SUSCEPTIBILITY TO THE STRUCTURE OF MOLECULES. *Journal of the American Chemical Society* **53**, 1367-1400 (1931).
80. Pauling, L. THE NATURE OF THE CHEMICAL BOND. III. THE TRANSITION FROM ONE EXTREME BOND TYPE TO ANOTHER. *Journal of the American Chemical Society* **54**, 988-1003 (1932).
81. Pauling, L. The discovery of the superoxide radical. *Trends in Biochemical Sciences* **4**, N270-N271 (1979).
82. Neuman, E.W. Potassium Superoxide and the Three-Electron Bond. *The Journal of Chemical Physics* **2**, 31-33 (1934).
83. Fridovich, I. The biology of oxygen radicals. *Science* **201**, 875-880 (1978).
84. Bast, A. Is formation of reactive oxygen by cytochrome P-450 perilous and predictable? *Trends in Pharmacological Sciences* **7**, 266-270 (1986).
85. Hayyan, M., Hashim, M.A. & AlNashef, I.M. Superoxide Ion: Generation and Chemical Implications. *Chemical Reviews* **116**, 3029-3085 (2016).
86. Nordberg, J. & Arnér, E.S. Reactive oxygen species, antioxidants, and the mammalian thioredoxin system. *Free radical biology and medicine* **31**, 1287-1312 (2001).
87. Kussmaul, L. & Hirst, J. The mechanism of superoxide production by NADH:ubiquinone oxidoreductase (complex I) from bovine heart mitochondria. *Proceedings of the National Academy of Sciences* **103**, 7607-7612 (2006).
88. Han, D., Antunes, F., Canali, R., Rettori, D. & Cadenas, E. Voltage-dependent anion channels control the release of the superoxide anion from mitochondria to cytosol. *J Biol Chem* **278**, 5557-5563 (2003).
89. Lustgarten, M.S. *et al.* Complex I generated, mitochondrial matrix-directed superoxide is released from the mitochondria through voltage dependent anion channels. *Biochemical and biophysical research communications* **422**, 515-521 (2012).
90. Bus, J.S. & Gibson, J.E. Paraquat: model for oxidant-initiated toxicity. *Environmental Health Perspectives* **55**, 37-46 (1984).
91. Cocheme, H.M. & Murphy, M.P. Complex I Is the Major Site of Mitochondrial Superoxide Production by Paraquat. *Journal of Biological Chemistry Journal of Biological Chemistry* **283**, 1786-1798 (2008).
92. Hassan, H.M. [69] Exacerbation of superoxide radical formation by Paraquat, in *Methods in Enzymology*, Vol. 105 523-532 (Academic Press, 1984).
93. Robb, E.L. *et al.* Control of mitochondrial superoxide production by reverse electron transport at complex I. *The Journal of biological chemistry* **293**, 9869-9879 (2018).

94. Dukan, S. & Nyström, T. Oxidative stress defense and deterioration of growth-arrested Escherichia coli cells. *J Biol Chem* **274**, 26027-26032 (1999).
95. Van Remmen, H. *et al.* Life-long reduction in MnSOD activity results in increased DNA damage and higher incidence of cancer but does not accelerate aging. *Physiol Genomics* **16**, 29-37 (2003).
96. Yang, W., Li, J. & Hekimi, S. A Measurable increase in oxidative damage due to reduction in superoxide detoxification fails to shorten the life span of long-lived mitochondrial mutants of Caenorhabditis elegans. *Genetics* **177**, 2063-2074 (2007).
97. Tharmalingam, S., Alhasawi, A., Appanna, V.P., Lemire, J. & Appanna, V.D. Reactive nitrogen species (RNS)-resistant microbes: adaptation and medical implications. *Biol Chem* **398**, 1193-1208 (2017).
98. Ghosh, N., Das, A., Chaffee, S., Roy, S. & Sen, C.K. Chapter 4 - Reactive Oxygen Species, Oxidative Damage and Cell Death, in *Immunity and Inflammation in Health and Disease*. (eds. S. Chatterjee, W. Jungraithmayr & D. Bagchi) 45-55 (Academic Press, 2018).
99. Richter, C., Park, J.W. & Ames, B.N. Normal oxidative damage to mitochondrial and nuclear DNA is extensive. *Proceedings of the National Academy of Sciences* **85**, 6465-6467 (1988).
100. D'Errico, M., Parlanti, E. & Dogliotti, E. Mechanism of oxidative DNA damage repair and relevance to human pathology. *Mutat Res* **659**, 4-14 (2008).
101. Madugundu, G.S., Cadet, J. & Wagner, J.R. Hydroxyl-radical-induced oxidation of 5-methylcytosine in isolated and cellular DNA. *Nucleic acids research* **42**, 7450-7460 (2014).
102. Branco, M.R., Ficz, G. & Reik, W. Uncovering the role of 5-hydroxymethylcytosine in the epigenome. *Nature Reviews Genetics* **13**, 7-13 (2012).
103. Kreuz, S. & Fischle, W. Oxidative stress signaling to chromatin in health and disease. *Epigenomics* **8**, 843-862 (2016).
104. Nakabeppu, Y. Cellular Levels of 8-Oxoguanine in either DNA or the Nucleotide Pool Play Pivotal Roles in Carcinogenesis and Survival of Cancer Cells. *International journal of molecular sciences* **15**, 12543-12557 (2014).
105. Nagayoshi, Y. *et al.* Differences in oxidative stress markers based on the aetiology of heart failure: comparison of oxidative stress in patients with and without coronary artery disease. *Free radical research* **43**, 1159-1166 (2009).
106. Davies, M.J. Protein oxidation and peroxidation. *Biochemical Journal* **473**, 805-825 (2016).
107. Berlett, B.S. & Stadtman, E.R. Protein oxidation in aging, disease, and oxidative stress. *Journal of Biological Chemistry* **272**, 20313-20316 (1997).
108. Levine, R.L. Carbonyl modified proteins in cellular regulation, aging, and disease. *Free Radic Biol Med* **32**, 790-796 (2002).
109. Dalle-Donne, I., Rossi, R., Giustarini, D., Milzani, A. & Colombo, R. Protein carbonyl groups as biomarkers of oxidative stress. *Clinica Chimica Acta* **329**, 23-38 (2003).
110. Levine, R.L., Mosoni, L., Berlett, B.S. & Stadtman, E.R. Methionine residues as endogenous antioxidants in proteins. *Proceedings of the National Academy of Sciences of the United States of America* **93**, 15036-15040 (1996).

111. Stadtman, E.R. Metal ion-catalyzed oxidation of proteins: biochemical mechanism and biological consequences. *Free Radical Biology and Medicine* **9**, 315-325 (1990).
112. Yin, H., Xu, L. & Porter, N.A. Free Radical Lipid Peroxidation: Mechanisms and Analysis. *Chemical Reviews* **111**, 5944-5972 (2011).
113. Girotti, A.W. Mechanisms of lipid peroxidation. *Journal of free radicals in biology & medicine* **1**, 87-95 (1985).
114. D'Autreaux, B. & Toledano, M.B. ROS as signalling molecules: mechanisms that generate specificity in ROS homeostasis. *Nat Rev Mol Cell Biol* **8**, 813-824 (2007).
115. Nathan, C. Specificity of a third kind: reactive oxygen and nitrogen intermediates in cell signaling. *The Journal of clinical investigation* **111**, 769-778 (2003).
116. Halliwell, B. & Gutteridge, J.M. *Free radicals in biology and medicine*. (Oxford University Press, USA, 2015).
117. Imlay, J.A. Iron-sulphur clusters and the problem with oxygen. *Molecular Microbiology* **59**, 1073-1082 (2006).
118. Rees, D.C. Great metalloclusters in enzymology. *Annual review of biochemistry* **71**, 221-246 (2002).
119. Berkovitch, F., Nicolet, Y., Wan, J.T., Jarrett, J.T. & Drennan, C.L. Crystal structure of biotin synthase, an S-adenosylmethionine-dependent radical enzyme. *Science* **303**, 76-79 (2004).
120. Winterbourn, C.C. & Hampton, M.B. Thiol chemistry and specificity in redox signaling. *Free Radical Biology and Medicine* **45**, 549-561 (2008).
121. Klomsiri, C., Karplus, P.A. & Poole, L.B. Cysteine-based redox switches in enzymes. *Antioxidants & redox signaling* **14**, 1065-1077 (2011).
122. Rhee, S.G. H2O2, a necessary evil for cell signaling. *Science* **312**, 1882-1883 (2006).
123. Finkel, T. From sulfenylation to sulfhydration: what a thiolate needs to tolerate. *Sci. Signal.* **5**, pe10-pe10 (2012).
124. Schieber, M. & Chandel, N.S. ROS function in redox signaling and oxidative stress. *Curr Biol* **24**, R453-R462 (2014).
125. Liochev, S.I. & Fridovich, I. Superoxide and Iron: Partners in Crime. *IUBMB Life* **48**, 157-161 (1999).
126. McCord, J.M. Superoxide dismutase, lipid peroxidation, and bell-shaped dose response curves. *Dose Response* **6**, 223-238 (2008).
127. Hekimi, S., Lapointe, J. & Wen, Y. Taking a "good" look at free radicals in the aging process. *Trends Cell Biol* **21**, 569-576 (2011).
128. Fukai, T. & Ushio-Fukai, M. Superoxide dismutases: role in redox signaling, vascular function, and diseases. *Antioxidants & Redox Signaling* **15**, 1583-1606 (2011).
129. Wang, Y., Branicky, R., Noë, A. & Hekimi, S. Superoxide dismutases: Dual roles in controlling ROS damage and regulating ROS signaling. *Journal of Cell Biology* **217**, 1915-1928 (2018).
130. Chelikani, P., Fita, I. & Loewen, P.C. Diversity of structures and properties among catalases. *Cellular and Molecular Life Sciences CMLS* **61**, 192-208 (2004).
131. Loew, O. A new enzyme of general occurrence in organismis. *Science* **11**, 701-702 (1900).

132. Sumner, J.B. & Gralén, N. The molecular weight of crystalline catalase. *Science* **87**, 284-284 (1938).
133. Zámocký, M. & Koller, F. Understanding the structure and function of catalases: clues from molecular evolution and in vitro mutagenesis. *Prog Biophys Mol Biol* **72**, 19-66 (1999).
134. Zamocky, M., Furtmüller, P.G. & Obinger, C. Evolution of catalases from bacteria to humans. *Antioxidants & redox signaling* **10**, 1527-1548 (2008).
135. Nicholls, P., Fita, I. & Loewen, P.C. Enzymology and structure of catalases. *Advances in Inorganic Chemistry* **51**, 51-106 (2000).
136. Kirkman, H.N. & Gaetani, G.F. Mammalian catalase: a venerable enzyme with new mysteries. *Trends in biochemical sciences* **32**, 44-50 (2007).
137. Heck, D.E., Vetrano, A.M., Mariano, T.M. & Laskin, J.D. UVB light stimulates production of reactive oxygen species unexpected role for catalase. *Journal of Biological Chemistry* **278**, 22432-22436 (2003).
138. Ho, Y.-S., Xiong, Y., Ma, W., Spector, A. & Ho, D.S. Mice lacking catalase develop normally but show differential sensitivity to oxidant tissue injury. *Journal of Biological Chemistry* **279**, 32804-32812 (2004).
139. Johnston, A.D. & Ebert, P.R. The redox system in C. elegans, a phylogenetic approach. *Journal of toxicology* **2012** (2012).
140. Townsend, D.M., Tew, K.D. & Tapiero, H. The importance of glutathione in human disease. *Biomed Pharmacother* **57**, 145-155 (2003).
141. Anderson, M.E. Glutathione: an overview of biosynthesis and modulation. *Chem Biol Interact* **111-112**, 1-14 (1998).
142. Meister, A. Glutathione deficiency produced by inhibition of its synthesis, and its reversal; applications in research and therapy. *Pharmacology & therapeutics* **51**, 155-194 (1991).
143. Moinova, H.R. & Mulcahy, R.T. An electrophile responsive element (EpRE) regulates beta-naphthoflavone induction of the human gamma-glutamylcysteine synthetase regulatory subunit gene. Constitutive expression is mediated by an adjacent AP-1 site. *J Biol Chem* **273**, 14683-14689 (1998).
144. Arrick, B.A., Griffo, W., Cohn, Z. & Nathan, C. Hydrogen peroxide from cellular metabolism of cystine. A requirement for lysis of murine tumor cells by vernolepin, a glutathione-depleting antineoplastic. *J Clin Invest* **76**, 567-574 (1985).
145. Mullineaux, P. & Creissen, G. Oxidative Stress and the Molecular Biology of Antioxidant Defenses. (1997).
146. Lee, Y.J. *et al.* Glucose deprivation-induced cytotoxicity and alterations in mitogen-activated protein kinase activation are mediated by oxidative stress in multidrug-resistant human breast carcinoma cells. *J Biol Chem* **273**, 5294-5299 (1998).
147. Banki, K., Hutter, E., Gonchoroff, N.J. & Perl, A. Molecular ordering in HIV-induced apoptosis. Oxidative stress, activation of caspases, and cell survival are regulated by transaldolase. *J Biol Chem* **273**, 11944-11953 (1998).
148. Downey, J.S. *et al.* The LEC rat possesses reduced hepatic selenium, contributing to the severity of spontaneous hepatitis and sensitivity to carcinogenesis. *Biochem Biophys Res Commun* **244**, 463-467 (1998).

149. Rhee, S.G. Overview on Peroxiredoxin. *Mol Cells* **39**, 1-5 (2016).
150. De Armas, M.I. *et al.* Rapid peroxynitrite reduction by human peroxiredoxin 3: Implications for the fate of oxidants in mitochondria. *Free Radical Biology and Medicine* **130**, 369-378 (2019).
151. Poole, L.B. The catalytic mechanism of peroxiredoxins. *Subcell Biochem* **44**, 61-81 (2007).
152. Holmgren, A. *et al.* Thiol redox control via thioredoxin and glutaredoxin systems. *Biochemical Society Transactions* **33**, 1375-1377 (2005).
153. Rushworth, G.F. & Megson, I.L. Existing and potential therapeutic uses for N-acetylcysteine: the need for conversion to intracellular glutathione for antioxidant benefits. *Pharmacol Ther* **141**, 150-159 (2014).
154. Burgunder, J., Varriale, A. & Lauterburg, B. Effect of N-acetylcysteine on plasma cysteine and glutathione following paracetamol administration. *European journal of clinical pharmacology* **36**, 127-131 (1989).
155. Hurst, G.A., Shaw, P.B. & LeMaistre, C.A. Laboratory and clinical evaluation of the mucolytic properties of acetylcysteine. *American Review of Respiratory Disease* **96**, 962-970 (1967).
156. Heard, K.J. Acetylcysteine for acetaminophen poisoning. *N Engl J Med* **359**, 285-292 (2008).
157. Grinberg, L., Fibach, E., Amer, J. & Atlas, D. N-acetylcysteine amide, a novel cell-permeating thiol, restores cellular glutathione and protects human red blood cells from oxidative stress. *Free Radic Biol Med* **38**, 136-145 (2005).
158. Sandilands, E.A. *et al.* Mechanisms for an effect of acetylcysteine on renal function after exposure to radio-graphic contrast material: study protocol. *BMC clinical pharmacology* **12**, 3 (2012).
159. Gibson, K.R. *et al.* Evaluation of the antioxidant properties of N-acetylcysteine in human platelets: prerequisite for bioconversion to glutathione for antioxidant and antiplatelet activity. *Journal of cardiovascular pharmacology* **54**, 319-326 (2009).
160. Svirbely, J.L. & Szent-Györgyi, A. The chemical nature of vitamin C. *Biochemical Journal* **27**, 279 (1933).
161. Buettner, G.R., Schafer, F.Q. & Albert, S.-G. vitamin C identification. *Biochemist* **28**, 31 (2006).
162. Padayatty, S.J. & Levine, M. Vitamin C: the known and the unknown and Goldilocks. *Oral Dis* **22**, 463-493 (2016).
163. Priestley, J. XIX. Observations on different kinds of air. *Philosophical transactions of the royal society of London*, 147-264 (1772).
164. West, J.B. Joseph Priestley, oxygen, and the Enlightenment. *American Journal of Physiology-Lung Cellular and Molecular Physiology* **306**, L111-L119 (2014).
165. Gruetter, C.A. *et al.* Relaxation of bovine coronary artery and activation of coronary arterial guanylate cyclase by nitric oxide, nitroprusside and a carcinogenic nitrosoamine. *J Cyclic Nucleotide Res* **5**, 211-224 (1979).
166. Furchgott, R.F. & Zawadzki, J.V. The obligatory role of endothelial cells in the relaxation of arterial smooth muscle by acetylcholine. *Nature* **288**, 373-376 (1980).

167. Truskey, G.A. Endothelial Cell Vascular Smooth Muscle Cell Co-Culture Assay For High Throughput Screening Assays For Discovery of Anti-Angiogenesis Agents and Other Therapeutic Molecules. *Int J High Throughput Screen* **2010**, 171-181 (2010).
168. Furchgott, R.F. Role of endothelium in responses of vascular smooth muscle. *Circ Res* **53**, 557-573 (1983).
169. Cherry, P.D., Furchgott, R.F., Zawadzki, J.V. & Jothianandan, D. Role of endothelial cells in relaxation of isolated arteries by bradykinin. *Proc Natl Acad Sci U S A* **79**, 2106-2110 (1982).
170. Palmer, R.M., Ferrige, A.G. & Moncada, S. Nitric oxide release accounts for the biological activity of endothelium-derived relaxing factor. *Nature* **327**, 11-17 (1987).
171. Ignarro, L.J., Buga, G.M., Wood, K.S., Byrns, R.E. & Chaudhuri, G. Endothelium-derived relaxing factor produced and released from artery and vein is nitric oxide. *Proceedings of the National Academy of Sciences* **84**, 9265-9269 (1987).
172. Ignarro, L.J. Biological actions and properties of endothelium-derived nitric oxide formed and released from artery and vein. *Circ Res* **65**, 1-21 (1989).
173. Palmer, R.M.J., Ashton, D.S. & Moncada, S. Vascular endothelial cells synthesize nitric oxide from L-arginine. *Nature* **333**, 664-666 (1988).
174. Yetik-Anacak, G. & Catravas, J.D. Nitric oxide and the endothelium: History and impact on cardiovascular disease. *Vascular Pharmacology* **45**, 268-276 (2006).
175. Koshland, D. The molecule of the year. *Science* **258**, 1861-1861 (1992).
176. SoRelle, R. Nobel prize awarded to scientists for nitric oxide discoveries. *Circulation* **98**, 2365-2366 (1998).
177. Howlett, R. Nobel award stirs up debate on nitric oxide breakthrough. *Nature* **395**, 625-626 (1998).
178. Arnold, W.P., Mittal, C.K., Katsuki, S. & Murad, F. Nitric oxide activates guanylate cyclase and increases guanosine 3':5'-cyclic monophosphate levels in various tissue preparations. *Proceedings of the National Academy of Sciences of the United States of America* **74**, 3203-3207 (1977).
179. Boden, W.E., Padala, S.K., Cabral, K.P., Buschmann, I.R. & Sidhu, M.S. Role of short-acting nitroglycerin in the management of ischemic heart disease. *Drug Des Devel Ther* **9**, 4793-4805 (2015).
180. Stuehr, D.J. Mammalian nitric oxide synthases. *Biochimica et Biophysica Acta (BBA)-Bioenergetics* **1411**, 217-230 (1999).
181. Mayer, B. & Hemmens, B. Biosynthesis and action of nitric oxide in mammalian cells. *Trends in biochemical sciences* **22**, 477-481 (1997).
182. Shafirovich, V. & Lymar, S.V. Nitroxyl and its anion in aqueous solutions: Spin states, protic equilibria, and reactivities toward oxygen and nitric oxide. *Proceedings of the National Academy of Sciences* **99**, 7340-7345 (2002).
183. Lewis, R.S. & Deen, W.M. Kinetics of the Reaction of Nitric Oxide with Oxygen in Aqueous Solutions. *Chemical Research in Toxicology* **7**, 568-574 (1994).
184. Smith, B.C. & Marletta, M.A. Mechanisms of S-nitrosothiol formation and selectivity in nitric oxide signaling. *Current opinion in chemical biology* **16**, 498-506 (2012).
185. Wink, D.A. *et al.* DNA deaminating ability and genotoxicity of nitric oxide and its progenitors. *Science* **254**, 1001-1003 (1991).

186. Hausladen, A. & Fridovich, I. Superoxide and peroxynitrite inactivate aconitases, but nitric oxide does not. *J Biol Chem* **269**, 29405-29408 (1994).
187. Castro, L., Rodriguez, M. & Radi, R. Aconitase is readily inactivated by peroxynitrite, but not by its precursor, nitric oxide. *J Biol Chem* **269**, 29409-29415 (1994).
188. Beneš, L., Ďuračková, Z. & Ferenčik, M. Chemistry, physiology and pathology of free radicals. *Life sciences* **65**, 1865-1874 (1999).
189. Martínez, M.C. & Andriantsitohaina, R. Reactive nitrogen species: molecular mechanisms and potential significance in health and disease. *Antioxid Redox Signal* **11**, 669-702 (2009).
190. Di Meo, S., Reed, T.T., Venditti, P. & Victor, V.M. Role of ROS and RNS Sources in Physiological and Pathological Conditions. *Oxid Med Cell Longev* **2016**, 1245049 (2016).
191. Schulz, J.B., Matthews, R.T. & Beal, M.F. Role of nitric oxide in neurodegenerative diseases. *Current opinion in neurology* **8**, 480-486 (1995).
192. Uehara, T. *et al.* S-nitrosylated protein-disulphide isomerase links protein misfolding to neurodegeneration. *Nature* **441**, 513-517 (2006).
193. Zhang, N. *et al.* Nitric oxide-mediated pathways and its role in the degenerative diseases. *Frontiers in Bioscience - Landmark* **22**, 824-834 (2017).
194. Leon-Bollotte, L. *et al.* S-nitrosylation of the death receptor fas promotes fas ligand-mediated apoptosis in cancer cells. *Gastroenterology* **140**, 2009-2018, 2018.e2001-2004 (2011).
195. Baek, M.W. *et al.* Nitric oxide induces apoptosis in human gingival fibroblast through mitochondria-dependent pathway and JNK activation. *Int Endod J* **48**, 287-297 (2015).
196. Folkes, L.K. & O'Neill, P. DNA damage induced by nitric oxide during ionizing radiation is enhanced at replication. *Nitric Oxide* **34**, 47-55 (2013).
197. Pearce, L.L., Kanai, A.J., Epperly, M.W. & Peterson, J. Nitrosative stress results in irreversible inhibition of purified mitochondrial complexes I and III without modification of cofactors. *Nitric Oxide* **13**, 254-263 (2005).
198. Chae, I.H., Park, K.W., Kim, H.S. & Oh, B.H. Nitric oxide-induced apoptosis is mediated by Bax/Bcl-2 gene expression, transition of cytochrome c, and activation of caspase-3 in rat vascular smooth muscle cells. *Clin Chim Acta* **341**, 83-91 (2004).
199. Rathnasamy, G. *et al.* NF-κB–Mediated Nitric Oxide Production and Activation of Caspase-3 Cause Retinal Ganglion Cell Death in the Hypoxic Neonatal Retina. *Investigative ophthalmology & visual science* **55**, 5878-5889 (2014).
200. Saligrama, P.T. *et al.* IL-15 maintains T-cell survival via S-nitrosylation-mediated inhibition of caspase-3. *Cell Death Differ* **21**, 904-914 (2014).
201. Tuteja, N., Chandra, M., Tuteja, R. & Misra, M.K. Nitric Oxide as a Unique Bioactive Signaling Messenger in Physiology and Pathophysiology. *J Biomed Biotechnol* **2004**, 227-237 (2004).
202. Fukuto, J.M. Chemistry of nitric oxide: biologically relevant aspects. *Adv Pharmacol* **34**, 1-15 (1995).
203. Kerwin, J.F., Jr., Lancaster, J.R., Jr. & Feldman, P.L. Nitric oxide: a new paradigm for second messengers. *J Med Chem* **38**, 4343-4362 (1995).
204. Ziolo, M.T. & Bers, D.M. The Real Estate of NOS Signaling. *Circulation Research* **92**, 1279-1281 (2003).

205. Hobbs, A.J. Soluble guanylate cyclase: the forgotten sibling. *Trends in Pharmacological Sciences* **18**, 484-491 (1997).
206. Traylor, T.G. & Sharma, V.S. Why Nitric Oxide? *Biochemistry* **31**, 2847-2849 (1992).
207. Rall, T.W. & Sutherland, E.W. Formation of a cyclic adenine ribonucleotide by tissue particles. *J Biol Chem* **232**, 1065-1076 (1958).
208. Ashman, D.F., Lipton, R., Melicow, M.M. & Price, T.D. Isolation of adenosine 3', 5'-monophosphate and guanosine 3', 5'-monophosphate from rat urine. *Biochem Biophys Res Commun* **11**, 330-334 (1963).
209. White, A.A. & Aurbach, G.D. Detection of guanyl cyclase in mammalian tissues. *Biochimica et Biophysica Acta (BBA) - Enzymology* **191**, 686-697 (1969).
210. Hardman, J.G. & Sutherland, E.W. Guanyl cyclase, an enzyme catalyzing the formation of guanosine 3',5'-monophosphate from guanosine trihosphate. *J Biol Chem* **244**, 6363-6370 (1969).
211. Katsuki, S., Arnold, W., Mittal, C. & Murad, F. Stimulation of guanylate cyclase by sodium nitroprusside, nitroglycerin and nitric oxide in various tissue preparations and comparison to the effects of sodium azide and hydroxylamine. *J Cyclic Nucleotide Res* **3**, 23-35 (1977).
212. Denninger, J.W. & Marletta, M.A. Guanylate cyclase and the ·NO/cGMP signaling pathway. *Biochimica et Biophysica Acta (BBA) - Bioenergetics* **1411**, 334-350 (1999).
213. Gnipp, S. *et al.* Nitric oxide dependent signaling via cyclic GMP in dendritic cells regulates migration and T-cell polarization. *Scientific Reports* **8**, 10969 (2018).
214. Niedbala, W., Cai, B. & Liew, F.Y. Role of nitric oxide in the regulation of T cell functions. *Ann Rheum Dis* **65 Suppl 3**, iii37-iii40 (2006).
215. Warner, T.D., Mitchell, J.A., Sheng, H. & Murad, F. Effects of cyclic GMP on smooth muscle relaxation. *Adv Pharmacol* **26**, 171-194 (1994).
216. Buechler, W.A. *et al.* Soluble guanylyl cyclase and platelet function. *Ann N Y Acad Sci* **714**, 151-157 (1994).
217. Jaffrey, S.R. & Snyder, S.H. Nitric oxide: a neural messenger. *Annu Rev Cell Dev Biol* **11**, 417-440 (1995).
218. Bellamy, T.C., Wood, J. & Garthwaite, J. On the activation of soluble guanylyl cyclase by nitric oxide. *Proceedings of the National Academy of Sciences of the United States of America* **99**, 507-510 (2002).
219. RUSSWURM, M., BEHRENDS, S., HARTENECK, C. & KOESLING, D. Functional properties of a naturally occurring isoform of soluble guanylyl cyclase. *Biochemical Journal* **335**, 125-130 (1998).
220. Sharma, V.S., Traylor, T.G., Gardiner, R. & Mizukami, H. Reaction of nitric oxide with heme proteins and model compounds of hemoglobin. *Biochemistry* **26**, 3837-3843 (1987).
221. Zhao, Y., Brandish, P.E., Ballou, D.P. & Marletta, M.A. A molecular basis for nitric oxide sensing by soluble guanylate cyclase. *Proceedings of the National Academy of Sciences* **96**, 14753-14758 (1999).
222. Fernhoff, N.B., Derbyshire, E.R. & Marletta, M.A. A nitric oxide/cysteine interaction mediates the activation of soluble guanylate cyclase. *Proceedings of the National Academy of Sciences* **106**, 21602-21607 (2009).

223. Brown, G.C. Nitric oxide regulates mitochondrial respiration and cell functions by inhibiting cytochrome oxidase. *FEBS Lett* **369**, 136-139 (1995).
224. Brookes, P.S., Bolaños, J.P. & Heales, S.J. The assumption that nitric oxide inhibits mitochondrial ATP synthesis is correct. *FEBS letters* **446**, 261-263 (1999).
225. Moncada, S. & Erusalimsky, J.D. Does nitric oxide modulate mitochondrial energy generation and apoptosis? *Nature Reviews Molecular Cell Biology* **3**, 214-220 (2002).
226. Bolotina, V.M., Najibi, S., Palacino, J.J., Pagano, P.J. & Cohen, R.A. Nitric oxide directly activates calcium-dependent potassium channels in vascular smooth muscle. *Nature* **368**, 850-853 (1994).
227. Sekkaï, D., Aillet, F., Israël, N. & Lepoivre, M. Inhibition of NF-kappaB and HIV-1 long terminal repeat transcriptional activation by inducible nitric oxide synthase 2 activity. *J Biol Chem* **273**, 3895-3900 (1998).
228. Lander, H.M., Sehajpal, P.K. & Novogrodsky, A. Nitric oxide signaling: a possible role for G proteins. *The Journal of Immunology* **151**, 7182-7187 (1993).
229. Lander, H.M., Ogiste, J.S., Pearce, S.F., Levi, R. & Novogrodsky, A. Nitric oxide-stimulated guanine nucleotide exchange on p21ras. *J Biol Chem* **270**, 7017-7020 (1995).
230. Lander, H.M. *et al.* A molecular redox switch on p21(ras). Structural basis for the nitric oxide-p21(ras) interaction. *J Biol Chem* **272**, 4323-4326 (1997).
231. Li, J., Billiar, T.R., Talanian, R.V. & Kim, Y.M. Nitric Oxide Reversibly Inhibits Seven Members of the Caspase Family via S-Nitrosylation. *Biochemical and Biophysical Research Communications* **240**, 419-424 (1997).
232. Gow, A.J. & Stamler, J.S. Reactions between nitric oxide and haemoglobin under physiological conditions. *Nature* **391**, 169-173 (1998).
233. Xu, L., Eu, J.P., Meissner, G. & Stamler, J.S. Activation of the cardiac calcium release channel (ryanodine receptor) by poly-S-nitrosylation. *Science* **279**, 234-237 (1998).
234. Afanas'ev, I. ROS and RNS signaling in heart disorders: could antioxidant treatment be successful? *Oxidative medicine and cellular longevity* **2011**, 293769-293769 (2011).
235. Orsborne, C., Chaggar, P.S., Shaw, S.M. & Williams, S.G. The renin-angiotensin-aldosterone system in heart failure for the non-specialist: the past, the present and the future. *Postgraduate Medical Journal* **93**, 29-37 (2017).
236. Opie, L.H. & Sack, M.N. Enhanced Angiotensin II Activity in Heart Failure. *Circulation Research* **88**, 654-658 (2001).
237. Griendling, K.K., Minieri, C.A., Ollerenshaw, J.D. & Alexander, R.W. Angiotensin II stimulates NADH and NADPH oxidase activity in cultured vascular smooth muscle cells. *Circulation research* **74**, 1141-1148 (1994).
238. Pagano, P.J., Chanock, S.J., Siwik, D.A., Colucci, W.S. & Clark, J.K. Angiotensin II induces p67phox mRNA expression and NADPH oxidase superoxide generation in rabbit aortic adventitial fibroblasts. *Hypertension* **32**, 331-337 (1998).
239. Marumo, T., Schini-Kerth, V.r.B., Fisslthaler, B. & Busse, R. Platelet-derived growth factor–stimulated superoxide anion production modulates activation of transcription factor NF-κB and expression of monocyte chemoattractant protein 1 in human aortic smooth muscle cells. *Circulation* **96**, 2361-2367 (1997).
240. Ushio-Fukai, M., Alexander, R.W., Akers, M. & Griendling, K.K. p38 Mitogen-activated protein kinase is a critical component of the redox-sensitive signaling pathways

activated by angiotensin II Role in vascular smooth muscle cell hypertrophy. *Journal of Biological Chemistry* **273**, 15022-15029 (1998).
241. Griendling, K.K., Sorescu, D. & Ushio-Fukai, M. NAD (P) H oxidase: role in cardiovascular biology and disease. *Circulation research* **86**, 494-501 (2000).
242. Libby, P. *et al.* Atherosclerosis. *Nature Reviews Disease Primers* **5**, 56 (2019).
243. Warnholtz, A. *et al.* Increased NADH-oxidase–mediated superoxide production in the early stages of atherosclerosis: evidence for involvement of the renin-angiotensin system. *Circulation* **99**, 2027-2033 (1999).
244. Miller, F.J., Gutterman, D.D., Rios, C.D., Heistad, D.D. & Davidson, B.L. Superoxide production in vascular smooth muscle contributes to oxidative stress and impaired relaxation in atherosclerosis. *Circulation research* **82**, 1298-1305 (1998).
245. Suzuki, H., Swei, A., Zweifach, B.W. & Schmid-Schönbein, G.W. In vivo evidence for microvascular oxidative stress in spontaneously hypertensive rats: hydroethidine microfluorography. *Hypertension* **25**, 1083-1089 (1995).
246. Nakazono, K. *et al.* Does superoxide underlie the pathogenesis of hypertension? *Proceedings of the National Academy of Sciences* **88**, 10045-10048 (1991).
247. Apostolova, N. & Victor, V.M. Molecular strategies for targeting antioxidants to mitochondria: therapeutic implications. *Antioxidants & redox signaling* **22**, 686-729 (2015).
248. Brownlee, M. The pathobiology of diabetic complications: a unifying mechanism. *diabetes* **54**, 1615-1625 (2005).
249. Hernandez-Mijares, A. *et al.* Mitochondrial complex I impairment in leukocytes from type 2 diabetic patients. *Free Radical Biology and Medicine* **50**, 1215-1221 (2011).
250. Rovira-Llopis, S. *et al.* (Mary Ann Liebert, Inc. 140 Huguenot Street, 3rd Floor New Rochelle, NY 10801 USA, 2014).
251. Chacko, B.K. *et al.* Prevention of diabetic nephropathy in Ins2+/− AkitaJ mice by the mitochondria-targeted therapy MitoQ. *Biochemical Journal* **432**, 9-19 (2010).
252. Baxter, L.C., Caselli, R.J., Johnson, S.C., Reiman, E. & Osborne, D. Apolipoprotein E ε4 affects new learning in cognitively normal individuals at risk for Alzheimer's disease. *Neurobiology of aging* **24**, 947-952 (2003).
253. Lauderback, C.M. *et al.* Apolipoprotein E modulates Alzheimer's Aβ (1–42)-induced oxidative damage to synaptosomes in an allele-specific manner. *Brain research* **924**, 90-97 (2002).
254. Ramassamy, C. *et al.* Oxidative insults are associated with apolipoprotein E genotype in Alzheimer's disease brain. *Neurobiology of disease* **7**, 23-37 (2000).
255. Turner, P.R., O'Connor, K., Tate, W.P. & Abraham, W.C. Roles of amyloid precursor protein and its fragments in regulating neural activity, plasticity and memory. *Progress in neurobiology* **70**, 1-32 (2003).
256. Butterfield, D.A. & Boyd-Kimball, D. Amyloid β-Peptide (1-42) Contributes to the Oxidative Stress and Neurodegeneration Found in Alzheimer Disease Brain. *Brain Pathology* **14**, 426-432 (2004).
257. Glenner, G., Wong, C., Quaranta, V. & Eanes, E. The amyloid deposits in Alzheimer's disease: their nature and pathogenesis. *Applied pathology* **2**, 357-369 (1984).

258. Zarei, S. *et al.* A comprehensive review of amyotrophic lateral sclerosis. *Surg Neurol Int* **6**, 171-171 (2015).
259. Masrori, P. & Van Damme, P. Amyotrophic lateral sclerosis: a clinical review. *Eur J Neurol* **27**, 1918-1929 (2020).
260. Rosen, D.R. *et al.* Mutations in Cu/Zn superoxide dismutase gene are associated with familial amyotrophic lateral sclerosis. *Nature* **362**, 59-62 (1993).
261. Pansarasa, O. *et al.* SOD1 in Amyotrophic Lateral Sclerosis: "Ambivalent" Behavior Connected to the Disease. *International journal of molecular sciences* **19**, 1345 (2018).
262. Cuanalo-Contreras, K., Mukherjee, A. & Soto, C. Role of protein misfolding and proteostasis deficiency in protein misfolding diseases and aging. *Int J Cell Biol* **2013**, 638083 (2013).
263. Forsberg, K., Andersen, P.M., Marklund, S.L. & Brännström, T. Glial nuclear aggregates of superoxide dismutase-1 are regularly present in patients with amyotrophic lateral sclerosis. *Acta Neuropathol* **121**, 623-634 (2011).
264. Ames, B.N. Dietary carcinogens and anticarcinogens. Oxygen radicals and degenerative diseases. *Science* **221**, 1256-1264 (1983).
265. Loft, S. & Poulsen, H.E. Cancer risk and oxidative DNA damage in man. *J Mol Med (Berl)* **74**, 297-312 (1996).
266. Higinbotham, K.G. *et al.* GGT to GTT transversions in codon 12 of the K-ras oncogene in rat renal sarcomas induced with nickel subsulfide or nickel subsulfide/iron are consistent with oxidative damage to DNA. *Cancer Res* **52**, 4747-4751 (1992).
267. Ames, B.N., Shigenaga, M.K. & Gold, L.S. DNA lesions, inducible DNA repair, and cell division: three key factors in mutagenesis and carcinogenesis. *Environ Health Perspect* **101 Suppl 5**, 35-44 (1993).
268. Harris, C.C. & Hollstein, M. Clinical implications of the p53 tumor-suppressor gene. *N Engl J Med* **329**, 1318-1327 (1993).
269. Brash, D.E. *et al.* A role for sunlight in skin cancer: UV-induced p53 mutations in squamous cell carcinoma. *Proc Natl Acad Sci U S A* **88**, 10124-10128 (1991).
270. Szatrowski, T.P. & Nathan, C.F. Production of large amounts of hydrogen peroxide by human tumor cells. *Cancer Res* **51**, 794-798 (1991).
271. Poulsen, H.E., Prieme, H. & Loft, S. Role of oxidative DNA damage in cancer initiation and promotion. *Eur J Cancer Prev* **7**, 9-16 (1998).
272. Olinski, R. *et al.* DNA base modifications in chromatin of human cancerous tissues. *FEBS Lett* **309**, 193-198 (1992).
273. McCord, J.M. & Fridovich, I. Superoxide dismutase. An enzymic function for erythrocuprein (hemocuprein). *The Journal of biological chemistry* **244**, 6049-6055 (1969).
274. Mann, T. & Keilin, D. Haemocuprein and Hepatocuprein, Copper-Protein Compounds of Blood and Liver in Mammals. **126**, 303-315 (1938).
275. Kimmel, J., Markowitz, H. & Brown, D.M. Some chemical and physical properties of erythrocuprein. *Journal of Biological Chemistry* **234**, 46-50 (1959).
276. McCord, J.M. & Fridovich, I. The reduction of cytochrome c by milk xanthine oxidase. *J Biol Chem* **243**, 5753-5760 (1968).

277. McCord, J.M. The evolution of free radicals and oxidative stress. *Am J Med* **108**, 652-659 (2000).
278. Zelko, I.N., Mariani, T.J. & Folz, R.J. Superoxide dismutase multigene family: a comparison of the CuZn-SOD (SOD1), Mn-SOD (SOD2), and EC-SOD (SOD3) gene structures, evolution, and expression. *Free Radic Biol Med* **33**, 337-349 (2002).
279. Meyer, K.M. & Kump, L.R. Oceanic Euxinia in Earth History: Causes and Consequences. *Annual Review of Earth and Planetary Sciences* **36**, 251-288 (2008).
280. Saito, M.A., Sigman, D.M. & Morel, F.M.M. The bioinorganic chemistry of the ancient ocean: the co-evolution of cyanobacterial metal requirements and biogeochemical cycles at the Archean–Proterozoic boundary? *Inorganica Chimica Acta* **356**, 308-318 (2003).
281. Irving, H. & Williams, R.J.P. 637. The stability of transition-metal complexes. *Journal of the Chemical Society (Resumed)*, 3192-3210 (1953).
282. Yost, F.J., Jr. & Fridovich, I. An iron-containing superoxide dismutase from Escherichia coli. *J Biol Chem* **248**, 4905-4908 (1973).
283. Hatchikian, E.C. & Henry, Y.A. An iron-containing superoxide dismutase from the strict anaerobe Desulfovibrio desulfuricans (Norway 4). *Biochimie* **59**, 153-161 (1977).
284. Pesce, A. *et al.* Unique structural features of the monomeric Cu,Zn superoxide dismutase from Escherichia coli, revealed by X-ray crystallography. *J Mol Biol* **274**, 408-420 (1997).
285. Banci, L. *et al.* Atomic-resolution monitoring of protein maturation in live human cells by NMR. *Nature chemical biology* **9**, 297 (2013).
286. Wilkinson, S.R. *et al.* Functional characterisation of the iron superoxide dismutase gene repertoire in Trypanosoma brucei. *Free Radic Biol Med* **40**, 198-209 (2006).
287. Fink, R.C. & Scandalios, J.G. Molecular evolution and structure--function relationships of the superoxide dismutase gene families in angiosperms and their relationship to other eukaryotic and prokaryotic superoxide dismutases. *Arch Biochem Biophys* **399**, 19-36 (2002).
288. Miller, A.-F. Superoxide dismutases: Ancient enzymes and new insights. *FEBS Letters* **586**, 585-595 (2012).
289. Wolfe-Simon, F., Grzebyk, D., Schofield, O. & Falkowski, P.G. THE ROLE AND EVOLUTION OF SUPEROXIDE DISMUTASES IN ALGAE1. *Journal of Phycology* **41**, 453-465 (2005).
290. Dupont, C.L., Neupane, K., Shearer, J. & Palenik, B. Diversity, function and evolution of genes coding for putative Ni-containing superoxide dismutases. *Environ Microbiol* **10**, 1831-1843 (2008).
291. Wuerges, J. *et al.* Crystal structure of nickel-containing superoxide dismutase reveals another type of active site. *Proc Natl Acad Sci U S A* **101**, 8569-8574 (2004).
292. Culotta, V.C., Yang, M. & O'Halloran, T.V. Activation of superoxide dismutases: Putting the metal to the pedal. *Biochimica et Biophysica Acta (BBA) - Molecular Cell Research* **1763**, 747-758 (2006).
293. Rae, T.D., Torres, A.S., Pufahl, R.A. & O'Halloran, T.V. Mechanism of Cu,Zn-superoxide dismutase activation by the human metallochaperone hCCS. *J Biol Chem* **276**, 5166-5176 (2001).

294. Furukawa, Y., Torres, A.S. & O'Halloran, T.V. Oxygen-induced maturation of SOD1: a key role for disulfide formation by the copper chaperone CCS. *Embo j* **23**, 2872-2881 (2004).
295. Chang, L.-Y., Slot, J.W., Geuze, H.J. & Crapo, J.D. Molecular immunocytochemistry of the CuZn superoxide dismutase in rat hepatocytes. *The Journal of cell biology* **107**, 2169-2179 (1988).
296. Wang, M., Herrmann, C.J., Simonovic, M., Szklarczyk, D. & von Mering, C. Version 4.0 of PaxDb: Protein abundance data, integrated across model organisms, tissues, and cell-lines. *Proteomics* **15**, 3163-3168 (2015).
297. Archibald, F.S. & Fridovich, I. The scavenging of superoxide radical by manganous complexes: In vitro. **214**, 452-463 (1982).
298. Tainer, J.A., Getzoff, E.D., Richardson, J.S. & Richardson, D.C. Structure and mechanism of copper, zinc superoxide dismutase. **306**, 284-287 (1983).
299. Ighodaro, O.M. & Akinloye, O.A. First line defence antioxidants-superoxide dismutase (SOD), catalase (CAT) and glutathione peroxidase (GPX): Their fundamental role in the entire antioxidant defence grid. *Alexandria Journal of Medicine* **54**, 287-293 (2018).
300. Smirnov, V.V. & Roth, J.P. Mechanisms of electron transfer in catalysis by copper zinc superoxide dismutase. *J Am Chem Soc* **128**, 16424-16425 (2006).
301. Borgstahl, G.E.O. & Oberley-Deegan, R.E. Superoxide Dismutases (SODs) and SOD Mimetics. *Antioxidants (Basel, Switzerland)* **7**, 156 (2018).
302. Shin, D.S. *et al.* Superoxide dismutase from the eukaryotic thermophile Alvinella pompejana: structures, stability, mechanism, and insights into amyotrophic lateral sclerosis. *Journal of molecular biology* **385**, 1534-1555 (2009).
303. Perry, J.J.P., Shin, D.S., Getzoff, E.D. & Tainer, J.A. The structural biochemistry of the superoxide dismutases. *Biochim Biophys Acta* **1804**, 245-262 (2010).
304. Hart, P.J. *et al.* A structure-based mechanism for copper-zinc superoxide dismutase. *Biochemistry* **38**, 2167-2178 (1999).
305. Getzoff, E.D. *et al.* Faster superoxide dismutase mutants designed by enhancing electrostatic guidance. *Nature* **358**, 347-351 (1992).
306. Getzoff, E.D. *et al.* Electrostatic recognition between superoxide and copper, zinc superoxide dismutase. **306**, 287-290 (1983).
307. Tainer, J.A., Getzoff, E.D., Beem, K.M., Richardson, J.S. & Richardson, D.C. Determination and analysis of the 2 Å structure of copper, zinc superoxide dismutase. *Journal of Molecular Biology* **160**, 181-217 (1982).
308. Salin, M.L. & Wilson, W.W. Porcine superoxide dismutase : Isolation and characterization of a relatively basic cuprozinc enzyme. *Molecular and Cellular Biochemistry : An International Journal for Chemical Biology in Health and Disease* **36**, 157-161 (1981).
309. Malinowski, D.P. & Fridovich, I. Chemical modification of arginine at the active site of the bovine erythrocyte superoxide dismutase. *Biochemistry* **18**, 5909-5917 (1979).
310. Tokuda, E. *et al.* A copper-deficient form of mutant Cu/Zn-superoxide dismutase as an early pathological species in amyotrophic lateral sclerosis. *Biochimica et Biophysica Acta (BBA) - Molecular Basis of Disease* **1864**, 2119-2130 (2018).

311. Fielden, E.M. *et al.* The mechanism of action of superoxide dismutase from pulse radiolysis and electron paramagnetic resonance. Evidence that only half the active sites function in catalysis. *Biochemical Journal* **139**, 49-60 (1974).
312. Parge, H.E., Hallewell, R.A. & Tainer, J.A. Atomic structures of wild-type and thermostable mutant recombinant human Cu,Zn superoxide dismutase. *Proceedings of the National Academy of Sciences of the United States of America* **89**, 6109-6113 (1992).
313. Wang, J. *et al.* Copper-binding-site-null SOD1 causes ALS in transgenic mice: aggregates of non-native SOD1 delineate a common feature. *Human Molecular Genetics* **12**, 2753-2764 (2003).
314. Fisher, C.L., Cabelli, D.E., Tainer, J.A., Hallewell, R.A. & Getzoff, E.D. The role of arginine 143 in the electrostatics and mechanism of Cu, Zn superoxide dismutase: Computational and experimental evaluation by mutational analysis. **19**, 24-34 (1994).
315. Crapo, J.D., Oury, T., Rabouille, C., Slot, J.W. & Chang, L.Y. Copper,zinc superoxide dismutase is primarily a cytosolic protein in human cells. *Proc Natl Acad Sci U S A* **89**, 10405-10409 (1992).
316. Okado-Matsumoto, A. & Fridovich, I. Subcellular distribution of superoxide dismutases (SOD) in rat liver: Cu,Zn-SOD in mitochondria. *J Biol Chem* **276**, 38388-38393 (2001).
317. Slot, J.W., Geuze, H.J., Freeman, B.A. & Crapo, J.D. Intracellular localization of the copper-zinc and manganese superoxide dismutases in rat liver parenchymal cells. *Lab Invest* **55**, 363-371 (1986).
318. Murphy, Michael P. How mitochondria produce reactive oxygen species. *Biochemical Journal* **417**, 1-13 (2008).
319. Holmstrôm, K.M. & Finkel, T. Cellular mechanisms and physiological consequences of redox-dependent signalling. *Nature Reviews Molecular Cell Biology* **15**, 411-421 (2014).
320. Nguyen, A.D. *et al.* Fibulin-5 is a novel binding protein for extracellular superoxide dismutase. *Circ Res* **95**, 1067-1074 (2004).
321. Petersen, S.V. *et al.* Extracellular superoxide dismutase (EC-SOD) binds to type i collagen and protects against oxidative fragmentation. *J Biol Chem* **279**, 13705-13710 (2004).
322. Fukai, T., Folz, R.J., Landmesser, U. & Harrison, D.G. Extracellular superoxide dismutase and cardiovascular disease. *Cardiovasc Res* **55**, 239-249 (2002).
323. Marklund, S.L. Extracellular superoxide dismutase in human tissues and human cell lines. *The Journal of Clinical Investigation* **74**, 1398-1403 (1984).
324. Folz, R.J. & Crapo, J.D. Extracellular Superoxide Dismutase (SOD3): Tissue-Specific Expression, Genomic Characterization, and Computer-Assisted Sequence Analysis of the Human EC SOD Gene. *Genomics* **22**, 162-171 (1994).
325. Strålin, P., Karlsson, K., Johansson, B.O. & Marklund, S.L. The Interstitium of the Human Arterial Wall Contains Very Large Amounts of Extracellular Superoxide Dismutase. *Arteriosclerosis, Thrombosis, and Vascular Biology* **15**, 2032-2036 (1995).
326. Fattman, C.L., Schaefer, L.M. & Oury, T.D. Extracellular superoxide dismutase in biology and medicine. *Free Radical Biology and Medicine* **35**, 236-256 (2003).
327. Marletta, M.A., Yoon, P.S., Iyengar, R., Leaf, C.D. & Wishnok, J.S. Macrophage oxidation of L-arginine to nitrite and nitrate: nitric oxide is an intermediate. *Biochemistry* **27**, 8706-8711 (1988).

328. Mayer, B., Schmidt, K., Humbert, P. & Bohme, E. Biosynthesis of endothelium-derived relaxing factor: a cytosolic enzyme in porcine aortic endothelial cells Ca2+-dependently converts L-arginine into an activator of soluble guanylyl cyclase. *Biochem Biophys Res Commun* **164**, 678-685 (1989).
329. Knowles, R., Palacios-Callender, M., Palmer, R. & Moncada, S. Knowles RG, Palacios M, Palmer RMJ & Moncada S.Formation of nitric oxide from L-arginine in the central nervous system: a transduction mechanism for stimulation of the soluble guanylate cyclase. Proc Natl Acad Sci USA 86: 5159−5162. *Proceedings of the National Academy of Sciences of the United States of America* **86**, 5159-5162 (1989).
330. Bredt, D.S. & Snyder, S.H. Isolation of nitric oxide synthetase, a calmodulin-requiring enzyme. *Proc Natl Acad Sci U S A* **87**, 682-685 (1990).
331. Hevel, J.M., White, K.A. & Marletta, M.A. Purification of the inducible murine macrophage nitric oxide synthase. Identification as a flavoprotein. *J Biol Chem* **266**, 22789-22791 (1991).
332. Pollock, J.S. *et al.* Purification and characterization of particulate endothelium-derived relaxing factor synthase from cultured and native bovine aortic endothelial cells. *Proceedings of the National Academy of Sciences of the United States of America* **88**, 10480-10484 (1991).
333. Ghaffari, A. *et al.* A direct nitric oxide gas delivery system for bacterial and mammalian cell cultures. *Nitric Oxide* **12**, 129-140 (2005).
334. Förstermann, U. & Sessa, W.C. Nitric oxide synthases: regulation and function. *European Heart Journal* **33**, 829-837 (2011).
335. Marletta, M.A., Hurshman, A.R. & Rusche, K.M. Catalysis by nitric oxide synthase. *Current Opinion in Chemical Biology* **2**, 656-663 (1998).
336. Schmidt, H.H., Pollock, J.S., Nakane, M., Förstermann, U. & Murad, F. Ca2+/calmodulin-regulated nitric oxide synthases. *Cell Calcium* **13**, 427-434 (1992).
337. Wang, J., Rousseau, D.L., Abu-Soud, H.M. & Stuehr, D.J. Heme coordination of NO in NO synthase. *Proc Natl Acad Sci U S A* **91**, 10512-10516 (1994).
338. Iyengar, R., Stuehr, D.J. & Marletta, M.A. Macrophage synthesis of nitrite, nitrate, and N-nitrosamines: precursors and role of the respiratory burst. **84**, 6369-6373 (1987).
339. Feng, C. Mechanism of Nitric Oxide Synthase Regulation: Electron Transfer and Interdomain Interactions. *Coord Chem Rev* **256**, 393-411 (2012).
340. Alderton, W.K., Cooper, C.E. & Knowles, R.G. Nitric oxide synthases: structure, function and inhibition. *Biochemical journal* **357**, 593-615 (2001).
341. Zhu, Y. & Silverman, R.B. Revisiting heme mechanisms. A perspective on the mechanisms of nitric oxide synthase (NOS), Heme oxygenase (HO), and cytochrome P450s (CYP450s). *Biochemistry* **47**, 2231-2243 (2008).
342. Papale, D. *et al.* Oxygen activation in neuronal NO synthase: resolving the consecutive mono-oxygenation steps. *Biochem J* **443**, 505-514 (2012).
343. Torres Pazmino, D.E., Winkler, M., Glieder, A. & Fraaije, M.W. Monooxygenases as biocatalysts: Classification, mechanistic aspects and biotechnological applications. *J Biotechnol* **146**, 9-24 (2010).

344. Buga, G.M. *et al.* Arginase activity in endothelial cells: inhibition by NG-hydroxy-L-arginine during high-output NO production. *American Journal of Physiology-Heart and Circulatory Physiology* **271**, H1988-H1998 (1996).
345. Daff, S. NO synthase: structures and mechanisms. *Nitric Oxide* **23**, 1-11 (2010).
346. Garcin, E.D. *et al.* Structural basis for isozyme-specific regulation of electron transfer in nitric-oxide synthase. *Journal of biological chemistry* **279**, 37918-37927 (2004).
347. Wang, M. *et al.* Three-dimensional structure of NADPH–cytochrome P450 reductase: prototype for FMN-and FAD-containing enzymes. *Proceedings of the National Academy of Sciences* **94**, 8411-8416 (1997).
348. Bredt, D.S. *et al.* Cloned and expressed nitric oxide synthase structurally resembles cytochrome P-450 reductase. **351**, 714-718 (1991).
349. Roman, L.J., Martásek, P. & Masters, B.S.S. Intrinsic and extrinsic modulation of nitric oxide synthase activity. *Chemical reviews* **102**, 1179-1190 (2002).
350. Adak, S., Sharma, M., Meade, A.L. & Stuehr, D.J. A conserved flavin-shielding residue regulates NO synthase electron transfer and nicotinamide coenzyme specificity. *Proceedings of the National Academy of Sciences* **99**, 13516-13521 (2002).
351. Daff, S., Sagami, I. & Shimizu, T. The 42-amino acid insert in the FMN domain of neuronal nitric-oxide synthase exerts control over Ca2+/calmodulin-dependent electron transfer. *Journal of Biological Chemistry* **274**, 30589-30595 (1999).
352. Abu-Soud, H.M. & Stuehr, D.J. Nitric oxide synthases reveal a role for calmodulin in controlling electron transfer. *Proceedings of the National Academy of Sciences* **90**, 10769-10772 (1993).
353. Abu-Soud, H.M., Yoho, L.L. & Stuehr, D.J. Calmodulin controls neuronal nitric-oxide synthase by a dual mechanism. Activation of intra-and interdomain electron transfer. *Journal of Biological Chemistry* **269**, 32047-32050 (1994).
354. Feng, C. *et al.* Intraprotein electron transfer in a two-domain construct of neuronal nitric oxide synthase: the output state in nitric oxide formation. *Biochemistry* **45**, 6354-6362 (2006).
355. Griffith, O.W. & Stuehr, D.J. Nitric Oxide Synthases: Properties and Catalytic Mechanism. *Annual Review of Physiology* **57**, 707-734 (1995).
356. Nathan, C. & Xie, Q. Regulation of biosynthesis of nitric oxide. *Journal of Biological Chemistry* **269**, 13725-13728 (1994).
357. Förstermann, U. *et al.* Nitric oxide synthase isozymes. Characterization, purification, molecular cloning, and functions. *Hypertension* **23**, 1121-1131 (1994).
358. Pollock, J.S. *et al.* Characterization and localization of endothelial nitric oxide synthase using specific monoclonal antibodies. *Am J Physiol* **265**, C1379-1387 (1993).
359. Tracey, W.R., Pollock, J.S., Murad, F., Nakane, M. & Förstermann, U. Identification of an endothelial-like type III NO synthase in LLC-PK1 kidney epithelial cells. *Am J Physiol* **266**, C22-28 (1994).
360. Caviedes, A. *et al.* Endothelial Nitric Oxide Synthase Is Present in Dendritic Spines of Neurons in Primary Cultures. *Front Cell Neurosci* **11**, 180 (2017).
361. Laranjinha, J.o., Santos, R.M., Lourenço, C.t.F., Ledo, A. & Barbosa, R.M. Nitric oxide signaling in the brain: translation of dynamics into respiration control and neurovascular

coupling NO dynamics respiration and neurovascular coupling. *Annals of the New York Academy of Sciences* **1259**, 10-18 (2012).
362. Huang, P.L. Lessons learned from nitric oxide synthase knockout animals. *Seminars in Perinatology* **24**, 87-90 (2000).
363. Förstermann, U., Boissel, J.-p. & Kleinert, H. Expressional control of the 'constitutive'isoforms of nitric oxide synthase (NOS I and NOS III). *The FASEB Journal* **12**, 773-790 (1998).
364. Huang, Z. *et al.* Stimulation of unprimed macrophages with immune complexes triggers a low output of nitric oxide by calcium-dependent neuronal nitric-oxide synthase. *J Biol Chem* **287**, 4492-4502 (2012).
365. Förstermann, U. & Münzel, T. Endothelial Nitric Oxide Synthase in Vascular Disease. *Circulation* **113**, 1708-1714 (2006).
366. Lee, S.J. & Stull, J.T. Calmodulin-dependent regulation of inducible and neuronal nitric-oxide synthase. *J Biol Chem* **273**, 27430-27437 (1998).
367. Pautz, A. *et al.* Regulation of the expression of inducible nitric oxide synthase. *Nitric Oxide* **23**, 75-93 (2010).
368. Piazza, M., Guillemette, J.G. & Dieckmann, T. Dynamics of Nitric Oxide Synthase-Calmodulin Interactions at Physiological Calcium Concentrations. *Biochemistry* **54**, 1989-2000 (2015).
369. Maune, J., Klee, C. & Beckingham, K. Ca2+ binding and conformational change in two series of point mutations to the individual Ca (2+)-binding sites of calmodulin. *Journal of Biological Chemistry* **267**, 5286-5295 (1992).
370. Ross, A. *et al.* NDRL-NIST Solution Kinetics Database: Ver. 2.0. *National Institute of Standards and Technology, Gaithersburg, MD* (1994).
371. Radi, R. Peroxynitrite, a stealthy biological oxidant. *J Biol Chem* **288**, 26464-26472 (2013).
372. Sohal, R.S., Svensson, I., Sohal, B.H. & Brunk, U.T. Superoxide anion radical production in different animal species. *Mechanisms of Ageing and Development* **49**, 129-135 (1989).
373. Bredt, D. & Snyder, S.H. Nitric oxide: a physiologic messenger molecule. *Annual review of biochemistry* **63**, 175-195 (1994).
374. Ignarro, L.J. Biosynthesis and metabolism of endothelium-derived nitric oxide. *Annual review of pharmacology and toxicology* **30**, 535-560 (1990).
375. Huie, R.E. & Padmaja, S. The Reaction of NO With Superoxide. *fra Free Radical Research* **18**, 195-199 (1993).
376. Beckman, J.S. & Koppenol, W.H. Nitric oxide, superoxide, and peroxynitrite: the good, the bad, and ugly. *The American Journal of Physiology* **271**, 1424-1437 (1996).
377. Szabó, C., Ischiropoulos, H. & Radi, R. Peroxynitrite: biochemistry, pathophysiology and development of therapeutics. *Nature Reviews Drug Discovery* **6**, 662-680 (2007).
378. Koppenol, W.H. & Kissner, R. Can ONOOH Undergo Homolysis? *Chemical Research in Toxicology* **11**, 87-90 (1998).
379. Radi, R. Nitric oxide, oxidants, and protein tyrosine nitration. *Proc Natl Acad Sci U S A* **101**, 4003-4008 (2004).
380. Sawa, T., Akaike, T. & Maeda, H. Tyrosine Nitration by Peroxynitrite Formed from Nitric Oxide and Superoxide Generated by Xanthine Oxidase. **275**, 32467-32474 (2000).

381. Beckman, J.S. Ischaemic injury mediator. *Nature* **345**, 27-28 (1990).
382. Beckman, J.S., Beckman, T.W., Chen, J., Marshall, P.A. & Freeman, B.A. Apparent hydroxyl radical production by peroxynitrite: implications for endothelial injury from nitric oxide and superoxide. *Proceedings of the National Academy of Sciences* **87**, 1620-1624 (1990).
383. Tsai, J.-H.M. *et al.* Role of conformation of peroxynitrite anion (ONOO-) with its stability and toxicity. *Journal of the American Chemical Society* **116**, 4115-4116 (1994).
384. Tsai, H.-H., Hamilton, T.P., Tsai, J.-H.M. & Beckman, J.S. Ab initio studies of peroxynitrite anion-water complexes. *Structural Chemistry* **6**, 323-332 (1995).
385. Mallozzi, C., Stasi, A.M.D. & Minetti, M. Peroxynitrite modulates tyrosine-dependent signal transduction pathway of human erythrocyte band 3. *The FASEB Journal* **11**, 1281-1290 (1997).
386. Klotz, L.O., Schroeder, P. & Sies, H. Peroxynitrite signaling: receptor tyrosine kinases and activation of stress-responsive pathways. *Free Radic Biol Med* **33**, 737-743 (2002).
387. Mallozzi, C., Di Stasi, M.A. & Minetti, M. Peroxynitrite-dependent activation of src tyrosine kinases lyn and hck in erythrocytes is under mechanistically different pathways of redox control. *Free Radic Biol Med* **30**, 1108-1117 (2001).
388. Di Stasi, A.M., Mallozzi, C., Macchia, G., Petrucci, T.C. & Minetti, M. Peroxynitrite induces tryosine nitration and modulates tyrosine phosphorylation of synaptic proteins. *J Neurochem* **73**, 727-735 (1999).
389. Filep, J.G., Beauchamp, M., Baron, C. & Paquette, Y. Peroxynitrite mediates IL-8 gene expression and production in lipopolysaccharide-stimulated human whole blood. *J Immunol* **161**, 5656-5662 (1998).
390. Park, S.W., Huq, M.D., Hu, X. & Wei, L.N. Tyrosine nitration on p65: a novel mechanism to rapidly inactivate nuclear factor-kappaB. *Mol Cell Proteomics* **4**, 300-309 (2005).
391. Gilbert, R.S. & Herschman, H.R. Transforming growth factor beta differentially modulates the inducible nitric oxide synthase gene in distinct cell types. *Biochem Biophys Res Commun* **195**, 380-384 (1993).
392. Carreras, M.C., Pargament, G.A., Catz, S.D., Poderoso, J.J. & Boveris, A. Kinetics of nitric oxide and hydrogen peroxide production and formation of peroxynitrite during the respiratory burst of human neutrophils. *FEBS Lett* **341**, 65-68 (1994).
393. Allen, R.G. *et al.* Stressor-induced increase in microbicidal activity of splenic macrophages is dependent upon peroxynitrite production. *Infection and immunity* **80**, 3429-3437 (2012).
394. Hall, E.D., Wang, J.A. & Miller, D.M. Relationship of nitric oxide synthase induction to peroxynitrite-mediated oxidative damage during the first week after experimental traumatic brain injury. *Exp Neurol* **238**, 176-182 (2012).
395. Liaudet, L., Vassalli, G. & Pacher, P. Role of peroxynitrite in the redox regulation of cell signal transduction pathways. *Front Biosci (Landmark Ed)* **14**, 4809-4814 (2009).
396. Pacher, P. & Szabo, C. Role of the peroxynitrite-poly(ADP-ribose) polymerase pathway in human disease. *Am J Pathol* **173**, 2-13 (2008).
397. Szabó, C. & Dawson, V.L. Role of poly (ADP-ribose) synthetase in inflammation and ischaemia–reperfusion. *Trends in pharmacological sciences* **19**, 287-298 (1998).

398. Szabó, C. & Ohshima, H. DNA Damage Induced by Peroxynitrite: Subsequent Biological Effects. *Nitric Oxide* **1**, 373-385 (1997).
399. Yamaza, T. *et al.* Oxidative stress-induced DNA damage in the synovial cells of the temporomandibular joint in the rat. *J Dent Res* **83**, 619-624 (2004).
400. Burney, S., Caulfield, J.L., Niles, J.C., Wishnok, J.S. & Tannenbaum, S.R. The chemistry of DNA damage from nitric oxide and peroxynitrite. *Mutation Research/Fundamental and Molecular Mechanisms of Mutagenesis* **424**, 37-49 (1999).
401. Yu, H., Venkatarangan, L., Wishnok, J.S. & Tannenbaum, S.R. Quantitation of four guanine oxidation products from reaction of DNA with varying doses of peroxynitrite. *Chemical research in toxicology* **18**, 1849-1857 (2005).
402. Niles, J.C., Wishnok, J.S. & Tannenbaum, S.R. Peroxynitrite-induced oxidation and nitration products of guanine and 8-oxoguanine: structures and mechanisms of product formation. *Nitric Oxide* **14**, 109-121 (2006).
403. Szabo, C., Zingarelli, B., O'Connor, M. & SALzMAN, A.L. DNA strand breakage, activation of poly (ADP-ribose) synthetase, and cellular energy depletion are involved in the cytotoxicity of macrophages and smooth muscle cells exposed to peroxynitrite. *Proceedings of the National Academy of Sciences* **93**, 1753-1758 (1996).
404. Szabó, C. *et al.* Protection against peroxynitrite-induced fibroblast injury and arthritis development by inhibition of poly (ADP-ribose) synthase. *Proceedings of the National Academy of Sciences* **95**, 3867-3872 (1998).
405. Radi, R., Beckman, J.S., Bush, K.M. & Freeman, B.A. Peroxynitrite-induced membrane lipid peroxidation: the cytotoxic potential of superoxide and nitric oxide. *Arch Biochem Biophys* **288**, 481-487 (1991).
406. Hogg, N. & Kalyanaraman, B. Nitric oxide and lipid peroxidation. *Biochim Biophys Acta* **1411**, 378-384 (1999).
407. Richter, C. Biophysical consequences of lipid peroxidation in membranes. *Chem Phys Lipids* **44**, 175-189 (1987).
408. van der Veen, R.C. & Roberts, L.J. Contrasting roles for nitric oxide and peroxynitrite in the peroxidation of myelin lipids. *J Neuroimmunol* **95**, 1-7 (1999).
409. Leeuwenburgh, C. *et al.* Reactive nitrogen intermediates promote low density lipoprotein oxidation in human atherosclerotic intima. *Journal of Biological Chemistry* **272**, 1433-1436 (1997).
410. Graham, A. *et al.* Peroxynitrite modification of low-density lipoprotein leads to recognition by the macrophage scavenger receptor. *FEBS Lett* **330**, 181-185 (1993).
411. Hogg, N., Darley-Usmar, V.M., Graham, A. & Moncada, S. Peroxynitrite and atherosclerosis. *Biochem Soc Trans* **21**, 358-362 (1993).
412. Denicola, A. & Radi, R. Peroxynitrite and drug-dependent toxicity. *Toxicology* **208**, 273-288 (2005).
413. Alvarez, B. & Radi, R. Peroxynitrite reactivity with amino acids and proteins. *Amino Acids* **25**, 295-311 (2003).
414. Boccini, F. & Herold, S. Mechanistic studies of the oxidation of oxyhemoglobin by peroxynitrite. *Biochemistry* **43**, 16393-16404 (2004).

415. Herold, S., Exner, M. & Boccini, F. The mechanism of the peroxynitrite-mediated oxidation of myoglobin in the absence and presence of carbon dioxide. *Chemical research in toxicology* **16**, 390-402 (2003).
416. Thomson, L., Trujillo, M., Telleri, R. & Radi, R. Kinetics of cytochrome C2+ oxidation by peroxynitrite: implications for superoxide measurements in nitric oxide-producing biological-systems. *Archives of Biochemistry and Biophysics* **319**, 491-497 (1995).
417. Hühmer, A.F., Nishida, C.R., Ortiz de Montellano, P.R. & Schöneich, C. Inactivation of the inducible nitric oxide synthase by peroxynitrite. *Chem Res Toxicol* **10**, 618-626 (1997).
418. Zou, M.H., Cohen, R. & Ullrich, V. Peroxynitrite and vascular endothelial dysfunction in diabetes mellitus. *Endothelium* **11**, 89-97 (2004).
419. Murray, C.I. & Van Eyk, J.E. Chasing cysteine oxidative modifications: proteomic tools for characterizing cysteine redox status. *Circ Cardiovasc Genet* **5**, 591-591 (2012).
420. Radi, R., Beckman, J.S., Bush, K.M. & Freeman, B.A. Peroxynitrite oxidation of sulfhydryls. The cytotoxic potential of superoxide and nitric oxide. *The Journal of biological chemistry* **266**, 4244-4250 (1991).
421. Carballal, S. *et al.* Sulfenic acid formation in human serum albumin by hydrogen peroxide and peroxynitrite. *Biochemistry* **42**, 9906-9914 (2003).
422. Quijano, C., Alvarez, B., Gatti, R.M., Augusto, O. & Radi, R. Pathways of peroxynitrite oxidation of thiol groups. *The Biochemical journal* **322 (Pt 1)**, 167-173 (1997).
423. van der Vliet, A., Hoen, P.A., Wong, P.S., Bast, A. & Cross, C.E. Formation of S-nitrosothiols via direct nucleophilic nitrosation of thiols by peroxynitrite with elimination of hydrogen peroxide. *J Biol Chem* **273**, 30255-30262 (1998).
424. Madej, E., Folkes, L.K., Wardman, P., Czapski, G. & Goldstein, S. Thiyl radicals react with nitric oxide to form S-nitrosothiols with rate constants near the diffusion-controlled limit. *Free Radical Biology and Medicine* **44**, 2013-2018 (2008).
425. Brown, G.C. & Borutaite, V. Inhibition of mitochondrial respiratory complex I by nitric oxide, peroxynitrite and S-nitrosothiols. *Biochimica et Biophysica Acta (BBA) - Bioenergetics* **1658**, 44-49 (2004).
426. Graves, J.E., Lewis, S.J. & Kooy, N.W. Peroxynitrite-mediated vasorelaxation: evidence against the formation of circulatingS-nitrosothiols. *American Journal of Physiology-Heart and Circulatory Physiology* **274**, H1001-H1008 (1998).
427. Souza, J.M. & Radi, R. Glyceraldehyde-3-phosphate dehydrogenase inactivation by peroxynitrite. *Arch Biochem Biophys* **360**, 187-194 (1998).
428. Konorev, E.A., Hogg, N. & Kalyanaraman, B. Rapid and irreversible inhibition of creatine kinase by peroxynitrite. *FEBS Lett* **427**, 171-174 (1998).
429. Radi, R., Rodriguez, M., Castro, L. & Telleri, R. Inhibition of mitochondrial electron transport by peroxynitrite. *Arch Biochem Biophys* **308**, 89-95 (1994).
430. Radi, R., Cassina, A., Hodara, R., Quijano, C. & Castro, L. Peroxynitrite reactions and formation in mitochondria. *Free Radic Biol Med* **33**, 1451-1464 (2002).
431. Takakura, K., Beckman, J.S., MacMillan-Crow, L.A. & Crow, J.P. Rapid and irreversible inactivation of protein tyrosine phosphatases PTP1B, CD45, and LAR by peroxynitrite. *Arch Biochem Biophys* **369**, 197-207 (1999).

432. Battin, E.E. & Brumaghim, J.L. Antioxidant activity of sulfur and selenium: a review of reactive oxygen species scavenging, glutathione peroxidase, and metal-binding antioxidant mechanisms. *Cell biochemistry and biophysics* **55**, 1-23 (2009).
433. Sies, H., Sharov, V.S., Klotz, L.O. & Briviba, K. Glutathione peroxidase protects against peroxynitrite-mediated oxidations. A new function for selenoproteins as peroxynitrite reductase. *J Biol Chem* **272**, 27812-27817 (1997).
434. Koppal, T., Drake, J. & Butterfield, D.A. In vivo modulation of rodent glutathione and its role in peroxynitrite-induced neocortical synaptosomal membrane protein damage. *Biochimica et Biophysica Acta (BBA) - Molecular Basis of Disease* **1453**, 407-411 (1999).
435. Marshall, K.A., Reist, M., Jenner, P. & Halliwell, B. The neuronal toxicity of sulfite plus peroxynitrite is enhanced by glutathione depletion: implications for Parkinson's disease. *Free Radic Biol Med* **27**, 515-520 (1999).
436. Vargas, M.R., Pehar, M., Cassina, P., Beckman, J.S. & Barbeito, L. Increased glutathione biosynthesis by Nrf2 activation in astrocytes prevents p75NTR-dependent motor neuron apoptosis. *J Neurochem* **97**, 687-696 (2006).
437. Pacher, P., Obrosova, I.G., Mabley, J.G. & Szabó, C. Role of nitrosative stress and peroxynitrite in the pathogenesis of diabetic complications. Emerging new therapeutical strategies. *Curr Med Chem* **12**, 267-275 (2005).
438. Wang, W., Sawicki, G. & Schulz, R. Peroxynitrite-induced myocardial injury is mediated through matrix metalloproteinase-2. *Cardiovasc Res* **53**, 165-174 (2002).
439. Gürsoy-Ozdemir, Y., Can, A. & Dalkara, T. Reperfusion-induced oxidative/nitrative injury to neurovascular unit after focal cerebral ischemia. *Stroke* **35**, 1449-1453 (2004).
440. Okamoto, T. *et al.* Activation of matrix metalloproteinases by peroxynitrite-induced protein S-glutathiolation via disulfide S-oxide formation. *J Biol Chem* **276**, 29596-29602 (2001).
441. Mallozzi, C., Di Stasi, A.M. & Minetti, M. Nitrotyrosine mimics phosphotyrosine binding to the SH2 domain of the src family tyrosine kinase lyn. *FEBS Lett* **503**, 189-195 (2001).
442. Ahsan, H. 3-Nitrotyrosine: A biomarker of nitrogen free radical species modified proteins in systemic autoimmunogenic conditions. *Human Immunology* **74**, 1392-1399 (2013).
443. Gow, A.J., Farkouh, C.R., Munson, D.A., Posencheg, M.A. & Ischiropoulos, H. Biological significance of nitric oxide-mediated protein modifications. *Am J Physiol Lung Cell Mol Physiol* **287**, L262-268 (2004).
444. Schopfer, F.J., Baker, P.R. & Freeman, B.A. NO-dependent protein nitration: a cell signaling event or an oxidative inflammatory response? *Trends Biochem Sci* **28**, 646-654 (2003).
445. Ischiropoulos, H. Biological selectivity and functional aspects of protein tyrosine nitration. *Biochemical and Biophysical Research Communications* **305**, 776-783 (2003).
446. Beckman, J.S. *et al.* Kinetics of superoxide dismutase-and iron-catalyzed nitration of phenolics by peroxynitrite. *Archives of Biochemistry and Biophysics* **298**, 438-445 (1992).
447. Ischiropoulos, H. *et al.* Peroxynitrite-mediated tyrosine nitration catalyzed by superoxide dismutase. *Archives of biochemistry and biophysics* **298**, 431-437 (1992).

448. Beckmann, J.S. *et al.* Extensive nitration of protein tyrosines in human atherosclerosis detected by immunohistochemistry. *Biological chemistry Hoppe-Seyler* **375**, 81-88 (1994).
449. Ohshima, H., Friesen, M., Brouet, I. & Bartsch, H. Nitrotyrosine as a new marker for endogenous nitrosation and nitration of proteins. *Food and chemical toxicology* **28**, 647-652 (1990).
450. Brennan, M.-L. *et al.* A tale of two controversies defining both the role of peroxidases in nitrotyrosine formation in vivo using eosinophil peroxidase and myeloperoxidase-deficient mice, and the nature of peroxidase-generated reactive nitrogen species. *Journal of Biological Chemistry* **277**, 17415-17427 (2002).
451. Aslan, M. *et al.* Nitric Oxide-dependent Generation of Reactive Species in Sickle Cell Disease ACTIN TYROSINE NITRATION INDUCES DEFECTIVE CYTOSKELETAL POLYMERIZATION. *Journal of Biological Chemistry* **278**, 4194-4204 (2003).
452. Thomas, D.D., Espey, M.G., Vitek, M.P., Miranda, K.M. & Wink, D.A. Protein nitration is mediated by heme and free metals through Fenton-type chemistry: An alternative to the NO/O reaction. *Proceedings of the National Academy of Sciences* **99**, 12691-12696 (2002).
453. Pfeiffer, S., Schmidt, K. & Mayer, B. Dityrosine formation outcompetes tyrosine nitration at low steady-state concentrations of peroxynitrite implications for tyrosine modification by nitric oxide/superoxide in vivo. *Journal of Biological Chemistry* **275**, 6346-6352 (2000).
454. Kanski, J., Hong, S.J. & Schöneich, C. Proteomic analysis of protein nitration in aging skeletal muscle and identification of nitrotyrosine-containing sequences in vivo by nanoelectrospray ionization tandem mass spectrometry. *J Biol Chem* **280**, 24261-24266 (2005).
455. Kanski, J., Behring, A., Pelling, J. & Schöneich, C. Proteomic identification of 3-nitrotyrosine-containing rat cardiac proteins: effects of biological aging. *Am J Physiol Heart Circ Physiol* **288**, H371-381 (2005).
456. Aulak, K.S. *et al.* Proteomic method identifies proteins nitrated in vivo during inflammatory challenge. *Proc Natl Acad Sci U S A* **98**, 12056-12061 (2001).
457. Souza, J.M., Daikhin, E., Yudkoff, M., Raman, C.S. & Ischiropoulos, H. Factors Determining the Selectivity of Protein Tyrosine Nitration. *Archives of Biochemistry and Biophysics* **371**, 169-178 (1999).
458. Ischiropoulos, H. Biological Tyrosine Nitration: A Pathophysiological Function of Nitric Oxide and Reactive Oxygen Species. *Archives of Biochemistry and Biophysics* **356**, 1-11 (1998).
459. Beckmann, J.S. *et al.* Extensive nitration of protein tyrosines in human atherosclerosis detected by immunohistochemistry. *Biol Chem Hoppe Seyler* **375**, 81-88 (1994).
460. Greenacre, S.A. & Ischiropoulos, H. Tyrosine nitration: localisation, quantification, consequences for protein function and signal transduction. *Free Radic Res* **34**, 541-581 (2001).
461. MacMillan-Crow, L.A. & Thompson, J.A. Tyrosine modifications and inactivation of active site manganese superoxide dismutase mutant (Y34F) by peroxynitrite. *Arch Biochem Biophys* **366**, 82-88 (1999).

462. MacMillan-Crow, L.A., Cruthirds, D.L., Ahki, K.M., Sanders, P.W. & Thompson, J.A. Mitochondrial tyrosine nitration precedes chronic allograft nephropathy. *Free Radic Biol Med* **31**, 1603-1608 (2001).
463. MacMillan-Crow, L.A., Crow, J.P., Kerby, J.D., Beckman, J.S. & Thompson, J.A. Nitration and inactivation of manganese superoxide dismutase in chronic rejection of human renal allografts. *Proc Natl Acad Sci U S A* **93**, 11853-11858 (1996).
464. Aoyama, K. *et al.* Nitration of manganese superoxide dismutase in cerebrospinal fluids is a marker for peroxynitrite-mediated oxidative stress in neurodegenerative diseases. *Ann Neurol* **47**, 524-527 (2000).
465. Xu, S. *et al.* Detection of sequence-specific tyrosine nitration of manganese SOD and SERCA in cardiovascular disease and aging. *Am J Physiol Heart Circ Physiol* **290**, H2220-2227 (2006).
466. Van Der Loo, B. *et al.* Enhanced peroxynitrite formation is associated with vascular aging. *The Journal of experimental medicine* **192**, 1731-1744 (2000).
467. Boven, L.A. *et al.* Increased peroxynitrite activity in AIDS dementia complex: implications for the neuropathogenesis of HIV-1 infection. *J Immunol* **162**, 4319-4327 (1999).
468. Strong, M.J. Neurofilament metabolism in sporadic amyotrophic lateral sclerosis. *J Neurol Sci* **169**, 170-177 (1999).
469. Tohgi, H. *et al.* Remarkable increase in cerebrospinal fluid 3-nitrotyrosine in patients with sporadic amyotrophic lateral sclerosis. *Ann Neurol* **46**, 129-131 (1999).
470. Wong, N.K. & Strong, M.J. Nitric oxide synthase expression in cervical spinal cord in sporadic amyotrophic lateral sclerosis. *Eur J Cell Biol* **77**, 338-343 (1998).
471. Beal, M.F. *et al.* Increased 3-nitrotyrosine in both sporadic and familial amyotrophic lateral sclerosis. *Ann Neurol* **42**, 644-654 (1997).
472. Chou, S.M., Wang, H.S. & Taniguchi, A. Role of SOD-1 and nitric oxide/cyclic GMP cascade on neurofilament aggregation in ALS/MND. *J Neurol Sci* **139 Suppl**, 16-26 (1996).
473. Hensley, K. *et al.* Electrochemical analysis of protein nitrotyrosine and dityrosine in the Alzheimer brain indicates region-specific accumulation. *J Neurosci* **18**, 8126-8132 (1998).
474. Smith, M.A., Richey Harris, P.L., Sayre, L.M., Beckman, J.S. & Perry, G. Widespread peroxynitrite-mediated damage in Alzheimer's disease. *J Neurosci* **17**, 2653-2657 (1997).
475. Su, J.H., Deng, G. & Cotman, C.W. Neuronal DNA damage precedes tangle formation and is associated with up-regulation of nitrotyrosine in Alzheimer's disease brain. *Brain Res* **774**, 193-199 (1997).
476. Tohgi, H. *et al.* Alterations of 3-nitrotyrosine concentration in the cerebrospinal fluid during aging and in patients with Alzheimer's disease. *Neurosci Lett* **269**, 52-54 (1999).
477. Liu, J.S., Zhao, M.L., Brosnan, C.F. & Lee, S.C. Expression of inducible nitric oxide synthase and nitrotyrosine in multiple sclerosis lesions. *The American journal of pathology* **158**, 2057-2066 (2001).
478. Good, P.F., Hsu, A., Werner, P., Perl, D.P. & Olanow, C.W. Protein nitration in Parkinson's disease. *J Neuropathol Exp Neurol* **57**, 338-342 (1998).
479. Komori, T., Shibata, N., Kobayashi, M., Sasaki, S. & Iwata, M. Inducible nitric oxide synthase (iNOS)-like immunoreactivity in argyrophilic, tau-positive astrocytes in progressive supranuclear palsy. *Acta Neuropathologica* **95**, 338-344 (1998).

480. Forster, C., Clark, H.B., Ross, M.E. & Iadecola, C. Inducible nitric oxide synthase expression in human cerebral infarcts. *Acta Neuropathol* **97**, 215-220 (1999).
481. Klein, A.M., Kowall, N.W. & Ferrante, R.J. Neurotoxicity and oxidative damage of beta amyloid 1-42 versus beta amyloid 1-40 in the mouse cerebral cortex. *Ann N Y Acad Sci* **893**, 314-320 (1999).
482. Bruijn, L.I. *et al.* Elevated free nitrotyrosine levels, but not protein-bound nitrotyrosine or hydroxyl radicals, throughout amyotrophic lateral sclerosis (ALS)-like disease implicate tyrosine nitration as an aberrant in vivo property of one familial ALS-linked superoxide dismutase 1 mutant. *Proc Natl Acad Sci U S A* **94**, 7606-7611 (1997).
483. Ferrante, R.J. *et al.* Increased 3-nitrotyrosine and oxidative damage in mice with a human copper/zinc superoxide dismutase mutation. *Ann Neurol* **42**, 326-334 (1997).
484. Matthews, R.T. & Flint Beal, M. Increased 3-nitrotyrosine in brains of Apo E-deficient mice. *Brain Research* **718**, 181-184 (1996).
485. Takizawa, S., Fukuyama, N., Hirabayashi, H., Nakazawa, H. & Shinohara, Y. Dynamics of nitrotyrosine formation and decay in rat brain during focal ischemia-reperfusion. *J Cereb Blood Flow Metab* **19**, 667-672 (1999).
486. Cross, A.H., Manning, P.T., Stern, M.K. & Misko, T.P. Evidence for the production of peroxynitrite in inflammatory CNS demyelination. *J Neuroimmunol* **80**, 121-130 (1997).
487. Eliasson, M.J. *et al.* Neuronal nitric oxide synthase activation and peroxynitrite formation in ischemic stroke linked to neural damage. *J Neurosci* **19**, 5910-5918 (1999).
488. Schulz, J.B. *et al.* Striatal Malonate Lesions Are Attenuated in Neuronal Nitric Oxide Synthase Knockout Mice. *Journal of Neurochemistry* **67**, 430-433 (1996).
489. Imam, S.Z. *et al.* Methamphetamine generates peroxynitrite and produces dopaminergic neurotoxicity in mice: protective effects of peroxynitrite decomposition catalyst. *Brain Research* **837**, 15-21 (1999).
490. Pennathur, S., Jackson-Lewis, V., Przedborski, S. & Heinecke, J.W. Mass spectrometric quantification of 3-nitrotyrosine, ortho-tyrosine, and o,o'-dityrosine in brain tissue of 1-methyl-4-phenyl-1,2,3, 6-tetrahydropyridine-treated mice, a model of oxidative stress in Parkinson's disease. *J Biol Chem* **274**, 34621-34628 (1999).
491. Ara, J. *et al.* Inactivation of tyrosine hydroxylase by nitration following exposure to peroxynitrite and 1-methyl-4-phenyl-1,2,3,6-tetrahydropyridine (MPTP). *Proc Natl Acad Sci U S A* **95**, 7659-7663 (1998).
492. Tabrizi, S.J. *et al.* Mitochondrial dysfunction and free radical damage in the Huntington R6/2 transgenic mouse. *Ann Neurol* **47**, 80-86 (2000).
493. Mésenge, C. *et al.* Reduction of tyrosine nitration after N(omega)-nitro-L-arginine-methylester treatment of mice with traumatic brain injury. *Eur J Pharmacol* **353**, 53-57 (1998).
494. Neufeld, A.H. Nitric oxide: a potential mediator of retinal ganglion cell damage in glaucoma. *Surv Ophthalmol* **43 Suppl 1**, S129-135 (1999).
495. Cromheeke, K.M. *et al.* Inducible nitric oxide synthase colocalizes with signs of lipid oxidation/peroxidation in human atherosclerotic plaques. *Cardiovasc Res* **43**, 744-754 (1999).

496. Depre, C., Havaux, X., Renkin, J., Vanoverschelde, J.L. & Wijns, W. Expression of inducible nitric oxide synthase in human coronary atherosclerotic plaque. *Cardiovascular research* **41**, 465-472 (1999).
497. Szabolcs, M.J. *et al.* Apoptosis and increased expression of inducible nitric oxide synthase in human allograft rejection. *Transplantation* **65**, 804-812 (1998).
498. Matata, B.M., Sosnowski, A.W. & Galiñanes, M. Off-pump bypass graft operation significantly reduces oxidative stress and inflammation. *Ann Thorac Surg* **69**, 785-791 (2000).
499. Hambrecht, R. *et al.* Exercise intolerance in patients with chronic heart failure and increased expression of inducible nitric oxide synthase in the skeletal muscle. *J Am Coll Cardiol* **33**, 174-179 (1999).
500. Kooy, N.W. *et al.* Extensive tyrosine nitration in human myocardial inflammation: evidence for the presence of peroxynitrite. *Crit Care Med* **25**, 812-819 (1997).
501. Roggensack, A.M., Zhang, Y. & Davidge, S.T. Evidence for peroxynitrite formation in the vasculature of women with preeclampsia. *Hypertension* **33**, 83-89 (1999).
502. Kossenjans, W., Eis, A., Sahay, R., Brockman, D. & Myatt, L. Role of peroxynitrite in altered fetal-placental vascular reactivity in diabetes or preeclampsia. *American Journal of Physiology-Heart and Circulatory Physiology* **278**, H1311-H1319 (2000).
503. Ravalli, S. *et al.* Inducible nitric oxide synthase expression in smooth muscle cells and macrophages of human transplant coronary artery disease. *Circulation* **97**, 2338-2345 (1998).
504. Aji, W. *et al.* L-arginine prevents xanthoma development and inhibits atherosclerosis in LDL receptor knockout mice. *Circulation* **95**, 430-437 (1997).
505. Bachmaier, K. *et al.* iNOS expression and nitrotyrosine formation in the myocardium in response to inflammation is controlled by the interferon regulatory transcription factor 1. *Circulation* **96**, 585-591 (1997).
506. Kooy, N.W., Royall, J.A., Ye, Y.Z., Kelly, D.R. & Beckman, J.S. Evidence for in vivo peroxynitrite production in human acute lung injury. *Am J Respir Crit Care Med* **151**, 1250-1254 (1995).
507. Haddad, I.Y. *et al.* Quantitation of nitrotyrosine levels in lung sections of patients and animals with acute lung injury. *J Clin Invest* **94**, 2407-2413 (1994).
508. Gole, M.D. *et al.* Plasma proteins modified by tyrosine nitration in acute respiratory distress syndrome. *Am J Physiol Lung Cell Mol Physiol* **278**, L961-967 (2000).
509. Saleh, D., Ernst, P., Lim, S., Barnes, P.J. & Giaid, A. Increased formation of the potent oxidant peroxynitrite in the airways of asthmatic patients is associated with induction of nitric oxide synthase: effect of inhaled glucocorticoid. *Faseb j* **12**, 929-937 (1998).
510. Banks, B.A., Ischiropoulos, H., McClelland, M., Ballard, P.L. & Ballard, R.A. Plasma 3-nitrotyrosine is elevated in premature infants who develop bronchopulmonary dysplasia. *Pediatrics* **101**, 870-874 (1998).
511. Petruzzelli, S. *et al.* Plasma 3-nitrotyrosine in cigarette smokers. *Am J Respir Crit Care Med* **156**, 1902-1907 (1997).
512. Hallman, M., Bry, K., Turbow, R., Waffarn, F. & Lappalainen, U. Pulmonary toxicity associated with nitric oxide in term infants with severe respiratory failure. *The Journal of Pediatrics* **132**, 827-829 (1998).

513. Aikio, O., Vuopala, K., Pokela, M.L. & Hallman, M. Diminished inducible nitric oxide synthase expression in fulminant early-onset neonatal pneumonia. *Pediatrics* **105**, 1013-1019 (2000).
514. Hansen, P.R., Holm, A.M., Svendsen, U.G., Olsen, P.S. & Andersen, C.B. Apoptosis and formation of peroxynitrite in the lungs of patients with obliterative bronchiolitis. *The Journal of Heart and Lung Transplantation* **19**, 160-166 (2000).
515. Sato, M., Fukuyama, N., Sakai, M. & Nakazawa, H. Increased nitric oxide in nasal lavage fluid and nitrotyrosine formation in nasal mucosa--indices for severe perennial nasal allergy. *Clin Exp Allergy* **28**, 597-605 (1998).
516. Cuzzocrea, S. *et al.* Role of IL-6 in the pleurisy and lung injury caused by carrageenan. *J Immunol* **163**, 5094-5104 (1999).
517. Adler, H. *et al.* Suppression of herpes simplex virus type 1 (HSV-1)-induced pneumonia in mice by inhibition of inducible nitric oxide synthase (iNOS, NOS2). *J Exp Med* **185**, 1533-1540 (1997).
518. Jackson, R.M., Helton, E.S., Viera, L. & Ohman, T. Survival, lung injury, and lung protein nitration in heterozygous MnSOD knockout mice in hyperoxia. *Exp Lung Res* **25**, 631-646 (1999).
519. Akaike, T. *et al.* Pathogenesis of influenza virus-induced pneumonia: involvement of both nitric oxide and oxygen radicals. *Proc Natl Acad Sci U S A* **93**, 2448-2453 (1996).
520. Yamazaki, C. *et al.* Production of superoxide and nitric oxide by alveolar macrophages in the bleomycin-induced interstitial pneumonia mice model. *Jpn J Pharmacol* **78**, 69-73 (1998).
521. Kristof, A.S., Goldberg, P., Laubach, V. & Hussain, S.N. Role of inducible nitric oxide synthase in endotoxin-induced acute lung injury. *Am J Respir Crit Care Med* **158**, 1883-1889 (1998).
522. WEINBERGER, B. *et al.* Inhaled Nitric Oxide Primes Lung Macrophages to Produce Reactive Oxygen and Nitrogen Intermediates. *American Journal of Respiratory and Critical Care Medicine* **158**, 931-938 (1998).
523. ter Steege, J.C., Koster-Kamphuis, L., van Straaten, E.A., Forget, P.P. & Buurman, W.A. Nitrotyrosine in plasma of celiac disease patients as detected by a new sandwich ELISA. *Free Radic Biol Med* **25**, 953-963 (1998).
524. Szaleczky, E., Prónai, L., Nakazawa, H. & Tulassay, Z. Evidence of in vivo peroxynitrite formation in patients with colorectal carcinoma, higher plasma nitrate/nitrite levels, and lower protection against oxygen free radicals. *J Clin Gastroenterol* **30**, 47-51 (2000).
525. Goto, T. *et al.* Enhanced expression of inducible nitric oxide synthase and nitrotyrosine in gastric mucosa of gastric cancer patients. *Clinical cancer research : an official journal of the American Association for Cancer Research* **5**, 1411-1415 (1999).
526. Sakaguchi, A.A. *et al.* Increased expression of inducible nitric oxide synthase and peroxynitrite in Helicobacter pylori gastric ulcer. *Free Radic Biol Med* **27**, 781-789 (1999).
527. Mannick, E.E. *et al.* Inducible nitric oxide synthase, nitrotyrosine, and apoptosis in Helicobacter pylori gastritis: effect of antibiotics and antioxidants. *Cancer Res* **56**, 3238-3243 (1996).
528. Dijkstra, G. *et al.* Expression of nitric oxide synthases and formation of nitrotyrosine and reactive oxygen species in inflammatory bowel disease. *J Pathol* **186**, 416-421 (1998).

529. Ford, H., Watkins, S., Reblock, K. & Rowe, M. The role of inflammatory cytokines and nitric oxide in the pathogenesis of necrotizing enterocolitis. *J Pediatr Surg* **32**, 275-282 (1997).
530. Kato, H. *et al.* Nitrotyrosine in esophageal squamous cell carcinoma and relevance to p53 expression. *Cancer Lett* **153**, 121-127 (2000).
531. MacMillan-Crow, L.A., Greendorfer, J.S., Vickers, S.M. & Thompson, J.A. Tyrosine nitration of c-SRC tyrosine kinase in human pancreatic ductal adenocarcinoma. *Arch Biochem Biophys* **377**, 350-356 (2000).
532. Kimura, H. *et al.* Increased expression of an inducible isoform of nitric oxide synthase and the formation of peroxynitrite in colonic mucosa of patients with active ulcerative colitis. *Gut* **42**, 180-187 (1998).
533. Suarez-Pinzon, W.L., Szabó, C. & Rabinovitch, A. Development of autoimmune diabetes in NOD mice is associated with the formation of peroxynitrite in pancreatic islet beta-cells. *Diabetes* **46**, 907-911 (1997).
534. Zingarelli, B., Szabó, C. & Salzman, A.L. Blockade of Poly(ADP-ribose) synthetase inhibits neutrophil recruitment, oxidant generation, and mucosal injury in murine colitis. *Gastroenterology* **116**, 335-345 (1999).
535. Cuzzocrea, S. *et al.* IL-6 knock-out mice exhibit resistance to splanchnic artery occlusion shock. *J Leukoc Biol* **66**, 471-480 (1999).
536. Jaiswal, M., LaRusso, N.F., Burgart, L.J. & Gores, G.J. Inflammatory cytokines induce DNA damage and inhibit DNA repair in cholangiocarcinoma cells by a nitric oxide-dependent mechanism. *Cancer Res* **60**, 184-190 (2000).
537. Cuzzocrea, S., Zingarelli, B., Villari, D., Caputi, A.P. & Longo, G. Evidence for in vivo peroxynitrite production in human chronic hepatitis. *Life Sci* **63**, Pl25-30 (1998).
538. Morikawa, A. *et al.* Role of nitric oxide in lipopolysaccharide-induced hepatic injury in D-galactosamine-sensitized mice as an experimental endotoxic shock model. *Infect Immun* **67**, 1018-1024 (1999).
539. Hinson, J.A., Michael, S.L., Ault, S.G. & Pumford, N.R. Western blot analysis for nitrotyrosine protein adducts in livers of saline-treated and acetaminophen-treated mice. *Toxicol Sci* **53**, 467-473 (2000).
540. Fukuyama, N. *et al.* Clinical evidence of peroxynitrite formation in chronic renal failure patients with septic shock. *Free Radic Biol Med* **22**, 771-774 (1997).
541. Thuraisingham, R.C., Nott, C.A., Dodd, S.M. & Yaqoob, M.M. Increased nitrotyrosine staining in kidneys from patients with diabetic nephropathy. *Kidney Int* **57**, 1968-1972 (2000).
542. COMBET, S. *et al.* Vascular Proliferation and Enhanced Expression of Endothelial Nitric Oxide Synthase in Human Peritoneum Exposed to Long-Term Peritoneal Dialysis. *Journal of the American Society of Nephrology* **11**, 717-728 (2000).
543. Noiri, E. *et al.* Reduced tolerance to acute renal ischemia in mice with a targeted disruption of the osteopontin gene. *Kidney International* **56**, 74-82 (1999).
544. Bank, N. *et al.* Inhibition of nitric oxide synthase ameliorates cellular injury in sickle cell mouse kidneys. *Kidney International* **58**, 82-89 (2000).
545. Bank, N. *et al.* Peroxynitrite formation and apoptosis in transgenic sickle cell mouse kidneys. *Kidney International* **54**, 1520-1528 (1998).

546. Hukkanen, M. *et al.* Nitric Oxide in the Local Host Reaction to Total Hip Replacement. *Clinical Orthopaedics and Related Research®* **352** (1998).
547. Kaur, H. & Halliwell, B. Evidence for nitric oxide-mediated oxidative damage in chronic inflammation. Nitrotyrosine in serum and synovial fluid from rheumatoid patients. *FEBS Lett* **350**, 9-12 (1994).
548. Szabó, C. *et al.* Protection against peroxynitrite-induced fibroblast injury and arthritis development by inhibition of poly(ADP-ribose) synthase. *Proc Natl Acad Sci U S A* **95**, 3867-3872 (1998).
549. Nakatsuka, M. *et al.* Generation of peroxynitrite and apoptosis in placenta of patients with chorioamnionitis: possible implications in placental abruption. *Hum Reprod* **14**, 1101-1106 (1999).
550. Yang, C.C., Alvarez, R.B., Engel, W.K., Heller, S.L. & Askanas, V. Nitric oxide-induced oxidative stress in autosomal recessive and dominant inclusion-body myopathies. *Brain* **121**, 1089-1097 (1998).
551. Banno, S., Tamada, Y., Matsumoto, Y. & Ohashi, M. Apoptotic cell death of neutrophils in development of skin lesions of patients with anaphylactoid purpura. *J Dermatol* **24**, 94-99 (1997).
552. Ahmed, B. & Van Den Oord, J.J. Expression of the inducible isoform of nitric oxide synthase in pigment cell lesions of the skin. *Br J Dermatol* **142**, 432-440 (2000).
553. Cotton, S.A., Herrick, A.L., Jayson, M.I. & Freemont, A.J. Endothelial expression of nitric oxide synthases and nitrotyrosine in systemic sclerosis skin. *J Pathol* **189**, 273-278 (1999).
554. Hattori, Y. *et al.* 8-hydroxy-2'-deoxyguanosine is increased in epidermal cells of hairless mice after chronic ultraviolet B exposure. *J Invest Dermatol* **107**, 733-737 (1996).
555. Robertson, F.M., Long, B.W., Tober, K.L., Ross, M.S. & Oberyszyn, T.M. Gene expression and cellular sources of inducible nitric oxide synthase during tumor promotion. *Carcinogenesis* **17**, 2053-2059 (1996).
556. Oates, J.C., Christensen, E.F., Reilly, C.M., Self, S.E. & Gilkeson, G.S. Prospective measure of serum 3-nitrotyrosine levels in systemic lupus erythematosus: correlation with disease activity. *Proc Assoc Am Physicians* **111**, 611-621 (1999).
557. Facchetti, F. *et al.* Expression of inducible nitric oxide synthase in human granulomas and histiocytic reactions. *The American journal of pathology* **154**, 145-152 (1999).
558. Haddad, I.Y. *et al.* High levels of peroxynitrite are generated in the lungs of irradiated mice given cyclophosphamide and allogeneic T cells. A potential mechanism of injury after marrow transplantation. *Am J Respir Cell Mol Biol* **20**, 1125-1135 (1999).
559. Gal, A., Tamir, S., Kennedy, L.J., Tannenbaum, S.R. & Wogan, G.N. Nitrotyrosine formation, apoptosis, and oxidative damage: relationships to nitric oxide production in SJL mice bearing the RcsX tumor. *Cancer Res* **57**, 1823-1828 (1997).
560. Stadtman, E.R., Moskovitz, J. & Levine, R.L. Oxidation of methionine residues of proteins: biological consequences. *Antioxid Redox Signal* **5**, 577-582 (2003).
561. Yamakura, F. & Ikeda, K. Modification of tryptophan and tryptophan residues in proteins by reactive nitrogen species. *Nitric Oxide* **14**, 152-161 (2006).
562. Alvarez, B. *et al.* Inactivation of human Cu,Zn superoxide dismutase by peroxynitrite and formation of histidinyl radical. *Free Radic Biol Med* **37**, 813-822 (2004).

563. Tsunoda, S., Kibe, N., Kurahashi, T. & Fujii, J. Differential responses of SOD1-deficient mouse embryonic fibroblasts to oxygen concentrations. *Archives of biochemistry and biophysics* **537**, 5-11 (2013).
564. Zhang, Y. *et al.* Loss of manganese superoxide dismutase leads to abnormal growth and signal transduction in mouse embryonic fibroblasts. *FRB Free Radical Biology and Medicine* **49**, 1255-1262 (2010).
565. Cramer-Morales, K., Heer, C.D., Mapuskar, K.A. & Domann, F.E. SOD2 targeted gene editing by CRISPR/Cas9 yields Human cells devoid of MnSOD. *Free Radical Biology and Medicine* **89**, 379-386 (2015).
566. Fritzen, S. *et al.* Neuronal nitric oxide synthase (NOS-I) knockout increases the survival rate of neural cells in the hippocampus independently of BDNF. *Mol Cell Neurosci* **35**, 261-271 (2007).
567. Kuhlencordt, P.J. *et al.* Role of endothelial nitric oxide synthase in endothelial activation: insights from eNOS knockout endothelial cells. *Am J Physiol Cell Physiol* **286**, C1195-1202 (2004).
568. Garg, U.C. & Hassid, A. Nitric oxide-generating vasodilators and 8-bromo-cyclic guanosine monophosphate inhibit mitogenesis and proliferation of cultured rat vascular smooth muscle cells. *The Journal of clinical investigation* **83**, 1774-1777 (1989).
569. Jeremy, J.Y., Rowe, D., Emsley, A.M. & Newby, A.C. Nitric oxide and the proliferation of vascular smooth muscle cells. *Cardiovascular Research* **43**, 580-594 (1999).
570. Gurjar, M.V., Sharma, R.V. & Bhalla, R.C. eNOS Gene Transfer Inhibits Smooth Muscle Cell Migration and MMP-2 and MMP-9 Activity. *Arteriosclerosis, Thrombosis, and Vascular Biology* **19**, 2871-2877 (1999).
571. Casscells, W. Migration of smooth muscle and endothelial cells. Critical events in restenosis. *Circulation* **86**, 723-729 (1992).
572. Muller, F.L. *et al.* Absence of CuZn superoxide dismutase leads to elevated oxidative stress and acceleration of age-dependent skeletal muscle atrophy. *Free Radic Biol Med* **40**, 1993-2004 (2006).
573. Flood, D.G. *et al.* Hindlimb motor neurons require Cu/Zn superoxide dismutase for maintenance of neuromuscular junctions. *Am J Pathol* **155**, 663-672 (1999).
574. Zhang, Y. *et al.* A new role for oxidative stress in aging: The accelerated aging phenotype in Sod1-/- mice is correlated to increased cellular senescence. *Redox Biol* **11**, 30-37 (2017).
575. Iuchi, Y. *et al.* Spontaneous skin damage and delayed wound healing in SOD1-deficient mice. *Mol Cell Biochem* **341**, 181-194 (2010).
576. Reaume, A.G. *et al.* Motor neurons in Cu/Zn superoxide dismutase-deficient mice develop normally but exhibit enhanced cell death after axonal injury. *Nat Genet* **13**, 43-47 (1996).
577. Fischer, L.R., Li, Y., Asress, S.A., Jones, D.P. & Glass, J.D. Absence of SOD1 leads to oxidative stress in peripheral nerve and causes a progressive distal motor axonopathy. *Exp Neurol* **233**, 163-171 (2012).
578. Shi, Y. *et al.* The lack of CuZnSOD leads to impaired neurotransmitter release, neuromuscular junction destabilization and reduced muscle strength in mice. *PLoS One* **9**, e100834 (2014).

579. Garratt, M., Pichaud, N., Glaros, E.N., Kee, A.J. & Brooks, R.C. Superoxide dismutase deficiency impairs olfactory sexual signaling and alters bioenergetic function in mice. *Proc Natl Acad Sci U S A* **111**, 8119-8124 (2014).
580. Matzuk, M.M., Dionne, L., Guo, Q., Kumar, T.R. & Lebovitz, R.M. Ovarian function in superoxide dismutase 1 and 2 knockout mice. *Endocrinology* **139**, 4008-4011 (1998).
581. Imamura, Y. *et al.* Drusen, choroidal neovascularization, and retinal pigment epithelium dysfunction in SOD1-deficient mice: a model of age-related macular degeneration. *Proc Natl Acad Sci U S A* **103**, 11282-11287 (2006).
582. Yoshihara, D. *et al.* The absence of the SOD1 gene causes abnormal monoaminergic neurotransmission and motivational impairment-like behavior in mice. *Free Radic Res* **50**, 1245-1256 (2016).
583. Lebovitz, R.M. *et al.* Neurodegeneration, myocardial injury, and perinatal death in mitochondrial superoxide dismutase-deficient mice. *Proc Natl Acad Sci U S A* **93**, 9782-9787 (1996).
584. Li, Y. *et al.* Dilated cardiomyopathy and neonatal lethality in mutant mice lacking manganese superoxide dismutase. *Nat Genet* **11**, 376-381 (1995).
585. Huang, T.T. *et al.* Genetic modification of prenatal lethality and dilated cardiomyopathy in Mn superoxide dismutase mutant mice. *Free Radic Biol Med* **31**, 1101-1110 (2001).
586. Asikainen, T.M. *et al.* Increased sensitivity of homozygous Sod2 mutant mice to oxygen toxicity. *Free Radic Biol Med* **32**, 175-186 (2002).
587. Melov, S. *et al.* Mitochondrial disease in superoxide dismutase 2 mutant mice. *Proc Natl Acad Sci U S A* **96**, 846-851 (1999).
588. Van Remmen, H. *et al.* Knockout mice heterozygous for Sod2 show alterations in cardiac mitochondrial function and apoptosis. *Am J Physiol Heart Circ Physiol* **281**, H1422-1432 (2001).
589. Nojiri, H. *et al.* Oxidative stress causes heart failure with impaired mitochondrial respiration. *J Biol Chem* **281**, 33789-33801 (2006).
590. Kuwahara, H. *et al.* Oxidative stress in skeletal muscle causes severe disturbance of exercise activity without muscle atrophy. *Free Radic Biol Med* **48**, 1252-1262 (2010).
591. Lustgarten, M.S. *et al.* MnSOD deficiency results in elevated oxidative stress and decreased mitochondrial function but does not lead to muscle atrophy during aging. *Aging Cell* **10**, 493-505 (2011).
592. Lustgarten, M.S. *et al.* Conditional knockout of Mn-SOD targeted to type IIB skeletal muscle fibers increases oxidative stress and is sufficient to alter aerobic exercise capacity. *Am J Physiol Cell Physiol* **297**, C1520-1532 (2009).
593. Ikegami, T. *et al.* Model mice for tissue-specific deletion of the manganese superoxide dismutase (MnSOD) gene. *Biochem Biophys Res Commun* **296**, 729-736 (2002).
594. Konzack, A. *et al.* Mitochondrial Dysfunction Due to Lack of Manganese Superoxide Dismutase Promotes Hepatocarcinogenesis. *Antioxid Redox Signal* **23**, 1059-1075 (2015).
595. Lenart, J., Dombrowski, F., Gorlach, A. & Kietzmann, T. Deficiency of manganese superoxide dismutase in hepatocytes disrupts zonated gene expression in mouse liver. *Arch Biochem Biophys* **462**, 238-244 (2007).

596. Parajuli, N. *et al.* Generation and characterization of a novel kidney-specific manganese superoxide dismutase knockout mouse. *Free Radic Biol Med* **51**, 406-416 (2011).
597. Sasaki, T. *et al.* Superoxide dismutase deficiency enhances superoxide levels in brain tissues during oxygenation and hypoxia-reoxygenation. *J Neurosci Res* **89**, 601-610 (2011).
598. Izuo, N. *et al.* Brain-Specific Superoxide Dismutase 2 Deficiency Causes Perinatal Death with Spongiform Encephalopathy in Mice. *Oxid Med Cell Longev* **2015**, 238914 (2015).
599. Case, A.J., Madsen, J.M., Motto, D.G., Meyerholz, D.K. & Domann, F.E. Manganese superoxide dismutase depletion in murine hematopoietic stem cells perturbs iron homeostasis, globin switching, and epigenetic control in erythrocyte precursor cells. *Free Radic Biol Med* **56**, 17-27 (2013).
600. Misawa, H. *et al.* Conditional knockout of Mn superoxide dismutase in postnatal motor neurons reveals resistance to mitochondrial generated superoxide radicals. *Neurobiol Dis* **23**, 169-177 (2006).
601. Treiber, N. *et al.* Accelerated aging phenotype in mice with conditional deficiency for mitochondrial superoxide dismutase in the connective tissue. *Aging Cell* **10**, 239-254 (2011).
602. Case, A.J. & Domann, F.E. Manganese superoxide dismutase is dispensable for post-natal development and lactation in the murine mammary gland. *Free Radic Res* **46**, 1361-1368 (2012).
603. Case, A.J. *et al.* Elevated mitochondrial superoxide disrupts normal T cell development, impairing adaptive immune responses to an influenza challenge. *Free Radic Biol Med* **50**, 448-458 (2011).
604. Jones, M.K. *et al.* Loss of parietal cell superoxide dismutase leads to gastric oxidative stress and increased injury susceptibility in mice. *Am J Physiol Gastrointest Liver Physiol* **301**, G537-546 (2011).
605. Carlsson, L.M., Jonsson, J., Edlund, T. & Marklund, S.L. Mice lacking extracellular superoxide dismutase are more sensitive to hyperoxia. *Proc Natl Acad Sci U S A* **92**, 6264-6268 (1995).
606. Jung, O. *et al.* Extracellular superoxide dismutase is a major determinant of nitric oxide bioavailability: in vivo and ex vivo evidence from ecSOD-deficient mice. *Circ Res* **93**, 622-629 (2003).
607. Gongora, M.C. *et al.* Loss of extracellular superoxide dismutase leads to acute lung damage in the presence of ambient air: a potential mechanism underlying adult respiratory distress syndrome. *Am J Pathol* **173**, 915-926 (2008).
608. Lob, H.E. *et al.* Role of vascular extracellular superoxide dismutase in hypertension. *Hypertension* **58**, 232-239 (2011).
609. Lob, H.E. *et al.* Induction of hypertension and peripheral inflammation by reduction of extracellular superoxide dismutase in the central nervous system. *Hypertension* **55**, 277-283, 276p following 283 (2010).
610. Tsunoda, S., Kawano, N., Miyado, K., Kimura, N. & Fujii, J. Impaired fertilizing ability of superoxide dismutase 1-deficient mouse sperm during in vitro fertilization. *Biol Reprod* **87**, 121 (2012).

611. Deepa, S.S. *et al.* Accelerated sarcopenia in Cu/Zn superoxide dismutase knockout mice. *Free Radical Biology and Medicine* **132**, 19-23 (2019).
612. Larkin, L.M. *et al.* Skeletal muscle weakness due to deficiency of CuZn-superoxide dismutase is associated with loss of functional innervation. *Am J Physiol Regul Integr Comp Physiol* **301**, R1400-1407 (2011).
613. Jang, Y.C. *et al.* Increased superoxide in vivo accelerates age-associated muscle atrophy through mitochondrial dysfunction and neuromuscular junction degeneration. *Faseb j* **24**, 1376-1390 (2010).
614. Brooks, S.V. & Faulkner, J.A. Skeletal muscle weakness in old age: underlying mechanisms. *Med Sci Sports Exerc* **26**, 432-439 (1994).
615. Jang, Y.C. & Van Remmen, H. Age-associated alterations of the neuromuscular junction. *Exp Gerontol* **46**, 193-198 (2011).
616. Zhang, Y. *et al.* CuZnSOD gene deletion targeted to skeletal muscle leads to loss of contractile force but does not cause muscle atrophy in adult mice. *Faseb j* **27**, 3536-3548 (2013).
617. Sentman, M.-L. *et al.* Phenotypes of Mice Lacking Extracellular Superoxide Dismutase and Copper- and Zinc-containing Superoxide Dismutase. *Journal of Biological Chemistry* **281**, 6904-6909 (2006).
618. Sakellariou, G.K. *et al.* Comparison of Whole Body SOD1 Knockout with Muscle-Specific SOD1 Knockout Mice Reveals a Role for Nerve Redox Signaling in Regulation of Degenerative Pathways in Skeletal Muscle. *Antioxid Redox Signal* **28**, 275-295 (2018).
619. Flood, D.G. *et al.* Hindlimb Motor Neurons Require Cu/Zn Superoxide Dismutase for Maintenance of Neuromuscular Junctions. *The American Journal of Pathology* **155**, 663-672 (1999).
620. Imamura, Y. *et al.* Drusen, choroidal neovascularization, and retinal pigment epithelium dysfunction in SOD1-deficient mice: a model of age-related macular degeneration. *Proceedings of the National Academy of Sciences of the United States of America* **103**, 11282-11287 (2006).
621. Iuchi, Y. *et al.* Spontaneous skin damage and delayed wound healing in SOD1-deficient mice. *Molecular and Cellular Biochemistry* **341**, 1-2 (2010).
622. Fischer, L.R., Li, Y., Asress, S.A., Jones, D.P. & Glass, J.D. Absence of SOD1 leads to oxidative stress in peripheral nerve and causes a progressive distal motor axonopathy. *Experimental Neurology* **233**, 163-171 (2012).
623. Zhang, Y. *et al.* Dietary restriction attenuates the accelerated aging phenotype of Sod1 mice. *Free Radical Biology and Medicine* **60**, 300-306 (2013).
624. Garratt, M., Pichaud, N., Glaros, E.N., Kee, A.J. & Brooks, R.C. Superoxide dismutase deficiency impairs olfactory sexual signaling and alters bioenergetic function in mice. *Proceedings of the National Academy of Sciences* **111**, 8119-8124 (2014).
625. Yoshihara, D. *et al.* The absence of the SOD1 gene causes abnormal monoaminergic neurotransmission and motivational impairment-like behavior in mice. *Free Radical Research* **50**, 1245-1256 (2016).
626. Oh, S.S. *et al.* Neurodegeneration and early lethality in superoxide dismutase 2-deficient mice: a comprehensive analysis of the central and peripheral nervous systems. *Neuroscience* **212**, 201-213 (2012).

627. Li, Y. *et al.* Dilated cardiomyopathy and neonatal lethality in mutant mice lacking manganese superoxide dismutase. *Nature genetics* **11**, 376-381 (1995).
628. Lebovitz, R.M. *et al.* Neurodegeneration, myocardial injury, and perinatal death in mitochondrial superoxide dismutase-deficient mice. *Proceedings of the National Academy of Sciences* **93**, 9782-9787 (1996).
629. Kokoszka, J.E., Coskun, P., Esposito, L.A. & Wallace, D.C. Increased mitochondrial oxidative stress in the Sod2 (+/−) mouse results in the age-related decline of mitochondrial function culminating in increased apoptosis. *Proceedings of the National Academy of Sciences* **98**, 2278-2283 (2001).
630. Remmen, H.V. *et al.* Knockout mice heterozygous for Sod2 show alterations in cardiac mitochondrial function and apoptosis. *American Journal of Physiology-Heart and Circulatory Physiology* **281**, H1422-H1432 (2001).
631. Silva, J.P. *et al.* SOD2 overexpression: enhanced mitochondrial tolerance but absence of effect on UCP activity. *The EMBO Journal* **24**, 4061-4070 (2005).
632. Hu, D. *et al.* Hippocampal long-term potentiation, memory, and longevity in mice that overexpress mitochondrial superoxide dismutase. *Neurobiology of Learning and Memory* **87**, 372-384 (2007).
633. Lee, S., Van Remmen, H. & Csete, M. Sod2 overexpression preserves myoblast mitochondrial mass and function, but not muscle mass with aging. *Aging Cell* **8**, 296-310 (2009).
634. Izuo, N. *et al.* Brain-Specific Superoxide Dismutase 2 Deficiency Causes Perinatal Death with Spongiform Encephalopathy in Mice. *Oxidative Medicine and Cellular Longevity* **2015**, 238914 (2015).
635. Benov, L. How superoxide radical damages the cell. *Protoplasma* **217**, 33-36 (2001).
636. Kuwahara, H. *et al.* Oxidative stress in skeletal muscle causes severe disturbance of exercise activity without muscle atrophy. *Free Radical Biology and Medicine* **48**, 1252-1262 (2010).
637. Brown, G.C. & Borutaite, V. Nitric oxide and mitochondrial respiration in the heart. *Cardiovascular Research* **75**, 283-290 (2007).
638. Jung, O. *et al.* Extracellular Superoxide Dismutase Is a Major Determinant of Nitric Oxide Bioavailability. *Circulation Research* **93**, 622-629 (2003).
639. Gongora, M.C. *et al.* Loss of extracellular superoxide dismutase leads to acute lung damage in the presence of ambient air: a potential mechanism underlying adult respiratory distress syndrome. *The American journal of pathology* **173**, 915-926 (2008).
640. Morishita, T. *et al.* Nephrogenic diabetes insipidus in mice lacking all nitric oxide synthase isoforms. *Proceedings of the National Academy of Sciences of the United States of America* **102**, 10616-10621 (2005).
641. Moroi, M. *et al.* Interaction of genetic deficiency of endothelial nitric oxide, gender, and pregnancy in vascular response to injury in mice. *The Journal of Clinical Investigation* **101**, 1225-1232 (1998).
642. Tsutsui, M. *et al.* Significance of nitric oxide synthases: Lessons from triple nitric oxide synthases null mice. *Journal of Pharmacological Sciences* **127**, 42-52 (2015).

643. Ortiz, P.A. & Garvin, J.L. Cardiovascular and renal control in NOS-deficient mouse models. *American Journal of Physiology-Regulatory, Integrative and Comparative Physiology* **284**, R628-R638 (2003).
644. Morishita, T. *et al.* Vasculoprotective roles of neuronal nitric oxide synthase. *The FASEB journal : official publication of the Federation of American Societies for Experimental Biology* **16**, 1994-1996 (2002).
645. Nakata, S. *et al.* Spontaneous myocardial infarction in mice lacking all nitric oxide synthase isoforms. *Circulation* **117**, 2211-2223 (2008).
646. Shibata, K. *et al.* Spontaneous development of left ventricular hypertrophy and diastolic dysfunction in mice lacking all nitric oxide synthases. *Circulation Journal* **74**, 2681-2692 (2010).
647. Mitter, S.S., Shah, S.J. & Thomas, J.D. A Test in Context: E/A and E/e' to Assess Diastolic Dysfunction and LV Filling Pressure. *Journal of the American College of Cardiology* **69**, 1451-1464 (2017).
648. Takaki , A. *et al.* Crucial role of nitric oxide synthases system in endothelium-dependent hyperpolarization in mice. *Journal of Experimental Medicine* **205**, 2053-2063 (2008).
649. Morisada, N. *et al.* Complete Disruption of All Nitric Oxide Synthase Genes Causes Markedly Accelerated Renal Lesion Formation Following Unilateral Ureteral Obstruction in Mice In Vivo. *Journal of Pharmacological Sciences* **114**, 379-389 (2010).
650. Sabanai, K. *et al.* Genetic Disruption of All NO Synthase Isoforms Enhances BMD and Bone Turnover in Mice In Vivo: Involvement of the Renin-Angiotensin System. *Journal of Bone and Mineral Research* **23**, 633-643 (2008).
651. Gough, D.R. & Cotter, T.G. Hydrogen peroxide: a Jekyll and Hyde signalling molecule. *Cell death & disease* **2** (2011).
652. Hewitt, J. & Morris, J.G. Superoxide dismutase in some obligately anaerobic bacteria. *FEBS Letters* **50**, 315-318 (1975).
653. Forman, H.J. & Fridovich, I. Superoxide dismutase: a comparison of rate constants. *Archives of biochemistry and biophysics* **158**, 396-400 (1973).
654. Day, R.M. & Suzuki, Y.J. Cell proliferation, reactive oxygen and cellular glutathione. *Dose Response* **3**, 425-442 (2006).
655. Ji, A.-R. *et al.* Reactive oxygen species enhance differentiation of human embryonic stem cells into mesendodermal lineage. *Exp Mol Med* **42**, 175-186 (2010).
656. Cardoso, A.R. *et al.* Mitochondrial compartmentalization of redox processes. *Free Radical Biology and Medicine* **52**, 2201-2208 (2012).
657. Meitzler, J.L. *et al.* NADPH Oxidases: A Perspective on Reactive Oxygen Species Production in Tumor Biology. *Antioxidants & Redox Signaling* **20**, 2873-2889 (2013).
658. Fisher, A.B. Redox Signaling Across Cell Membranes. *Antioxidants & Redox Signaling* **11**, 1349-1356 (2008).
659. Bradley, A., Evans, M., Kaufman, M.H. & Robertson, E. Formation of germ-line chimaeras from embryo-derived teratocarcinoma cell lines. *Nature* **309**, 255-256 (1984).
660. Livak, K.J. & Schmittgen, T.D. Analysis of relative gene expression data using real-time quantitative PCR and the 2(-Delta Delta C(T)) Method. *Methods* **25**, 402-408 (2001).
661. Troy, C.M., Derossi, D., Prochiantz, A., Greene, L.A. & Shelanski, M.L. Downregulation of Cu/Zn superoxide dismutase leads to cell death via the nitric oxide-peroxynitrite

pathway. *The Journal of Neuroscience : The Official Journal of the Society for Neuroscience* **16**, 253-261 (1996).
662. Kim, H., Kim, M., Im, S.-K. & Fang, S. Mouse Cre-LoxP system: general principles to determine tissue-specific roles of target genes. *Lab Anim Res* **34**, 147-159 (2018).
663. Koyanagi, M., Kawakabe, S. & Arimura, Y. A comparative study of colorimetric cell proliferation assays in immune cells. *Cytotechnology Cytotechnology : Incorporating Methods in Cell ScienceInternational Journal of Cell Culture and Biotechnology* **68**, 1489-1498 (2016).
664. Budihardjo, I., Oliver, H., Lutter, M., Luo, X. & Wang, X. Biochemical Pathways of Caspase Activation During Apoptosis. *Annu. Rev. Cell Dev. Biol. Annual Review of Cell and Developmental Biology* **15**, 269-290 (1999).
665. Chang, L.Y., Slot, J.W., Geuze, H.J. & Crapo, J.D. Molecular immunocytochemistry of the CuZn superoxide dismutase in rat hepatocytes. *The Journal of cell biology* **107**, 2169-2179 (1988).
666. Yamakura, F. & Kawasaki, H. Post-translational modifications of superoxide dismutase. *BBAPAP BBA - Proteins and Proteomics* **1804**, 318-325 (2010).
667. Winterbourn, C.C. Reconciling the chemistry and biology of reactive oxygen species. *Nature Chemical Biology* **4**, 278-286 (2008).
668. Bienert, G.P., Schjoerring, J.K. & Jahn, T.P. Membrane transport of hydrogen peroxide. *Biochimica et Biophysica Acta (BBA) - Biomembranes* **1758**, 994-1003 (2006).
669. Takac, I. *et al.* The E-loop is involved in hydrogen peroxide formation by the NADPH oxidase Nox4. *J Biol Chem* **286**, 13304-13313 (2011).
670. Sansone, R.A. & Sansone, L.A. Getting a Knack for NAC: N-Acetyl-Cysteine. *Innov Clin Neurosci* **8**, 10-14 (2011).
671. Cnubben, N.H.P., Rietjens, I.M.C.M., Wortelboer, H., van Zanden, J. & van Bladeren, P.J. The interplay of glutathione-related processes in antioxidant defense. *Environmental Toxicology and Pharmacology* **10**, 141-152 (2001).
672. Bos, J.L. ras Oncogenes in Human Cancer: A Review. *Cancer Research* **49**, 4682-4689 (1989).
673. Prior, I.A., Lewis, P.D. & Mattos, C. A comprehensive survey of Ras mutations in cancer. *Cancer research* **72**, 2457-2467 (2012).
674. Liou, G.-Y. *et al.* Mutant KRas-Induced Mitochondrial Oxidative Stress in Acinar Cells Upregulates EGFR Signaling to Drive Formation of Pancreatic Precancerous Lesions. *Cell reports* **14**, 2325-2336 (2016).
675. Storz, P. KRas, ROS and the initiation of pancreatic cancer. *Small GTPases* **8**, 38-42 (2017).
676. Jackson, E.L. *et al.* Analysis of lung tumor initiation and progression using conditional expression of oncogenic K-ras. *Genes Dev* **15**, 3243-3248 (2001).
677. Víteček, J., Lojek, A., Valacchi, G. & Kubala, L. Arginine-based inhibitors of nitric oxide synthase: therapeutic potential and challenges. *Mediators of inflammation* **2012**, 318087-318087 (2012).
678. Derbyshire, E.R. & Marletta, M.A. Structure and Regulation of Soluble Guanylate Cyclase. *Annual Review of Biochemistry* **81**, 533-559 (2012).

679. Wolfertstetter, S., Huettner, J.P. & Schlossmann, J. cGMP-Dependent Protein Kinase Inhibitors in Health and Disease. *Pharmaceuticals (Basel)* **6**, 269-286 (2013).
680. Garthwaite, J. *et al.* Potent and selective inhibition of nitric oxide-sensitive guanylyl cyclase by 1H-[1,2,4]oxadiazolo[4,3-a]quinoxalin-1-one. *Mol Pharmacol* **48**, 184-188 (1995).
681. Martínez-Ruiz, A., Cadenas, S. & Lamas, S. Nitric oxide signaling: Classical, less classical, and nonclassical mechanisms. *Free Radical Biology and Medicine* **51**, 17-29 (2011).
682. Han, S.J. *et al.* Assay of the redox state of the tumor suppressor PTEN by mobility shift. *Methods* **77-78**, 58-62 (2015).
683. Son, Y., Kim, S., Chung, H.T. & Pae, H.O. Reactive oxygen species in the activation of MAP kinases. *Methods Enzymol* **528**, 27-48 (2013).
684. McCubrey, J.A., Lahair, M.M. & Franklin, R.A. Reactive oxygen species-induced activation of the MAP kinase signaling pathways. *Antioxid Redox Signal* **8**, 1775-1789 (2006).
685. Lee, S.R. *et al.* Reversible inactivation of the tumor suppressor PTEN by H2O2. *The Journal of Biological Chemistry* **277**, 20336-20342 (2002).
686. Leslie, N.R. *et al.* Redox regulation of PI 3-kinase signalling via inactivation of PTEN. *The EMBO journal* **22**, 5501-5510 (2003).
687. Pouysségur, J. & Mechta-Grigoriou, F. Redox regulation of the hypoxia-inducible factor. *Biol Chem* **387**, 1337-1346 (2006).
688. Morgan, M.J. & Liu, Z.G. Crosstalk of reactive oxygen species and NF-κB signaling. *Cell Res* **21**, 103-115 (2011).
689. Weydert, C.J. & Cullen, J.J. Measurement of superoxide dismutase, catalase and glutathione peroxidase in cultured cells and tissue. *Nat Protoc* **5**, 51-66 (2010).
690. Weisiger, R.A. & Fridovich, I. Mitochondrial superoxide simutase. Site of synthesis and intramitochondrial localization. *J Biol Chem* **248**, 4793-4796 (1973).
691. Marklund, S.L. Human copper-containing superoxide dismutase of high molecular weight. *Proceedings of the National Academy of Sciences* **79**, 7634-7638 (1982).
692. Pèrez, V.I. *et al.* Is the oxidative stress theory of aging dead? *BBAGEN BBA - General Subjects* **1790**, 1005-1014 (2009).
693. Deepa, S.S. *et al.* A new mouse model of frailty: the Cu/Zn superoxide dismutase knockout mouse. *Geroscience* **39**, 187-198 (2017).
694. Ho, Y.S. *et al.* Reduced fertility in female mice lacking copper-zinc superoxide dismutase. *J Biol Chem* **273**, 7765-7769 (1998).
695. Keithley, E.M. *et al.* Cu/Zn superoxide dismutase and age-related hearing loss. *Hear Res* **209**, 76-85 (2005).
696. Olofsson, E.M., Marklund, S.L. & Behndig, A. Glucose-induced cataract in CuZn-SOD null lenses: an effect of nitric oxide? *Free radical biology & medicine* **42**, 1098-1105 (2007).
697. Watanabe, K. *et al.* Superoxide dismutase 1 loss disturbs intracellular redox signaling, resulting in global age-related pathological changes. *Biomed Res Int* **2014**, 140165-140165 (2014).
698. Grindley, N.D., Whiteson, K.L. & Rice, P.A. Mechanisms of site-specific recombination. *Annu Rev Biochem* **75**, 567-605 (2006).

699. Ghosh, K., Lau, C.-K., Gupta, K. & Van Duyne, G.D. Preferential synapsis of loxP sites drives ordered strand exchange in Cre-loxP site-specific recombination. *Nature Chemical Biology* **1**, 275-282 (2005).
700. Holliday, R. A mechanism for gene conversion in fungi. *Genetical Research* **5**, 282-304 (1964).
701. Guo, F., Gopaul, D.N. & Van Duyne, G.D. Structure of Cre recombinase complexed with DNA in a site-specific recombination synapse. *Nature* **389**, 40-46 (1997).
702. O'Neil, K.T., Hoess, R.H. & DeGrado, W.F. Design of DNA-binding peptides based on the leucine zipper motif. *Science* **249**, 774-778 (1990).
703. Metzger, D. & Chambon, P. Site- and time-specific gene targeting in the mouse. *Methods* **24**, 71-80 (2001).
704. Brocard, J. *et al.* Spatio-temporally controlled site-specific somatic mutagenesis in the mouse. *Proc Natl Acad Sci U S A* **94**, 14559-14563 (1997).
705. Indra, A.K. *et al.* Temporally-controlled site-specific mutagenesis in the basal layer of the epidermis: comparison of the recombinase activity of the tamoxifen-inducible Cre-ER(T) and Cre-ER(T2) recombinases. *Nucleic acids research* **27**, 4324-4327 (1999).
706. Gow, A.J., Luchsinger, B.P., Pawloski, J.R., Singel, D.J. & Stamler, J.S. The oxyhemoglobin reaction of nitric oxide. *Proceedings of the National Academy of Sciences of the United States of America* **96**, 9027-9032 (1999).
707. Yoshida, K., Kasama, K., Kitabatake, M., Okuda, M. & Imai, M. Metabolic fate of nitric oxide. *International Archives of Occupational and Environmental Health* **46**, 71-77 (1980).
708. Gardner, P.R. Hemoglobin: a nitric-oxide dioxygenase. *Scientifica (Cairo)* **2012**, 683729-683729 (2012).
709. Lancaster, J.R., Jr. Simulation of the diffusion and reaction of endogenously produced nitric oxide. *Proc Natl Acad Sci U S A* **91**, 8137-8141 (1994).
710. Helms, C. & Kim-Shapiro, D.B. Hemoglobin-mediated nitric oxide signaling. *Free radical biology & medicine* **61**, 464-472 (2013).
711. Wang, Y. & Hekimi, S. Mitochondrial respiration without ubiquinone biosynthesis. **22**, 4768-4783 (2013).
712. Lønbro, S. *et al.* Reliability of blood lactate as a measure of exercise intensity in different strains of mice during forced treadmill running. *PloS one* **14**, e0215584-e0215584 (2019).
713. Rodrigues, W.F., Miguel, C.B., Napimoga, M.H., Oliveira, C.J.F. & Lazo-Chica, J.E. Establishing standards for studying renal function in mice through measurements of body size-adjusted creatinine and urea levels. *Biomed Res Int* **2014**, 872827-872827 (2014).
714. Hayashi, S. & McMahon, A.P. Efficient Recombination in Diverse Tissues by a Tamoxifen-Inducible Form of Cre: A Tool for Temporally Regulated Gene Activation/Inactivation in the Mouse. *Developmental Biology* **244**, 305-318 (2002).
715. Mondola, P., Damiano, S., Sasso, A. & Santillo, M. The Cu, Zn Superoxide Dismutase: Not Only a Dismutase Enzyme. *Front Physiol* **7**, 594-594 (2016).

716. Hayashi, S. & McMahon, A.P. Efficient Recombination in Diverse Tissues by a Tamoxifen-Inducible Form of Cre: A Tool for Temporally Regulated Gene Activation/Inactivation in the Mouse. *YDBIO</cja:jid> Developmental Biology* **244**, 305-318 (2002).
717. Berridge, B., Van Vleet, J. & Herman, E. Cardiac, vascular, and skeletal muscle systems. , in *Haschek and Rousseaux's Handbook of Toxicologic Pathology*. (eds. W. Haschek *et al.*) 1635-1665 (Elsevier, Amsterdam; 2013).
718. Parikh, S. *et al.* Diagnosis and management of mitochondrial disease: a consensus statement from the Mitochondrial Medicine Society. *Genet Med* **17**, 689-701 (2015).
719. Mitochondrial Medicine Society's Committee on, D. *et al.* The in-depth evaluation of suspected mitochondrial disease. *Mol Genet Metab* **94**, 16-37 (2008).
720. Philp, A., Macdonald, A.L. & Watt, P.W. Lactate – a signal coordinating cell and systemic function. *Journal of Experimental Biology* **208**, 4561-4575 (2005).
721. Sakellariou, G.K. *et al.* Role of superoxide-nitric oxide interactions in the accelerated age-related loss of muscle mass in mice lacking Cu,Zn superoxide dismutase. *Aging Cell* **10**, 749-760 (2011).
722. Al Shoyaib, A., Archie, S.R. & Karamyan, V.T. Intraperitoneal Route of Drug Administration: Should it Be Used in Experimental Animal Studies? *Pharmaceutical Research* **37**, 12 (2019).
723. Pavathuparambil Abdul Manaph, N., Al-Hawwas, M. & Zhou, X.-F. A direct and non-invasive method for kidney delivery of therapeutics in mice. *MethodsX* **5**, 1440-1446 (2018).
724. Wiedmeyer, C.E., Ruben, D. & Franklin, C. Complete blood count, clinical chemistry, and serology profile by using a single tube of whole blood from mice. *J Am Assoc Lab Anim Sci* **46**, 59-64 (2007).
725. O'Connell, K.E. *et al.* Practical Murine Hematopathology: A Comparative Review and Implications for Research. *Comparative Medicine* **65**, 96-113 (2015).
726. Roscoe, B.J.M.L. & Green, E.L. *Biology of the laboratory mouse*, Edn. 2d ed. (Blakiston Division, McGraw-Hill, New York; 1966).
727. Rai, M., Nongthomba, U. & Grounds, M.D. Chapter Nine - Skeletal Muscle Degeneration and Regeneration in Mice and Flies, in *Current Topics in Developmental Biology*, Vol. 108. (ed. B. Galliot) 247-281 (Academic Press, 2014).
728. Bruschetta, G. *et al.* FeTPPS Reduces Secondary Damage and Improves Neurobehavioral Functions after Traumatic Brain Injury. *Frontiers in Neuroscience* **11** (2017).
729. Kalayci, R. *et al.* Long-term L-NAME treatment potentiates the blood-brain barrier disruption during pentylenetetrazole-induced seizures in rats. *Life sciences* **79**, 16-20 (2006).
730. Suda, O. *et al.* Long-Term Treatment With N ω -Nitro- l -Arginine Methyl Ester Causes Arteriosclerotic Coronary Lesions in Endothelial Nitric Oxide Synthase-Deficient Mice. *Circulation* **106**, 1729-1735 (2002).
731. Pechánová, O., Bernátová, I. & Babal, P. Structural alterations in the heart after long-term L-NAME and D-NAME treatment. *General physiology and biophysics* **18 Suppl 1**, 6-9 (2000).
732. Castro, B. & Kuang, S. Evaluation of Muscle Performance in Mice by Treadmill Exhaustion Test and Whole-limb Grip Strength Assay. *Bio Protoc* **7**, e2237 (2017).

733. Baverstock, H., Jeffery, N.S. & Cobb, S.N. The morphology of the mouse masticatory musculature. *J Anat* **223**, 46-60 (2013).
734. Hakim, C.H. *et al.* An improved method for studying mouse diaphragm function. *Scientific Reports* **9**, 19453 (2019).
735. Russwurm, M. & Koesling, D. NO activation of guanylyl cyclase. *EMBJ The EMBO Journal* **23**, 4443-4450 (2004).
736. Bogdan, C. Nitric oxide and the immune response. *Nature immunology* **2**, 907-916 (2001).
737. Snyder, S.H. Nitric oxide: first in a new class of neurotransmitters. *Science (New York, N.Y.)* **257**, 494-496 (1992).
738. Radi, R. Oxygen radicals, nitric oxide, and peroxynitrite: Redox pathways in molecular medicine. *Proceedings of the National Academy of Sciences* **115**, 5839-5848 (2018).
739. Bonner, R.F. & Nossal, R. Principles of Laser-Doppler Flowmetry, in *Laser-Doppler Blood Flowmetry*. (eds. A.P. Shepherd & P.Å. Öberg) 17-45 (Springer US, Boston, MA; 1990).
740. Yin, H., Price, F. & Rudnicki, M.A. Satellite cells and the muscle stem cell niche. *Physiological reviews* **93**, 23-67 (2013).
741. Snow, M.H. Myogenic cell formation in regenerating rat skeletal muscle injured by mincing. II. An autoradiographic study. *Anat Rec* **188**, 201-217 (1977).
742. Gibson, M.C. & Schultz, E. The distribution of satellite cells and their relationship to specific fiber types in soleus and extensor digitorum longus muscles. *Anat Rec* **202**, 329-337 (1982).
743. Schmalbruch, H. & Hellhammer, U. The number of nuclei in adult rat muscles with special reference to satellite cells. *Anat Rec* **189**, 169-175 (1977).
744. Christov, C. *et al.* Muscle satellite cells and endothelial cells: close neighbors and privileged partners. *Mol Biol Cell* **18**, 1397-1409 (2007).
745. Chen, K., Pittman, R.N. & Popel, A.S. Nitric oxide in the vasculature: where does it come from and where does it go? A quantitative perspective. *Antioxidants & redox signaling* **10**, 1185-1198 (2008).
746. Bartosz, G. Peroxynitrite: mediator of the toxic action of nitric oxide. *Acta Biochim Pol* **43**, 645-659 (1996).
747. Ross, A. *et al.* NDRL-NIST solution kinetics database. *Notre Dame Radiation Laboratory, Gaithersburg* (1998).
748. Hao, Y. *et al.* Thioredoxin shapes the C. elegans sensory response to Pseudomonas produced nitric oxide. *Elife* **7**, e36833 (2018).
749. Lin, M.T. & Flint Beal, M. The oxidative damage theory of aging. *Clinical Neuroscience Research* **2**, 305-315 (2003).
750. Liochev, S.I. Reactive oxygen species and the free radical theory of aging. *Free Radical Biology and Medicine* **60**, 1-4 (2013).
751. Powers, S.K., Ji, L.L., Kavazis, A.N. & Jackson, M.J. Reactive oxygen species: impact on skeletal muscle. *Compr Physiol* **1**, 941-969 (2011).
752. Powers, S.K. *et al.* Influence of exercise and fiber type on antioxidant enzyme activity in rat skeletal muscle. *Am J Physiol* **266**, R375-380 (1994).

753. Picard, M., Hepple, R.T. & Burelle, Y. Mitochondrial functional specialization in glycolytic and oxidative muscle fibers: tailoring the organelle for optimal function. *American Journal of Physiology-Cell Physiology* **302**, C629-C641 (2012).
754. Davies, K.J., Maguire, J.J., Brooks, G.A., Dallman, P.R. & Packer, L. Muscle mitochondrial bioenergetics, oxygen supply, and work capacity during dietary iron deficiency and repletion. *American Journal of Physiology-Endocrinology and Metabolism* **242**, E418-E427 (1982).
755. Roubenoff, R. & Hughes, V.A. Sarcopenia: current concepts. *J Gerontol A Biol Sci Med Sci* **55**, M716-724 (2000).
756. Sataranatarajan, K. *et al.* Neuron specific reduction in CuZnSOD is not sufficient to initiate a full sarcopenia phenotype. *Redox Biology* **5**, 140-148 (2015).
757. Dobrowolny, G., Aucello, M. & Musarò, A. Muscle atrophy induced by SOD1G93A expression does not involve the activation of caspase in the absence of denervation. *Skeletal Muscle* **1**, 3 (2011).
758. Gurney, M.E. *et al.* Motor neuron degeneration in mice that express a human Cu,Zn superoxide dismutase mutation. *Science* **264**, 1772-1775 (1994).
759. Higgins, C.M.J., Jung, C. & Xu, Z. ALS-associated mutant SOD1G93A causes mitochondrial vacuolation by expansion of the intermembrane space and by involvement of SOD1 aggregation and peroxisomes. *BMC Neuroscience* **4**, 16 (2003).
760. Kapur, S., Bédard, S., Marcotte, B., Côté, C.H. & Marette, A. Expression of nitric oxide synthase in skeletal muscle: a novel role for nitric oxide as a modulator of insulin action. *Diabetes* **46**, 1691-1700 (1997).
761. Stamler, J.S. & Meissner, G. Physiology of Nitric Oxide in Skeletal Muscle. *Physiological Reviews* **81**, 209-237 (2001).
762. Kobzik, L., Reid, M.B., Bredt, D.S. & Stamler, J.S. Nitric oxide in skeletal muscle. *Nature* **372**, 546-548 (1994).
763. Lau, K.S. *et al.* Skeletal muscle contractions stimulate cGMP formation and attenuate vascular smooth muscle myosin phosphorylation via nitric oxide. *FEBS Lett* **431**, 71-74 (1998).
764. Thiemermann, C., Bowes, J., Myint, F.P. & Vane, J.R. Inhibition of the activity of poly(ADP ribose) synthetase reduces ischemia-reperfusion injury in the heart and skeletal muscle. *Proc Natl Acad Sci U S A* **94**, 679-683 (1997).
765. Kaliman, P., Canicio, J., Testar, X., Palacín, M. & Zorzano, A. Insulin-like growth factor-II, phosphatidylinositol 3-kinase, nuclear factor-kappaB and inducible nitric-oxide synthase define a common myogenic signaling pathway. *J Biol Chem* **274**, 17437-17444 (1999).
766. Klebl, B.M., Ayoub, A.T. & Pette, D. Protein oxidation, tyrosine nitration, and inactivation of sarcoplasmic reticulum Ca2+-ATPase in low-frequency stimulated rabbit muscle. *FEBS Lett* **422**, 381-384 (1998).
767. Hussain, S.N. Activity of nitric oxide synthase in the ventilatory muscle vasculature. *Comp Biochem Physiol A Mol Integr Physiol* **119**, 191-201 (1998).
768. Kobzik, L., Stringer, B., Balligand, J.L., Reid, M.B. & Stamler, J.S. Endothelial type nitric oxide synthase in skeletal muscle fibers: mitochondrial relationships. *Biochem Biophys Res Commun* **211**, 375-381 (1995).

769. Punkt, K. *et al.* Fibre-related nitric oxide synthase (NOS) in Duchenne muscular dystrophy. *Acta Histochem* **109**, 228-236 (2007).
770. Gossrau, R. Caveolin-3 and nitric oxide synthase I in healthy and diseased skeletal muscle. *Acta Histochemica* **100**, 99-112 (1998).
771. Godfrey, E.W., Longacher, M., Neiswender, H., Schwarte, R.C. & Browning, D.D. Guanylate cyclase and cyclic GMP-dependent protein kinase regulate agrin signaling at the developing neuromuscular junction. *Developmental biology* **307**, 195-201 (2007).
772. Chao, D.S. *et al.* Nitric oxide synthase and cyclic GMP-dependent protein kinase concentrated at the neuromuscular endplate. *Neuroscience* **76**, 665-672 (1997).
773. Lyons, T.W., Reinhard, C.T. & Planavsky, N.J. The rise of oxygen in Earth's early ocean and atmosphere. *Nature* **506**, 307-315 (2014).
774. Brocks, J.J., Logan, G.A., Buick, R. & Summons, R.E. Archean molecular fossils and the early rise of eukaryotes. *Science* **285**, 1033-1036 (1999).
775. Andreakis, N. *et al.* Evolution of the Nitric Oxide Synthase Family in Metazoans. *Molecular Biology and Evolution* **28**, 163-179 (2010).
776. Moroz, L.L. & Kohn, A.B. Parallel evolution of nitric oxide signaling: diversity of synthesis and memory pathways. *Front Biosci (Landmark Ed)* **16**, 2008-2051 (2011).
777. Robberecht, W. & Philips, T. The changing scene of amyotrophic lateral sclerosis. *Nature Reviews Neuroscience* **14**, 248-264 (2013).
778. Andersen, P.M. & Al-Chalabi, A. Clinical genetics of amyotrophic lateral sclerosis: what do we really know? *Nature Reviews Neurology* **7**, 603-615 (2011).
779. Taylor, J.P., Brown, R.H. & Cleveland, D.W. Decoding ALS: from genes to mechanism. *Nature* **539**, 197-206 (2016).
780. Du, M.Q., Carmichael, P.L. & Phillips, D.H. Induction of activating mutations in the human c-Ha-ras-1 proto-oncogene by oxygen free radicals. *Mol Carcinog* **11**, 170-175 (1994).
781. Waris, G. & Ahsan, H. Reactive oxygen species: role in the development of cancer and various chronic conditions. *J Carcinog* **5**, 14-14 (2006).
782. Panieri, E. & Santoro, M.M. ROS homeostasis and metabolism: a dangerous liason in cancer cells. *Cell Death & Disease* **7**, e2253-e2253 (2016).
783. Sabharwal, S.S. & Schumacker, P.T. Mitochondrial ROS in cancer: initiators, amplifiers or an Achilles' heel? *Nature Reviews Cancer* **14**, 709-721 (2014).
784. Cantley, L.C. The Phosphoinositide 3-Kinase Pathway. *Science* **296**, 1655-1657 (2002).
785. Chandel, N.S. *et al.* Reactive oxygen species generated at mitochondrial complex III stabilize hypoxia-inducible factor-1alpha during hypoxia: a mechanism of O2 sensing. *J Biol Chem* **275**, 25130-25138 (2000).
786. Semenza, G.L. Targeting HIF-1 for cancer therapy. *Nature Reviews Cancer* **3**, 721-732 (2003).
787. Mitsuishi, Y. *et al.* Nrf2 Redirects Glucose and Glutamine into Anabolic Pathways in Metabolic Reprogramming. *Cancer Cell* **22**, 66-79 (2012).
788. Hempel, N., Carrico, P.M. & Melendez, J.A. Manganese superoxide dismutase (Sod2) and redox-control of signaling events that drive metastasis. *Anticancer Agents Med Chem* **11**, 191-201 (2011).

789. Tribble, D.L. *et al.* Fatty streak formation in fat-fed mice expressing human copper-zinc superoxide dismutase. *Arteriosclerosis, thrombosis, and vascular biology* **17**, 1734-1740 (1997).
790. Rafieian-Kopaei, M., Setorki, M., Doudi, M., Baradaran, A. & Nasri, H. Atherosclerosis: process, indicators, risk factors and new hopes. *Int J Prev Med* **5**, 927-946 (2014).
791. Crow, J.P. & Beckman, J.S. Reactions between Nitric Oxide, Superoxide, and Peroxynitrite: Footprints of Peroxynitrite in Vivo, in *Advances in Pharmacology*, Vol. 34. (eds. L. Ignarro & F. Murad) 17-43 (Academic Press, 1995).
792. Chen, J.-y. *et al.* Nitric oxide bioavailability dysfunction involves in atherosclerosis. *Biomedicine & Pharmacotherapy* **97**, 423-428 (2018).
793. Wang, G.R., Zhu, Y., Halushka, P.V., Lincoln, T.M. & Mendelsohn, M.E. Mechanism of platelet inhibition by nitric oxide: in vivo phosphorylation of thromboxane receptor by cyclic GMP-dependent protein kinase. *Proceedings of the National Academy of Sciences of the United States of America* **95**, 4888-4893 (1998).
794. Jenkins, D. *et al.* Roles of nitric oxide in tumor growth. *Proceedings of the National Academy of Sciences* **92**, 4392-4396 (1995).
795. Xu, W., Liu, L.Z., Loizidou, M., Ahmed, M. & Charles, I.G. The role of nitric oxide in cancer. *Cell Research* **12**, 311-320 (2002).
796. Knott, A.B. & Bossy-Wetzel, E. Nitric oxide in health and disease of the nervous system. *Antioxidants & redox signaling* **11**, 541-554 (2009).
797. Farah, C., Michel, L.Y.M. & Balligand, J.-L. Nitric oxide signalling in cardiovascular health and disease. *Nature Reviews Cardiology* **15**, 292-316 (2018).